

The state of phytoplankton and bacterioplankton on the Scotian Shelf and Slope: Atlantic Zone Monitoring Program 1997-2013

W.K.W. Li

Ocean and Ecosystem Sciences Division
Maritimes Region
Fisheries and Oceans Canada

Bedford Institute of Oceanography
P.O. Box 1006
Dartmouth, Nova Scotia
Canada B2Y 4A2

2014

**Canadian Technical Report of
Hydrography and Ocean Sciences 303**



Fisheries and Oceans
Canada

Pêches et Océans
Canada

Canada

Canadian Technical Report of Hydrography and Ocean Sciences

Technical reports contain scientific and technical information of a type that represents a contribution to existing knowledge but which is not normally found in the primary literature. The subject matter is generally related to programs and interests of the Oceans and Science sectors of Fisheries and Oceans Canada.

Technical reports may be cited as full publications. The correct citation appears above the abstract of each report. Each report is abstracted in the data base *Aquatic Sciences and Fisheries Abstracts*.

Technical reports are produced regionally but are numbered nationally. Requests for individual reports will be filled by the issuing establishment listed on the front cover and title page.

Regional and headquarters establishments of Ocean Science and Surveys ceased publication of their various report series as of December 1981. A complete listing of these publications and the last number issued under each title are published in the *Canadian Journal of Fisheries and Aquatic Sciences*, Volume 38: Index to Publications 1981. The current series began with Report Number 1 in January 1982.

Rapport technique canadien sur l'hydrographie et les sciences océaniques

Les rapports techniques contiennent des renseignements scientifiques et techniques qui constituent une contribution aux connaissances actuelles mais que l'on ne trouve pas normalement dans les revues scientifiques. Le sujet est généralement rattaché aux programmes et intérêts des secteurs des Océans et des Sciences de Pêches et Océans Canada.

Les rapports techniques peuvent être cités comme des publications à part entière. Le titre exact figure au-dessus du résumé de chaque rapport. Les rapports techniques sont résumés dans la base de données *Résumés des sciences aquatiques et halieutiques*.

Les rapports techniques sont produits à l'échelon régional, mais numérotés à l'échelon national. Les demandes de rapports seront satisfaites par l'établissement auteur dont le nom figure sur la couverture et la page de titre.

Les établissements de l'ancien secteur des Sciences et Levés océaniques dans les régions et à l'administration centrale ont cessé de publier leurs diverses séries de rapports en décembre 1981. Vous trouverez dans l'index des publications du volume 38 du *Journal canadien des sciences halieutiques et aquatiques*, la liste de ces publications ainsi que le dernier numéro paru dans chaque catégorie. La nouvelle série a commencé avec la publication du rapport numéro 1 en janvier 1982.

Canadian Technical Report of
Hydrography and Ocean Sciences 303

2014

The state of phytoplankton and bacterioplankton
on the Scotian Shelf and Slope:
Atlantic Zone Monitoring Program 1997-2013

by

W.K.W. Li

Ocean and Ecosystem Sciences Division
Maritimes Region
Fisheries and Oceans Canada

Bedford Institute of Oceanography
P.O. Box 1006
Dartmouth, Nova Scotia
Canada B2Y 4A2
E-mail: Bill.Li@dfo-mpo.gc.ca

© Her Majesty the Queen in Right of Canada, 2014

Cat. No. Fs97-18/303E ISBN 978-1-100-25285-8 ISSN 0711-6764 (print version)

Cat. No. Fs97-18/303E-PDF ISBN 978-1-100-25286-5 ISSN 1488-5417 (PDF version)

Correct citation for this publication:

Li, W.K.W. 2014. The state of phytoplankton and bacterioplankton on the Scotian Shelf and Slope: Atlantic Zone Monitoring Program 1997-2013. Can. Tech. Rep. Hydrogr. Ocean. Sci. 303: xx + 140 p.

TABLE OF CONTENTS

| | |
|---|-------|
| LIST OF TABLES | v |
| LIST OF FIGURES | vi |
| ABSTRACT | xvii |
| RÉSUMÉ | xviii |
| PREFACE..... | xix |
| 1. INTRODUCTION | 1 |
| 1.1 AIMS AND STRATEGY | 1 |
| 1.2 BACKGROUND | 1 |
| 1.3 PURPOSE | 2 |
| 2. METHODS | 3 |
| 2.1 SAMPLING AND ANALYSES..... | 3 |
| 2.2 DATA HANDLING | 4 |
| 2.3 DATA PRESENTATION | 5 |
| 2.4 DATA SUMMARY | 6 |
| 2.5 DATA AVAILABILITY | 6 |
| 3. RESULTS | 7 |
| 3.1 TEMPERATURE | 7 |
| 3.2 SALINITY | 7 |
| 3.3 STRATIFICATION (Δ SIGMA-THETA)..... | 7 |
| 3.4 OXYGEN | 7 |
| 3.5 NITRATE..... | 8 |
| 3.6 PHOSPHATE | 8 |
| 3.7 SILICATE..... | 8 |
| 3.8 BACTERIA..... | 8 |
| 3.9 CHLOROPHYLL <i>a</i> | 9 |
| 3.10 <i>SYNECHOCOCCUS</i> | 9 |
| 3.11 PICOEUKARYOTES | 9 |
| 3.12 PICOPHYTOPLANKTON | 10 |
| 3.13 NANOPHYTOPLANKTON..... | 10 |
| 3.14 DIAGNOSTIC PIGMENTS | 11 |

| | |
|--|----|
| 3.15 MICROPHYTOPLANKTON PIGMENTS | 11 |
| 3.16 NANOPHYTOPLANKTON PIGMENTS | 11 |
| 3.17 PICOPHYTOPLANKTON PIGMENTS..... | 12 |
| 3.18 MICROPHYTOPLANKTON FRACTION | 12 |
| 3.19 NANOPHYTOPLANKTON FRACTION | 12 |
| 3.20 PICOPHYTOPLANKTON FRACTION | 13 |
| 3.21 PARTICULATE ORGANIC CARBON..... | 13 |
| 3.22 POC:PON..... | 13 |
| 3.23 BROWNS BANK LINE SUMMARY | 13 |
| 3.24 HALIFAX LINE SUMMARY | 14 |
| 3.25 LOUISBOURG LINE SUMMARY | 14 |
| 3.26 SHELF-WIDE SUMMARY | 15 |
| 3.27 GRAND MEAN SUMMARY | 15 |
| 4. DISCUSSION..... | 16 |
| 4.1 SCIENTIFIC METHOD..... | 16 |
| 4.2 ANNUAL SHELF-WIDE PATTERN | 17 |
| 4.3 SEASONAL PATTERN..... | 18 |
| 4.4 CASE PATTERN..... | 19 |
| 4.5 FOOD WEB IMPLICATIONS | 20 |
| ACKNOWLEDGMENTS | 21 |
| REFERENCES | 22 |
| TABLES | 25 |
| FIGURES..... | 30 |

LIST OF TABLES

- Table 1. List of AZMP Scotian Shelf cruises 1997-2013
- Table 2. Climatological mean values on BBL in spring and fall
- Table 3. Climatological mean values on HL in spring and fall
- Table 4. Climatological mean values on LL in spring and fall
- Table 5. Change in absolute values of variables from 1998 to 2013 on LL in fall

LIST OF FIGURES

Figure 1: Map of the Scotian Shelf and Slope showing AZMP core stations 1 to 7 on Browns Bank Line (BBL), Halifax Line (HL), and Louisbourg Line (LL).

Figure 2: Temperature profiles of time-averaged depth-binned values in the upper 100 m layer on Browns Bank Line in spring and fall at Stations 1-7. Lower right panel is the along transect distribution of time-averaged and depth-averaged temperature.

Figure 3: Temperature time series of depth-averaged values on Browns Bank Line in spring and fall at Stations 1-7. Lower right panel is the along transect distribution of standardised multiyear change in depth-averaged temperature.

Figure 4: Temperature profiles of time-averaged depth-binned values in the upper 100 m layer on Halifax Line in spring and fall at Stations 1-7. Lower right panel is the along transect distribution of time-averaged and depth-averaged temperature.

Figure 5: Temperature time series of depth-averaged values on Halifax Line in spring and fall at Stations 1-7. Lower right panel is the along transect distribution of standardised multiyear change in depth-averaged temperature.

Figure 6: Temperature profiles of time-averaged depth-binned values in the upper 100 m layer on Louisbourg Line in spring and fall at Stations 1-7. Lower right panel is the along transect distribution of time-averaged and depth-averaged temperature.

Figure 7: Temperature time series of depth-averaged values on Louisbourg Line in spring and fall at Stations 1-7. Lower right panel is the along transect distribution of standardised multiyear change in depth-averaged temperature.

Figure 8: Salinity profiles of time-averaged depth-binned values in the upper 100 m layer on Browns Bank Line in spring and fall at Stations 1-7. Lower right panel is the along transect distribution of time-averaged and depth-averaged salinity.

Figure 9: Salinity time series of depth-averaged values on Browns Bank Line in spring and fall at Stations 1-7. Lower right panel is the along transect distribution of standardised multiyear change in depth-averaged salinity.

Figure 10: Salinity profiles of time-averaged depth-binned values in the upper 100 m layer on Halifax Line in spring and fall at Stations 1-7. Lower right panel is the along transect distribution of time-averaged and depth-averaged salinity.

Figure 11: Salinity time series of depth-averaged values on Halifax Line in spring and fall at Stations 1-7. Lower right panel is the along transect distribution of standardised multiyear change in depth-averaged salinity.

Figure 12: Salinity profiles of time-averaged depth-binned values in the upper 100 m layer on Louisbourg Line in spring and fall at Stations 1-7. Lower right panel is the along transect distribution of time-averaged and depth-averaged salinity.

Figure 13: Salinity time series of depth-averaged values on Louisbourg Line in spring and fall at Stations 1-7. Lower right panel is the along transect distribution of standardised multiyear change in depth-averaged salinity.

Figure 14: Density profiles of time-averaged depth-binned values in the upper 100 m layer on Browns Bank Line in spring and fall at Stations 1-7. Lower right panel is the along transect distribution of time-averaged values for the difference between maximum and minimum density ($\sigma_{\theta_{max}} - \sigma_{\theta_{min}}$) in the upper 100m layer.

Figure 15: Density difference ($\sigma_{\theta_{max}} - \sigma_{\theta_{min}}$) time series on Browns Bank Line in spring and fall at Stations 1-7. Lower right panel is the along transect distribution of standardised multiyear change in density difference.

Figure 16: Density profiles of time-averaged depth-binned values in the upper 100 m layer on Halifax Line in spring and fall at Stations 1-7. Lower right panel is the along transect distribution of time-averaged values for the difference between maximum and minimum density ($\sigma_{\theta_{max}} - \sigma_{\theta_{min}}$) in the upper 100m layer.

Figure 17: Density difference ($\sigma_{\theta_{max}} - \sigma_{\theta_{min}}$) time series on Halifax Line in spring and fall at Stations 1-7. Lower right panel is the along transect distribution of standardised multiyear change in density difference.

Figure 18: Density profiles of time-averaged depth-binned values in the upper 100 m layer on Louisbourg Line in spring and fall at Stations 1-7. Lower right panel is the along transect distribution of time-averaged values for the difference between maximum and minimum density ($\sigma_{\theta_{max}} - \sigma_{\theta_{min}}$) in the upper 100m layer.

Figure 19: Density difference ($\sigma_{\theta_{max}} - \sigma_{\theta_{min}}$) time series on Louisbourg Line in spring and fall at Stations 1-7. Lower right panel is the along transect distribution of standardised multiyear change in density difference.

Figure 20: Dissolved oxygen profiles of time-averaged depth-binned values in the upper 100 m layer on Browns Bank Line in spring and fall at Stations 1-7. Lower right panel is the along transect distribution of time-averaged and depth-averaged dissolved oxygen.

Figure 21: Dissolved oxygen time series of depth-averaged values on Browns Bank Line in spring and fall at Stations 1-7. Lower right panel is the along transect distribution of standardised multiyear change in depth-averaged dissolved oxygen.

Figure 22: Dissolved oxygen profiles of time-averaged depth-binned values in the upper 100 m layer on Halifax Line in spring and fall at Stations 1-7. Lower right panel is the along transect distribution of time-averaged and depth-averaged dissolved oxygen.

Figure 23: Dissolved oxygen time series of depth-averaged values on Halifax Line in spring and fall at Stations 1-7. Lower right panel is the along transect distribution of standardised multiyear change in depth-averaged dissolved oxygen.

Figure 24: Dissolved oxygen profiles of time-averaged depth-binned values in the upper 100 m layer on Louisbourg Line in spring and fall at Stations 1-7. Lower right panel is the along transect distribution of time-averaged and depth-averaged dissolved oxygen.

Figure 25: Dissolved oxygen time series of depth-averaged values on Louisbourg Line in spring and fall at Stations 1-7. Lower right panel is the along transect distribution of standardised multiyear change in depth-averaged dissolved oxygen.

Figure 26: Nitrate profiles of time-averaged depth-binned values in the upper 100 m layer on Browns Bank Line in spring and fall at Stations 1-7. Lower right panel is the along transect distribution of time-averaged and depth-averaged nitrate.

Figure 27: Nitrate time series of depth-averaged values on Browns Bank Line in spring and fall at Stations 1-7. Lower right panel is the along transect distribution of standardised multiyear change in depth-averaged nitrate.

Figure 28: Nitrate profiles of time-averaged depth-binned values in the upper 100 m layer on Halifax Line in spring and fall at Stations 1-7. Lower right panel is the along transect distribution of time-averaged and depth-averaged nitrate.

Figure 29: Nitrate time series of depth-averaged values on Halifax Line in spring and fall at Stations 1-7. Lower right panel is the along transect distribution of standardised multiyear change in depth-averaged nitrate.

Figure 30: Nitrate profiles of time-averaged depth-binned values in the upper 100 m layer on Louisbourg Line in spring and fall at Stations 1-7. Lower right panel is the along transect distribution of time-averaged and depth-averaged nitrate.

Figure 31: Nitrate time series of depth-averaged values on Louisbourg Line in spring and fall at Stations 1-7. Lower right panel is the along transect distribution of standardised multiyear change in depth-averaged nitrate.

Figure 32: Phosphate profiles of time-averaged depth-binned values in the upper 100 m layer on Browns Bank Line in spring and fall at Stations 1-7. Lower right panel is the along transect distribution of time-averaged and depth-averaged phosphate.

Figure 33: Phosphate time series of depth-averaged values on Browns Bank Line in spring and fall at Stations 1-7. Lower right panel is the along transect distribution of standardised multiyear change in depth-averaged phosphate.

Figure 34: Phosphate profiles of time-averaged depth-binned values in the upper 100 m layer on Halifax Line in spring and fall at Stations 1-7. Lower right panel is the along transect distribution of time-averaged and depth-averaged phosphate.

Figure 35: Phosphate time series of depth-averaged values on Halifax Line in spring and fall at Stations 1-7. Lower right panel is the along transect distribution of standardised multiyear change in depth-averaged phosphate.

Figure 36: Phosphate profiles of time-averaged depth-binned values in the upper 100 m layer on Louisbourg Line in spring and fall at Stations 1-7. Lower right panel is the along transect distribution of time-averaged and depth-averaged phosphate.

Figure 37: Phosphate time series of depth-averaged values on Louisbourg Line in spring and fall at Stations 1-7. Lower right panel is the along transect distribution of standardised multiyear change in depth-averaged phosphate.

Figure 38: Silicate profiles of time-averaged depth-binned values in the upper 100 m layer on Browns Bank Line in spring and fall at Stations 1-7. Lower right panel is the along transect distribution of time-averaged and depth-averaged silicate.

Figure 39: Silicate time series of depth-averaged values on Browns Bank Line in spring and fall at Stations 1-7. Lower right panel is the along transect distribution of standardised multiyear change in depth-averaged silicate.

Figure 40: Silicate profiles of time-averaged depth-binned values in the upper 100 m layer on Halifax Line in spring and fall at Stations 1-7. Lower right panel is the along transect distribution of time-averaged and depth-averaged silicate.

Figure 41: Silicate time series of depth-averaged values on Halifax Line in spring and fall at Stations 1-7. Lower right panel is the along transect distribution of standardised multiyear change in depth-averaged silicate.

Figure 42: Silicate profiles of time-averaged depth-binned values in the upper 100 m layer on Louisbourg Line in spring and fall at Stations 1-7. Lower right panel is the along transect distribution of time-averaged and depth-averaged silicate.

Figure 43: Silicate time series of depth-averaged values on Louisbourg Line in spring and fall at Stations 1-7. Lower right panel is the along transect distribution of standardised multiyear change in depth-averaged silicate.

Figure 44: Bacteria profiles of time-averaged depth-binned values in the upper 100 m layer on Browns Bank Line in spring and fall at Stations 1-7. Lower right panel is the along transect distribution of time-averaged and depth-averaged bacteria.

Figure 45: Bacteria time series of depth-averaged values on Browns Bank Line in spring and fall at Stations 1-7. Lower right panel is the along transect distribution of standardised multiyear change in depth-averaged bacteria.

Figure 46: Bacteria profiles of time-averaged depth-binned values in the upper 100 m layer on Halifax Line in spring and fall at Stations 1-7. Lower right panel is the along transect distribution of time-averaged and depth-averaged bacteria.

Figure 47: Bacteria time series of depth-averaged values on Halifax Line in spring and fall at Stations 1-7. Lower right panel is the along transect distribution of standardised multiyear change in depth-averaged bacteria.

Figure 48: Bacteria profiles of time-averaged depth-binned values in the upper 100 m layer on Louisbourg Line in spring and fall at Stations 1-7. Lower right panel is the along transect distribution of time-averaged and depth-averaged bacteria.

Figure 49: Bacteria time series of depth-averaged values on Louisbourg Line in spring and fall at Stations 1-7. Lower right panel is the along transect distribution of standardised multiyear change in depth-averaged bacteria.

Figure 50: Chlorophyll *a* profiles of time-averaged depth-binned values in the upper 100 m layer on Browns Bank Line in spring and fall at Stations 1-7. Lower right panel is the along transect distribution of time-averaged and depth-averaged chlorophyll *a*.

Figure 51: Chlorophyll *a* time series of depth-averaged values on Browns Bank Line in spring and fall at Stations 1-7. Lower right panel is the along transect distribution of standardised multiyear change in depth-averaged chlorophyll *a*.

Figure 52: Chlorophyll *a* profiles of time-averaged depth-binned values in the upper 100 m layer on Halifax Line in spring and fall at Stations 1-7. Lower right panel is the along transect distribution of time-averaged and depth-averaged chlorophyll *a*.

Figure 53: Chlorophyll *a* time series of depth-averaged values on Halifax Line in spring and fall at Stations 1-7. Lower right panel is the along transect distribution of standardised multiyear change in depth-averaged chlorophyll *a*.

Figure 54: Chlorophyll *a* profiles of time-averaged depth-binned values in the upper 100 m layer on Louisbourg Line in spring and fall at Stations 1-7. Lower right panel is the along transect distribution of time-averaged and depth-averaged chlorophyll *a*.

Figure 55: Chlorophyll *a* time series of depth-averaged values on Louisbourg Line in spring and fall at Stations 1-7. Lower right panel is the along transect distribution of standardised multiyear change in depth-averaged chlorophyll *a*.

Figure 56: *Synechococcus* profiles of time-averaged depth-binned values in the upper 100 m layer on Browns Bank Line in spring and fall at Stations 1-7. Lower right panel is the along transect distribution of time-averaged and depth-averaged *Synechococcus*.

Figure 57: *Synechococcus* time series of depth-averaged values on Browns Bank Line in spring and fall at Stations 1-7. Lower right panel is the along transect distribution of standardised multiyear change in depth-averaged *Synechococcus*.

Figure 58: *Synechococcus* profiles of time-averaged depth-binned values in the upper 100 m layer on Halifax Line in spring and fall at Stations 1-7. Lower right panel is the along transect distribution of time-averaged and depth-averaged *Synechococcus*.

Figure 59: *Synechococcus* time series of depth-averaged values on Halifax Line in spring and fall at Stations 1-7. Lower right panel is the along transect distribution of standardised multiyear change in depth-averaged *Synechococcus*.

Figure 60: *Synechococcus* profiles of time-averaged depth-binned values in the upper 100 m layer on Louisbourg Line in spring and fall at Stations 1-7. Lower right panel is the along transect distribution of time-averaged and depth-averaged *Synechococcus*.

Figure 61: *Synechococcus* time series of depth-averaged values on Louisbourg Line in spring and fall at Stations 1-7. Lower right panel is the along transect distribution of standardised multiyear change in depth-averaged *Synechococcus*.

Figure 62: Picoeukaryotes profiles of time-averaged depth-binned values in the upper 100 m layer on Browns Bank Line in spring and fall at Stations 1-7. Lower right panel is the along transect distribution of time-averaged and depth-averaged picoeukaryotes.

Figure 63: Picoeukaryotes time series of depth-averaged values on Browns Bank Line in spring and fall at Stations 1-7. Lower right panel is the along transect distribution of standardised multiyear change in depth-averaged picoeukaryotes.

Figure 64: Picoeukaryotes profiles of time-averaged depth-binned values in the upper 100 m layer on Halifax Line in spring and fall at Stations 1-7. Lower right panel is the along transect distribution of time-averaged and depth-averaged picoeukaryotes.

Figure 65: Picoeukaryotes time series of depth-averaged values on Halifax Line in spring and fall at Stations 1-7. Lower right panel is the along transect distribution of standardised multiyear change in depth-averaged picoeukaryotes.

Figure 66: Picoeukaryotes profiles of time-averaged depth-binned values in the upper 100 m layer on Louisbourg Line in spring and fall at Stations 1-7. Lower right panel is the along transect distribution of time-averaged and depth-averaged picoeukaryotes.

Figure 67: Picoeukaryotes time series of depth-averaged values on Louisbourg Line in spring and fall at Stations 1-7. Lower right panel is the along transect distribution of standardised multiyear change in depth-averaged picoeukaryotes.

Figure 68: Picophytoplankton profiles of time-averaged depth-binned values in the upper 100 m layer on Browns Bank Line in spring and fall at Stations 1-7. Lower right panel is the along transect distribution of time-averaged and depth-averaged picophytoplankton.

Figure 69: Picophytoplankton time series of depth-averaged values on Browns Bank Line in spring and fall at Stations 1-7. Lower right panel is the along transect distribution of standardised multiyear change in depth-averaged picophytoplankton.

Figure 70: Picophytoplankton profiles of time-averaged depth-binned values in the upper 100 m layer on Halifax Line in spring and fall at Stations 1-7. Lower right panel is the along transect distribution of time-averaged and depth-averaged picophytoplankton.

Figure 71: Picophytoplankton time series of depth-averaged values on Halifax Line in spring and fall at Stations 1-7. Lower right panel is the along transect distribution of standardised multiyear change in depth-averaged picophytoplankton.

Figure 72: Picophytoplankton profiles of time-averaged depth-binned values in the upper 100 m layer on Louisbourg Line in spring and fall at Stations 1-7. Lower right panel is the along transect distribution of time-averaged and depth-averaged picophytoplankton.

Figure 73: Picophytoplankton time series of depth-averaged values on Louisbourg Line in spring and fall at Stations 1-7. Lower right panel is the along transect distribution of standardised multiyear change in depth-averaged picophytoplankton.

Figure 74: Nanophytoplankton profiles of time-averaged depth-binned values in the upper 100 m layer on Browns Bank Line in spring and fall at Stations 1-7. Lower right panel is the along transect distribution of time-averaged and depth-averaged nanophytoplankton.

Figure 75: Nanophytoplankton time series of depth-averaged values on Browns Bank Line in spring and fall at Stations 1-7. Lower right panel is the along transect distribution of standardised multiyear change in depth-averaged nanophytoplankton.

Figure 76: Nanophytoplankton profiles of time-averaged depth-binned values in the upper 100 m layer on Halifax Line in spring and fall at Stations 1-7. Lower right panel is the along transect distribution of time-averaged and depth-averaged nanophytoplankton.

Figure 77: Nanophytoplankton time series of depth-averaged values on Halifax Line in spring and fall at Stations 1-7. Lower right panel is the along transect distribution of standardised multiyear change in depth-averaged nanophytoplankton.

Figure 78: Nanophytoplankton profiles of time-averaged depth-binned values in the upper 100 m layer on Louisbourg Line in spring and fall at Stations 1-7. Lower right panel is the along transect distribution of time-averaged and depth-averaged nanophytoplankton.

Figure 79: Nanophytoplankton time series of depth-averaged values on Louisbourg Line in spring and fall at Stations 1-7. Lower right panel is the along transect distribution of standardised multiyear change in depth-averaged nanophytoplankton.

Figure 80: Diagnostic pigments time series of near-surface values on Browns Bank Line in spring and fall at Stations 1-7. Lower right panel is the along transect distribution of standardised multiyear change in near-surface diagnostic pigments.

Figure 81: Diagnostic pigments time series of near-surface values on Halifax Line in spring and fall at Stations 1-7. Lower right panel is the along transect distribution of standardised multiyear change in near-surface diagnostic pigments.

Figure 82: Diagnostic pigments time series of near-surface values on Louisbourg Line in spring and fall at Stations 1-7. Lower right panel is the along transect distribution of standardised multiyear change in near-surface diagnostic pigments.

Figure 83: Microphytoplankton pigments time series of near-surface values on Browns Bank Line in spring and fall at Stations 1-7. Lower right panel is the along transect distribution of standardised multiyear change in near-surface microphytoplankton pigments.

Figure 84: Microphytoplankton pigments time series of near-surface values on Halifax Line in spring and fall at Stations 1-7. Lower right panel is the along transect distribution of standardised multiyear change in near-surface microphytoplankton pigments.

Figure 85: Microphytoplankton pigments time series of near-surface values on Louisbourg Line in spring and fall at Stations 1-7. Lower right panel is the along transect distribution of standardised multiyear change in near-surface microphytoplankton pigments.

Figure 86: Nanophytoplankton pigments time series of near-surface values on Browns Bank Line in spring and fall at Stations 1-7. Lower right panel is the along transect distribution of standardised multiyear change in near-surface nanophytoplankton pigments.

Figure 87: Nanophytoplankton pigments time series of near-surface values on Halifax Line in spring and fall at Stations 1-7. Lower right panel is the along transect distribution of standardised multiyear change in near-surface nanophytoplankton pigments.

Figure 88: Nanophytoplankton pigments time series of near-surface values on Louisbourg Line in spring and fall at Stations 1-7. Lower right panel is the along transect distribution of standardised multiyear change in near-surface nanophytoplankton pigments.

Figure 89: Picophytoplankton pigments time series of near-surface values on Browns Bank Line in spring and fall at Stations 1-7. Lower right panel is the along transect distribution of standardised multiyear change in near-surface picophytoplankton pigments.

Figure 90: Picophytoplankton pigments time series of near-surface values on Halifax Line in spring and fall at Stations 1-7. Lower right panel is the along transect distribution of standardised multiyear change in near-surface picophytoplankton pigments.

Figure 91: Picophytoplankton pigments time series of near-surface values on Louisbourg Line in spring and fall at Stations 1-7. Lower right panel is the along transect distribution of standardised multiyear change in near-surface picophytoplankton pigments.

Figure 92: Percent of microphytoplankton pigments (f-micro) time series of near-surface values on Browns Bank Line in spring and fall at Stations 1-7. Lower right panel is the along transect distribution of standardised multiyear change in near-surface f-micro.

Figure 93: Percent of microphytoplankton pigments (f-micro) time series of near-surface values on Halifax Line in spring and fall at Stations 1-7. Lower right panel

is the along transect distribution of standardised multiyear change in near-surface f-micro.

Figure 94: Percent of microphytoplankton pigments (f-micro) time series of near-surface values on Louisbourg Line in spring and fall at Stations 1-7. Lower right panel is the along transect distribution of standardised multiyear change in near-surface f-micro.

Figure 95: Percent of nanophytoplankton pigments (f-nano) time series of near-surface values on Browns Bank Line in spring and fall at Stations 1-7. Lower right panel is the along transect distribution of standardised multiyear change in near-surface f-nano.

Figure 96: Percent of nanophytoplankton pigments (f-nano) time series of near-surface values on Halifax Line in spring and fall at Stations 1-7. Lower right panel is the along transect distribution of standardised multiyear change in near-surface f-nano.

Figure 97: Percent of nanophytoplankton pigments (f-nano) time series of near-surface values on Louisbourg Line in spring and fall at Stations 1-7. Lower right panel is the along transect distribution of standardised multiyear change in near-surface f-nano.

Figure 98: Percent of picophytoplankton pigments (f-pico) time series of near-surface values on Browns Bank Line in spring and fall at Stations 1-7. Lower right panel is the along transect distribution of standardised multiyear change in near-surface f-pico.

Figure 99: Percent of picophytoplankton pigments (f-pico) time series of near-surface values on Halifax Line in spring and fall at Stations 1-7. Lower right panel is the along transect distribution of standardised multiyear change in near-surface f-pico.

Figure 100: Percent of picophytoplankton pigments (f-pico) time series of near-surface values on Louisbourg Line in spring and fall at Stations 1-7. Lower right panel is the along transect distribution of standardised multiyear change in near-surface f-pico.

Figure 101: POC time series of near-surface values on Browns Bank Line in spring and fall at Stations 1-7. Lower right panel is the along transect distribution of standardised multiyear change in near-surface POC.

Figure 102: POC time series of near-surface values on Halifax Line in spring and fall at Stations 1-7. Lower right panel is the along transect distribution of standardised multiyear change in near-surface POC.

Figure 103: POC time series of near-surface values on Louisbourg Line in spring and fall at Stations 1-7. Lower right panel is the along transect distribution of standardised multiyear change in near-surface POC.

Figure 104: POC:PON time series of near-surface values on Browns Bank Line in spring and fall at Stations 1-7. Lower right panel is the along transect distribution of standardised multiyear change in near-surface POC:PON.

Figure 105: POC:PON time series of near-surface values on Halifax Line in spring and fall at Stations 1-7. Lower right panel is the along transect distribution of standardised multiyear change in near-surface POC:PON.

Figure 106: POC:PON time series of near-surface values on Louisbourg Line in spring and fall at Stations 1-7. Lower right panel is the along transect distribution of standardised multiyear change in near-surface POC:PON.

Figure 107: Multiyear change in physical, chemical, and biological variables on Browns Bank Line in spring and fall, ranked from strongest positive change to strongest negative change in common units of standard deviates per year.

Figure 108: Multiyear change in physical, chemical, and biological variables on Halifax Line in spring and fall, ranked from strongest positive change to strongest negative change in common units of standard deviates per year.

Figure 109: Multiyear change in physical, chemical, and biological variables on Louisbourg Line in spring and fall, ranked from strongest positive change to strongest negative change in common units of standard deviates per year.

Figure 110: Multiyear change in physical, chemical, and biological variables on the Scotian Shelf (BBL, HL, LL average) in spring and fall, ranked from strongest positive change to strongest negative change in common units of standard deviates per year.

Figure 111: Multiyear change in physical, chemical, and biological variables on the Scotian Shelf (BBL, HL, LL average) on an annual basis (spring, fall average), ranked from strongest positive change to strongest negative change in common units of standard deviates per year.

ABSTRACT

Li, W.K.W. 2014. The state of phytoplankton and bacterioplankton on the Scotian Shelf and Slope: Atlantic Zone Monitoring Program 1997-2013. Can. Tech. Rep. Hydrogr. Ocean. Sci. 303: xx + 140 p.

Since inception, the Atlantic Zone Monitoring Program has undertaken dedicated oceanographic sampling on the Scotian Shelf and Slope in spring and fall, which regularly includes 7 stations on each of 3 cross-shelf sections extending from near-coast to the off-shelf slope: the Browns Bank Line (BBL) on the Western Scotian Shelf (WSS), the Halifax Line (HL) on the Central Scotian Shelf (CSS), and the Louisbourg Line (LL) on the Eastern Scotian Shelf (ESS). This report presents a detailed record of microbial plankton and their environment at these 21 stations from 1997 to 2013. It provides information on microbes that is supplementary to annual data of the core program reported to the Canadian Science Advisory Secretariat. Descriptions are given for both the climatological mean state and the interannual change for picophytoplankton, nanophytoplankton, bacterioplankton, and associated phytoplankton pigments. Multiyear changes in physical, chemical, and biological variables are compared on the common basis of dimensionless standard anomalies. The result of such comparisons is an ordered sequence of variables ranked by relative change over the period of observation, from the strongest positive change to the strongest negative change. The analysis leads to a proposed canonical model type of climate-induced microbial change in thermohaline stratified nutrient limited oceans, which is characterised by an increasing ecological importance of picophytoplankton in the marine ecosystem.

RÉSUMÉ

Li, W.K.W. 2014. Situation du phytoplancton et du bactérioplancton sur le plateau et le talus néo-écossais : Programme de monitoring de la zone Atlantique 1997-2013. Rapp. tech. can. hydrogr. sci. océan. 303: xx + 140 p.

Depuis sa création, le Programme de monitoring de la zone Atlantique a entrepris un échantillonnage océanographique dédié sur le plateau et le talus néo-écossais au printemps et à l'automne effectué régulièrement à sept stations situées sur chacun des trois transects s'étendant de la proximité du littoral jusqu'au talus : le transect du banc Browns dans l'Ouest du plateau néo-écossais, le transect d'Halifax, au centre du plateau néo-écossais et le transect de Louisbourg dans l'Est du plateau néo-écossais. Ce rapport présente un dossier détaillé sur le plancton microbien et son environnement à ces 21 stations de 1997 à 2013. Il fournit des renseignements sur les microbes qui viennent compléter les données annuelles du programme de base déclarées au Secrétariat canadien de consultation scientifique. Les descriptions sont fournies pour l'état moyen du climat et la variation interannuelle du picophytoplancton, du nanophytoplancton, du bactérioplancton ainsi que des pigments phytoplanctoniques associés. Les variations pluriannuelles des variables physiques, chimiques et biologiques sont comparées sur une base commune d'anomalies adimensionnelles standard. Le résultat de ces comparaisons est une séquence ordonnée de variables classées par variation relative au cours de la période d'observation, de la variation positive la plus forte à la variation négative la plus forte. L'analyse permet d'élaborer une proposition de type de modèle classique de variation microbienne liée au climat dans les eaux océaniques stratifiées en thermoclines limitées en nutriments, qui est caractérisé par l'importance écologique grandissante du picophytoplancton dans l'écosystème marin.

PREFACE

This is one in a set of three reports that document the mean state and interannual change of phytoplankton and bacterioplankton in the ocean waters of Atlantic Canada from program inception to the end of 2013. This report documents the observations made on the Scotian Shelf and Slope in the Atlantic Zone Monitoring Program. The companion reports document observations made in the Labrador Sea in the Atlantic Zone Off-Shelf Monitoring Program¹, and at the Compass Buoy Station in the Bedford Basin Monitoring Program². Together, this set of three reports comprises an integrated technical output of the core non-research component of microbial oceanographic activity in Ocean and Ecosystem Sciences Division aligned to the DFO hierarchical program architecture of Sustainable Aquatic Ecosystems / Oceans Management / Ecosystem Assessments / Aquatic Ecosystems Science.

¹ Li, W.K.W. and W.G. Harrison 2014. The state of phytoplankton and bacterioplankton in the Labrador Sea: Atlantic Zone Off Shelf Monitoring Program 1994-2013. Can. Tech. Rep. Hydrogr. Ocean. Sci. 302: xviii + 181 p.

² Li, W.K.W. 2014. The state of phytoplankton and bacterioplankton at the Compass Buoy Station : Bedford Basin Monitoring Program 1992-2013. Can. Tech. Rep. Hydrogr. Ocean. Sci. 304: xiv + 122p.

This page is intentionally left blank.

1. INTRODUCTION

1.1 AIMS AND STRATEGY

The Atlantic Zone Monitoring Program (AZMP) aims to describe, understand, and forecast the state of the marine ecosystem in the shelf waters of Atlantic Canada, and to quantify the changes in the oceans and the predator-prey relationships of marine resources therein. To this end, the objectives are to collect and analyse biological, chemical, and physical data for characterising and understanding the causes of oceanic variability at the seasonal, interannual, and decadal scales; furthermore, to provide the multidisciplinary data sets that can be used to establish relationships among the biological, chemical, and physical variables (Therriault et al. 1998; Pepin et al. 2005).

In stating this aspirational goal, AZMP has ostensibly adopted an analytic strategy to link cause and effect - a focus on mechanistic oceanographic processes over indeterminate complex environmental history, which, arguably, may be a useful alternative to a synthetic approach for managing ecological futures. With this strategy, AZMP is firmly grounded in phenomenological description of the cumulative oceanographic data collection. The ensuing data reduction and statistical predictions are not explicitly referenced to a null hypothesis in the tradition of hypothetico-deductive science amenable to strong test. Instead, AZMP collects circumstantial evidence that corroborates (or not) the alternative hypothesis of biological change produced by a physical or chemical cause of interest. In this reductionist heuristic, we accept that the reification of statistics constructs the knowledge representation which enables us to understand and explain, at least in a probabilistic manner.

1.2 BACKGROUND

Since inception, AZMP has undertaken dedicated oceanographic sampling on the Scotian Shelf and Slope in spring and fall, which regularly includes, *inter alia*, seven stations on each of three cross-shelf sections extending from near-coast to the off-shelf slope: the Browns Bank Line (BBL) on the Western Scotian Shelf (WSS), the Halifax Line (HL) on the Central Scotian Shelf (CSS), and the Louisbourg Line (LL) on the Eastern Scotian Shelf (ESS). The standard measurements are of conductivity, temperature, pressure, dissolved oxygen, red fluorescence, and photosynthetically active radiation (all in continuous profiling mode); nitrate, phosphate, silicate, and bulk chlorophyll *a* (all from selected discrete depths); mesozooplankton (integrated vertical haul); and Secchi light attenuation when possible.

At these stations, the primary trophic level is solely monitored by the measurement of bulk chlorophyll *a*, which is a cellular biomarker indicating the photosynthetically-competent portion of the plankton community. Although potentially rich in information, this bulk descriptor is nevertheless no more than a high level aggregate of the extensive biological diversity contributing to oxygenic photolithotrophic primary production. To disaggregate the bulk, the component organisms can be classified in a number of different ways: by their systematic names (taxonomy), by their evolutionary lineage (phylogeny), by their metabolism (trophic mode), by their biological attributes and habits (functional traits), by their chemical composition (stoichiometry), or by their physical size (allometry). These and other classifications reflect different facets of life: arguably, no facet is inherently pre-eminent in ecological enquiry; rather, each facet can be more or less useful in particular contexts.

With respect to organism size, the unicellular forms of plankton in the ocean span three orders of magnitude (a thousand-fold) in linear dimension, which is equivalent to nine orders of magnitude (a billion-fold) in volume or mass dimension. By convention (Sieburth et al. 1978), unicellular plankton are grouped into three size classes that are designated by linear dimensions of equivalent spherical diameter but adhere to a nomenclature that corresponds approximately to the live weights of the organisms at the upper end of their range. Thus, picoplankton, nanoplankton, and microplankton occupy the respective size windows of 0.2-2.0 μm , 2-20 μm , and 20-200 μm ; and they have respective live weights of approximately unit picogram, nanogram, and microgram. In each of these microbial size classes, there are members that are primary producers (picophytoplankton, nanophytoplankton, microphytoplankton), members that are primary consumers (bacterioplankton, nanoheterotrophic protists, microheterotrophic protists), and members that are mixotrophic, contributing to both primary and secondary production (Flynn et al. 2013).

1.3 PURPOSE

The present report has a two-fold purpose. First, it describes both the climatological mean state and the interannual change for picophytoplankton, nanophytoplankton, bacterioplankton, and associated phytoplankton pigments at the aforementioned 21 stations over the 17 year period (1997-2013). Second, this report relates the change over time of microbial plankton variables to their physical and chemical environment. This is done by comparing all variables on the common basis of dimensionless standard anomalies. The result of such comparisons is an ordered sequence of variables ranked by relative change over the period of observation, from the strongest positive change to the strongest negative change. This report is a detailed evidentiary record of knowledge

of microbial plankton and their environment in the Scotian Shelf and Slope, against which scientific hypotheses may be tested.

2. METHODS

2.1 SAMPLING AND ANALYSES

Data reported in this document were collected from 30 cruises on the Scotian Shelf and Slope from 1997 to 2013: 15 in the spring, and 15 in the fall (Table 1). The earliest start of a spring cruise was day 91 (April 1, 2005), and the latest start was day 121 (May 1, 2001). On average, the spring cruises started on day 101 ± 8 . The earliest start of a fall cruise was day 264 (September 21, 2013), and the latest start was day 297 (October 24, 2001). On average, the fall cruises started on day 280 ± 12 .

For this report, data were selected only from sampling depths no greater than 100 m, because phytoplankton (though not bacterioplankton) were generally at the threshold of analytical detection at greater depths. Further, data were only selected from stations 1 to 7 of BBL, HL, and LL (Figure 1) because these core stations have been consistently sampled since inception of the program. Together, these 21 stations map the cross-shelf gradient normal to the alongshore gradient from the eastern shelf, to the central shelf, to the western shelf. Nominal geographic coordinates for these stations are available from the AZMP website³.

Standard AZMP method protocols were used to record hydrographic profiles, to collect water samples, and to analyse nutrients and chlorophyll *a* (Mitchell et al. 2002). Particulate organic carbon (POC) and nitrogen (PON) were measured by Perkin Elmer Series II CHNS/O Analyzer 2400. For picophytoplankton (picoeukaryotic algae and *Synechococcus* cyanobacteria), nanophytoplankton, and bacterioplankton, the protocols for fixing and analysing samples by flow cytometry have been previously described (Li and Dickie 2001).

For diagnostic phytoplankton pigments, the method of high performance liquid chromatography (Stuart and Head 2005) was used to distinguish fucoxanthin [Fuco], peridinin [Peri], 19'-butanoyloxyfucoxanthin [But-fuco], 19'-hexanoyloxyfucoxanthin [Hex-fuco], alloxanthin [Allo], chlorophyll *b* [TChl*b*], and zeaxanthin [Zea]. Following Uitz et al. (2006), we apportioned diagnostic pigments to cell size classes as follows:

³ www.meds-sdmm.dfo-mpo.gc.ca/isdm-gdsi/azmp-pmza/hydro/azmp_pmza_coordinates_coordonnees-eng.csv

Microphytoplankton pigments (mg m^{-3})

$$\text{MICROPIG} = 1.41[\text{Fuco}] + 1.41[\text{Peri}]$$

Nanophytoplankton pigments (mg m^{-3})

$$\text{NANOPIG} = 1.27[\text{Hex-fuco}] + 0.35[\text{But-fuco}] + 0.60[\text{Allo}]$$

Picophytoplankton pigments (mg m^{-3})

$$\text{PICOPIG} = 1.01[\text{TChl}b] + 0.86[\text{Zea}]$$

Thus the weighted sum of diagnostic pigments (mg m^{-3}) is given by:

$$\text{DIAGPIG} = \text{MICROPIG} + \text{NANOPIG} + \text{PICOPIG}$$

And the fractional contribution of each size class to the sum is given by:

$$\text{FMICRO} = \text{MICROPIG}/\text{DIAGPIG}$$

$$\text{FNANO} = \text{NANOPIG}/\text{DIAGPIG}$$

$$\text{FPICO} = \text{PICOPIG}/\text{DIAGPIG}$$

It should be noted that since we did not undertake a local calibration of this general method to obtain custom weighting coefficients for Scotian Shelf phytoplankton, there may be some uncertainty in the quantitative assignment of the 7 pigments to the 3 size classes.

2.2 DATA HANDLING

At the time of collection, each water sample was assigned a unique 6-digit identification number that served to link all variously-measured physical, chemical, and biological variables to the date, time, geographic location, and depth of sampling. Metadata included cruise number and station name.

Hydrographic data (temperature, salinity, pressure, density, oxygen) were extracted from continuous vertical profiles to match the actual depths from which water samples were collected. A measure of stratification (Δ sigma-theta) was calculated by taking the arithmetic difference between maximum and minimum values of water density (sigma-theta) in the upper 100 m.

For nutrients, chlorophyll *a*, and microbial plankton, samples were nominally collected at 10 m depth intervals from the surface to 100 m. For POC/PON and phytoplankton pigments, only near-surface samples were collected. All data were compiled and consolidated into a single flat file. For ease of manipulation, all data (which were pressure-referenced) were assigned to 10 m depth bins using the Microsoft

Excel built-in function “mround”. Data manipulations were handled using an Excel pivot table created from the flat file.

2.3 DATA PRESENTATION

2.3.1 Climatological mean state

2.3.1.1 Vertical distribution: For each variable at each station during each season, we plot the 10 m depth-resolved vertical profile by taking the average of all appropriate measurements within each depth-bin made over the entire 17-year time series. POC/PON and phytoplankton pigment variables are excluded because these were only sampled near-surface.

2.3.1.2 Cross-shelf gradient: For each section (BBL, HL, LL) during each season, we plot the 7-station gradient from near-coast to off-shelf slope by taking the depth-average (0-100 m) of each time-averaged variable (from 2.3.1.1). POC/PON and phytoplankton pigment variables are excluded because these were only sampled near-surface.

2.3.2 Interannual change

2.3.2.1 Time series: For each variable at each station during each season, we plot the 17-year time series of the depth-average (0-100 m) of each variable, or the time series of the near-surface value for POC/PON and phytoplankton pigment variables. For plankton and pigment variables, a logarithmic transform was first applied to the measurements. The first-order multiyear trend is indicated by simple linear regression in the plots by a dashed line.

2.3.2.2 Intensity of change: The interannual departure from climatological mean state for each variable is reported using the dimensionless standardised (or normalised) anomaly, as follows. From each time series (in 2.3.2.1), the mean (M) and standard deviation (S) are calculated over the entire period. The standard anomaly A for any year y of the measured value X is given by $A_y = (X_y - M)/S$. Thus, for y extending over the entire period of observation, the intensity of interannual change is reported as the slope of the linear regression of A_y on y . We refer to this quantity as the “slope of change” over time, and because it has the same units (standard deviates per year) for all variables, it is a common basis for comparison across physics, chemistry, and biology. For each variable at each station during each season, we plot the “slope of change” over time in cross-shelf gradients on each hydrographic section (BBL, HL, LL).

2.4 DATA SUMMARY

For each hydrographic section at each season, we calculated the average value of the “slope of change” over time across the 7 stations for all variables. We then ranked the variables in descending order from the most strongly positive change to the most strongly negative change. Thus, variables close to each other in rank reflect a degree of similarity in their temporal dynamics. Vice versa, variables far apart from each other in rank with opposite signs of change reflect a degree of inverse similarity. This allows the visualisation of any coherence in the manner in which suites of these variables changed over time.

For a higher level of system aggregation to represent the seasonal pattern over the Scotian Shelf as a whole, we averaged the “slope of change” for variables, combining the 3 hydrographic sections by season, and then ranked the shelf-wide spring pattern and fall pattern separately. Finally, at the highest level of aggregation possible with the dataset, we averaged the shelf-wide “slope of change” combining spring and fall, giving a grand mean that was then ranked in the same manner, describing the annual shelf-wide pattern.

2.5 DATA AVAILABILITY

The data in this report are available from the BioChem database maintained by DFO Integrated Science Data Management⁴. The data have also been submitted to the International Council for the Exploration of the Sea (ICES) Working Group on Phytoplankton and Microbial Ecology (WGMPE)⁵, as well as the UNESCO Intergovernmental Oceanographic Commission (IOC) International Group for Marine Ecological Time Series (IGMETS)⁶.

⁴ <http://www.meds-sdmm.dfo-mpo.gc.ca/biochem/biochem-eng.htm>

⁵ <http://wgpme.net>

⁶ <http://igmets.net>

3. RESULTS

The description of salient results is based on Figures 2-106 and Tables 2-4.

3.1 TEMPERATURE

[Figures 2-7, Tables 2-4]

Temperature is everywhere lower near-coast than off-shelf, except at LL in the fall. Temperature increases from east to west (LL<HL<BBL). Needless to note, temperature is lower in spring than in fall. Slopes of change in temperature are generally positive everywhere, and generally more positive in the fall than in the spring.

3.2 SALINITY

[Figures 8-13, Tables 2-4]

Salinity is everywhere lower near-coast than off-shelf. Salinity increases from east to west (LL<HL<BBL). Salinity is generally lower in spring than in fall at BBL, generally the same in spring and fall at HL, but generally lower in fall than in spring at LL. Slopes of change in salinity are generally positive in both spring and fall at BBL and HL. In contrast, the slopes are generally negative in both spring and fall at LL.

3.3 STRATIFICATION (Δ SIGMA-THETA)

[Figures 14-19, Tables 2-4]

Stratification is everywhere weaker in spring than in fall. Slopes of change in stratification are generally negative everywhere in spring; but they are positive everywhere in fall without exception. This observation of increasing fall stratification over the entire survey area is an important phenomenon that will be shown to be associated with decreasing depth-averaged nutrient concentrations and selective change in plankton variables.

3.4 OXYGEN

[Figures 20-25, Tables 2-4]

Dissolved oxygen concentration is (unsurprisingly) everywhere higher in spring (when it is cold) than in fall (when it is warm). Depth-averaged and station-averaged oxygen decreases from the east transect to the west transect (LL>HL>BBL). Oxygen decreases from near-coast to off-shelf at BBL and HL, but not at LL. Slopes of change in oxygen are generally positive in both spring and fall everywhere, except that they are negative at BBL in fall.

3.5 NITRATE

[Figures 26-31, Tables 2-4]

In spring, there is residual nitrate in the surface layer; in fall, the surface is depleted but concentrations at depth are higher in fall than in spring. Depth-averaged and station-averaged nitrate increases from the east transect to the west transect (LL<HL<BBL). In spring, depth-averaged nitrate is lower near-coast than off-shelf at BBL and HL, but not at LL; but in fall, a cross-shelf nitrate gradient is not evident on any of the sections. Slopes of change in nitrate are generally negative: they are strongly negative at LL in spring and at BBL in fall; with some exceptions, the slope of nitrate change is positive at BBL in spring.

3.6 PHOSPHATE

[Figures 32-37, Tables 2-4]

Phosphate is not depleted anywhere, but it is lower in the surface than at depth. This vertical distribution is more accentuated in fall than in spring such that surface concentrations are lower in fall than in spring, and vice versa, deep concentrations are higher in fall than in spring. Depth-averaged concentrations are not greatly different between spring and fall. At BBL and HL, there is a negative phosphate gradient from near-coast to off-shelf in fall, but not in spring. With a single exception (HL1), all 20 other stations show a negative slope of phosphate change in fall.

3.7 SILICATE

[Figures 38-43, Tables 2-4]

Silicate, like phosphate, is not depleted anywhere, but it is lower in the surface than at depth. However, in contrast to phosphate, the depth-averaged concentrations of silicate are higher in fall than in spring. The cross-shelf patterns of silicate and phosphate are the same. Thus, at BBL and HL, there is a negative silicate gradient from near-coast to off-shelf in fall, but not in spring. Slopes of silicate change are generally negative everywhere in fall. Moreover, there is also strong negative silicate change at LL in spring; in contrast, there is strong positive silicate change at BBL in spring.

3.8 BACTERIA

[Figures 44-49, Tables 2-4]

Bacteria generally display a fairly uniform vertical distribution on the shelf in spring, but with fall stratification, a pronounced structure is developed in which bacterial concentrations are increased greatly in the upper 50 m. This vertical seasonal difference

is less evident at slope stations. Depth-averaged concentrations are generally higher in fall than in spring, and generally higher in the west than the east (LL<HL<BBL). Cross-shelf gradients are pronounced only at BBL, where there is an increase from near-coast to off-shelf in spring, but a decrease in the same direction in fall. Slopes of bacterial change are generally positive everywhere; they are especially strong and consistently positive at HL and LL in fall.

3.9 CHLOROPHYLL *a*

[Figures 50-55, Tables 2-4]

Chlorophyll *a*, in distinct contrast to bacteria, display greater vertical structure in spring than in fall. Depth-averaged concentrations are much higher in spring than in fall, averaging a 4-fold seasonal difference at BBL, a 5-fold difference at HL, and a 9-fold difference at LL. Cross-shelf gradients of depth-averaged chlorophyll are not remarkable. Slopes of chlorophyll change are generally positive in spring, and generally negative in fall (except at the offshore portion of HL).

3.10 SYNECHOCOCCUS

[Figures 56-61, Tables 2-4]

Synechococcus, a cyanobacterium, constitutes the prokaryotic component of the photosynthetic picoplankton in these waters. Similar to heterotrophic bacteria, *Synechococcus* has a fairly uniform vertical distribution in spring, but a strongly stratified vertical distribution in fall. Depth-averaged concentrations are very much higher in fall than in spring, being about 40-fold different between seasons at BBL and HL, and about 90-fold different at LL.

In the spring surveys, stations with a depth-averaged temperature of less than 5°C have much lower concentrations of *Synechococcus* than stations with a depth-averaged temperature of greater than 5°C (i.e. BBL5, BBL6, BBL7, HL6, HL7). The difference in *Synechococcus* concentration between high and low temperature stations is about 3-fold at BBL, and about 7-fold at HL. It can be noted that all stations at LL in spring are low in both temperature and *Synechococcus*.

Slopes of change in *Synechococcus* are generally positive in both seasons, with a weak exception at the offshore portion of BBL in fall. Notably, a strong increase in *Synechococcus* is evident all through LL in fall, similar to the pattern for heterotrophic bacteria.

3.11 PICOEUKARYOTES

[Figures 62-67, Tables 2-4]

Picoeukaryotic algae constitute the polyphyletic eukaryotic component of the photosynthetic picoplankton. As with *Synechococcus*, picoeukaryotes have a fairly uniform vertical distribution in spring, but a strongly stratified vertical distribution in fall. Depth-averaged concentrations are likewise higher in fall than in spring, but not as many-fold different. For picoeukaryotes, the seasonal difference is about 3-fold to 9-fold. In spring, there are more picoeukaryotes than *Synechococcus* (2- to 4-fold more), but in fall, the balance is reversed such that there are more *Synechococcus* than picoeukaryotes (3- to 7-fold more).

Slopes of change in picoeukaryotes are generally positive in both seasons, with a weak exception at the offshore portion of HL. Notably, a strong increase in picoeukaryotes is evident all through LL in fall, similar to the patterns for both heterotrophic bacteria and *Synechococcus* noted above.

3.12 PICOPHYTOPLANKTON

[Figures 68-73, Tables 2-4]

Picophytoplankton is simply the sum of the two photosynthetic picoplankton components: *Synechococcus* (Section 3.10) and picoeukaryotic algae (Section 3.11). It is useful to combine the 2 components into a single ataxonomic size class because the polyphyletic members can be considered as one ecological functional group. Although the patterns over depth, space, and time can, in principle, be deduced for the whole from the parts, we have carried out the calculations as if picophytoplankton were a separate entity for the sake of checking internal consistency in the dataset.

As a size class, picophytoplankton are more abundant in fall than in spring (7- to 38-fold more). There are more picophytoplankton off-shelf than near-coast, a pattern most evident in spring, but also to some extent in fall. Slopes of change in picophytoplankton are generally positive. All through LL, the increase of picophytoplankton in fall is remarkably evident.

3.13 NANOPHYTOPLANKTON

[Figures 74-79, Tables 2-4]

Nanophytoplankton in the upper 50 m are generally more abundant in fall than in spring, but the seasonal difference in depth-averaged concentrations are not pronounced, being no more than 1.7-fold higher in fall than in spring. There is no evident gradient from east-to-west alongshore (LL~HL~BBL) nor from near-coast to off-shelf. Slopes of change in nanophytoplankton are weak and do not indicate any notable pattern by season or by place.

3.14 DIAGNOSTIC PIGMENTS

[Figures 80-82, Tables2-4]

The weighted sum of diagnostic pigments (DIAGPIG) is a quasi-measure of total phytoplankton chlorophyll *a*. The quasi-measure is based on the weighted contribution of 7 photosynthetic pigments used as chemotaxonomic markers for constituent members of the phytoplankton community. In principle, the salient patterns of DIAGPIG should corroborate those of chlorophyll *a*. However, because DIAGPIG are concentrations of near-surface pigments, exact matches to the patterns for chlorophyll *a* averaged over a 100 m depth range (Section 3.9) are not expected.

DIAGPIG are everywhere higher in spring than in fall (about 2- to 4-fold), and generally higher near-coast than off-shelf (especially in fall). As with chlorophyll *a*, the slopes of change in DIAGPIG are generally positive in spring, and negative in fall. In fact, the general decrease of DIAGPIG in fall is even more pronounced than that of chlorophyll *a*, perhaps indicating that change in phytoplankton is stronger near the ocean surface and that this change is attenuated when averaged to depth.

3.15 MICROPHYTOPLANKTON PIGMENTS

[Figures 83-85, Tables2-4]

MICROPIG is a pigment-based estimate of the biomass of bacillariophytes and dinophytes (which are generally in the microplankton size class), but it is a biased estimator because fucoxanthin is also present in some prymnesiophytes, chrysophytes, pelagophytes, raphidophytes, and bolidophytes (which are generally in the nanoplankton and picoplankton size classes). A correction can be applied to reduce this bias (Devred et al. 2011), but we have not done so because the method, although based on reasonable assumptions, only corrects for nanoplankton but not picoplankton. The Devred method has yet to be validated with taxonomic counts, but it would be a challenging task since gene sequences of Scotian Shelf picoplankton indicate extensive phylogenetic diversity that includes pelagophytes and bolidophytes (Dasilva et al. 2014).

MICROPIG is everywhere much higher in spring than in fall (about 4- to 9-fold), and generally higher near coast than off-shelf (especially in fall). Slopes of change in MICROPIG are generally positive in spring, and almost all strongly negative in fall.

3.16 NANOPHYTOPLANKTON PIGMENTS

[Figures 86-88, Tables2-4]

NANOPIG is a pigment-based estimate of the biomass of nanophytoplankton in near-surface waters. Because of the aforementioned uncertainties in assigning chemotaxonomic markers to cell size classes, and because of low sampling intensity, NANOPIG may at best provide corroboration to the patterns indicated by the more complete dataset of nanophytoplankton abundance (Section 3.13). NANOPIG is everywhere higher in fall than in spring. There is a pronounced cross-shelf increase of NANOPIG at BBL and HL in spring, but the gradient seems to be reversed in fall. Slopes of change in NANOPIG are generally positive in spring, and generally negative in fall.

3.17 PICOPHYTOPLANKTON PIGMENTS

[Figures 89-91, Tables2-4]

PICOPIG is a pigment-based estimate of the biomass of picophytoplankton in near-surface waters. At best, it corroborates the patterns indicated by picophytoplankton abundance (Section 3.12). PICOPIG is generally higher in fall than in spring. There is a cross-shelf increase of PICOPIG in spring, but the gradient reverses in fall. Slopes of change in PICOPIG are generally positive in both spring and fall, with an exception in the offshore portion of HL – an echo of the trend in piceokaryote abundance there (Section 3.11).

3.18 MICROPHYTOPLANKTON FRACTION

[Figures 92-94, Tables2-4]

FMICRO is the fraction (or percentage) of total phytoplankton biomass (expressed as chlorophyll *a*) ascribed to the microplankton size class, assuming that all (and none but) fucoxanthin and peridinin are found in this class. FMICRO is much higher in spring (71-98%) than in fall (22-48%). FMICRO decreases from near-coast to off-shelf in both spring and fall, except at LL in spring when it remains high (94-98%) across the section. Slopes of change in FMICRO are almost all negative in both spring and fall, and most strongly negative at LL in fall.

3.19 NANOPHYTOPLANKTON FRACTION

[Figures 95-97, Tables2-4]

FNANO is the fraction (or percentage) of total phytoplankton biomass (expressed as chlorophyll *a*) ascribed to the nanoplankton size class, assuming that all (and none but) 19²-butanoyloxyfucoxanthin, 19³-hexanoyloxyfucoxanthin, and alloxanthin are found in this class. Essentially, the patterns and trends for FMICRO and FNANO are mirror opposites. FNANO is much higher in fall (28-49%) than in spring (1-20%). FNANO increases from near-coast to off-shelf in both spring and fall, except at LL in spring

when it remains low (1-4%) across the section. Slopes of change in FNANO are almost all positive in spring, but there is a mix of positive and negative slopes in the fall.

3.20 PICOPHYTOPLANKTON FRACTION

[Figures 98-100, Tables2-4]

FPICO is the fraction (or percentage) of total phytoplankton biomass (expressed as chlorophyll *a*) ascribed to the picoplankton size class, assuming that all (and none but) chlorophyll *b* and zeaxanthin are found in this class. FPICO is higher in fall (22-37%) than in spring (1-11%). There is no cross-shelf trend in FPICO either in spring or in fall. Slopes of change in FPICO are almost all positive. Most remarkably, not only is FPICO increasing at every station on LL in both spring and fall, but the relative rate of change in fall is approximately twice (2 ± 0.8) the relative rate of change in spring at every LL station.

3.21 PARTICULATE ORGANIC CARBON

[Figures 101-103, Tables2-4]

Particulate organic carbon (POC) measures both living and non-living carbon in seston. Dynamic processes for the two pools are very different. Nevertheless, a strong seasonal difference is evident, with spring values being at least twice as large as fall values. There is more POC near-coast than off-shelf in fall. Slopes of change in POC are mostly positive on HL, but mixed on BBL and LL.

3.22 POC:PON

[Figures 104-106, Tables2-4]

POC:PON is the stoichiometric molar ratio of organic carbon to organic nitrogen in seston. Its value on the Scotian Shelf is different from the historical Redfield ratio for living phytoplankton ($6.6 \text{ molC molN}^{-1}$), as expected because of non-phytoplankton components in the seston, and also because elemental ratios are now understood to emerge from complex nested hierarchical processes. On averaging over stations, the climatological means of POC:PON have a value of 8.2 ± 0.8 in spring, and a value of 7.8 ± 0.5 in fall. Slopes of change in POC:PON do not have a remarkable pattern.

3.23 BROWNS BANK LINE SUMMARY

[Figure 107]

A summary of the multiyear changes at BBL in spring and in fall is given in Figure 107 by ranking the variables from the strongest positive change to the strongest negative change.

3.23.1 Spring

Increasing small plankton variables (PICOPIG, NANOPIG) are juxtaposed against a decreasing large plankton variable (FMICRO) and decreasing stratification.

3.23.2 Fall

Increasing temperature, stratification, and small plankton variables (PICOPIG, FPICO) are juxtaposed against decreasing large plankton variables (MICROPIG, FMICRO) and nutrients.

3.24 HALIFAX LINE SUMMARY

[Figure 108]

A summary of the multiyear changes at HL in spring and in fall is given in Figure 108 by ranking the variables from the strongest positive change to the strongest negative change.

3.24.1 Spring

Increasing small plankton variables (PICOPIG, NANOPIG) are juxtaposed against decreasing stratification and a large plankton variable (FMICRO).

3.24.2 Fall

Increasing stratification and a small plankton variable (BACTERIA) are juxtaposed against decreasing diagnostic pigments and microplankton pigments.

3.25 LOUISBOURG LINE SUMMARY

[Figure 109]

A summary of the multiyear changes at LL in spring and in fall is given in Figure 109 by ranking the variables from the strongest positive change to the strongest negative change.

3.25.1 Spring

Increasing small plankton variables (NANOPIG, FPICO, FNANO, PICOPIG, PICOEUK, PICOPHYTO) are juxtaposed against decreasing nutrients and a large plankton variable (FMICRO).

3.25.2 Fall

Increasing small plankton variables (FPICO, PICOPHYTO, SYNECHO, PICOEUK, BACTERIA, PICOPIG), increasing stratification and temperature are all juxtaposed against decreasing large plankton variables (MICROPIG, FMICRO).

3.26 SHELF-WIDE SUMMARY

[Figure 110]

A summary of the multiyear shelf-wide changes in spring and in fall is given in Figure 110 by ranking the variables (average BBL, HL, LL) from the strongest positive change to the strongest negative change.

3.26.1 Spring

Increasing small plankton variables (NANOPIG, PICOPIG, FPICO, FNANO, PICOPHYTO) are juxtaposed against a decreasing large plankton variable (FMICRO) and decreasing stratification.

3.26.2 Fall

Increasing stratification, temperature, and small plankton variables (FPICO, BACTERIA, PICOPHYTO) are juxtaposed against decreasing large plankton variables (MICROPIG) and nutrients.

3.27 GRAND MEAN SUMMARY

[Figure 111]

A grand mean summary of the multiyear changes on an annual shelf-wide basis is given in Figure 111. At this highest level of data aggregation, the system shows positive change in all the small plankton variables (FPICO, PICOPIG, PICOPHYTO, PICOEUK, BACTERIA, SYNECHO) and positive change in the physical drivers (temperature, stratification), all juxtaposed against negative change in the large plankton variables (FMICRO, MICROPIG) and negative change in the nutrients.

4. DISCUSSION

4.1 SCIENTIFIC METHOD

This report presents a detailed evidentiary record of microbial plankton and their environment in the Scotian Shelf and Slope from 1997 to 2013. It provides information on microbes that is supplementary to annual data of the core program reported to the Canadian Science Advisory Secretariat (Hebert et al. 2013; Johnson et al. 2013). In this respect, the microbial data broaden AZMP ecosystem considerations to include all size classes of the phytoplankton and also the prokaryotic secondary producers. Amongst the small number of long-term oceanographic observation programs in the world carried out in support of ecosystem assessment and management, AZMP is one of the very few that includes direct measurements in explicit recognition of the new microbial paradigm (now 40-years old) of the ocean's food web (Pomeroy 1974).

The shelf-wide distribution of selected properties of the phytoplankton in the AZMP region is variously monitored: by direct sampling (*in vitro* and *in vivo* red fluorescence), by satellite remote sensing (ocean colour), and by Continuous Plankton Recorder on ships of opportunity (Phytoplankton Colour Index, diatoms, dinoflagellates). Due to different scales of sampling (Head and Pepin 2010), and importantly, due to differences in the fundamental characteristics of the measured variables, the results are not redundant, but are complementary. As Cullen (1982) once remarked: "It should not be assumed, *a priori* that fluorescence represents chlorophyll, chlorophyll represents biomass, or even that biomass represents acceptable food for herbivores".

To put a finer point on this important distinction, we note how, even within the unitary field of oceanography, there are differences amongst the sub-disciplines on how phytoplankton are tokened. To physical oceanographers, phytoplankton may be synonymous with fluorescence: the release of photons as electrons return to ground state after excitation. To optical oceanographers, phytoplankton may be synonymous with visible spectral radiometric signatures. To chemical oceanographers, phytoplankton may be synonymous with $C_{55}H_{72}O_5N_4Mg$ (chlorophyll *a*), a diagnostic molecule that can be measured with great analytical precision by absorption or chromatography when disaggregated from its native state in a test tube. To fisheries oceanographers, phytoplankton may be synonymous with green colouration on a silk mesh towed behind a vessel-of-opportunity. However, to biological oceanographers, phytoplankton are known in a myriad of ways (Section 1.2) representing the two great classes of biological processes: matter and energy transfer on the one hand, and the maintenance, transmission, and modification of genetically based information on the other hand (Eldredge 1986). The nexus of this dual hierarchy in ecology (elements to

molecules to organelles to organisms to populations to communities to meta-communities) and in evolution (genes to transcripts to organisms to species to phyla to domain) is the individual free-living organismal entity. To view mechanistic AZMP at this nexus of individual entities of algae and bacteria affirms the complementary of reductionism and organicism (Hull 1974).

Towards meeting the expressed goals and objectives of AZMP (Section 1.1), we offer in this report the multidisciplinary data sets that can be used to establish relationships among the organismal (phytoplankton and bacteria), chemotaxonomic (diagnostic pigments), chemical (nutrients and oxygen), and physical (temperature, salinity, stratification) variables. We use the method of hierarchical coarse-graining to progressively enlarge the scale of analysis to discern macroscopic pattern (Li and López-Urrutia 2013). Starting with point measurements in space and time, we progressively averaged over depth, over stations, over multi-station transects, over seasons, and over years. Phytoplankton and bacterioplankton interact at the short scales of microbial generation times and cellular distances which are below the detection capabilities of AZMP; but temporal and spatial averaging to increasingly large scales allows the detection of climate-related signals (Li et al. 2006; Li 2009).

Notwithstanding the short length of the time series, the relationships amongst variables presented in this report offer new insight on changes in the state of the Scotian Shelf ecosystem (Frank et al. 2011, 2013; Greene 2013). However, we note carefully that phenomenological ecology offers, at best, circumstantial evidence which corroborates one particular alternative hypothesis, but does not and cannot constitute a strong test of a null hypothesis (Strong 1980). Essentially, in ecological systems, causes are usually neither severally necessary nor jointly sufficient for their effects (Hull 1974). This means that although we may be able to explain (in statistical form), we may not always be able to predict. This is an ineluctable constraint.

4.2 ANNUAL SHELF-WIDE PATTERN

At the highest level of our data aggregation (Figure 111), we discern a multiyear, shelf-wide, annual-based increase in temperature, which (given the small change in salinity) leads to a logical deduction of increased stratification⁷, based on necessary and sufficient physical cause. From increasing stratification, a logical induction can be made of decreasing nutrients, which is confirmed in this system by the evidence, implying that (at this level of time and space integration) vertical water column

⁷ Note that it is only on the Louisbourg Line that salinity has a negative rate of multiyear change that would contribute to increased stratification (Figure 109).

processes are sufficient to characterise the nutrient field, without the necessity of other factors, for example horizontal physical processes. Finally, a logical abduction can be made that increasing picoplankton together with decreasing microplankton⁸ are sufficiently (but not necessarily) caused by decreasing nutrients, on the accepted premise that picoplankton can thrive on regenerated nutrients but that microplankton depend on new nutrients. This inference seems (to us) to offer the best explanation for the observed changes in plankton and nutrients. In principle, one might infer a reversal in cause-and-effect (i.e. top-down control of nutrients by phytoplankton), but increased stratification is a sufficient cause for decreased nutrients, and thus a more parsimonious explanation.

Parenthetically, given the strong counter-trends for picoplankton and microplankton together with a near-neutral trend for nanoplankton, a logical deduction can be made that any bulk descriptor of phytoplankton biomass should have a weak or neutral trend. This is confirmed by chlorophyll *a*⁹. Any regional scale analysis of multiyear phytoplankton change in the Scotian Shelf that is based on bulk properties *in situ* (or their remote-sensing proxies) would, by definition, be blind to the underlying trends of the parts which make up the whole.

4.3 SEASONAL PATTERN

In fact, the underlying trends are also seasonally different, increasing the complexity of causal relationships. Here we consider the shelf-wide patterns separately for spring and for fall (Figure 110).

In spring, almost all of the phytoplankton biomass can be attributed to the large size class (FMICRO = $87 \pm 8\%$), with only residual portions in the smaller size classes (FNANO = $6 \pm 5\%$; FPICO = $6 \pm 4\%$). Therefore, in spring, changes in community biomass are essentially driven by microplankton. Notwithstanding the dominance of microplankton biomass, there is a multiyear trend of spring picoplankton increase, even in the face of a multiyear trend of spring stratification decrease. One might therefore suggest that stratification increase is not a necessary condition for picoplankton increase during the time of year when nutrients have not yet been depleted from the surface; instead, increasing temperature may be a sufficient condition. Nevertheless, though the

⁸ Coincident with this microplankton decrease, the annual trend for the Phytoplankton Colour Index derived from Continuous Plankton Recorder is also negative in the Eastern Scotian Shelf over these years (Frank et al. 2011).

⁹ The trend for DIAGPIG also confirms the deduction but the slope of change is noticeably negative (Figure 111), an unsurprising result since this variable is less reliable than chlorophyll *a* because of sampling and methodological issues discussed previously.

relative rate of multiyear picoplankton increase is noteworthy as an organismal response to spring climate change, the impact of picoplankton to ecosystem function measured in absolute terms presumably remains extremely low in spring.

In fall, by contrast, there is a much more equitable distribution of biomass amongst the size classes ($33 \pm 7\%$, $39 \pm 6\%$, $29 \pm 4\%$ respectively). Therefore, in fall, community biomass changes are effectively driven by changes in all size classes. The strong multiyear fall increase in temperature and stratification¹⁰ can be construed as sufficient cause for fall decreases in nutrients, bulk phytoplankton biomass¹¹ (chlorophyll *a*, diagnostic pigments), and microphytoplankton; together with fall increases in picophytoplankton (*Synechococcus* and picoeukaryotes) and bacteria. We suggest that this fall pattern constitutes the canonical model type of climate-induced microbial change in thermohaline-stratified nutrient-limited oceans.

4.4 CASE PATTERN

We illustrate an actualisation of this model type using a case group comprising the 7 stations on LL representing the Eastern Scotian Shelf. The relative rate of multiyear change expressed as standard deviates per year (Figure 109) is a useful statistical device that allows common comparison amongst variables, between seasons, and amongst regions. However, when there is no need to adjust seasonal and regional responses to their norms, we can use a more intuitive indicator of change based on variables expressed in their native absolute measurement units, comparing them at the start (1998) and end (2013) of the time series. In Table 5, for variables that have increased, we indicate the ratio of end to start values; vice versa, for variables that have decreased, we indicate the inverse ratio of start to end values to emphasise mirror symmetry.

In this exemplar case, temperature has risen measurably by 1.2-fold (7.03 to 8.33 °C), and stratification has increased even more, by 1.4-fold (1 sigma-theta unit over a 100 m water column). Picophytoplankton abundance has almost tripled (19 to 54 thousand cells per milliliter), which is mirrored by the almost tripled decrease of microplankton pigment concentration (0.36 to 0.13 mg m⁻³). As a result, the distribution of phytoplankton biomass has shifted from microplankton dominance (47%) in 1998 to picoplankton dominance (39%) in 2013, with the consequence that total biomass has declined 1.6-fold (0.59 to 0.37 mg chlorophyll per m⁻³). Heterotrophic bacteria have increased 1.3-fold (4.8 to 6.2 hundred thousand cells per

¹⁰ Also noted by Frank et al. (2011) in their Figure S11.

¹¹ Also evident in Figure S12 of Frank et al. (2011) as a decrease in the fall season Phytoplankton Colour Index in the years after the mid 1990's. We are aware that PCI and chlorophyll *a* may bear little significant relationship to each other in the fall season at other times and places (Batten et al. 2003).

milliliter). The best explanation that can be abductively inferred from the realised plankton changes is that temperature and stratification of nutrients are the proximate causes, neither severally necessary nor jointly sufficient.

4.5 FOOD WEB IMPLICATIONS

In principle, an intensification of the microbial loop caused by higher abundance of picoplankton (*Synechococcus*, picoeukaryotic algae, heterotrophic bacteria) could lead to greater diversion of material and energy away from tertiary and higher trophic levels. Such a change in trophic flux might be expected in fall if the ongoing redistribution of phytoplankton biomass amongst size classes results in a change in class dominance, as seems to be happening. In spring, diatoms of the microplankton will remain overwhelmingly dominant and no significant change in trophic flux would be expected even as picoplankton are on a trajectory of increase from their normal extremely low concentrations in spring.

There is an important premise underlying these conjectures: namely that multiyear change proceeds in a linear fashion, as measured by the slope of inter-annual change over time. This is almost certainly an untenable premise in the long-term because natural systems tend to return to a basin of attraction. In other words, the linear trends ascribed to the period 1997-2013 may actually be only a short segment of a much longer multi-decadal cycle. But even if this were not the case, and if driving pressures are sustained, the system might abruptly shift into a new regime if there is not enough existing resilient capacity (Tett et al. 2013). In other words, beyond a critical point, the effects no longer change linearly with the causes. Evidence to test these conjectures lie beyond the scope of this report.

ACKNOWLEDGMENTS

I thank DFO Maritimes Science sector management, the AZMP Permanent Management Committee, the AZMP Maritimes Coordinating Committee, and the Canadian Coast Guard for supporting and enabling this work. The great many dedicated DFO staff persons who have served on these bodies since program inception are too numerous to list here by name. I also thank the many members of the Ocean and Ecosystem Science Division and the Program Coordination and Support Division who manage, coordinate, administer, and undertake the work at-sea, in the laboratory, and in the office. I especially thank my colleagues in the Marine Ecosystem Section (previously Ocean and Research Monitoring Section, previously Biological Oceanography Section) who have directly contributed to and supported activities of the spring and fall shelf cruises, including Anning (Jeff), Anstey (Carol), Burtch (Sandy), Caverhill (Carla), Cogswell (Andrew), Dickie (Paul), Evans Duchene (Barb), Harrison (Glen), Head (Erica), Hebert (Dave), Horne (Edward), Johnson (Catherine), Kennedy (Mary), Landry (Marilyn), Pauley (Kevin), Perry (Tim), Ringuette (Marc), and Spry (Jeff). I am also grateful to those who have worked in the flow cytometry laboratory over the years: Kelly Haussler, Peter Sykes, Diane Horn, Karen Scarcella, Chantal Giroux, and Gillian Forbes. I thank Catherine Johnson and Glen Harrison for their review of this report.

REFERENCES

- Batten, S.D., Walne, A.W., Edwards, M., and Groom, S.B. 2003. Phytoplankton biomass from continuous plankton recorder data: an assessment of the phytoplankton colour index. *J. Plankton Res.* 25: 697-702.
- Cullen, J.J. 1982. The deep chlorophyll maximum: comparing vertical profiles of chlorophyll *a*. *Can. J. Fish. Aquat. Sci.* 39: 791-803.
- Dasilva, C.R., Li, W.K.W., and Lovejoy, C. 2014. Phylogenetic diversity of eukaryotic marine microbial plankton on the Scotian Shelf Northwestern Atlantic Ocean. *J. Plankton Res.* 36: 344-363.
- Devred, E., Sathyendranath, S., Stuart, V., and Platt T. 2011. A three component classification of phytoplankton absorption spectra: Application to ocean-color data. *Remote Sensing of the Environment* 115: 2255-2266.
- Eldredge, N. 1986. Information, economics, and evolution. *Ann. Rev. Ecol. Syst.* 17: 351-369.
- Flynn, K.J., Stoecker, D.K., Mitra, A., Raven, J.A., Glibert, P.M., Hansen, P.J., Granéli, E., and Burkholder, J.M. 2013. Misuse of the phytoplankton-zooplankton dichotomy: the need to assign organisms as mixotrophs within plankton functional types. *J. Plankton Res.* 35:3-11.
- Frank, K.T., Petrie, B., Fisher, J.A.D., and Leggett, W.C. 2011. Transient dynamics of an altered large marine ecosystem. *Nature* 477:86–89.
- Frank, K.T., Petrie, B., Fisher, J.A.D., and Leggett, W.C. 2013. Setting the record straight on drivers of changing ecosystem states. *Fish. Oceanogr.* 22: 143-146.
- Greene, C.H. 2013. Towards a more balanced view of marine ecosystems. *Fish. Oceanogr.* 22:140-142.
- Head, E.J.H. and Pepin P. 2010. Monitoring changes in phytoplankton abundance and composition in the Northwest Atlantic: a comparison of results obtained by continuous plankton recorder sampling and colour satellite imagery. *J. Plankton Res.* 32: 1649–1660.
- Hebert, D., Pettipas, R., Brickman, D., and Dever M. 2013. Meteorological, sea ice and physical oceanographic conditions on the Scotian Shelf and in the Gulf of Maine during 2012. DFO Can. Sci. Advis. Sec. Res. Doc. 2013/058. v + 46 p.

- Hull, D.L. 1974. *Philosophy of Biological Science*. Prentice-Hall, New Jersey, 148p.
- Johnson, C., Harrison, G., Casault, B., Spry, J., Li, W., and Head, E. 2013. Optical, chemical, and biological oceanographic conditions on the Scotian Shelf and in the eastern Gulf of Maine in 2012. *DFO Can. Sci. Advis. Sec. Res. Doc.* 2013/070. v + 42 p.
- Li, W.K.W. 2009. From cytometry to macroecology: a quarter century quest in microbial oceanography. *Aquat. Microb. Ecol.* 57: 239-251.
- Li, W.K.W. and Dickie, P.M. 2001. Monitoring phytoplankton, bacterioplankton, and virioplankton in a coastal inlet (Bedford Basin) by flow cytometry. *Cytometry* 44:236-246.
- Li, W.K.W., Harrison, W.G., and Head, E.J.H. 2006. Coherent sign switching in multiyear trends of microbial plankton. *Science* 311: 1157-1160.
- Li, W.K.W. and López-Urrutia, A. 2013. Macroscopic patterns in marine plankton. *In: Encyclopedia of Biodiversity, Volume 4*. Edited by S.A. Levin. Academic Press, Waltham, MA. pp. 667-680.
- Mitchell, M.R., G. Harrison, K. Pauley, A. Gagné, G. Maillet, and P. Strain. 2002. Atlantic Zonal Monitoring Program Sampling Protocol. *Can. Tech. Rep. Hydrogr. Ocean Sci.* 223: iv + 23 pp.
- Pepin, P., Petrie, B., Therriault, J.-C., Narayanan, S., Harrison, G., Chassé, J., Colbourne, E., Gilbert, D., Gregory, D., Harvey, M., Maillet, G., Mitchel, M., and Starr, M. 2005. The Atlantic Zone Monitoring Program (AZMP): Review of 1998-2003. *Can. Tech. Rep. Hydrogr. Ocean Sci.* 242: v + 87 p.
- Pomeroy, L.R. 1974. The ocean's food web, a changing paradigm. *Bioscience* 24: 499-504.
- Sieburth, J.McN., Smetacek, V., and Lenz, J. 1978. Pelagic ecosystem structure: Heterotrophic compartments of the plankton and their relationship to plankton size fractions. *Limnol. Oceanogr.* 23:1256-1263.
- Strong, D.R. Jr. 1980. Null hypothesis in ecology. *In Conceptual Issues in Ecology*. Edited by E. Saarinen. D. Reidel Publishing, Dordrecht. pp. 245-259.
- Stuart, V. and Head, E.J.H. 2005. The BIO method. *In: The Second SeaWiFS HPLC Analysis Round-Robin Experiment (SeaHARRE-2)*. NASA/TM-2005-212785. National Aeronautics and Space Administration, Goddard Space Flight Center, Maryland, pp. 78-80.

- Tett, P. and 20 others. 2013. Framework for understanding marine ecosystem health. *Mar. Ecol. Prog. Ser.* 494:1-27.
- Therriault, J.-C., Petrie, B., Pepin, P., Gagnon, J., Gregory, D., Helbig, J., Herman, A., Lefavre, D., Mitchell, M., Pelchat, B., Runge, J., and Sarneoto, D. 1998. Proposal for a Northwest Atlantic Zonal Monitoring Program. *Can. Tech. Rep. Hydrogr. Ocean Sci.* 194: vii+57 p.
- Uitz, J., Claustre, H., Morel, A., and Hooker, S.B. 2006. Vertical distribution of phytoplankton communities in open ocean: An assessment based on surface chlorophyll. *J. Geophys. Res.* 111, C08005, doi:10.1029/2005JC003207.

TABLES

TABLE 1. List of AZMP Scotian Shelf cruises 1997-2013.

| SEASON | YEAR | CRUISE | DATE | | DAY OF YEAR | | # OF DAYS |
|---------------------------|--------|------------|-------------|-------------|-------------|------------|-----------|
| | | | START | END | START | END | |
| SPRING | 1997 | 97-003 | 18-Apr-1997 | 28-Apr-1997 | 108 | 118 | 11 |
| | 1998 | 98-002 | 8-Apr-1998 | 26-Apr-1998 | 98 | 116 | 19 |
| | 1999 | 99-003 | 8-Apr-1999 | 18-Apr-1999 | 98 | 108 | 11 |
| | 2000 | 00-002 | 6-Apr-2000 | 23-Apr-2000 | 97 | 114 | 18 |
| | 2001 | 01-009 | 1-May-2001 | 25-May-2001 | 121 | 145 | 25 |
| | 2003 | 03-005 | 12-Apr-2003 | 19-Apr-2003 | 102 | 109 | 8 |
| | 2004 | 04-009 | 18-Apr-2004 | 8-May-2004 | 109 | 129 | 21 |
| | 2005 | 05-004 | 1-Apr-2005 | 10-Apr-2005 | 91 | 100 | 10 |
| | 2006 | 06-008 | 20-Apr-2006 | 7-May-2006 | 110 | 127 | 18 |
| | 2007 | 07-001 | 4-Apr-2007 | 22-Apr-2007 | 94 | 112 | 19 |
| | 2008 | 08-004 | 10-Apr-2008 | 29-Apr-2008 | 101 | 120 | 20 |
| | 2009 | 09-005 | 9-Apr-2009 | 29-Apr-2009 | 99 | 119 | 21 |
| | 2010 | 10-006 | 8-Apr-2010 | 25-Apr-2010 | 98 | 115 | 18 |
| | 2011 | 11-004 | 7-Apr-2011 | 23-Apr-2011 | 97 | 113 | 17 |
| 2013 | 13-004 | 5-Apr-2013 | 26-Apr-2013 | 95 | 116 | 22 | |
| Average | | | | | 101 | 117 | 17 |
| Standard deviation | | | | | 8 | 10 | 5 |

| SEASON | YEAR | CRUISE | DATE | | DAY OF YEAR | | # OF DAYS |
|---------------------------|--------|-------------|-------------|-------------|-------------|------------|-----------|
| | | | START | END | START | END | |
| FALL | 1998 | 98-050 | 3-Oct-1998 | 20-Oct-1998 | 276 | 293 | 18 |
| | 1999 | 99-054 | 23-Oct-1999 | 12-Nov-1999 | 296 | 316 | 21 |
| | 2000 | 00-050 | 30-Sep-2000 | 16-Oct-2000 | 274 | 290 | 17 |
| | 2001 | 01-061 | 24-Oct-2001 | 7-Nov-2001 | 297 | 311 | 15 |
| | 2002 | 02-064 | 18-Oct-2002 | 31-Oct-2002 | 291 | 304 | 14 |
| | 2003 | 03-067 | 19-Oct-2003 | 31-Oct-2003 | 292 | 304 | 13 |
| | 2004 | 04-055 | 19-Oct-2004 | 29-Oct-2004 | 293 | 303 | 11 |
| | 2005 | 05-055 | 17-Oct-2005 | 1-Nov-2005 | 290 | 305 | 16 |
| | 2006 | 06-052 | 5-Oct-2006 | 20-Oct-2006 | 278 | 293 | 16 |
| | 2007 | 07-045 | 28-Sep-2007 | 18-Oct-2007 | 271 | 291 | 21 |
| | 2008 | 08-037 | 28-Sep-2008 | 20-Oct-2008 | 272 | 294 | 23 |
| | 2009 | 09-048 | 26-Sep-2009 | 19-Oct-2009 | 269 | 292 | 24 |
| | 2011 | 11-043 | 24-Sep-2011 | 14-Oct-2011 | 267 | 287 | 21 |
| | 2012 | 12-042 | 25-Sep-2012 | 15-Oct-2012 | 269 | 289 | 21 |
| 2013 | 13-037 | 21-Sep-2013 | 9-Oct-2013 | 264 | 282 | 19 | |
| Average | | | | | 280 | 297 | 18 |
| Standard Deviation | | | | | 12 | 10 | 4 |

TABLE 2. Climatological mean values on BBL in spring and fall. Units: Celsius (temperature); psu (salinity); kg m^{-3} (sigma-theta, Δ sigma-theta); ml l^{-1} (oxygen); mmol m^{-3} (nitrate, silicate, phosphate); cells ml^{-1} (bacteria, *Synechococcus*, picoeukaryotes, picophytoplankton, nanophytoplankton); mg m^{-3} (chlorophyll *a*, POC, PON, 19'-butanoyloxyfucoxanthin [BUT], 19'-hexanoyloxyfucoxanthin [HEX], alloxanthin [ALLO], chlorophyll *b* [CHLB], fucoxanthin [FUCO], peridinin [PERI], zeaxanthin [ZEA], diagnostic pigments [DIAGPIG], microphytoplankton pigments [MICROPIG], nanophytoplankton pigments [NANOPIG], picophytoplankton pigments [PICOPIG]); fraction (FMICRO, FNANO, FPICO); mol mol^{-1} (POC:PON).

| SEASON | STATION | DEPTH AVERAGE (0-100M) | | | | DEPTH AVERAGE (0-100M) | | | | | | | | | |
|--------|---------|------------------------|----------|-------------|----------------------|------------------------|---------|-----------|----------|-------------|----------|---------|---------|-----------|-----------|
| | | TEMPERATURE | SALINITY | SIGMA-THETA | Δ SIGMA-THETA | OXYGEN | NITRATE | PHOSPHATE | SILICATE | CHLOROPHYLL | BACTERIA | SYNECHO | PICOEUK | PICOPHYTO | NANOPHYTO |
| Spring | BBL1 | 2.57 | 31.51 | 25.13 | 0.34 | 7.25 | 3.09 | 0.61 | 3.18 | 3.41 | 429645 | 518 | 1842 | 2359 | 932 |
| Spring | BBL2 | 2.98 | 31.84 | 25.36 | 0.76 | 7.21 | 4.25 | 0.68 | 4.04 | 2.75 | 435675 | 607 | 1880 | 2485 | 1067 |
| Spring | BBL3 | 3.15 | 31.91 | 25.40 | 0.72 | 7.29 | 4.06 | 0.68 | 3.78 | 3.15 | 433913 | 675 | 2140 | 2815 | 1070 |
| Spring | BBL4 | 3.26 | 32.08 | 25.52 | 0.90 | 7.12 | 4.28 | 0.68 | 3.75 | 2.96 | 443725 | 564 | 1623 | 2187 | 917 |
| Spring | BBL5 | 5.97 | 33.12 | 26.01 | 1.21 | 6.63 | 5.34 | 0.63 | 3.58 | 2.12 | 593173 | 1426 | 2837 | 4262 | 959 |
| Spring | BBL6 | 6.67 | 33.43 | 26.19 | 1.07 | 6.30 | 5.99 | 0.64 | 3.70 | 2.05 | 644279 | 1668 | 2726 | 4395 | 873 |
| Spring | BBL7 | 6.92 | 33.52 | 26.22 | 1.03 | 6.46 | 5.30 | 0.60 | 3.24 | 2.11 | 726614 | 1795 | 3680 | 5472 | 1127 |
| Spring | AVERAGE | 4.50 | 32.49 | 25.69 | 0.86 | 6.90 | 4.61 | 0.65 | 3.61 | 2.65 | 529575 | 1036 | 2390 | 3425 | 992 |
| Fall | BBL1 | 9.29 | 31.88 | 24.59 | 1.77 | 5.65 | 4.19 | 0.67 | 4.31 | 0.60 | 728190 | 41627 | 8059 | 49687 | 1208 |
| Fall | BBL2 | 9.17 | 32.49 | 25.06 | 2.05 | 5.44 | 5.72 | 0.74 | 5.38 | 0.79 | 799463 | 39533 | 8197 | 47646 | 1715 |
| Fall | BBL3 | 10.14 | 32.69 | 25.08 | 1.87 | 5.36 | 5.68 | 0.71 | 5.03 | 0.82 | 753441 | 36958 | 7415 | 44423 | 1707 |
| Fall | BBL4 | 10.73 | 32.71 | 24.99 | 1.97 | 5.30 | 5.24 | 0.67 | 4.62 | 0.63 | 677115 | 36533 | 7146 | 43830 | 1305 |
| Fall | BBL5 | 10.97 | 33.02 | 25.17 | 2.79 | 5.23 | 5.67 | 0.66 | 4.49 | 0.40 | 653723 | 41265 | 7756 | 50352 | 1039 |
| Fall | BBL6 | 11.97 | 33.09 | 25.06 | 2.70 | 5.12 | 5.23 | 0.61 | 4.15 | 0.50 | 638632 | 32538 | 7009 | 42990 | 1100 |
| Fall | BBL7 | 13.83 | 33.74 | 25.19 | 2.69 | 4.98 | 5.04 | 0.54 | 3.43 | 0.43 | 560460 | 29577 | 11114 | 46599 | 1080 |
| Fall | AVERAGE | 10.87 | 32.80 | 25.02 | 2.26 | 5.30 | 5.25 | 0.66 | 4.49 | 0.60 | 687289 | 36862 | 8100 | 46504 | 1308 |

| SEASON | STATION | NEAR-SURFACE VALUE | | | | | | | | | | | | | | | | |
|--------|---------|--------------------|-----|---------|-------|-------|-------|-------|-------|-------|-------|---------|----------|---------|---------|--------|-------|-------|
| | | POC | PON | POC:PON | BUT | HEX | ALLO | CHLB | FUCO | PERI | ZEA | DIAGPIG | MICROPIG | NANOPIG | PICOPIG | FMICRO | FNANO | FPICO |
| Spring | BBL1 | 283 | 39 | 8.43 | 0.004 | 0.007 | 0.009 | 0.060 | 1.134 | 0.015 | 0.009 | 1.71 | 1.62 | 0.02 | 0.07 | 0.91 | 0.01 | 0.08 |
| Spring | BBL2 | 260 | 43 | 7.10 | 0.008 | 0.025 | 0.025 | 0.074 | 1.044 | 0.025 | 0.002 | 1.63 | 1.51 | 0.05 | 0.08 | 0.84 | 0.07 | 0.09 |
| Spring | BBL3 | 312 | 46 | 7.69 | 0.006 | 0.017 | 0.018 | 0.083 | 1.279 | 0.028 | 0.004 | 1.97 | 1.84 | 0.03 | 0.09 | 0.83 | 0.07 | 0.10 |
| Spring | BBL4 | 324 | 46 | 8.03 | 0.013 | 0.039 | 0.022 | 0.068 | 1.225 | 0.038 | 0.005 | 1.92 | 1.78 | 0.07 | 0.07 | 0.84 | 0.07 | 0.08 |
| Spring | BBL5 | 276 | 43 | 7.35 | 0.005 | 0.053 | 0.025 | 0.087 | 1.165 | 0.033 | 0.002 | 1.86 | 1.69 | 0.08 | 0.09 | 0.86 | 0.06 | 0.08 |
| Spring | BBL6 | 295 | 57 | 7.25 | 0.003 | 0.045 | 0.025 | 0.085 | 0.911 | 0.025 | 0.005 | 1.48 | 1.32 | 0.07 | 0.09 | 0.84 | 0.07 | 0.09 |
| Spring | BBL7 | 277 | 45 | 7.04 | 0.007 | 0.077 | 0.039 | 0.124 | 0.809 | 0.049 | 0.003 | 1.46 | 1.21 | 0.12 | 0.13 | 0.81 | 0.09 | 0.10 |
| Spring | AVERAGE | 290 | 45 | 7.55 | 0.006 | 0.038 | 0.023 | 0.083 | 1.081 | 0.030 | 0.004 | 1.72 | 1.57 | 0.06 | 0.09 | 0.85 | 0.06 | 0.09 |
| Fall | BBL1 | 159 | 26 | 7.41 | 0.023 | 0.134 | 0.026 | 0.115 | 0.373 | 0.034 | 0.027 | 0.91 | 0.57 | 0.19 | 0.14 | 0.39 | 0.32 | 0.30 |
| Fall | BBL2 | 182 | 30 | 7.09 | 0.025 | 0.185 | 0.057 | 0.167 | 0.271 | 0.043 | 0.033 | 0.92 | 0.48 | 0.28 | 0.20 | 0.39 | 0.33 | 0.31 |
| Fall | BBL3 | 190 | 27 | 8.28 | 0.026 | 0.192 | 0.044 | 0.161 | 0.311 | 0.036 | 0.028 | 0.96 | 0.53 | 0.30 | 0.19 | 0.40 | 0.36 | 0.30 |
| Fall | BBL4 | 150 | 24 | 7.34 | 0.020 | 0.199 | 0.046 | 0.162 | 0.275 | 0.036 | 0.026 | 0.91 | 0.44 | 0.29 | 0.19 | 0.36 | 0.37 | 0.27 |
| Fall | BBL5 | 127 | 20 | 7.47 | 0.026 | 0.150 | 0.027 | 0.123 | 0.077 | 0.023 | 0.036 | 0.51 | 0.15 | 0.22 | 0.16 | 0.26 | 0.39 | 0.37 |
| Fall | BBL6 | 148 | 21 | 8.10 | 0.027 | 0.149 | 0.024 | 0.112 | 0.156 | 0.019 | 0.028 | 0.60 | 0.25 | 0.21 | 0.14 | 0.32 | 0.38 | 0.30 |
| Fall | BBL7 | 113 | 16 | 8.17 | 0.027 | 0.143 | 0.016 | 0.094 | 0.087 | 0.014 | 0.026 | 0.46 | 0.17 | 0.20 | 0.12 | 0.28 | 0.45 | 0.32 |
| Fall | AVERAGE | 153 | 23 | 7.69 | 0.025 | 0.165 | 0.034 | 0.133 | 0.222 | 0.029 | 0.029 | 0.75 | 0.37 | 0.24 | 0.16 | 0.34 | 0.37 | 0.31 |

TABLE 3. Climatological mean values on HL in spring and fall. Units: Celsius (temperature); psu (salinity); kg m^{-3} (sigma-theta, Δ sigma-theta); ml l^{-1} (oxygen); mmol m^{-3} (nitrate, silicate, phosphate); cells ml^{-1} (bacteria, *Synechococcus*, picoeukaryotes, picophytoplankton, nanophytoplankton); mg m^{-3} (chlorophyll *a*, POC, PON, 19'-butanoyloxyfucoxanthin [BUT], 19'-hexanoyloxyfucoxanthin [HEX], alloxanthin [ALLO], chlorophyll *b* [CHLB], fucoxanthin [FUCO], peridinin [PERI], zeaxanthin [ZEA], diagnostic pigments [DIAGPIG], microphytoplankton pigments [MICROPIG], nanophytoplankton pigments [NANOPIG], picophytoplankton pigments [PICOPIG]); fraction (FMICRO, FNANO, FPICO); mol mol^{-1} (POC:PON).

| SEASON | STATION | DEPTH AVERAGE (0-100M) | | | | DEPTH AVERAGE (0-100M) | | | | | | | | | |
|--------|---------|------------------------|----------|-------------|----------------------|------------------------|---------|-----------|----------|-------------|----------|---------|---------|-----------|-----------|
| | | TEMPERATURE | SALINITY | SIGMA-THETA | Δ SIGMA-THETA | OXYGEN | NITRATE | PHOSPHATE | SILICATE | CHLOROPHYLL | BACTERIA | SYNECHO | PICOEUK | PICOPHYTO | NANOPHYTO |
| Spring | HL1 | 1.41 | 31.43 | 25.14 | 0.63 | 8.14 | 2.42 | 0.62 | 2.39 | 2.96 | 431848 | 271 | 1173 | 1416 | 850 |
| Spring | HL2 | 1.96 | 31.77 | 25.37 | 1.07 | 7.53 | 2.78 | 0.65 | 2.69 | 2.39 | 421935 | 284 | 1086 | 1347 | 775 |
| Spring | HL3 | 3.86 | 32.48 | 25.77 | 1.25 | 6.92 | 4.19 | 0.68 | 3.32 | 1.42 | 593811 | 477 | 2067 | 2530 | 878 |
| Spring | HL4 | 4.08 | 32.58 | 25.83 | 1.03 | 6.90 | 3.41 | 0.60 | 2.81 | 1.41 | 512232 | 466 | 1926 | 2391 | 1079 |
| Spring | HL5 | 4.34 | 32.96 | 26.10 | 0.87 | 6.82 | 3.95 | 0.62 | 3.16 | 1.83 | 455878 | 384 | 1353 | 1737 | 976 |
| Spring | HL6 | 6.46 | 33.59 | 26.29 | 0.97 | 6.54 | 4.03 | 0.54 | 2.50 | 2.08 | 585225 | 2471 | 4048 | 6518 | 1278 |
| Spring | HL7 | 6.34 | 33.64 | 26.35 | 0.79 | 6.56 | 4.59 | 0.58 | 2.89 | 2.42 | 615015 | 2921 | 2955 | 5860 | 1073 |
| Spring | AVERAGE | 4.06 | 32.64 | 25.84 | 0.94 | 7.06 | 3.63 | 0.61 | 2.82 | 2.07 | 516563 | 1039 | 2087 | 3114 | 987 |
| Fall | HL1 | 8.81 | 31.31 | 24.17 | 2.80 | 5.62 | 4.02 | 0.64 | 4.76 | 0.46 | 569901 | 30899 | 5632 | 36531 | 1095 |
| Fall | HL2 | 8.85 | 31.69 | 24.45 | 3.64 | 5.55 | 4.62 | 0.66 | 4.66 | 0.48 | 655902 | 43814 | 7169 | 50982 | 1198 |
| Fall | HL3 | 9.27 | 32.42 | 24.97 | 3.43 | 5.35 | 4.92 | 0.60 | 4.36 | 0.38 | 652972 | 44319 | 6989 | 51308 | 1180 |
| Fall | HL4 | 10.81 | 32.51 | 24.78 | 2.91 | 5.39 | 3.88 | 0.51 | 3.47 | 0.38 | 674581 | 43839 | 7189 | 51028 | 1248 |
| Fall | HL5 | 9.95 | 32.74 | 25.10 | 2.96 | 5.47 | 4.33 | 0.55 | 3.66 | 0.41 | 675429 | 43243 | 9653 | 52761 | 971 |
| Fall | HL6 | 12.21 | 33.39 | 25.18 | 2.90 | 5.27 | 3.98 | 0.48 | 3.06 | 0.39 | 567862 | 33925 | 12073 | 47049 | 1101 |
| Fall | HL7 | 14.21 | 33.76 | 25.06 | 2.83 | 5.07 | 3.66 | 0.44 | 2.54 | 0.29 | 491910 | 27989 | 20945 | 56656 | 813 |
| Fall | AVERAGE | 10.59 | 32.54 | 24.82 | 3.07 | 5.39 | 4.20 | 0.55 | 3.79 | 0.40 | 612651 | 38290 | 9950 | 49474 | 1086 |

| SEASON | STATION | NEAR-SURFACE VALUE | | | | | | | | | | | | | | | | |
|--------|---------|--------------------|-----|---------|-------|-------|-------|-------|-------|-------|-------|---------|----------|---------|---------|--------|-------|-------|
| | | POC | PON | POC:PON | BUT | HEX | ALLO | CHLB | FUCO | PERI | ZEA | DIAGPIG | MICROPIG | NANOPIG | PICOPIG | FMICRO | FNANO | FPICO |
| Spring | HL1 | 308 | 45 | 8.35 | 0.004 | 0.006 | 0.013 | 0.050 | 0.944 | 0.009 | 0.002 | 1.41 | 1.34 | 0.02 | 0.05 | 0.93 | 0.03 | 0.04 |
| Spring | HL2 | 320 | 44 | 8.67 | 0.005 | 0.015 | 0.013 | 0.047 | 1.062 | 0.015 | 0.004 | 1.60 | 1.61 | 0.03 | 0.05 | 0.84 | 0.06 | 0.10 |
| Spring | HL3 | 274 | 40 | 7.77 | 0.002 | 0.035 | 0.013 | 0.075 | 0.622 | 0.029 | 0.006 | 1.05 | 0.92 | 0.05 | 0.08 | 0.82 | 0.08 | 0.10 |
| Spring | HL4 | 233 | 35 | 7.72 | 0.007 | 0.044 | 0.024 | 0.056 | 0.472 | 0.035 | 0.007 | 0.85 | 0.72 | 0.07 | 0.06 | 0.82 | 0.11 | 0.07 |
| Spring | HL5 | 206 | 32 | 7.64 | 0.009 | 0.053 | 0.020 | 0.059 | 0.632 | 0.058 | 0.006 | 1.12 | 0.97 | 0.08 | 0.07 | 0.85 | 0.08 | 0.07 |
| Spring | HL6 | 224 | 35 | 7.54 | 0.008 | 0.104 | 0.037 | 0.081 | 0.661 | 0.040 | 0.004 | 1.23 | 0.99 | 0.16 | 0.09 | 0.71 | 0.20 | 0.09 |
| Spring | HL7 | 262 | 41 | 7.62 | 0.005 | 0.059 | 0.021 | 0.105 | 0.767 | 0.029 | 0.004 | 1.32 | 1.12 | 0.09 | 0.11 | 0.72 | 0.16 | 0.11 |
| Spring | AVERAGE | 261 | 39 | 7.90 | 0.006 | 0.045 | 0.020 | 0.068 | 0.737 | 0.031 | 0.005 | 1.23 | 1.10 | 0.07 | 0.07 | 0.81 | 0.10 | 0.08 |
| Fall | HL1 | 146 | 23 | 7.65 | 0.014 | 0.118 | 0.018 | 0.075 | 0.134 | 0.038 | 0.019 | 0.50 | 0.24 | 0.17 | 0.09 | 0.42 | 0.37 | 0.22 |
| Fall | HL2 | 139 | 21 | 7.95 | 0.015 | 0.129 | 0.028 | 0.119 | 0.090 | 0.033 | 0.025 | 0.50 | 0.17 | 0.19 | 0.14 | 0.29 | 0.37 | 0.34 |
| Fall | HL3 | 114 | 17 | 7.87 | 0.024 | 0.133 | 0.012 | 0.078 | 0.078 | 0.023 | 0.023 | 0.43 | 0.14 | 0.18 | 0.10 | 0.29 | 0.46 | 0.26 |
| Fall | HL4 | 113 | 17 | 7.70 | 0.030 | 0.120 | 0.005 | 0.067 | 0.058 | 0.005 | 0.021 | 0.34 | 0.09 | 0.17 | 0.09 | 0.26 | 0.49 | 0.25 |
| Fall | HL5 | 117 | 17 | 8.51 | 0.029 | 0.119 | 0.004 | 0.076 | 0.047 | 0.011 | 0.023 | 0.34 | 0.08 | 0.16 | 0.10 | 0.24 | 0.46 | 0.30 |
| Fall | HL6 | 109 | 14 | 8.75 | 0.024 | 0.109 | 0.006 | 0.064 | 0.046 | 0.011 | 0.024 | 0.31 | 0.08 | 0.15 | 0.08 | 0.24 | 0.47 | 0.29 |
| Fall | HL7 | 88 | 13 | 8.36 | 0.026 | 0.078 | 0.000 | 0.040 | 0.034 | 0.000 | 0.025 | 0.22 | 0.05 | 0.11 | 0.06 | 0.22 | 0.46 | 0.32 |
| Fall | AVERAGE | 118 | 17 | 8.11 | 0.023 | 0.115 | 0.010 | 0.074 | 0.070 | 0.017 | 0.023 | 0.38 | 0.12 | 0.16 | 0.09 | 0.28 | 0.44 | 0.28 |

TABLE 4. Climatological mean values on LL in spring and fall. Units: Celsius (temperature); psu (salinity); kg m^{-3} (sigma-theta, Δ sigma-theta); ml l^{-1} (oxygen); mmol m^{-3} (nitrate, silicate, phosphate); cells ml^{-1} (bacteria, *Synechococcus*, picoeukaryotes, picophytoplankton, nanophytoplankton); mg m^{-3} (chlorophyll *a*, POC, PON, 19'-butanoyloxyfucoxanthin [BUT], 19'-hexanoyloxyfucoxanthin [HEX], alloxanthin [ALLO], chlorophyll *b* [CHLB], fucoxanthin [FUCO], peridinin [PERI], zeaxanthin [ZEA], diagnostic pigments [DIAGPIG], microphytoplankton pigments [MICROPIG], nanophytoplankton pigments [NANOPIG], picophytoplankton pigments [PICOPIG]); fraction (FMICRO, FNANO, FPICO); mol mol^{-1} (POC:PON).

| SEASON | STATION | DEPTH AVERAGE (0-100M) | | | | DEPTH AVERAGE (0-100M) | | | | | | | | | |
|--------|---------|------------------------|----------|-------------|----------------------|------------------------|---------|-----------|----------|-------------|----------|---------|---------|-----------|-----------|
| | | TEMPERATURE | SALINITY | SIGMA-THETA | Δ SIGMA-THETA | OXYGEN | NITRATE | PHOSPHATE | SILICATE | CHLOROPHYLL | BACTERIA | SYNECHO | PICOEUK | PICOPHYTO | NANOPHYTO |
| Spring | LL1 | 0.08 | 31.08 | 24.94 | 1.11 | 7.97 | 2.52 | 0.64 | 2.59 | 3.92 | 508793 | 261 | 974 | 1234 | 1070 |
| Spring | LL2 | 0.59 | 31.54 | 25.28 | 1.28 | 7.62 | 3.81 | 0.71 | 3.77 | 3.25 | 441645 | 338 | 991 | 1311 | 700 |
| Spring | LL3 | 0.67 | 31.64 | 25.35 | 1.02 | 7.81 | 3.68 | 0.68 | 3.49 | 4.60 | 408446 | 294 | 886 | 1169 | 874 |
| Spring | LL4 | 1.01 | 31.77 | 25.44 | 0.67 | 7.64 | 3.62 | 0.67 | 3.38 | 4.31 | 404248 | 307 | 923 | 1213 | 835 |
| Spring | LL5 | 1.26 | 31.95 | 25.58 | 0.53 | 7.67 | 3.78 | 0.65 | 3.22 | 4.18 | 433748 | 313 | 826 | 1133 | 823 |
| Spring | LL6 | 1.83 | 32.10 | 25.66 | 0.21 | 7.92 | 1.36 | 0.52 | 1.17 | 5.88 | 471124 | 298 | 910 | 1204 | 832 |
| Spring | LL7 | 2.13 | 32.54 | 25.98 | 0.84 | 7.58 | 3.40 | 0.63 | 3.08 | 4.02 | 620871 | 466 | 1462 | 1913 | 1063 |
| Spring | AVERAGE | 1.08 | 31.80 | 25.46 | 0.81 | 7.74 | 3.17 | 0.64 | 2.96 | 4.31 | 469839 | 325 | 996 | 1311 | 886 |
| Fall | LL1 | 8.37 | 30.76 | 23.82 | 3.22 | 5.85 | 2.96 | 0.60 | 4.00 | 0.63 | 558524 | 16438 | 6573 | 23011 | 1058 |
| Fall | LL2 | 7.51 | 31.12 | 24.19 | 3.62 | 5.87 | 3.73 | 0.65 | 4.20 | 0.54 | 532233 | 22019 | 7448 | 29467 | 1157 |
| Fall | LL3 | 6.92 | 31.33 | 24.43 | 3.47 | 5.82 | 4.38 | 0.71 | 4.90 | 0.49 | 533404 | 29087 | 7816 | 36903 | 1172 |
| Fall | LL4 | 6.83 | 31.40 | 24.48 | 3.16 | 5.74 | 4.77 | 0.73 | 5.38 | 0.40 | 559696 | 33376 | 6756 | 40133 | 1152 |
| Fall | LL5 | 7.04 | 31.54 | 24.55 | 3.27 | 5.74 | 4.67 | 0.72 | 5.10 | 0.40 | 538840 | 31671 | 5351 | 37022 | 1137 |
| Fall | LL6 | 9.03 | 31.47 | 24.25 | 2.54 | 5.72 | 3.04 | 0.60 | 3.92 | 0.51 | 626113 | 35171 | 5179 | 40319 | 1260 |
| Fall | LL7 | 8.17 | 32.28 | 25.07 | 2.99 | 5.82 | 3.89 | 0.62 | 3.82 | 0.44 | 505612 | 33530 | 5640 | 40941 | 1206 |
| Fall | AVERAGE | 7.70 | 31.41 | 24.40 | 3.18 | 5.79 | 3.92 | 0.66 | 4.48 | 0.49 | 550632 | 28756 | 6395 | 35399 | 1163 |

| SEASON | STATION | NEAR-SURFACE VALUE | | | | | | | | | | | | | | | | |
|--------|---------|--------------------|-----|---------|-------|-------|-------|-------|-------|-------|-------|---------|----------|---------|---------|--------|-------|-------|
| | | POC | PON | POC:PON | BUT | HEX | ALLO | CHLB | FUCO | PERI | ZEA | DIAGPIG | MICROPIG | NANOPIG | PICOPIG | FMICRO | FNANO | FPICO |
| Spring | LL1 | 334 | 47 | 8.33 | 0.004 | 0.000 | 0.008 | 0.039 | 1.422 | 0.002 | 0.002 | 2.05 | 2.01 | 0.01 | 0.04 | 0.94 | 0.03 | 0.02 |
| Spring | LL2 | 338 | 40 | 9.36 | 0.001 | 0.001 | 0.004 | 0.027 | 1.057 | 0.001 | 0.002 | 1.52 | 1.49 | 0.00 | 0.03 | 0.95 | 0.04 | 0.02 |
| Spring | LL3 | 403 | 45 | 9.84 | 0.000 | 0.003 | 0.004 | 0.033 | 1.825 | 0.011 | 0.003 | 2.63 | 2.59 | 0.01 | 0.04 | 0.95 | 0.02 | 0.03 |
| Spring | LL4 | 336 | 43 | 8.94 | 0.000 | 0.005 | 0.004 | 0.016 | 1.408 | 0.001 | 0.000 | 2.01 | 1.99 | 0.01 | 0.02 | 0.97 | 0.02 | 0.01 |
| Spring | LL5 | 365 | 47 | 8.72 | 0.001 | 0.003 | 0.003 | 0.024 | 1.409 | 0.004 | 0.012 | 2.03 | 1.99 | 0.01 | 0.03 | 0.98 | 0.01 | 0.01 |
| Spring | LL6 | 417 | 49 | 9.82 | 0.004 | 0.006 | 0.006 | 0.040 | 1.372 | 0.015 | 0.002 | 2.01 | 1.96 | 0.01 | 0.04 | 0.97 | 0.01 | 0.02 |
| Spring | LL7 | 438 | 63 | 8.10 | 0.000 | 0.004 | 0.005 | 0.050 | 1.789 | 0.017 | 0.008 | 2.61 | 2.55 | 0.01 | 0.06 | 0.97 | 0.01 | 0.02 |
| Spring | AVERAGE | 376 | 48 | 9.01 | 0.001 | 0.003 | 0.005 | 0.033 | 1.469 | 0.007 | 0.004 | 2.13 | 2.08 | 0.01 | 0.04 | 0.96 | 0.02 | 0.02 |
| Fall | LL1 | 165 | 27 | 7.27 | 0.011 | 0.147 | 0.046 | 0.176 | 0.152 | 0.096 | 0.018 | 0.76 | 0.35 | 0.22 | 0.19 | 0.48 | 0.28 | 0.24 |
| Fall | LL2 | 142 | 24 | 7.01 | 0.009 | 0.157 | 0.042 | 0.173 | 0.121 | 0.045 | 0.022 | 0.66 | 0.23 | 0.23 | 0.19 | 0.34 | 0.35 | 0.31 |
| Fall | LL3 | 130 | 21 | 7.31 | 0.012 | 0.161 | 0.034 | 0.152 | 0.135 | 0.049 | 0.024 | 0.66 | 0.26 | 0.23 | 0.17 | 0.37 | 0.35 | 0.28 |
| Fall | LL4 | 127 | 20 | 7.24 | 0.019 | 0.147 | 0.029 | 0.140 | 0.097 | 0.042 | 0.031 | 0.58 | 0.20 | 0.21 | 0.17 | 0.30 | 0.36 | 0.34 |
| Fall | LL5 | 130 | 19 | 8.05 | 0.008 | 0.139 | 0.033 | 0.115 | 0.077 | 0.040 | 0.027 | 0.50 | 0.17 | 0.20 | 0.14 | 0.31 | 0.38 | 0.31 |
| Fall | LL6 | 124 | 19 | 7.66 | 0.014 | 0.118 | 0.029 | 0.077 | 0.064 | 0.060 | 0.022 | 0.44 | 0.19 | 0.17 | 0.10 | 0.37 | 0.39 | 0.27 |
| Fall | LL7 | 130 | 20 | 7.63 | 0.022 | 0.166 | 0.026 | 0.101 | 0.074 | 0.044 | 0.022 | 0.52 | 0.17 | 0.23 | 0.12 | 0.30 | 0.44 | 0.26 |
| Fall | AVERAGE | 135 | 21 | 7.45 | 0.014 | 0.148 | 0.034 | 0.133 | 0.103 | 0.054 | 0.024 | 0.59 | 0.22 | 0.21 | 0.16 | 0.35 | 0.36 | 0.29 |

TABLE 5. Change in absolute values of variables from 1998 to 2013, interpolated from linear regression of time series representing the average conditions on the 7 stations of the Louisbourg Line in fall.

| LOUISBOURG LINE - FALL VARIABLE | YEAR | | RATIO | |
|--------------------------------------|--------|--------|-----------|-----------|
| | 1998 | 2013 | 2013/1998 | 1998/2013 |
| SYNECHOCOCCUS (cells/ml) | 15468 | 43762 | 2.8 | |
| FPICO (%) | 14% | 39% | 2.8 | |
| PICOPHYTO (cells/ml) | 19396 | 53820 | 2.8 | |
| PICOEUK (cells/ml) | 4379 | 8912 | 2.0 | |
| PICOPIG (mg/m ³) | 0.11 | 0.19 | 1.6 | |
| DELTASIGMATHETA (kg/m ³) | 2.70 | 3.71 | 1.4 | |
| BACTERIA (cells/ml) | 483789 | 617337 | 1.3 | |
| POC (mg/m ³) | 116 | 148 | 1.3 | |
| TEMPERATURE (C) | 7.03 | 8.33 | 1.2 | |
| OXYGEN (ml/l) | 5.69 | 5.94 | 1.0 | |
| NITRATE (mmol/m ³) | 3.91 | 3.97 | 1.0 | |
| NANOPHYTO (cells/ml) | 1167 | 1167 | 1.0 | |
| SALINITY (psu) | 31.47 | 31.30 | | 1.0 |
| POC:PON (mol/mol) | 7.54 | 7.39 | | 1.0 |
| SILICATE (mmol/m ³) | 4.63 | 4.32 | | 1.1 |
| FNANO (%) | 39% | 35% | | 1.1 |
| PHOSPHATE (mmol/m ³) | 0.71 | 0.61 | | 1.2 |
| CHLOROPHYLL (mg/m ³) | 0.59 | 0.37 | | 1.6 |
| DIAGPIG (mg/m ³) | 0.80 | 0.45 | | 1.8 |
| FMICRO (%) | 47% | 26% | | 1.8 |
| NANOPIG (mg/m ³) | 0.33 | 0.14 | | 2.3 |
| MICROPIG (mg/m ³) | 0.36 | 0.13 | | 2.8 |

FIGURES

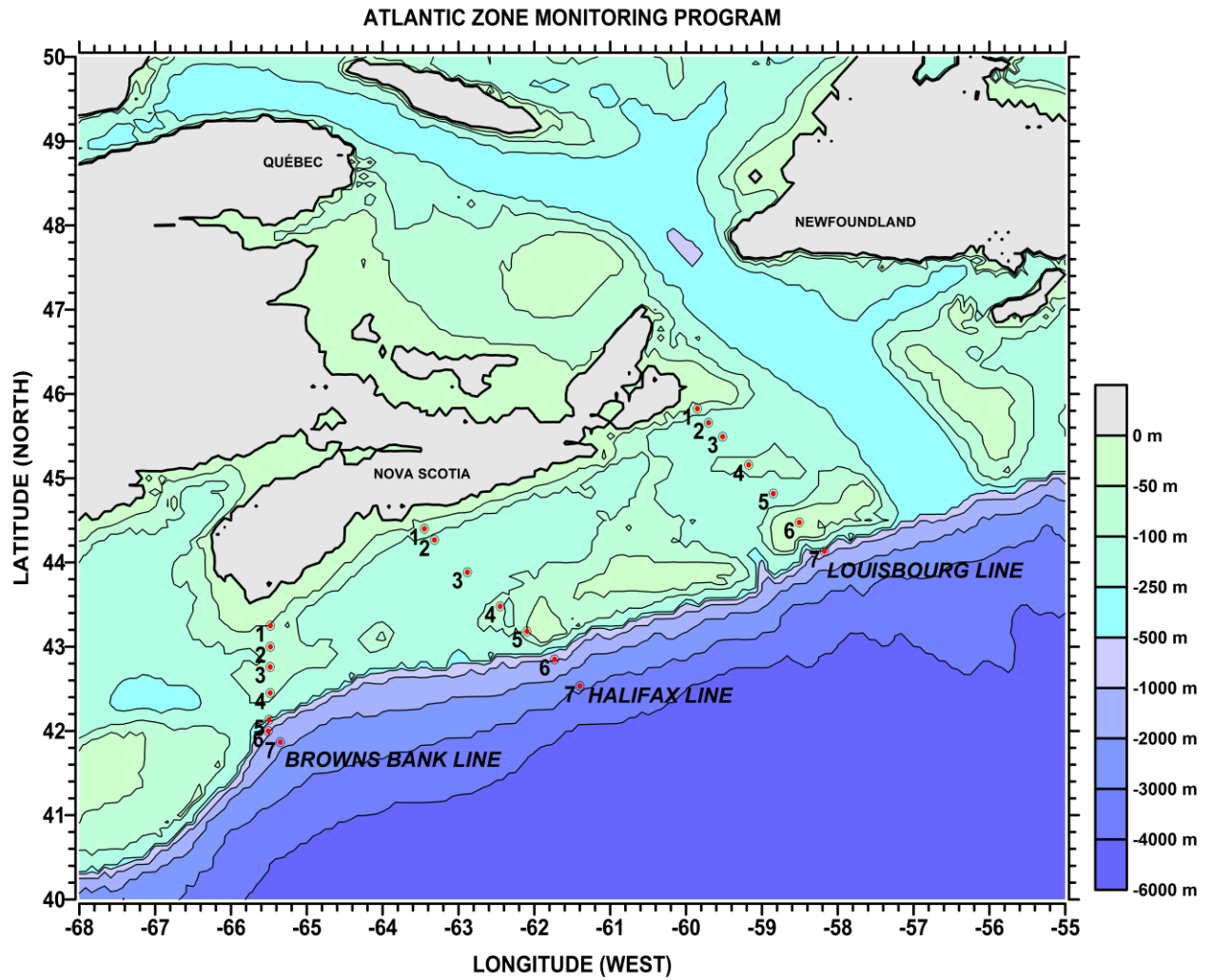


Figure 1. Map of the Scotian Shelf and Slope showing AZMP core stations 1 to 7 on Browns Bank Line (BBL), Halifax Line (HL), and Louisbourg Line (LL). Station coordinates are available at http://www.meds-sdmm.dfo-mpo.gc.ca/isdm-gdsi/azmp-pmza/hydro/azmp_pmza_coordinates_coordonnees-eng.csv

Figure 2

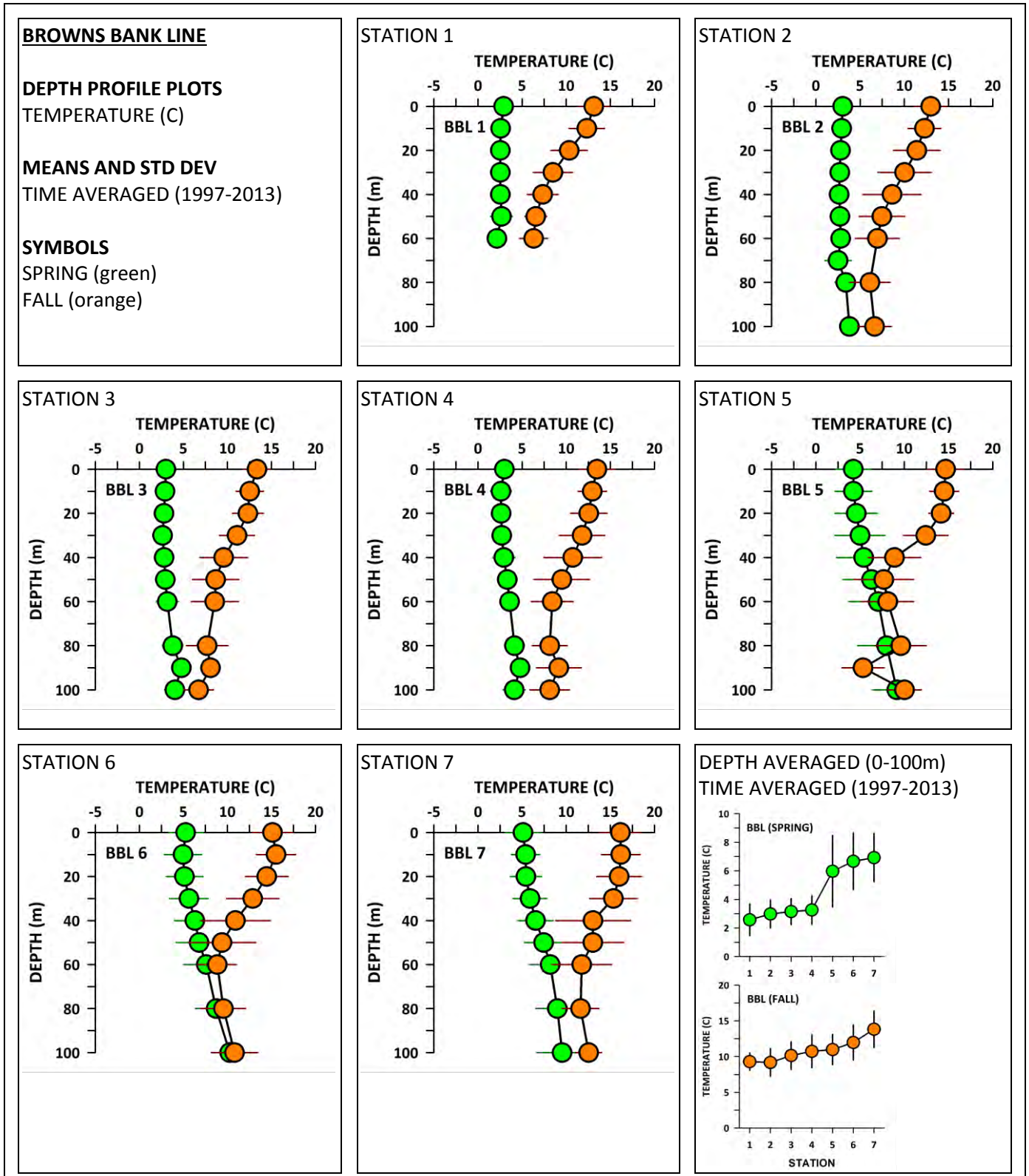


Figure 3

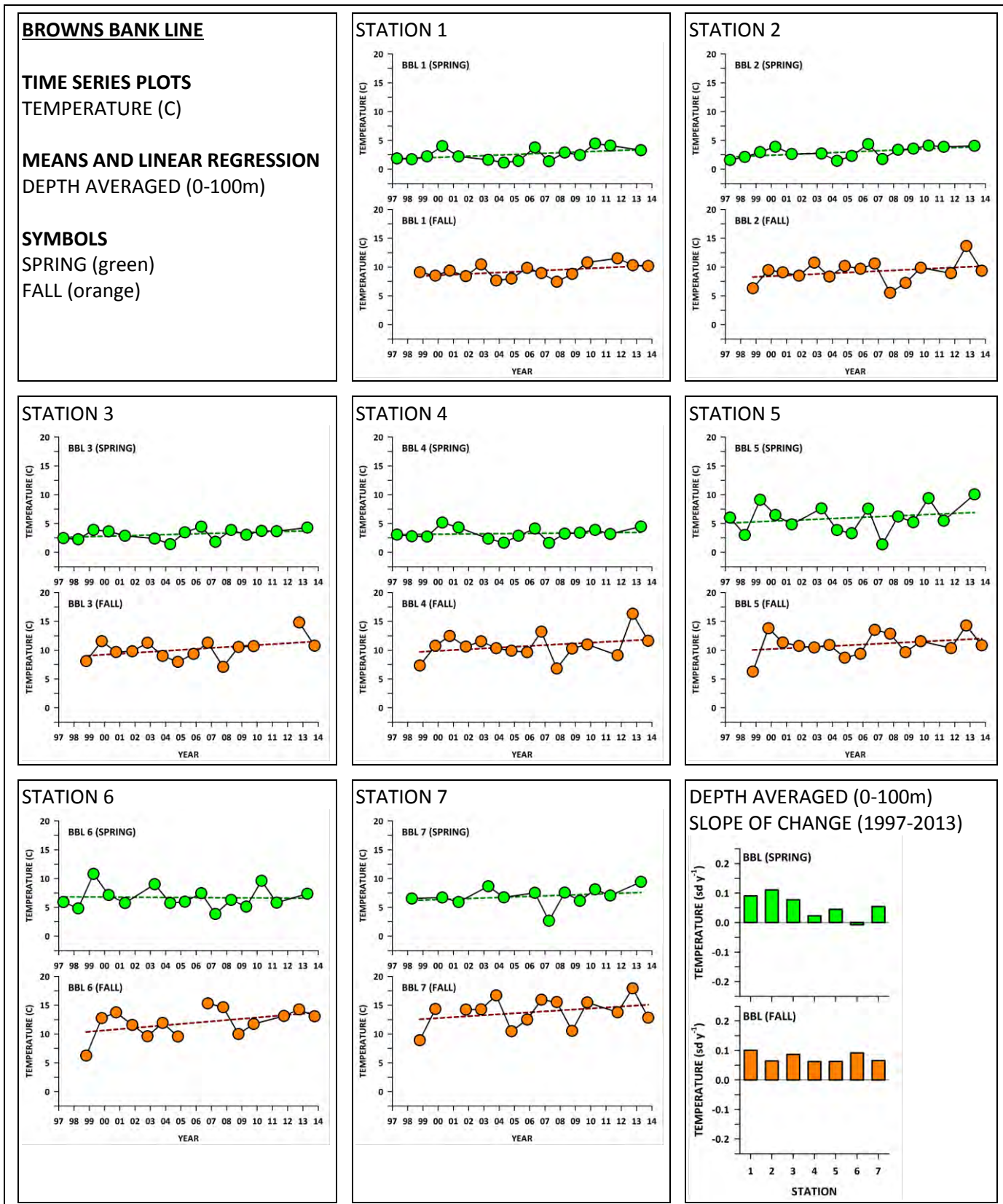


Figure 4

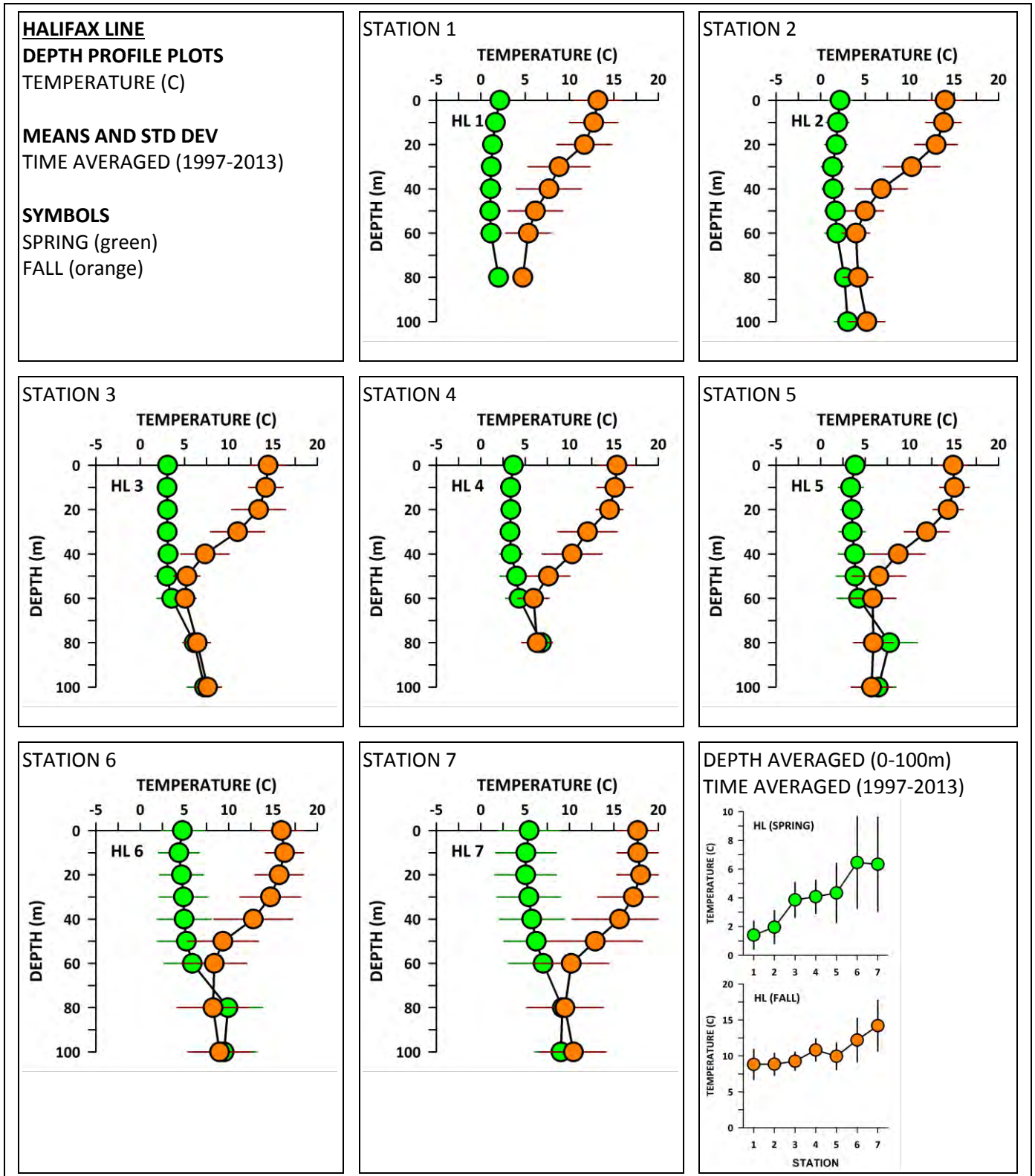


Figure 5

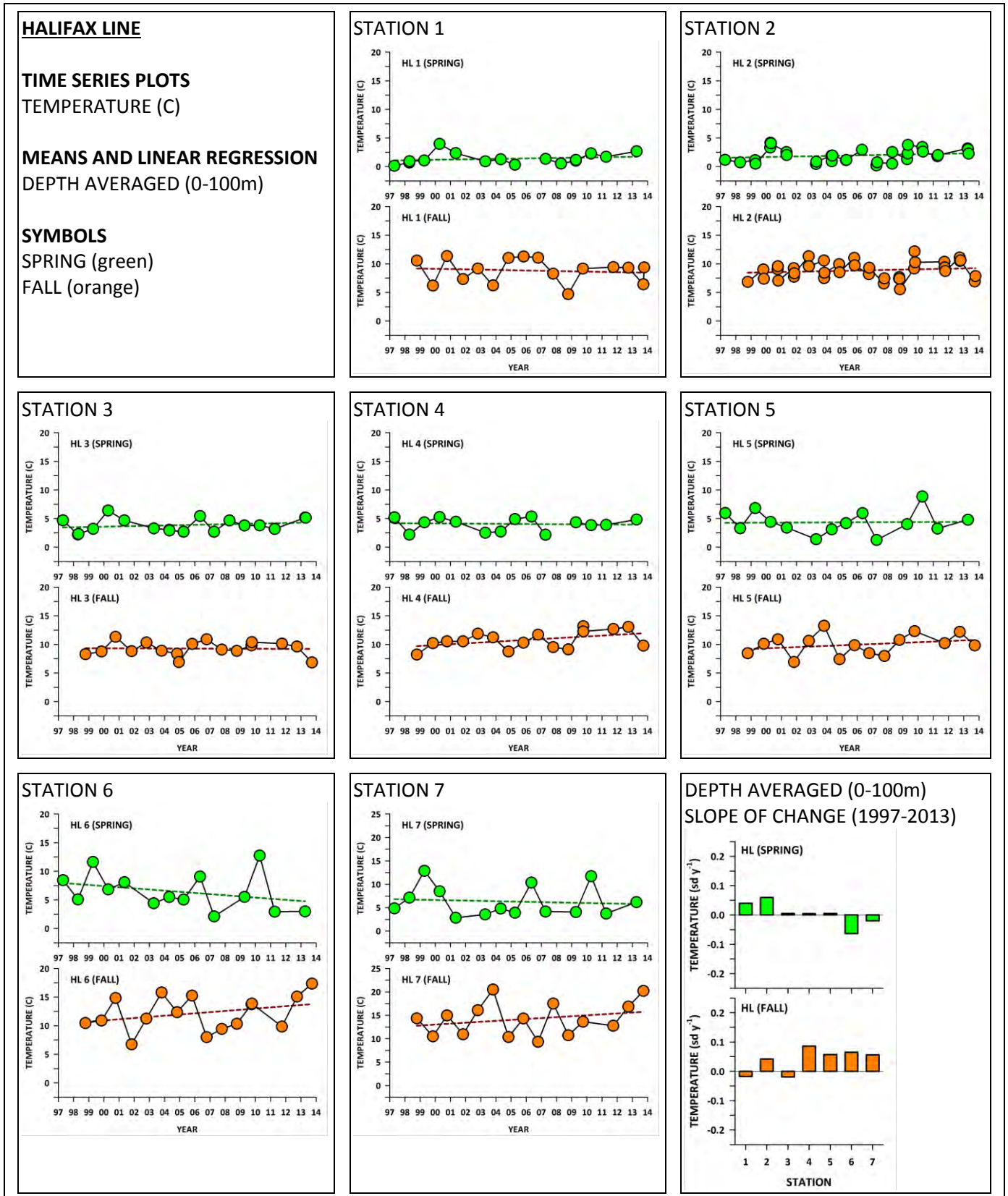


Figure 6

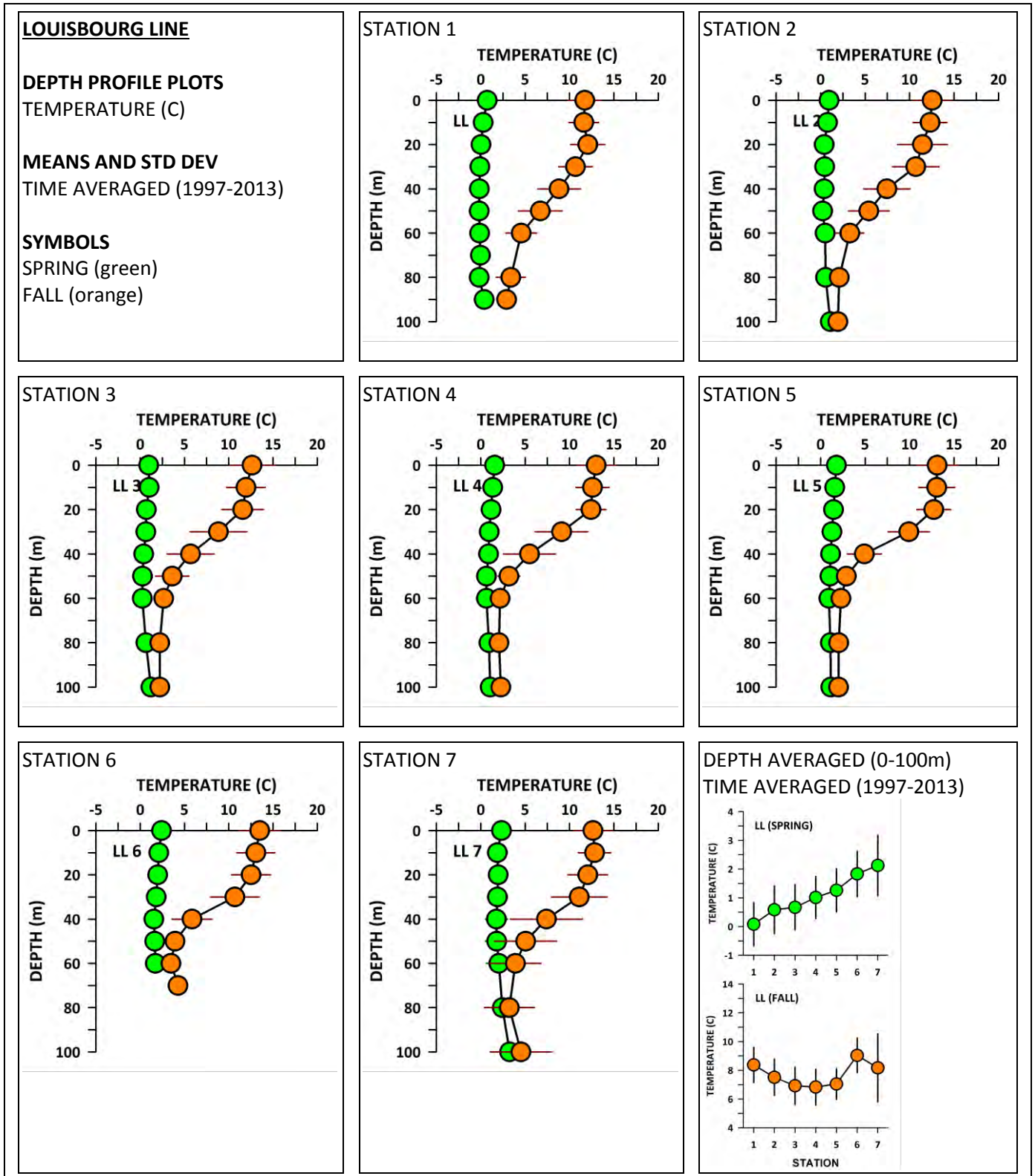


Figure 7

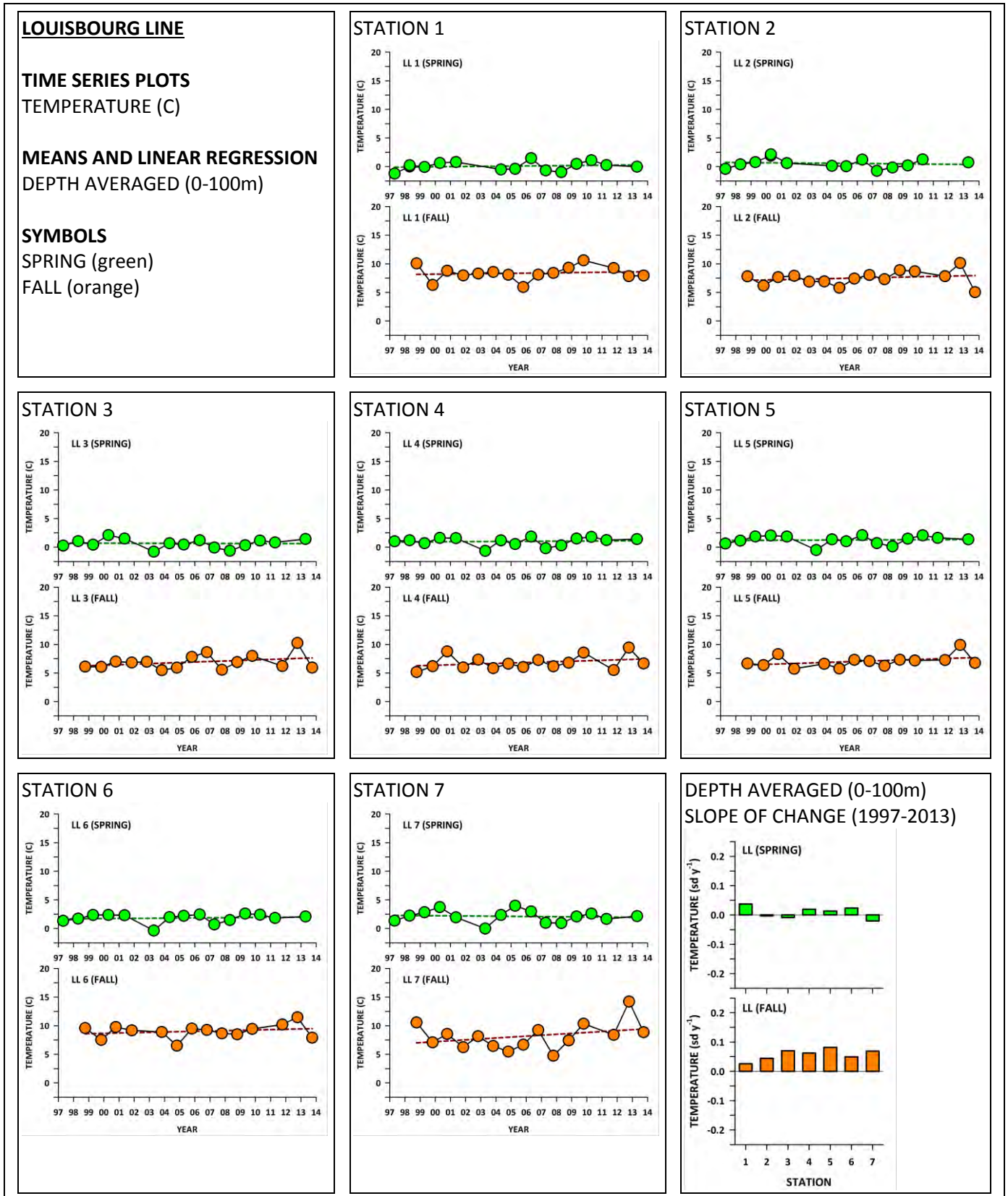


Figure 8

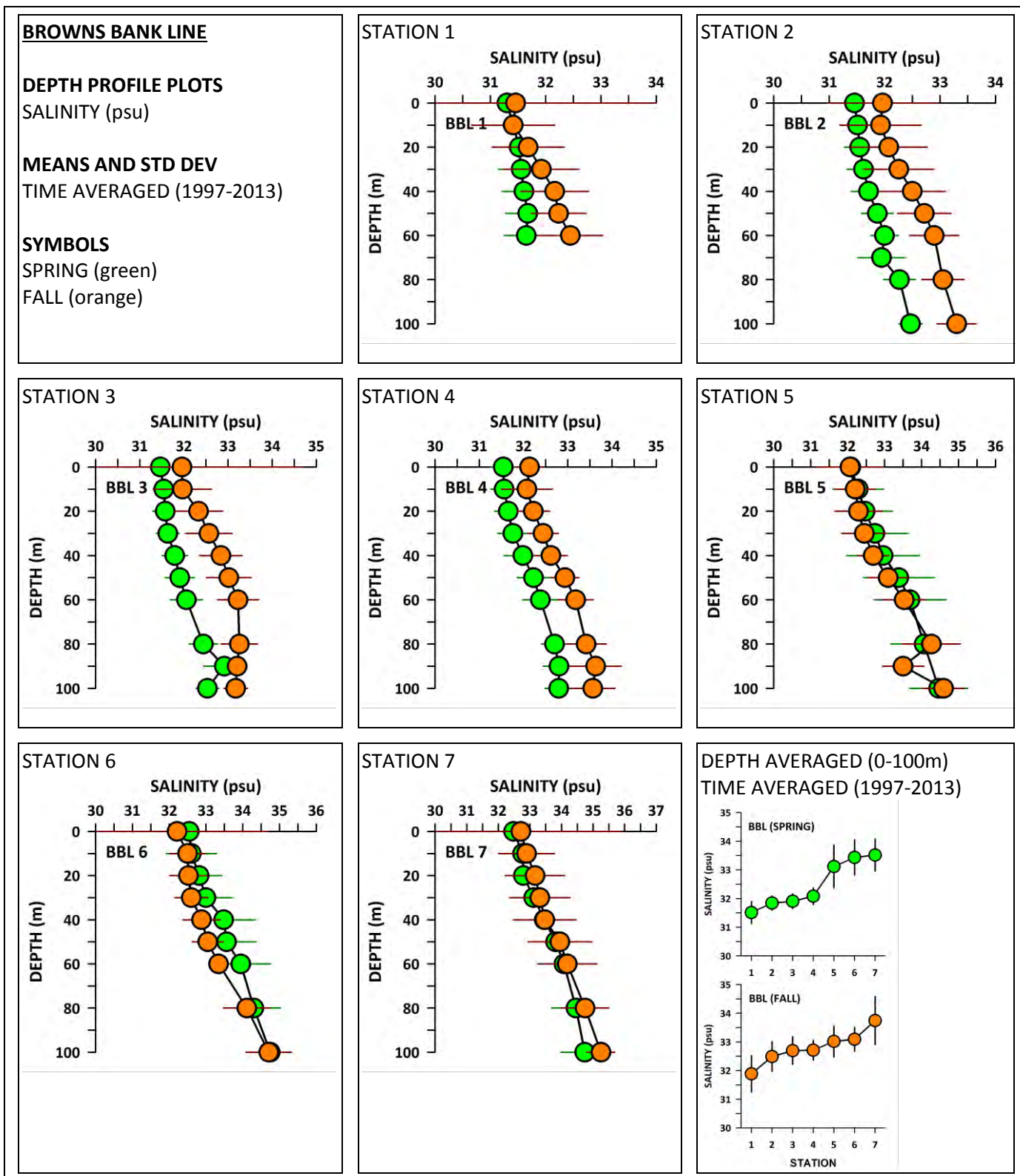


Figure 9

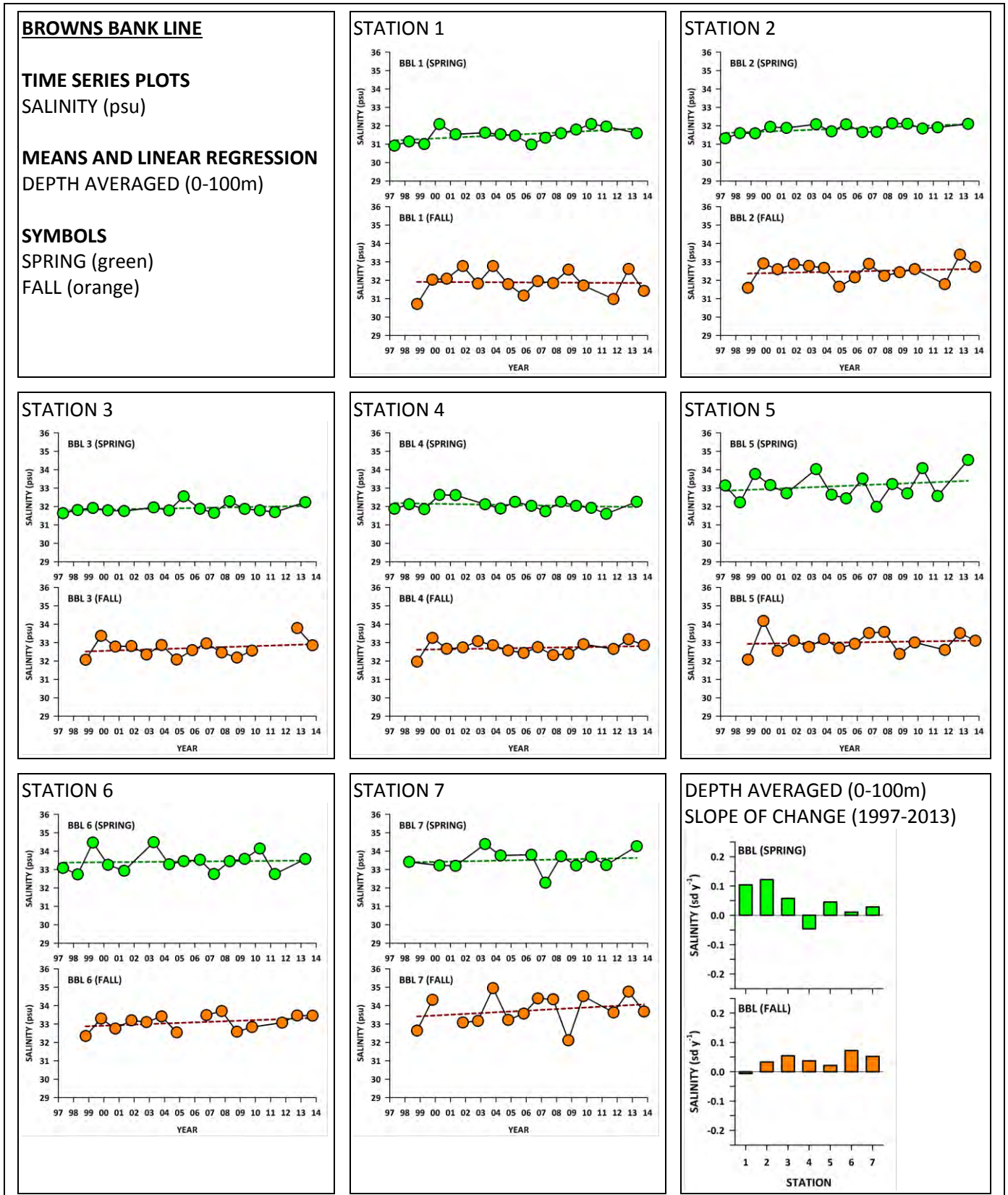


Figure 10

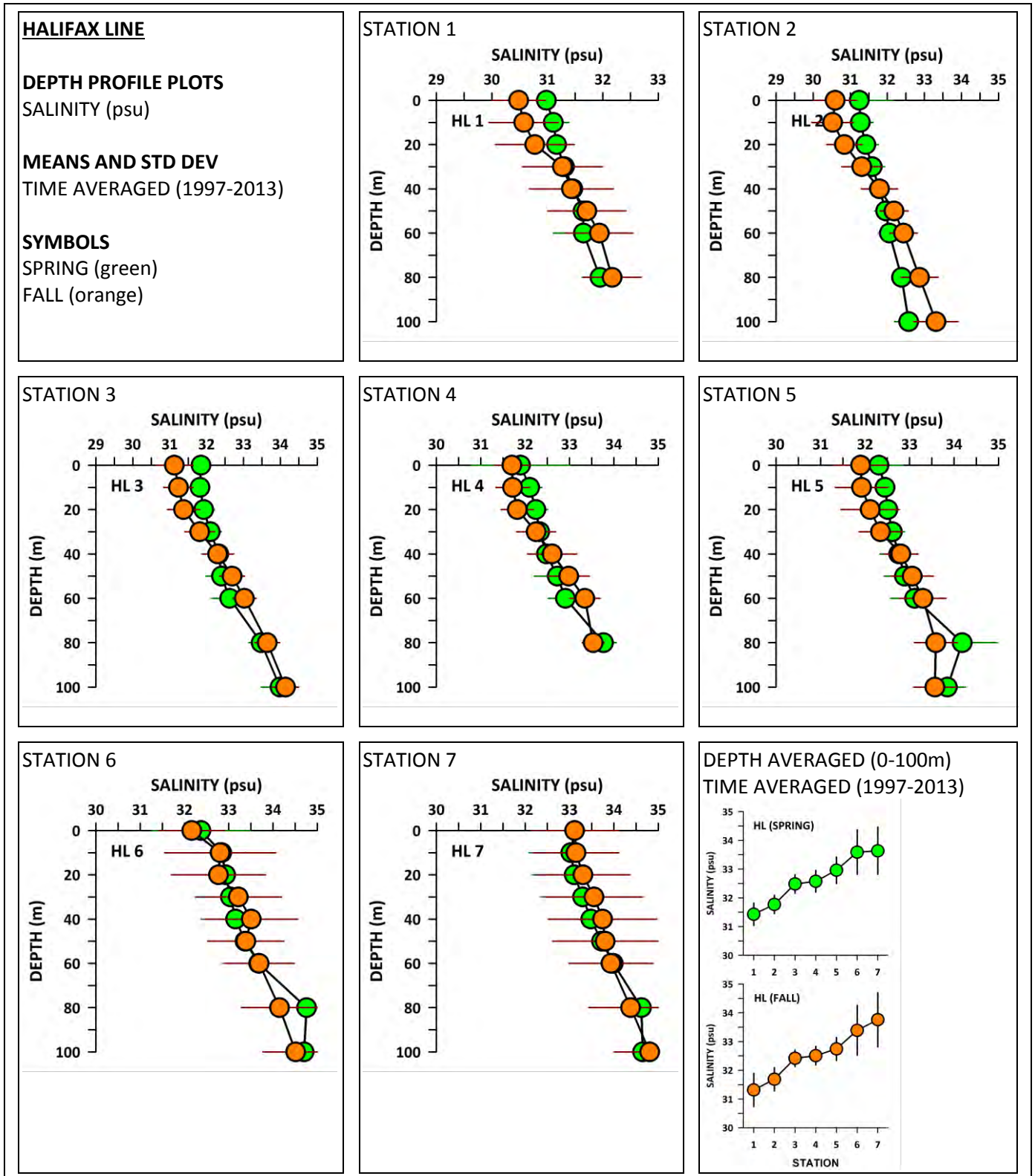


Figure 11

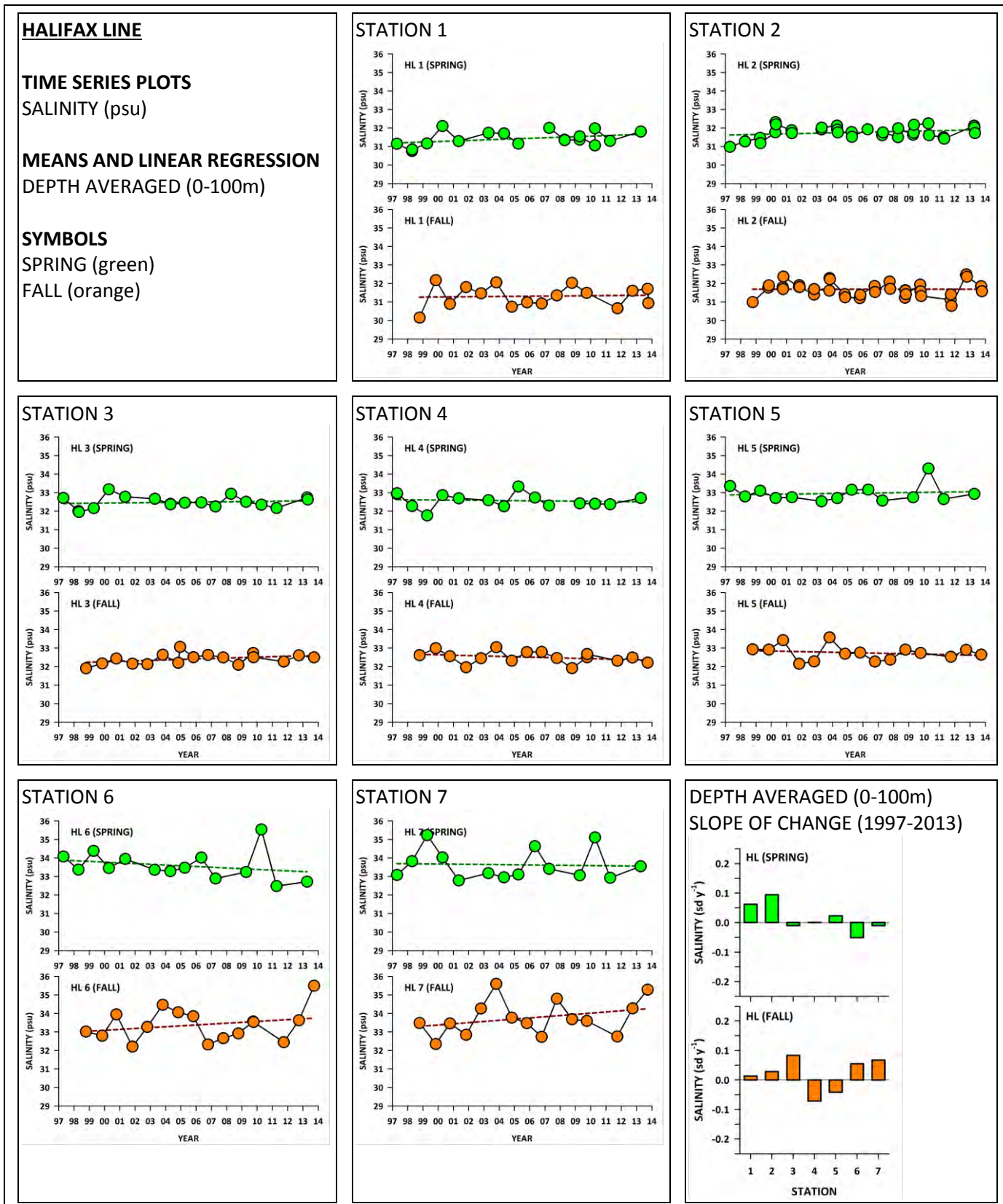


Figure 12

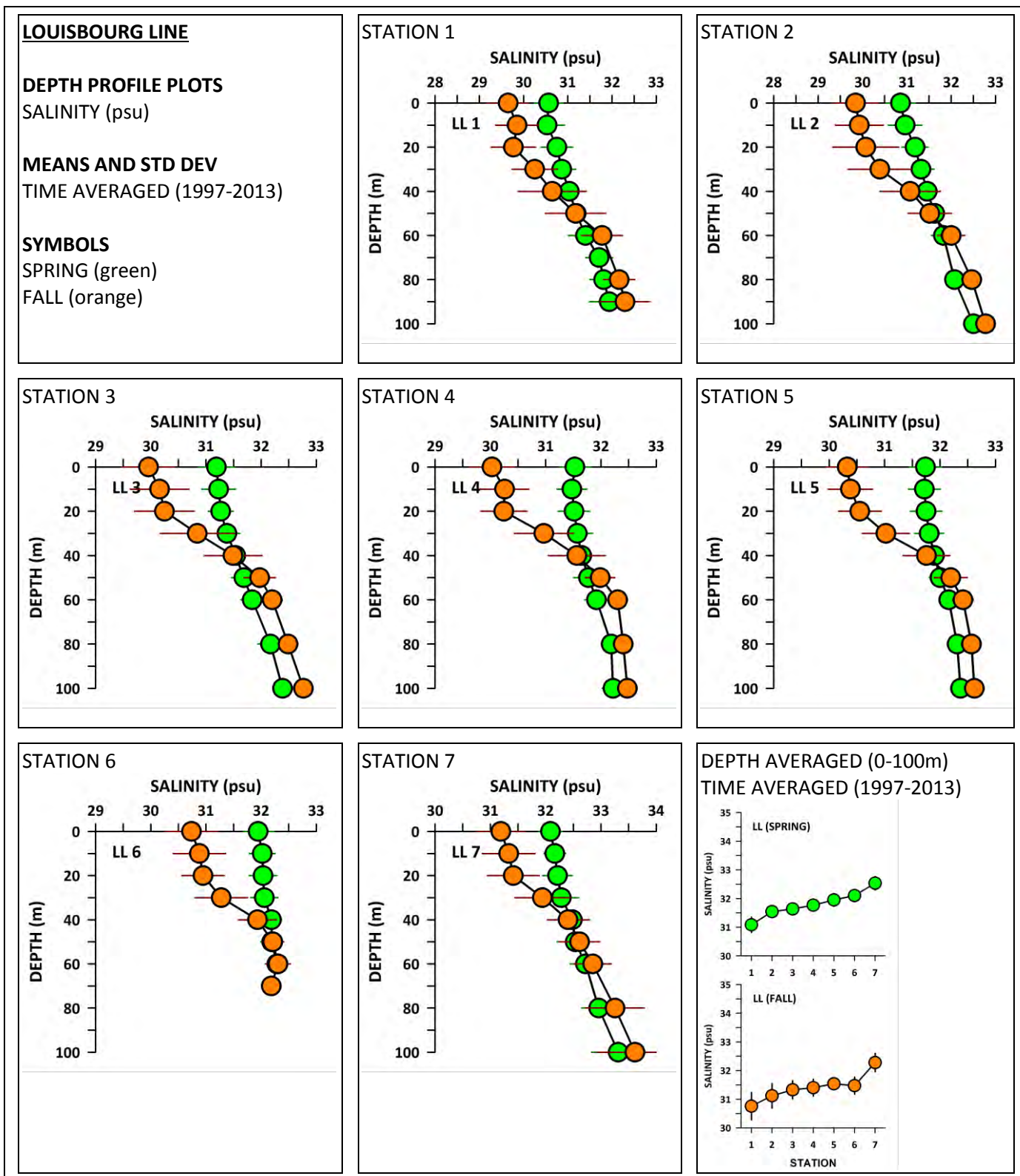


Figure 13

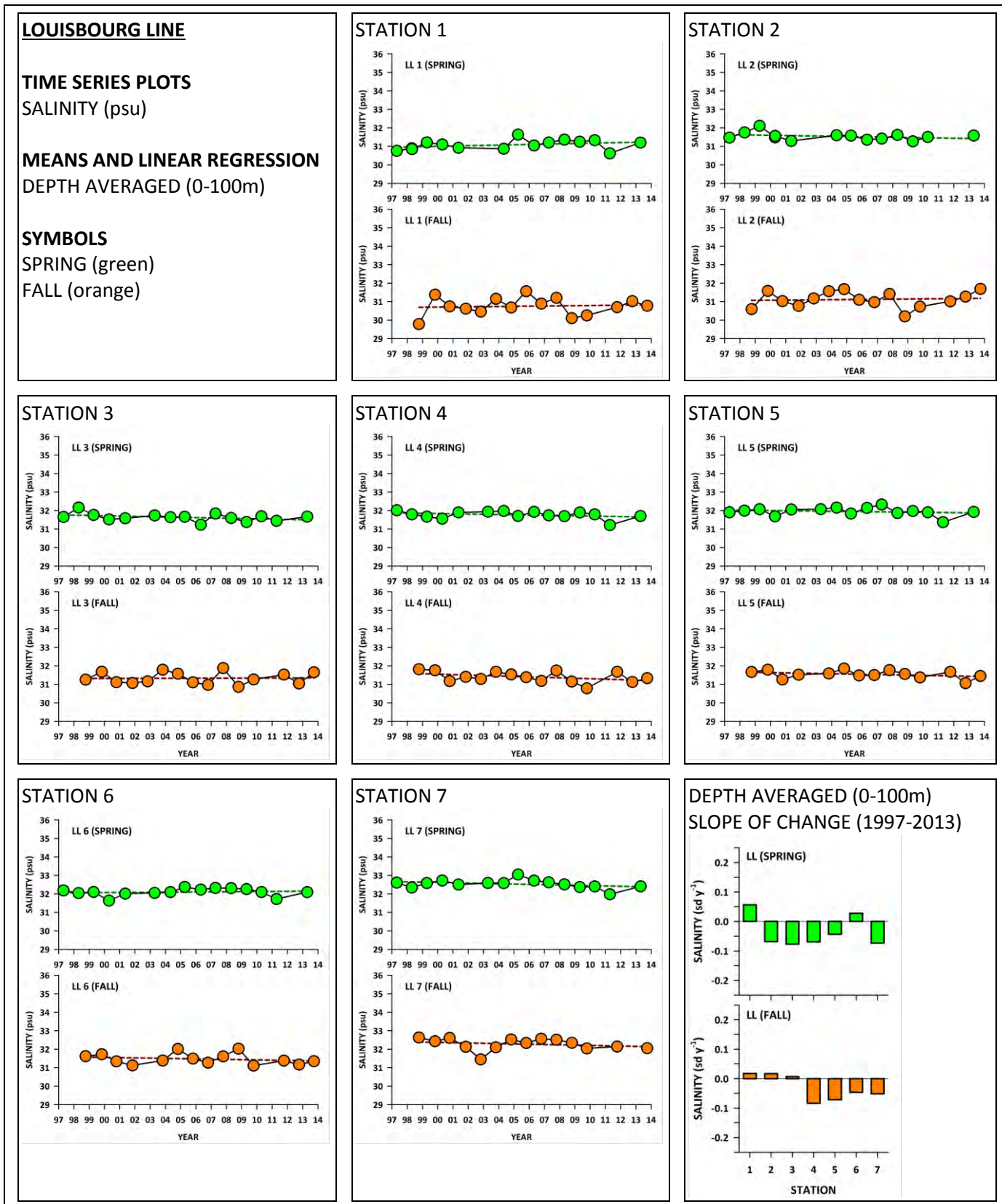


Figure 14

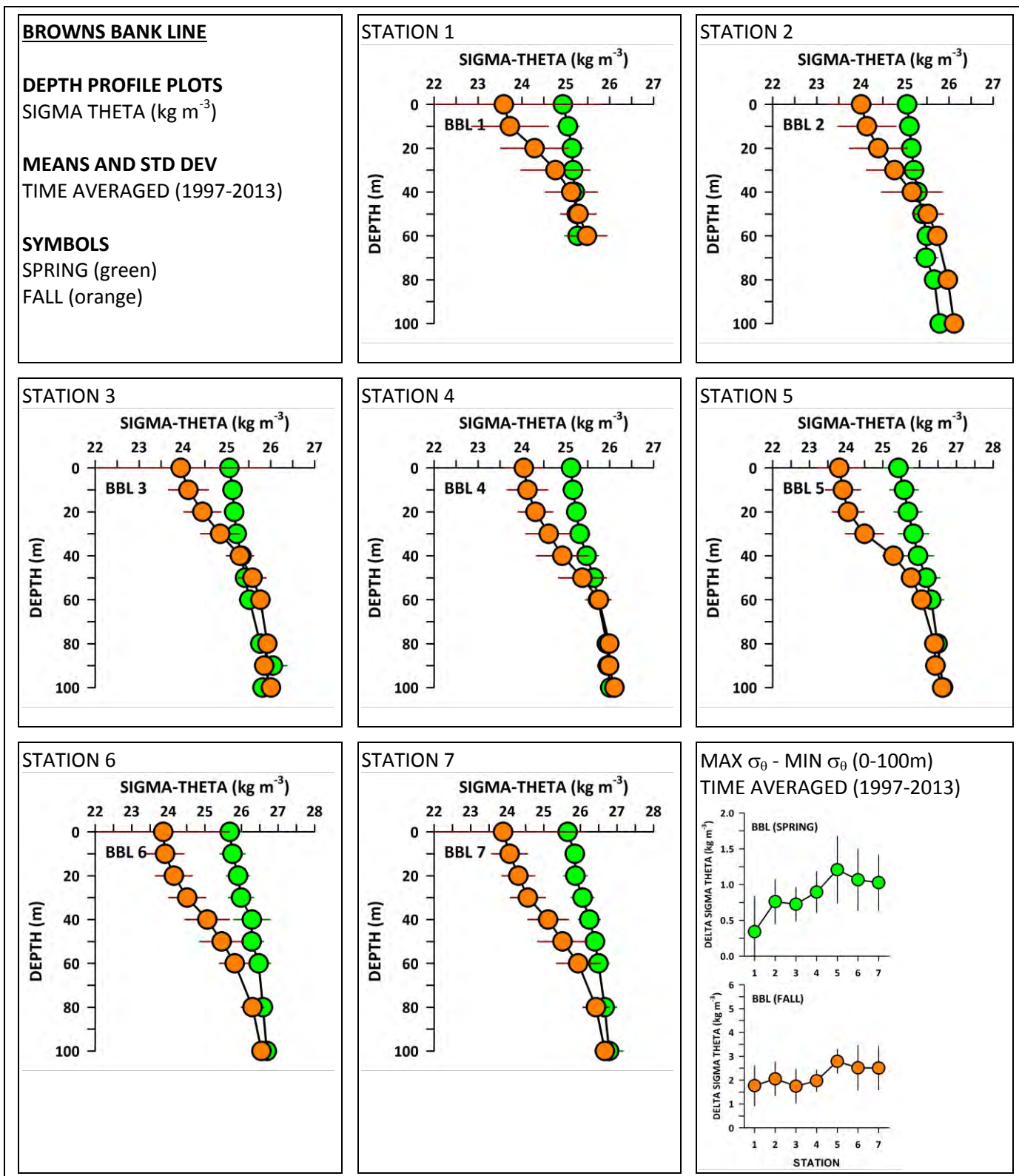


Figure 15

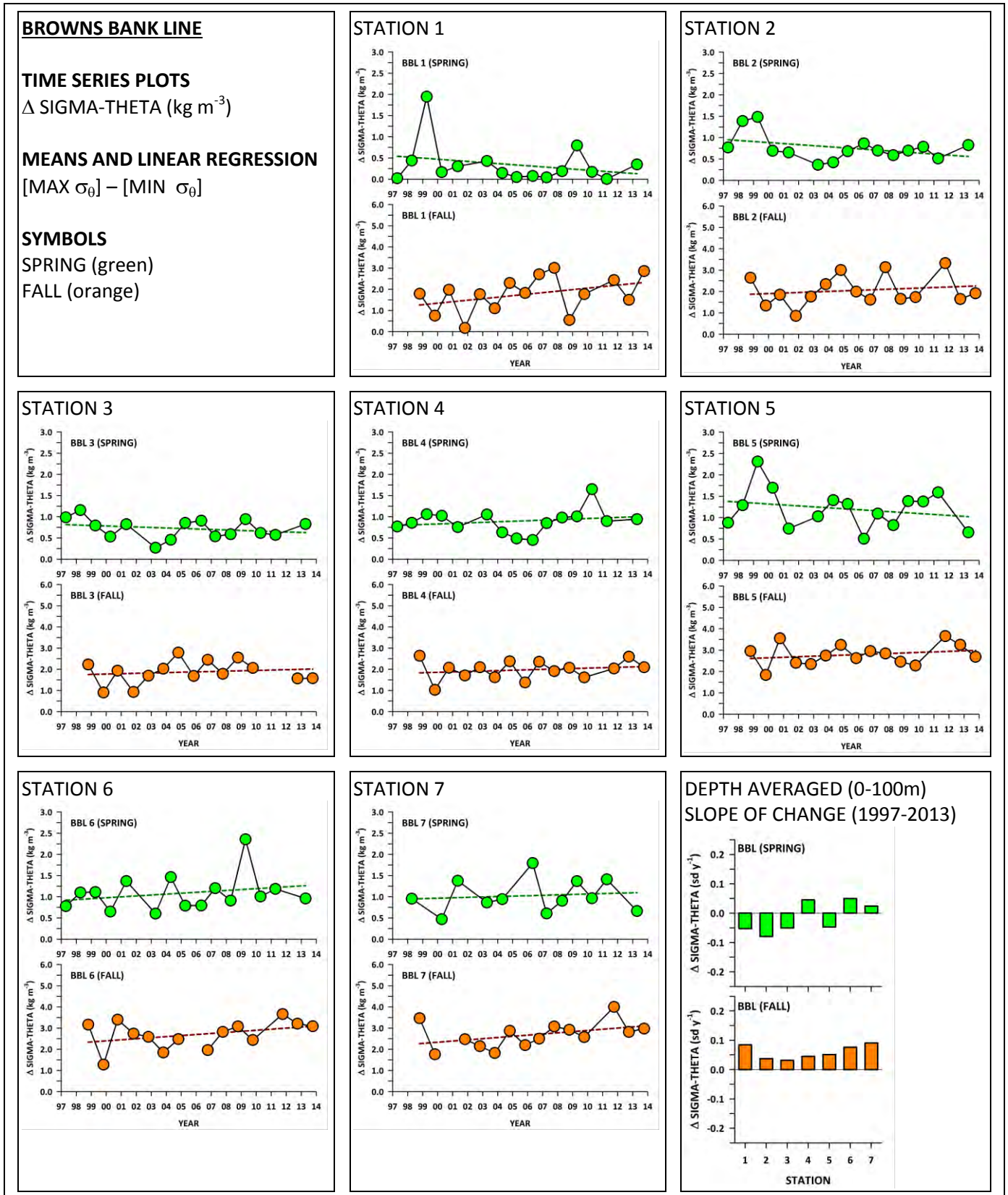


Figure 16

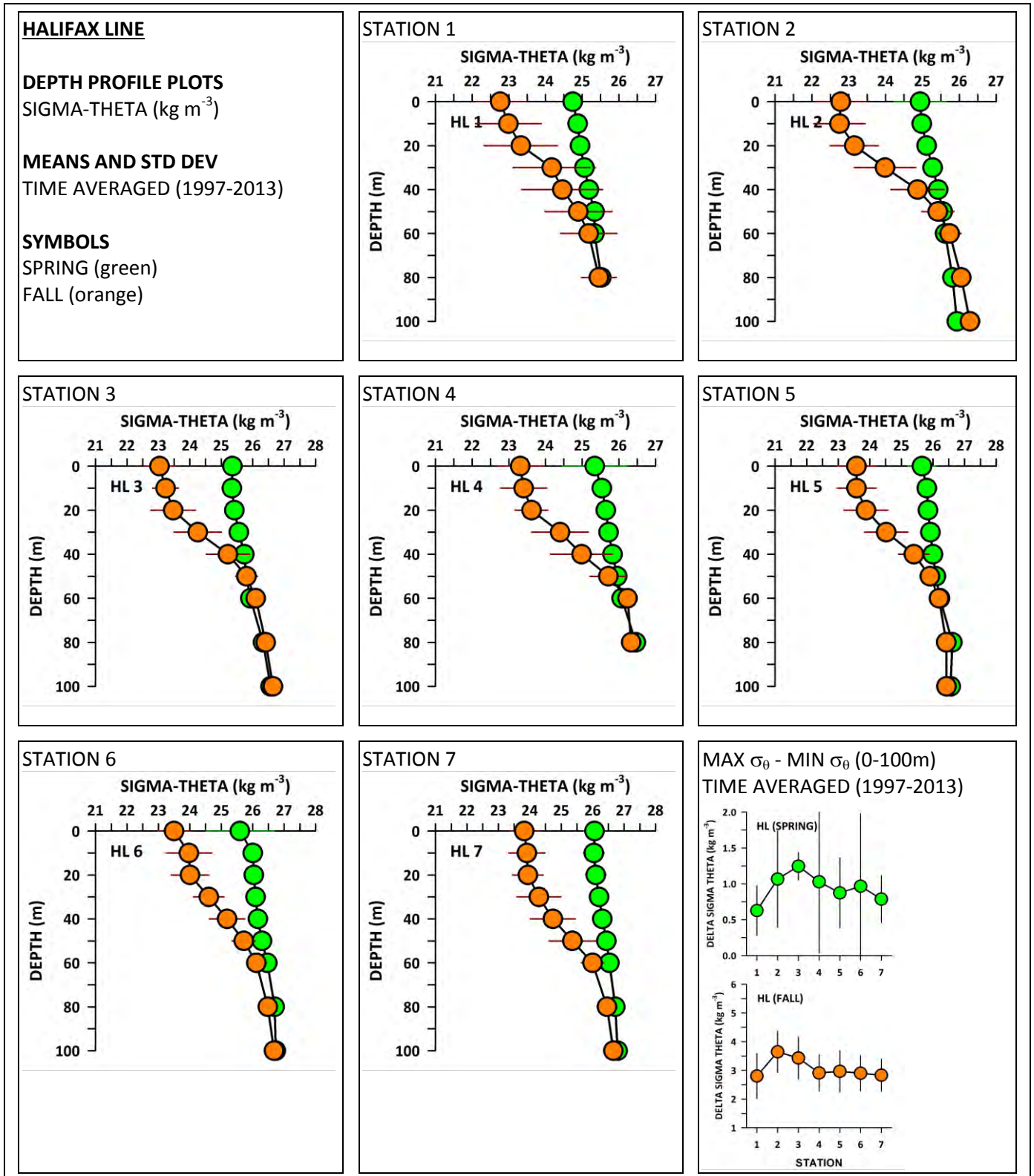


Figure 17

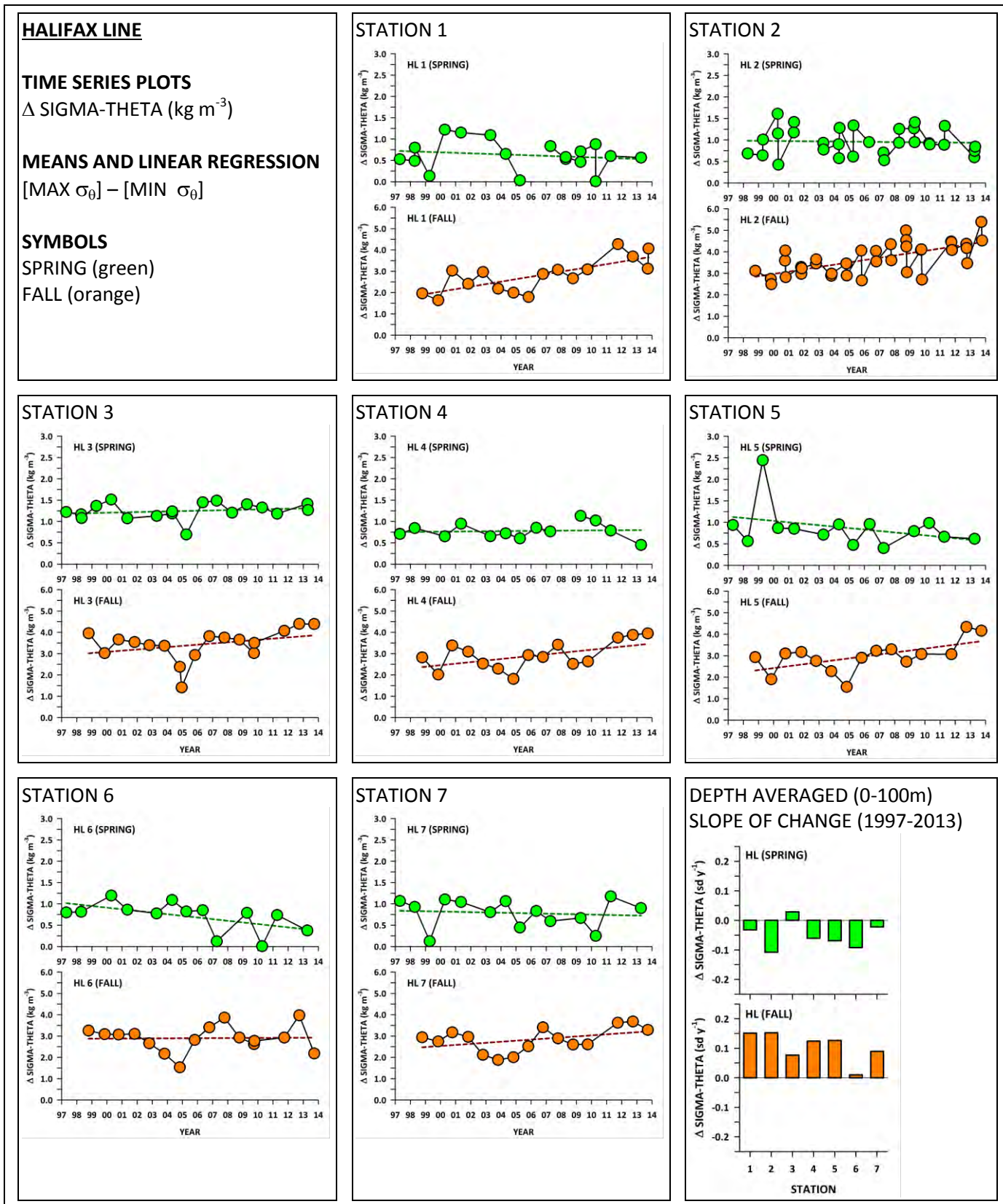


Figure 18

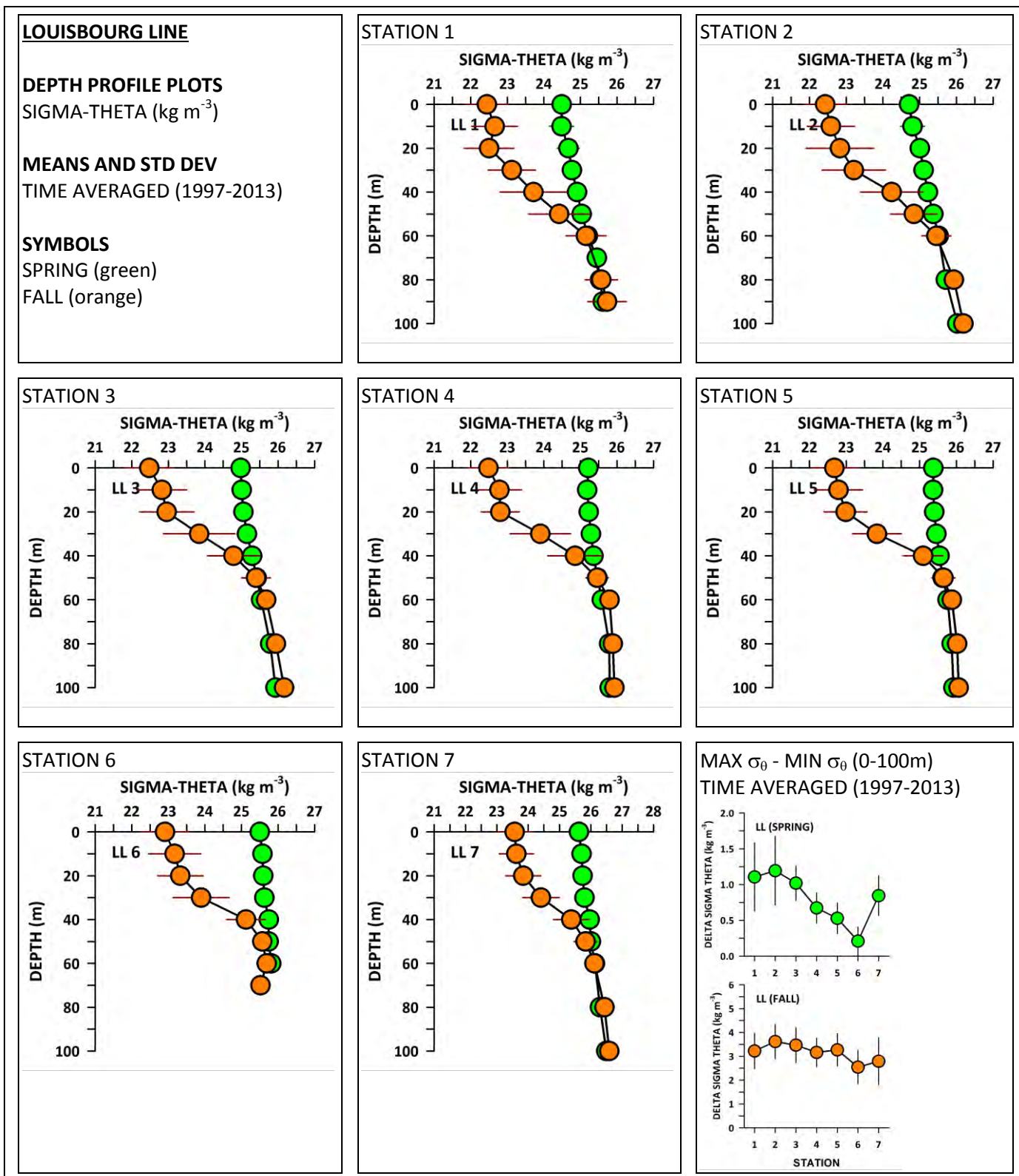


Figure 19

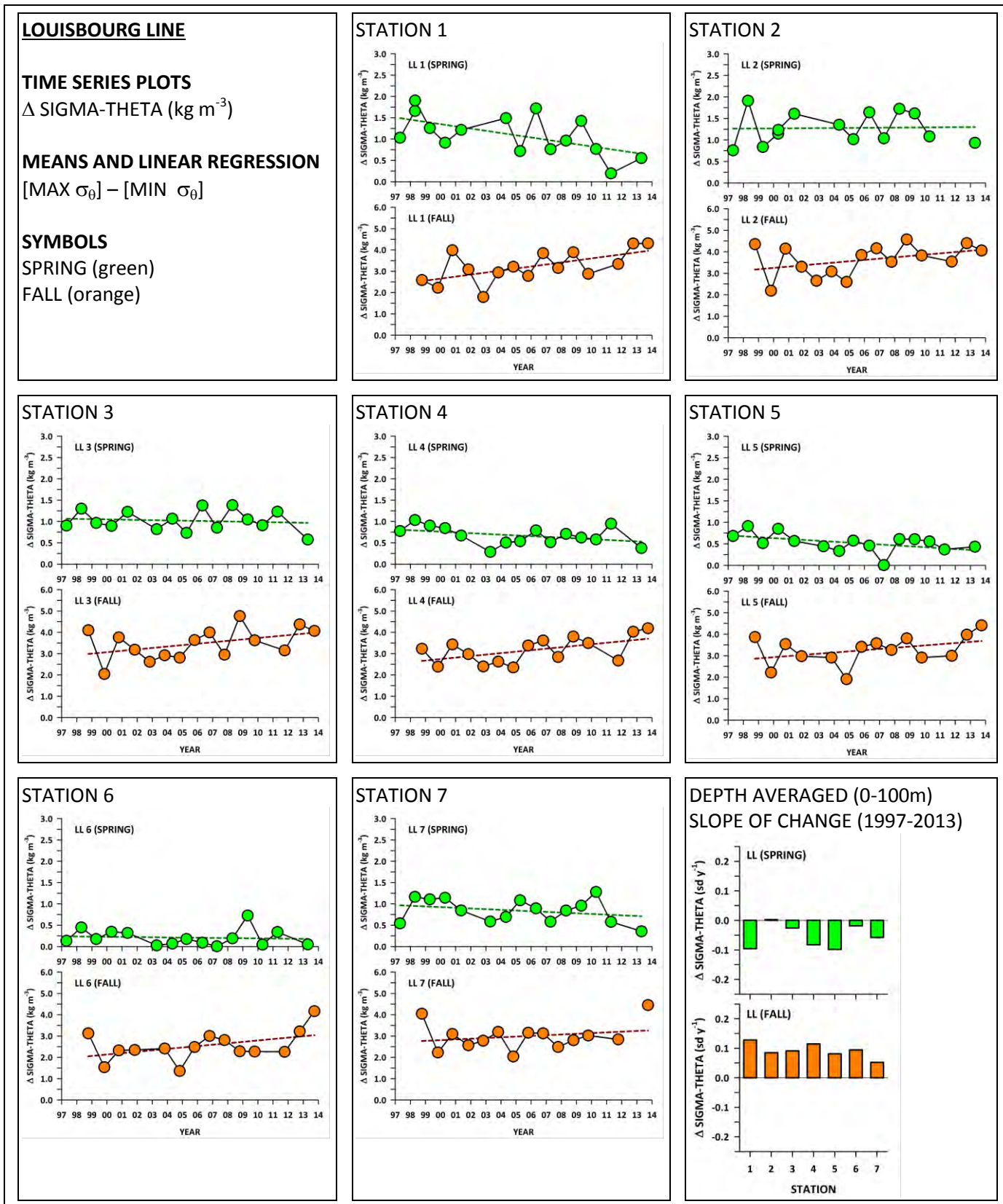


Figure 20

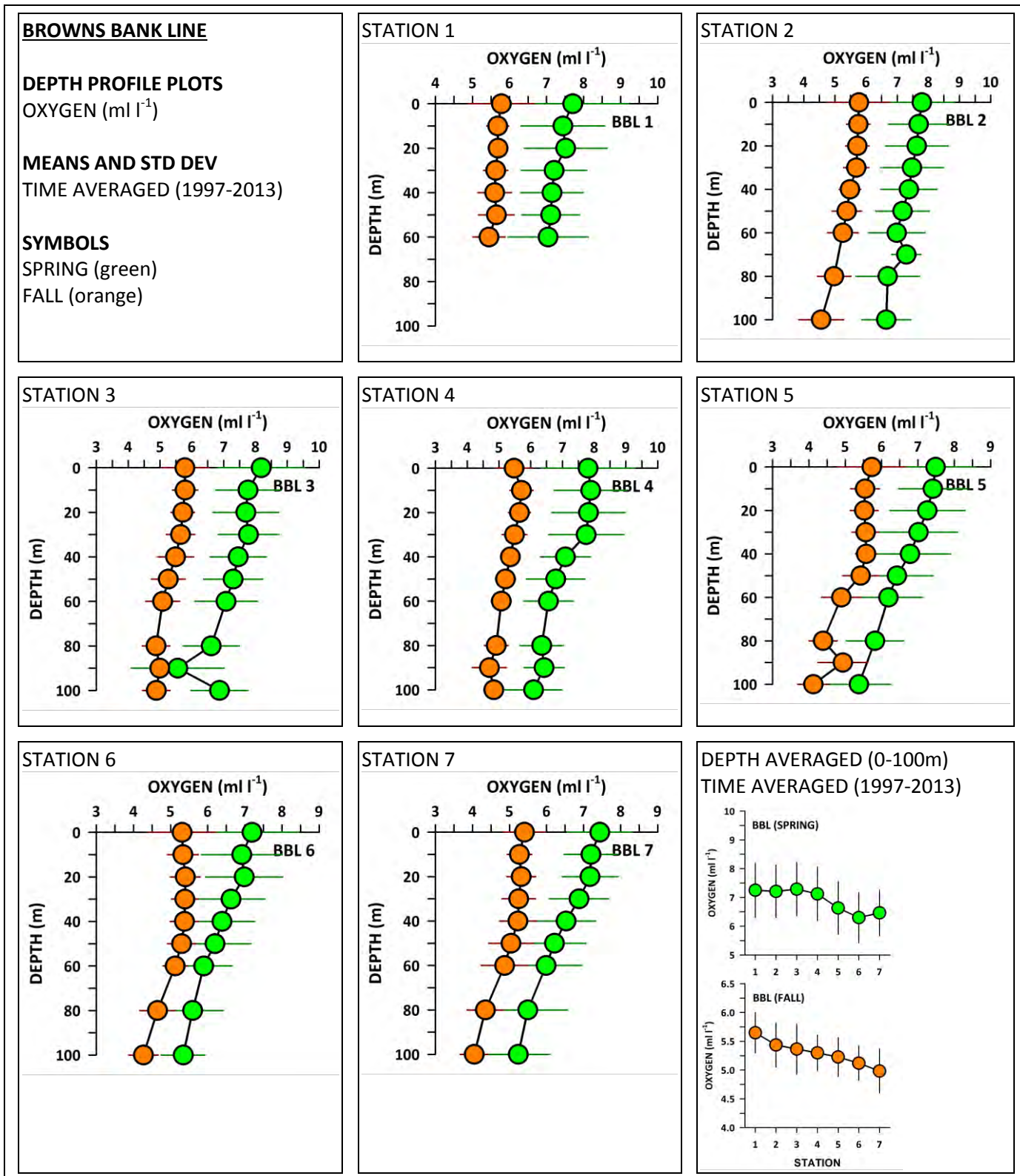


Figure 21

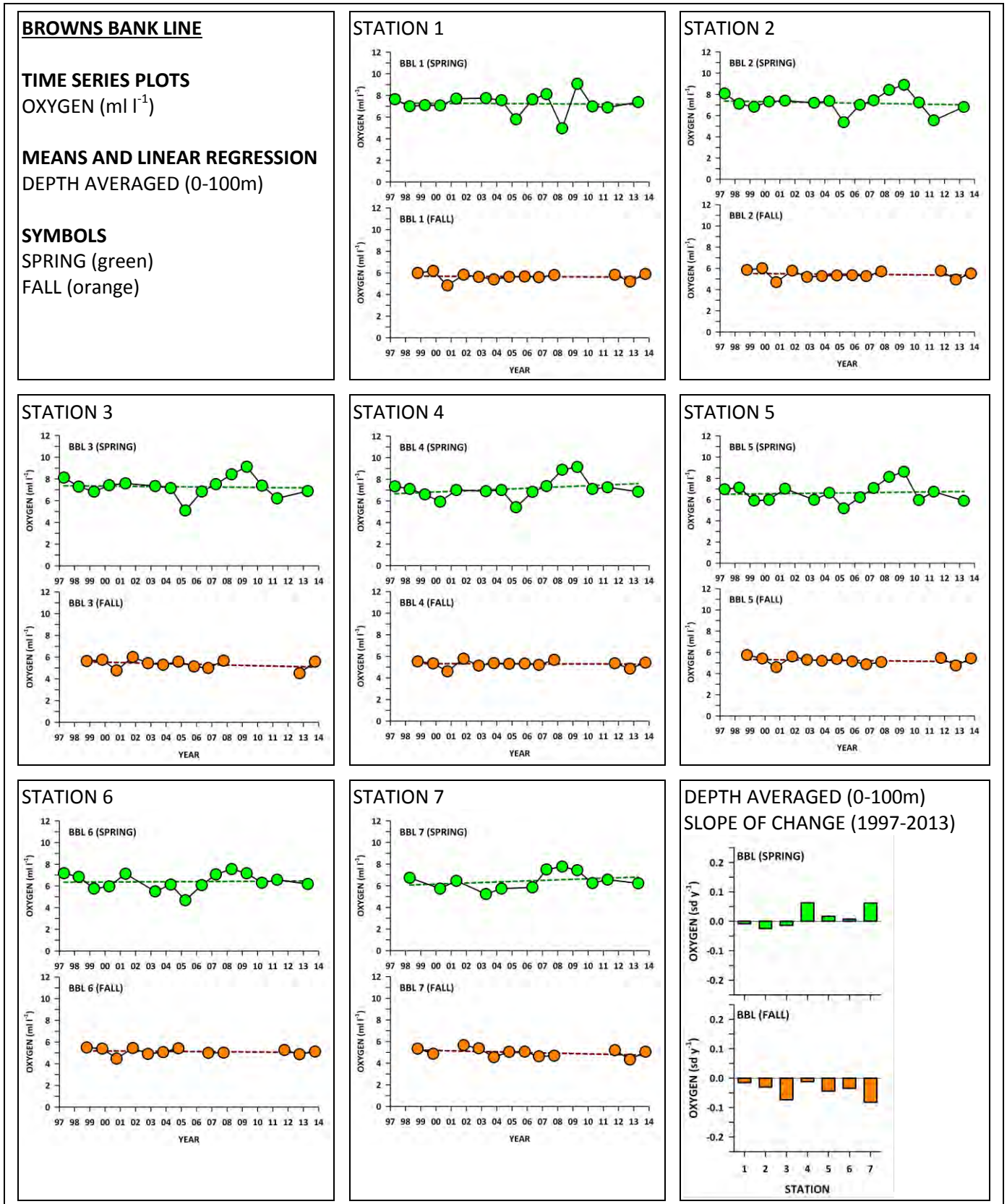


Figure 22

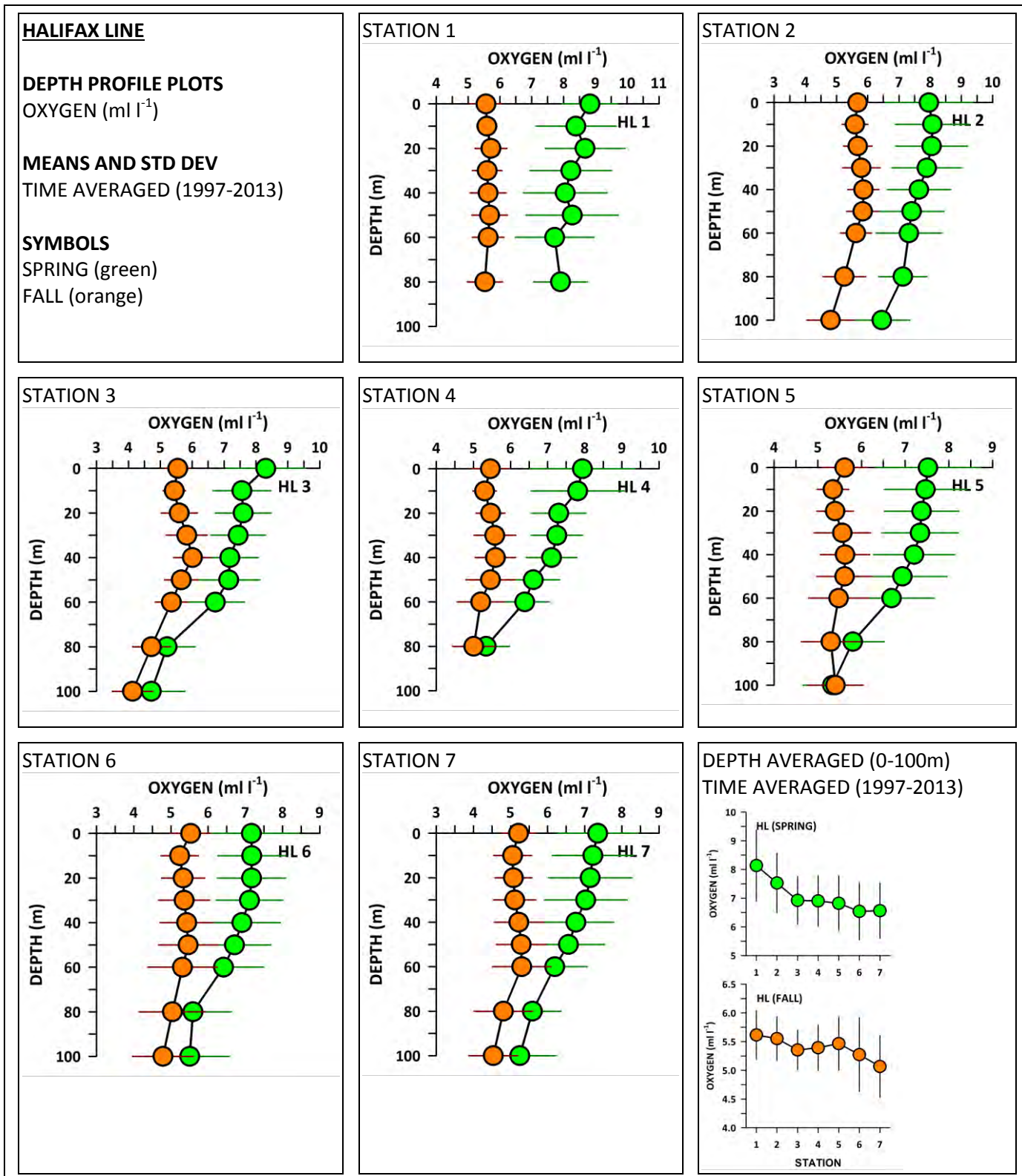


Figure 23

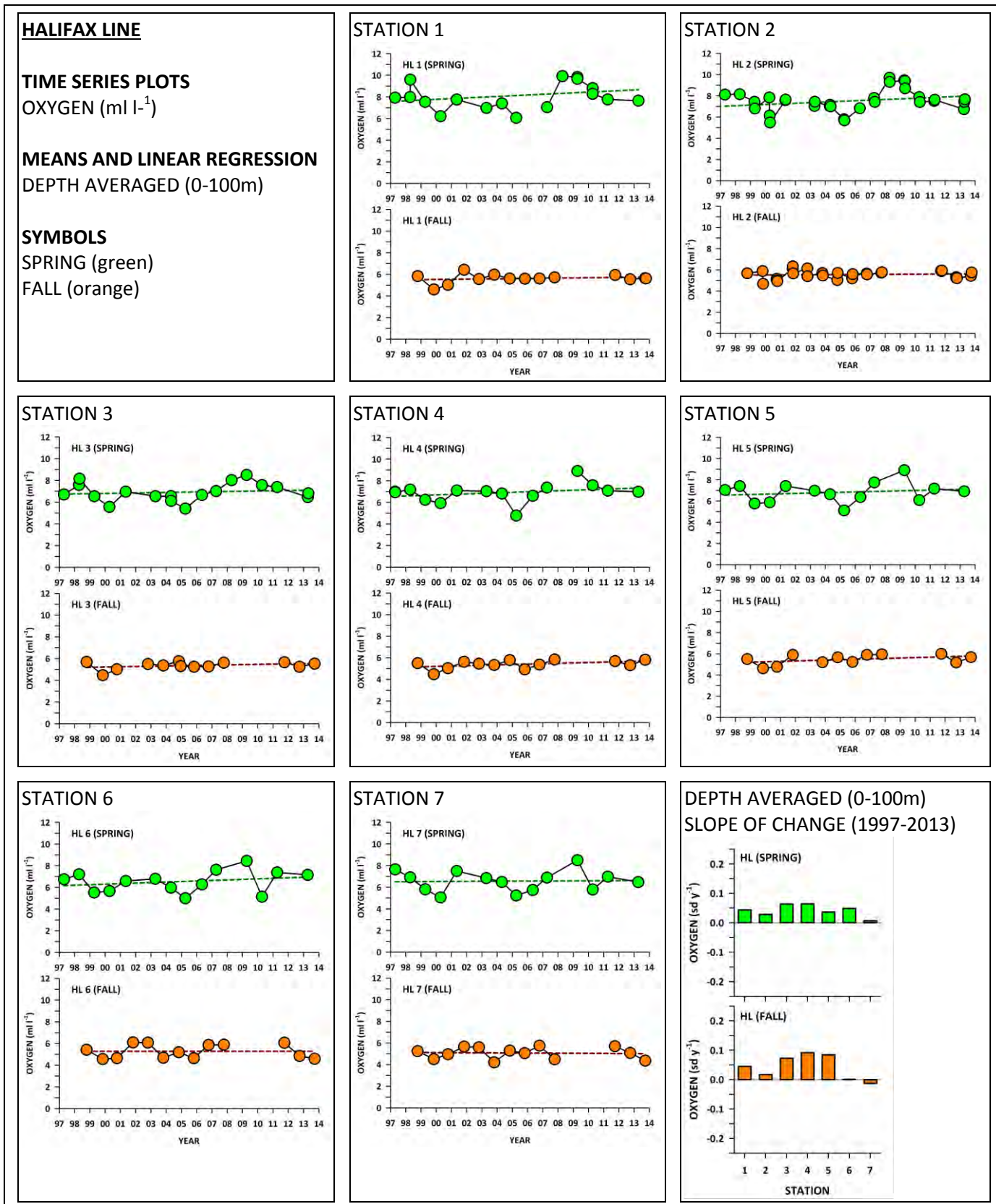


Figure 24

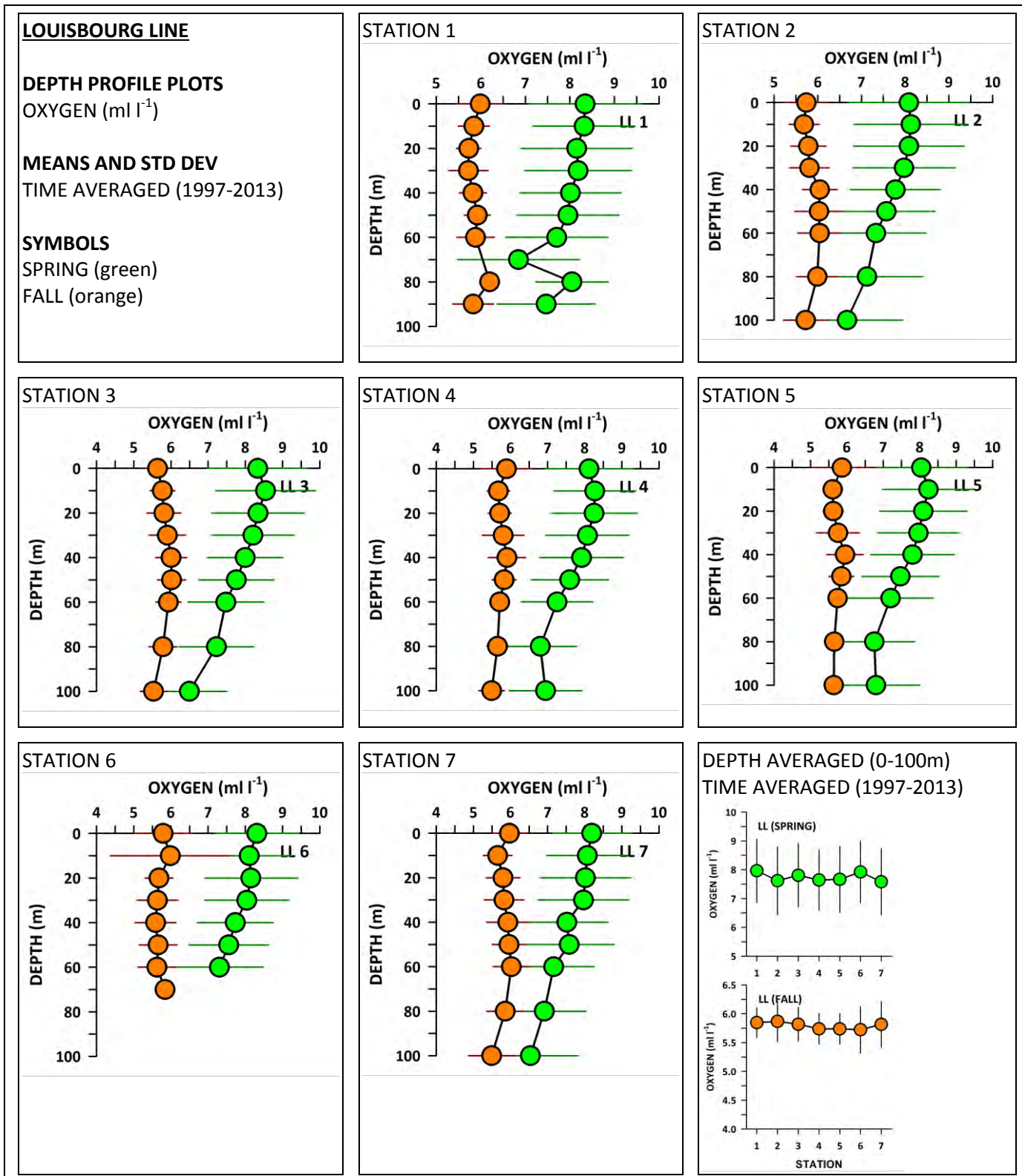


Figure 25

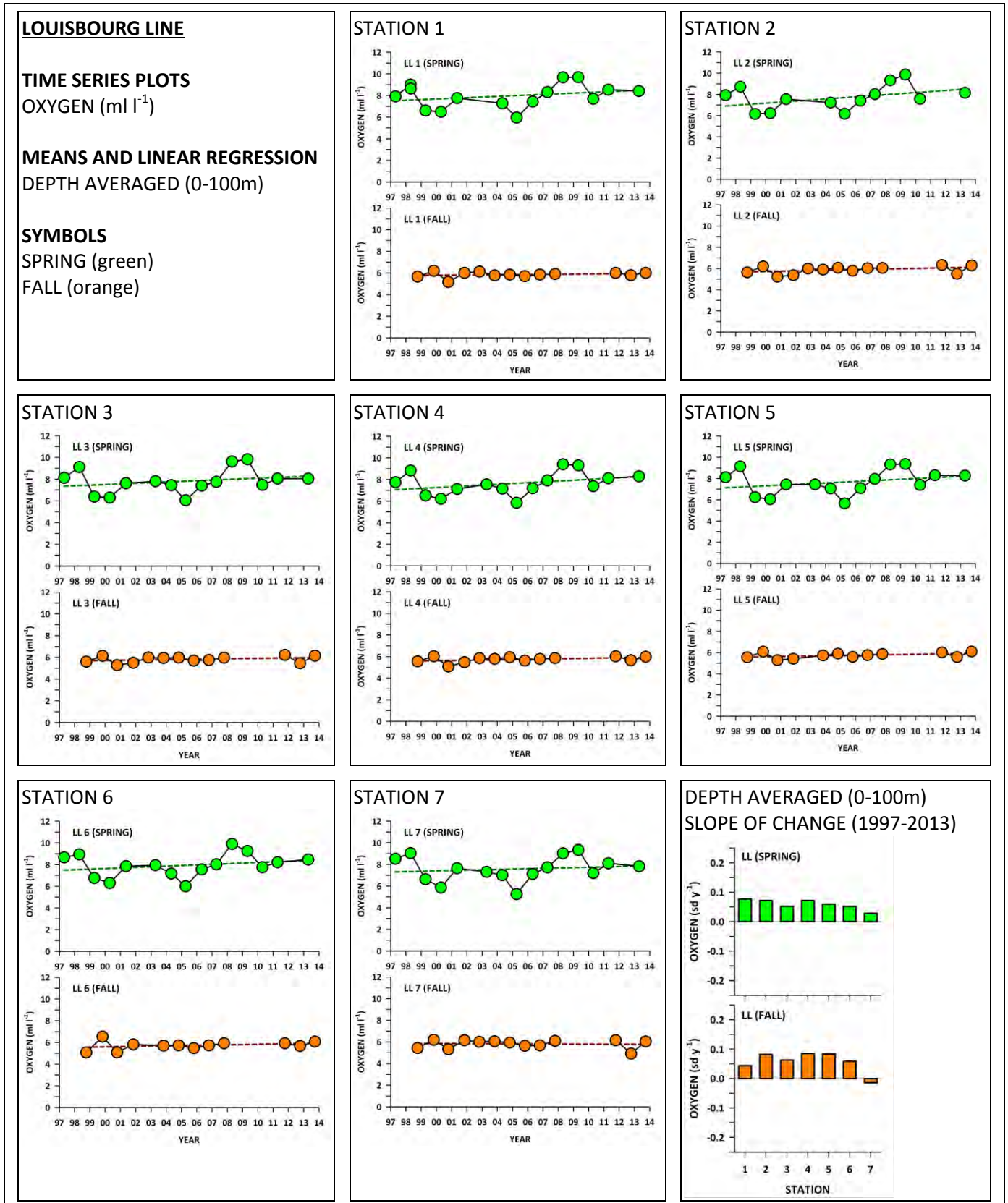


Figure 26

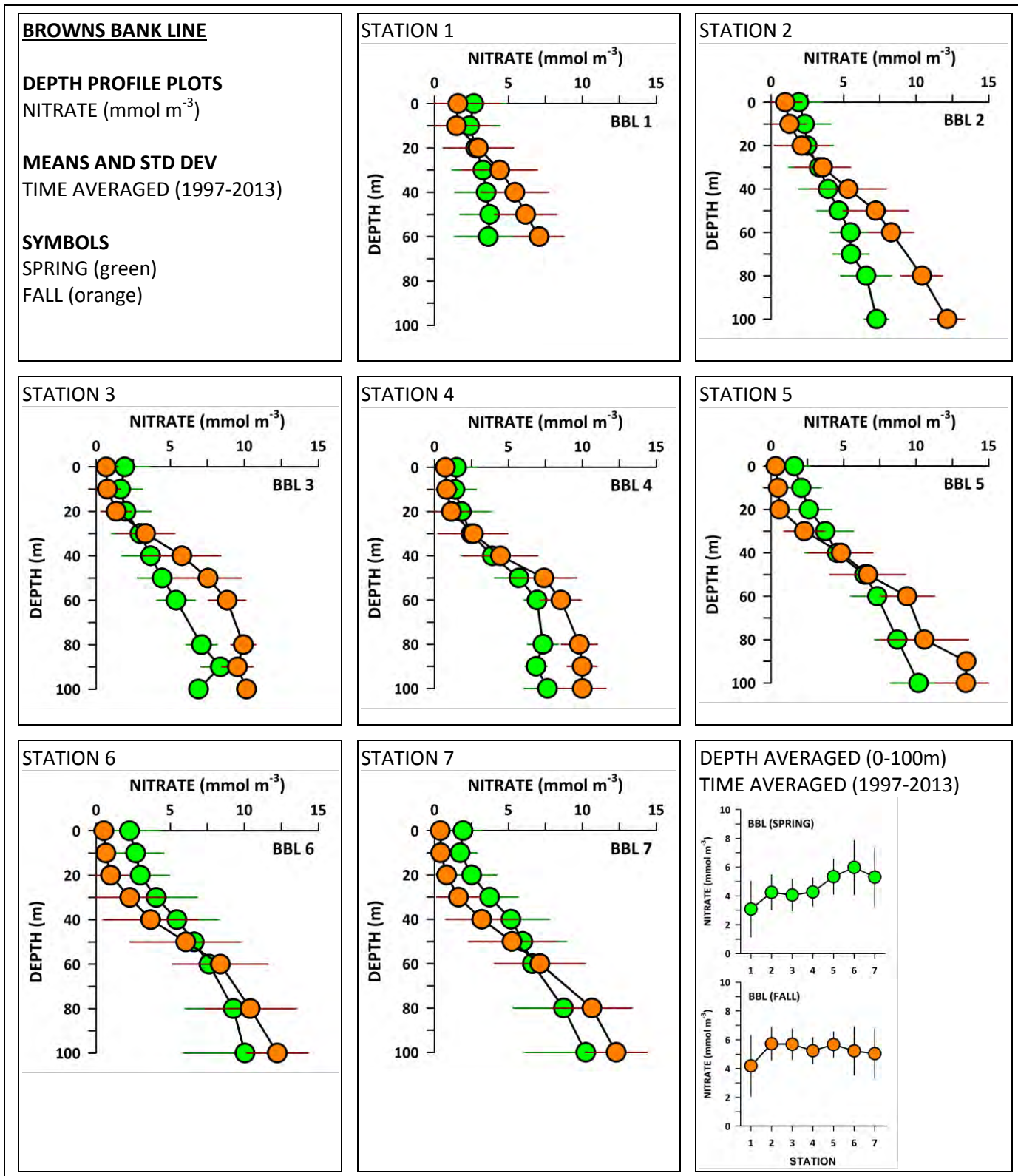


Figure 27

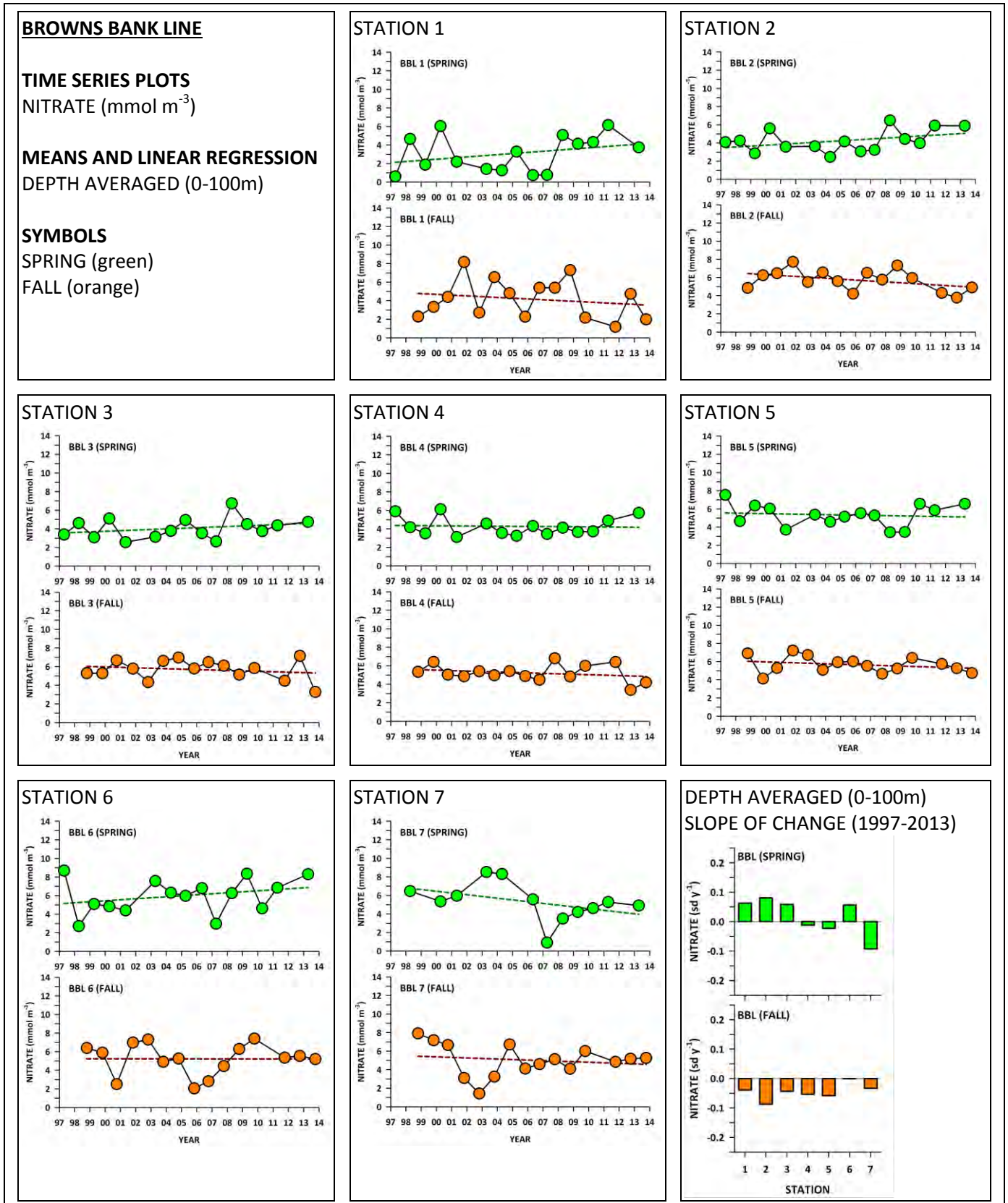


Figure 28

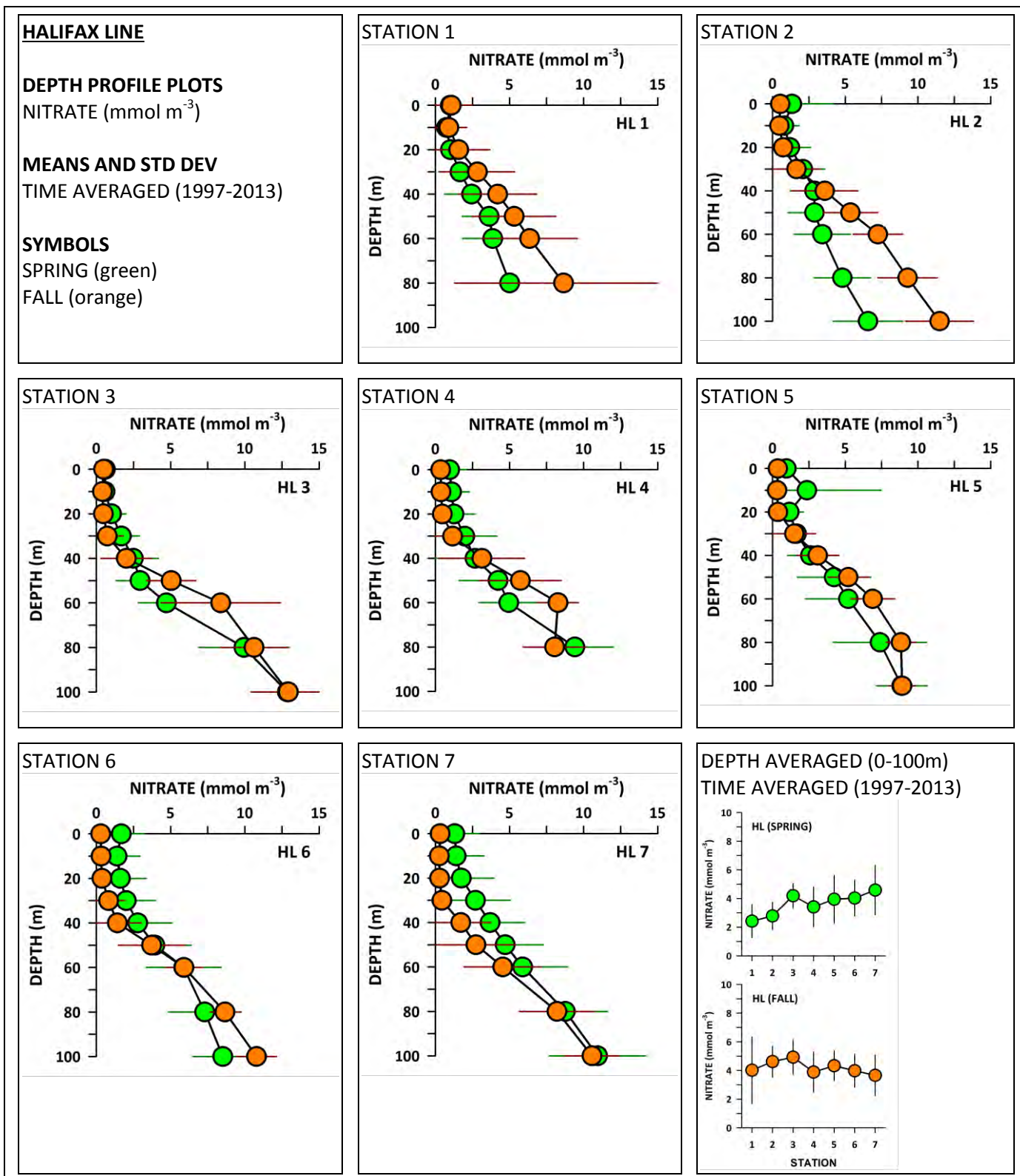


Figure 29

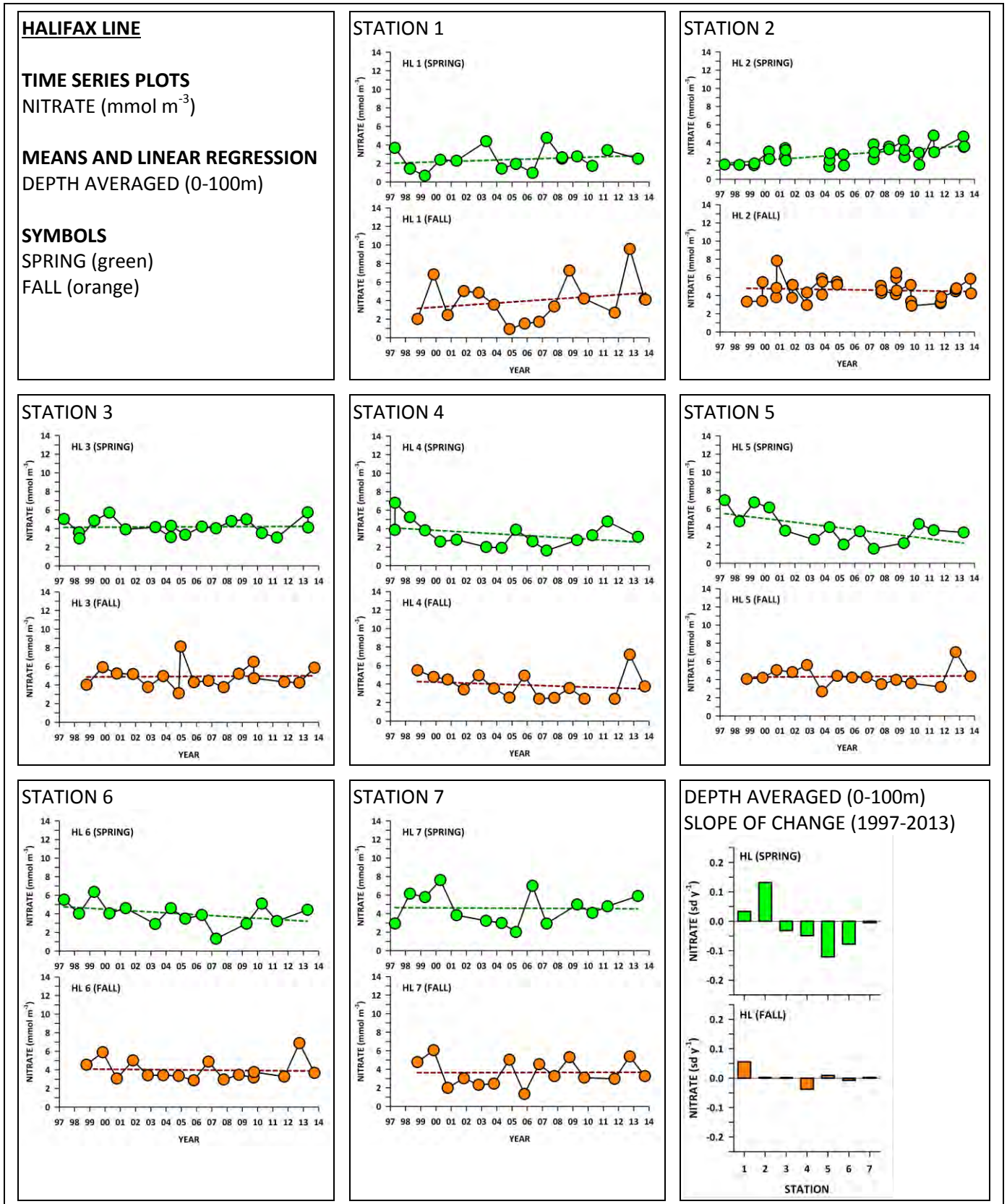


Figure 30

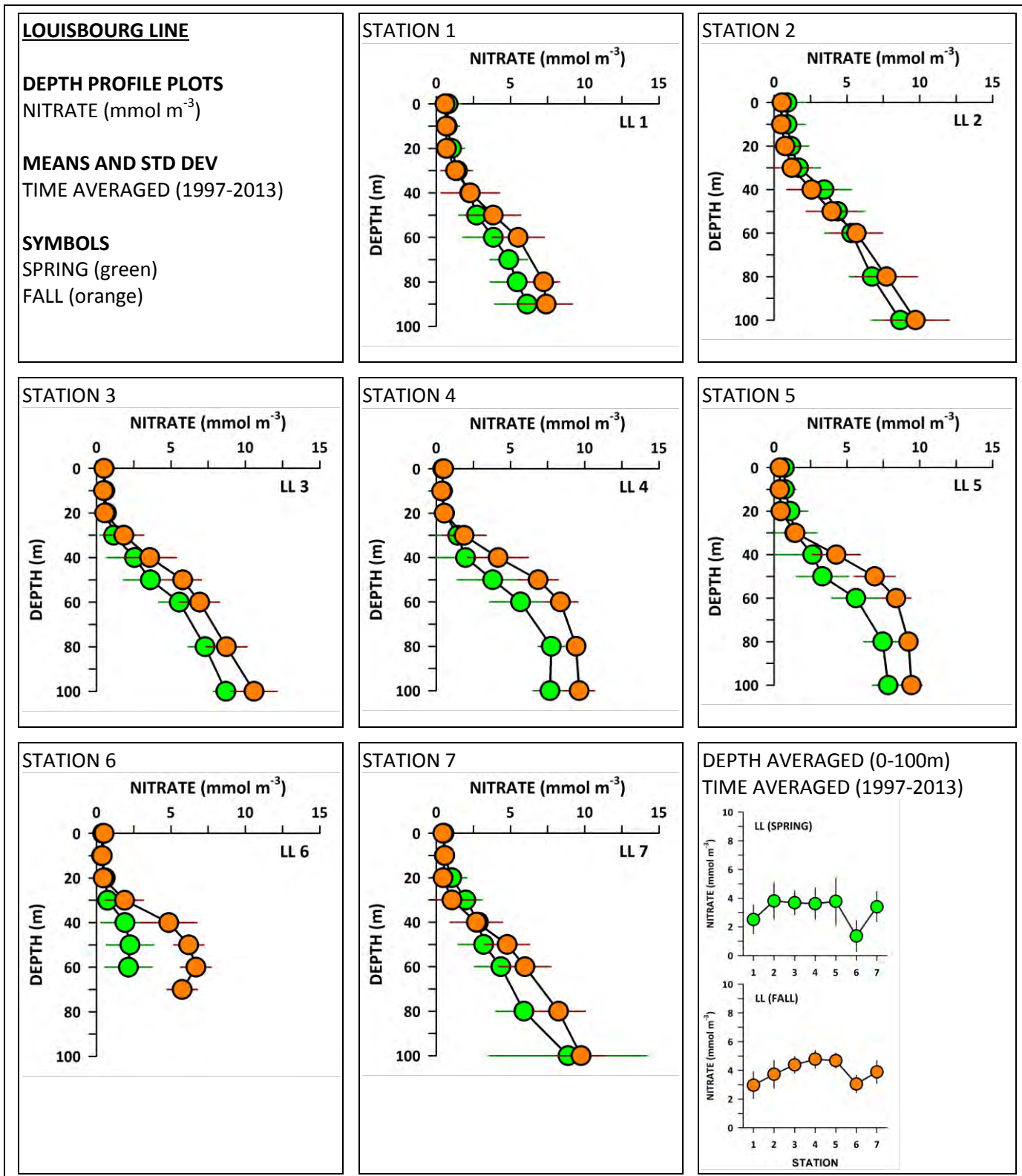


Figure 31

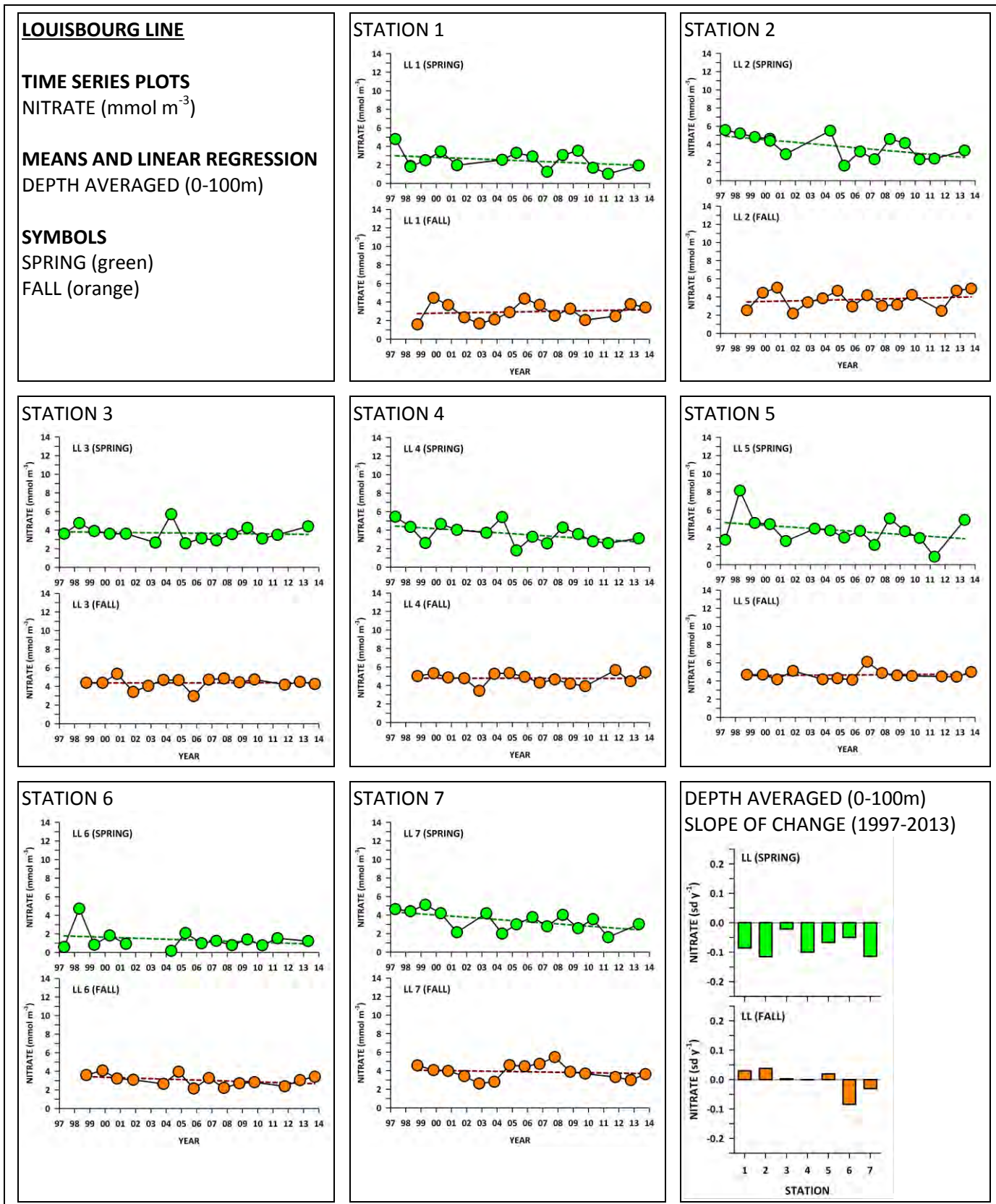


Figure 32

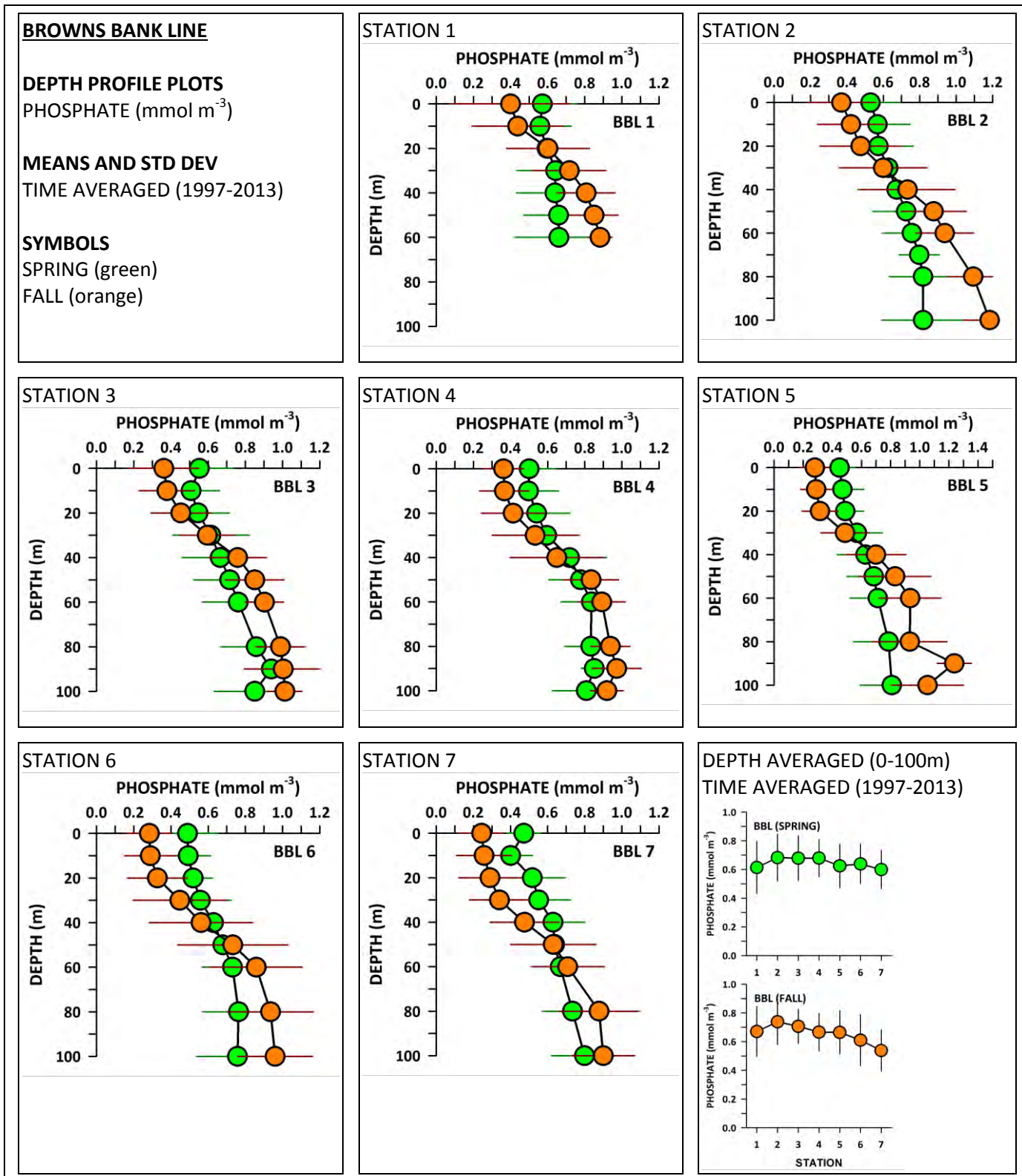


Figure 33

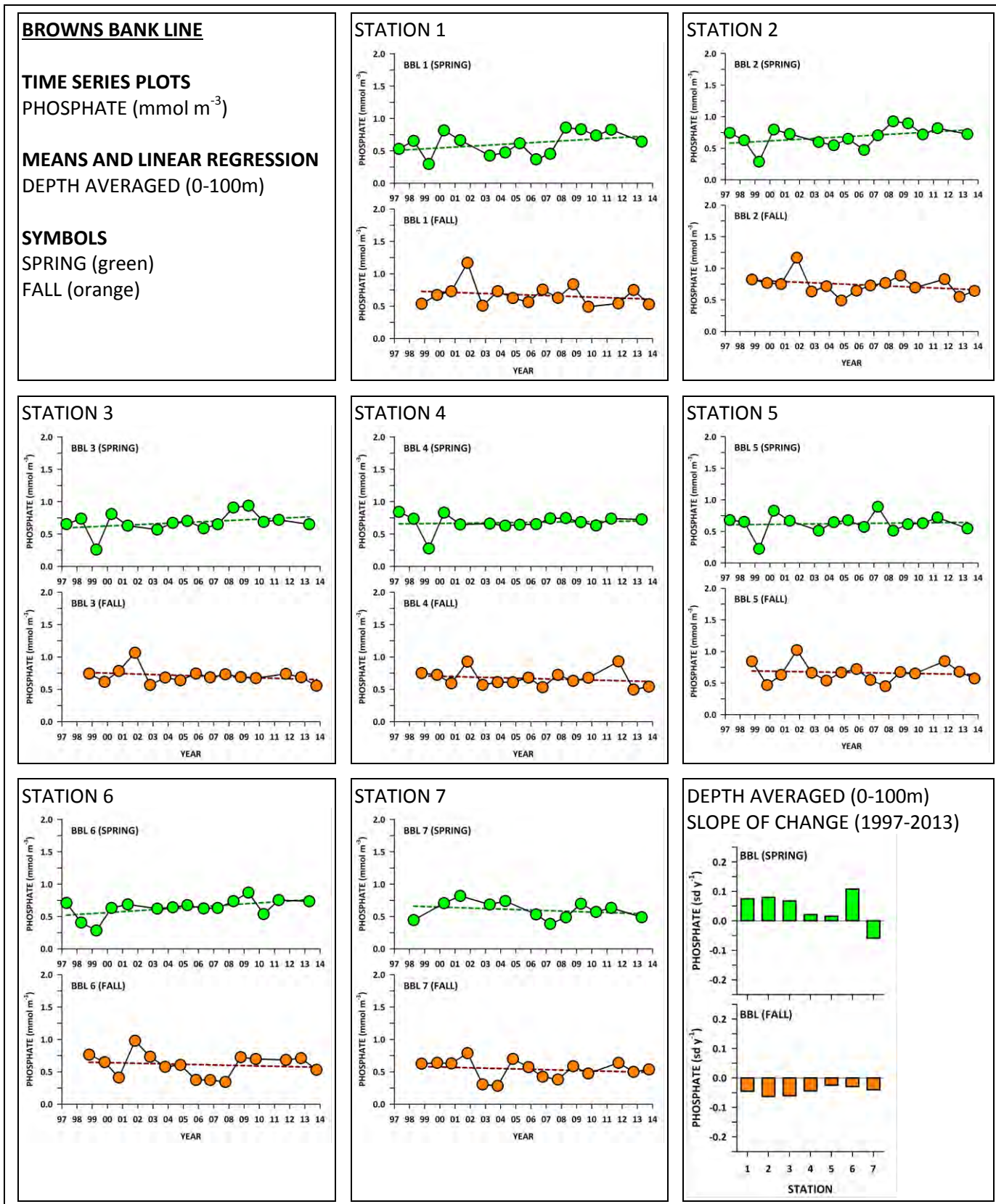


Figure 34

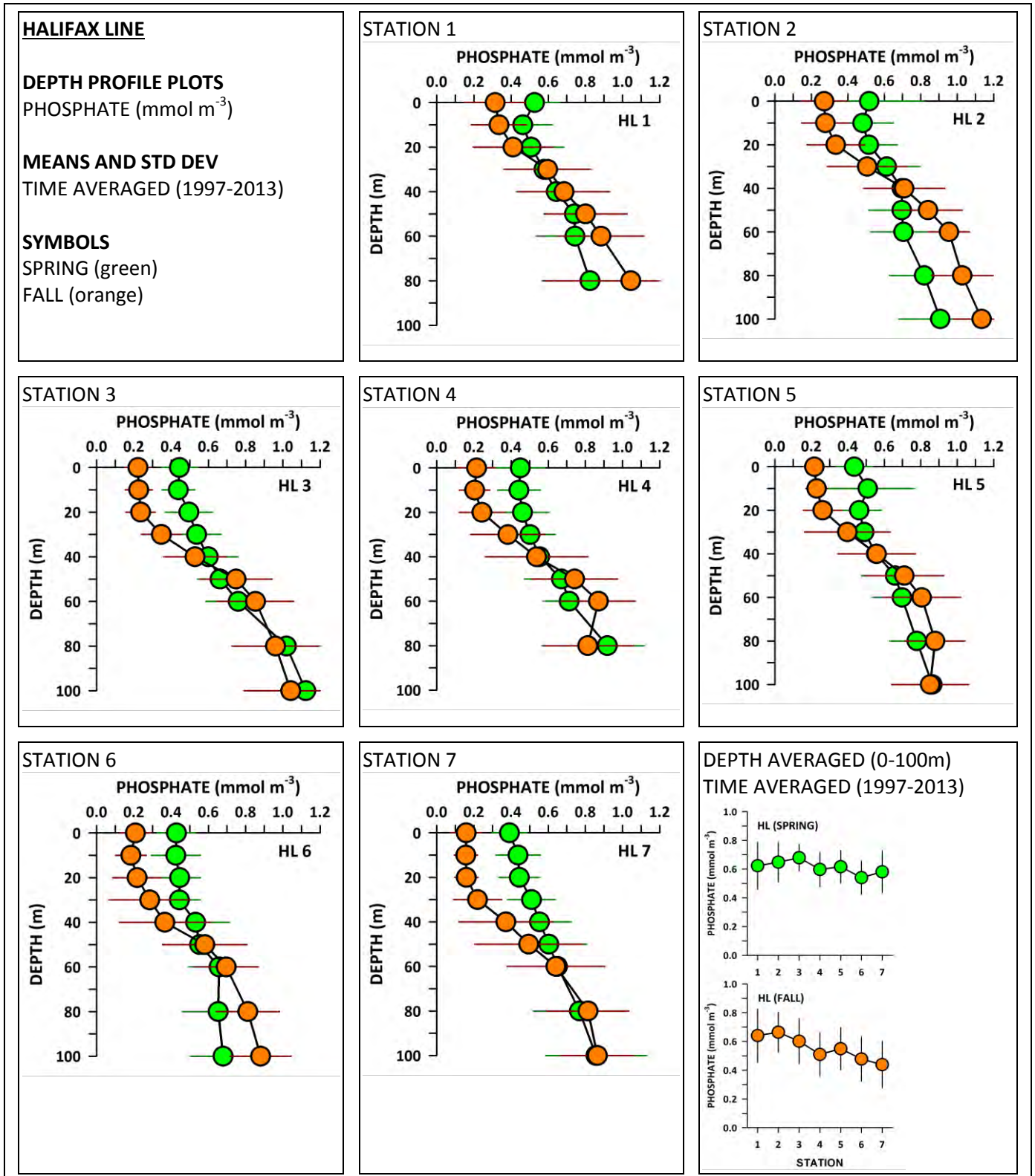


Figure 35

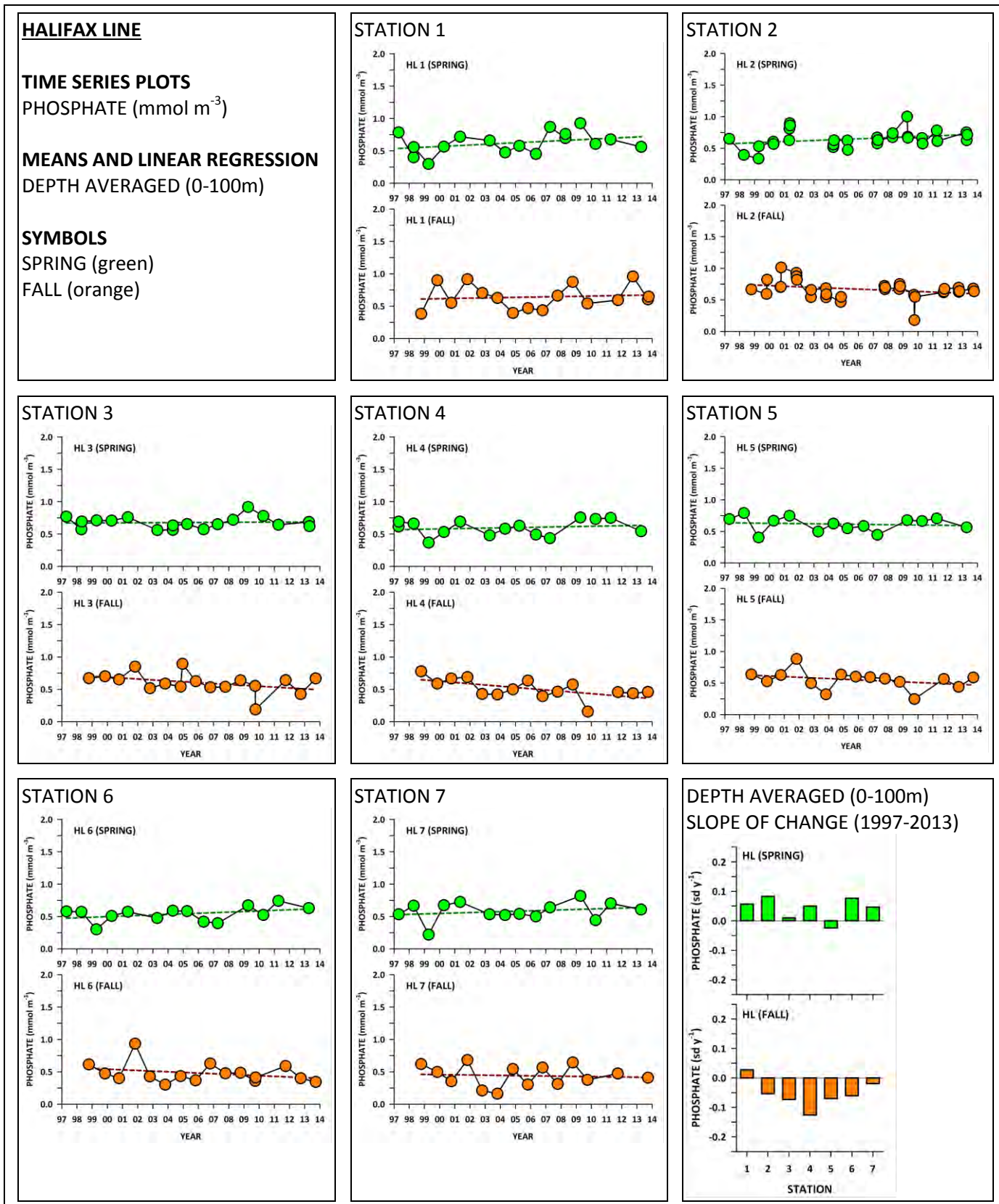


Figure 36

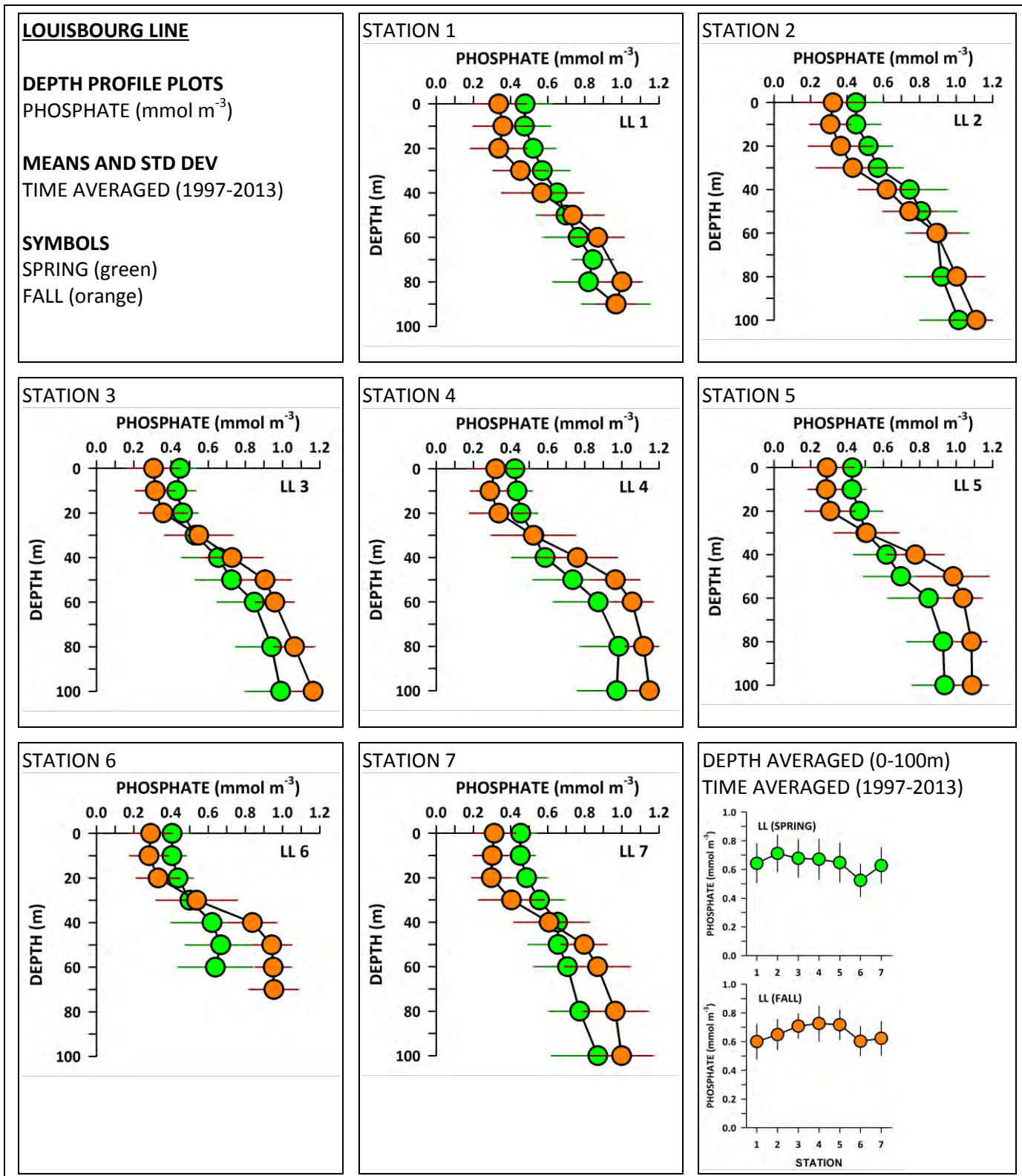


Figure 37

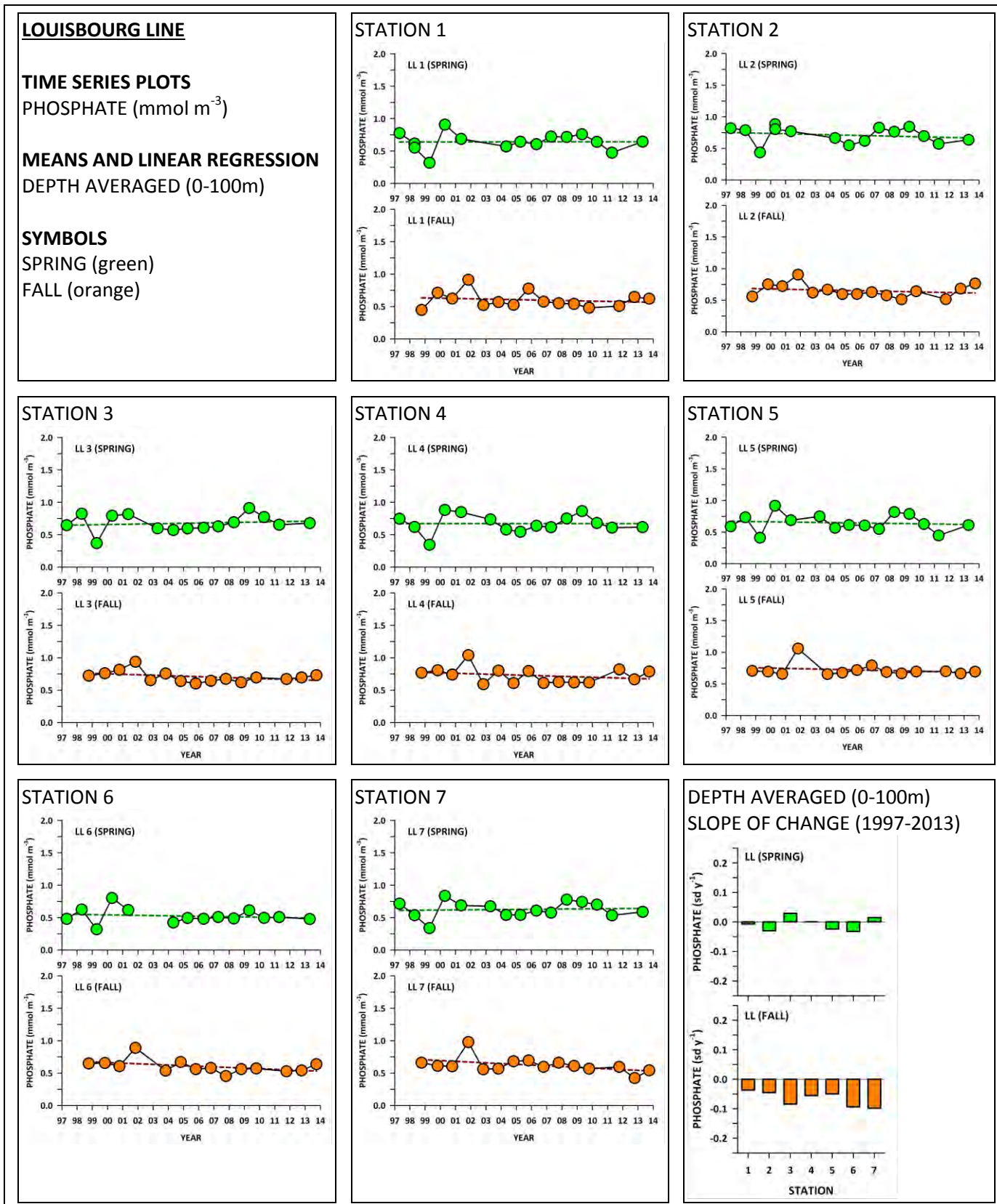


Figure 38

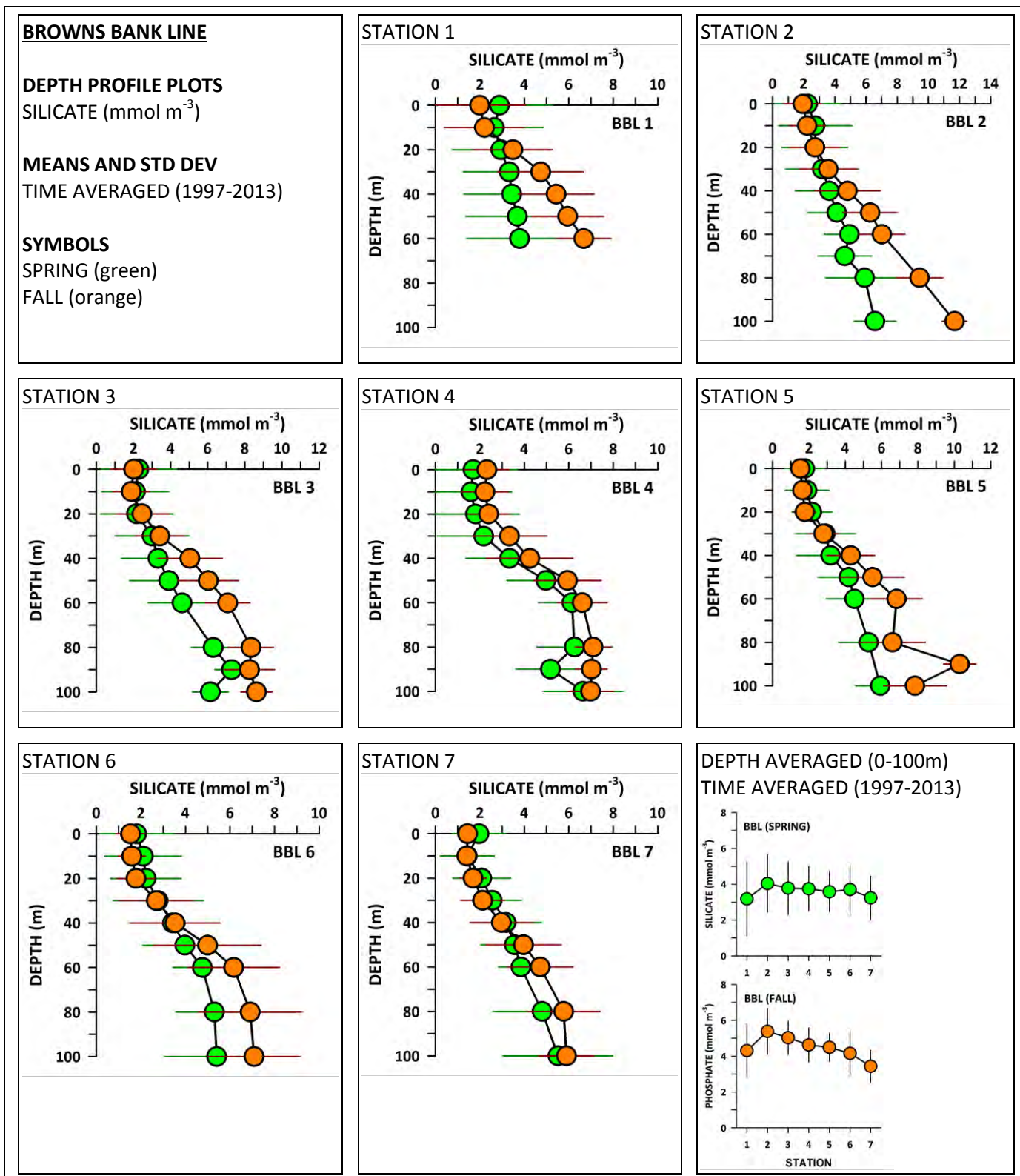


Figure 39

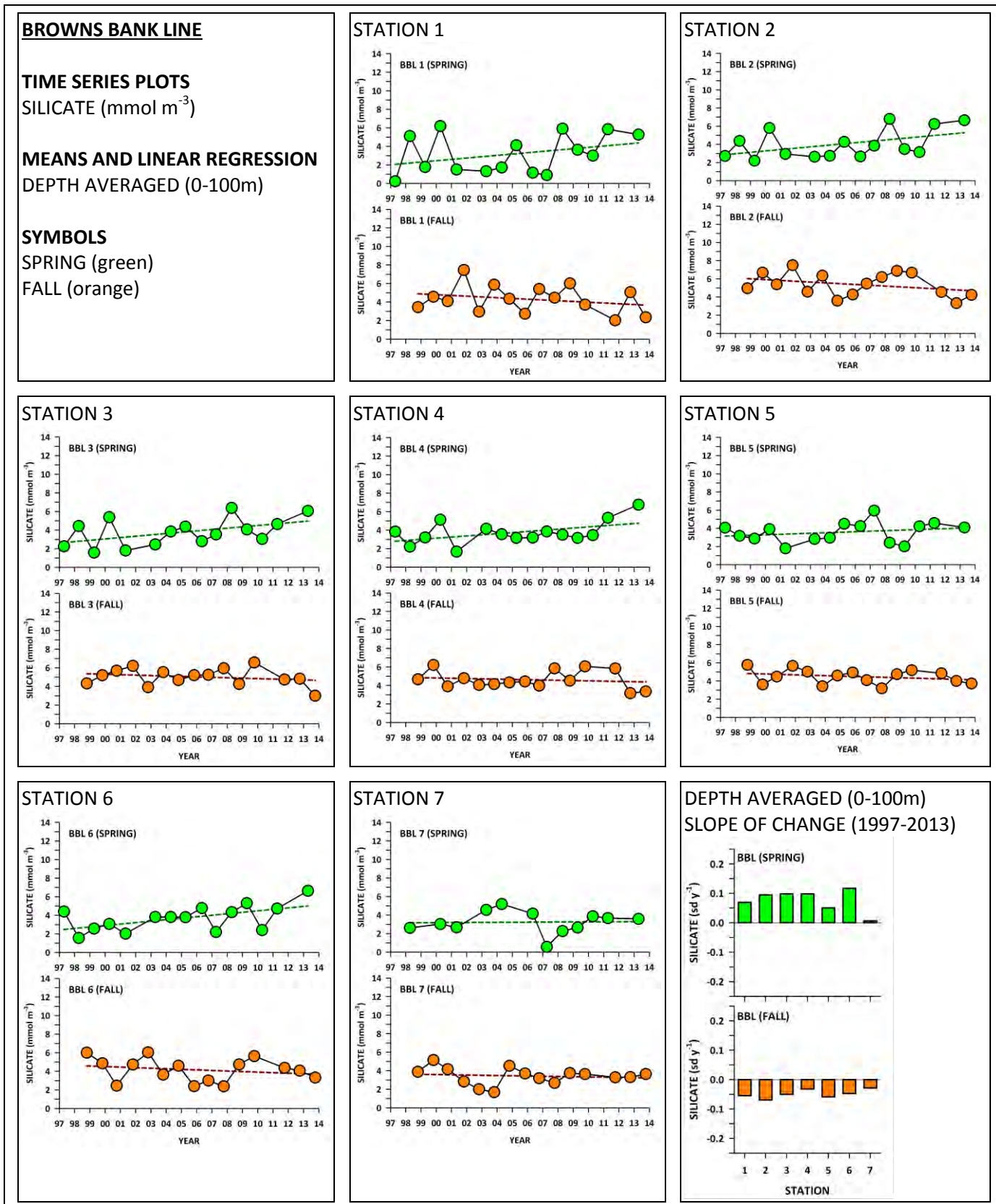


Figure 40

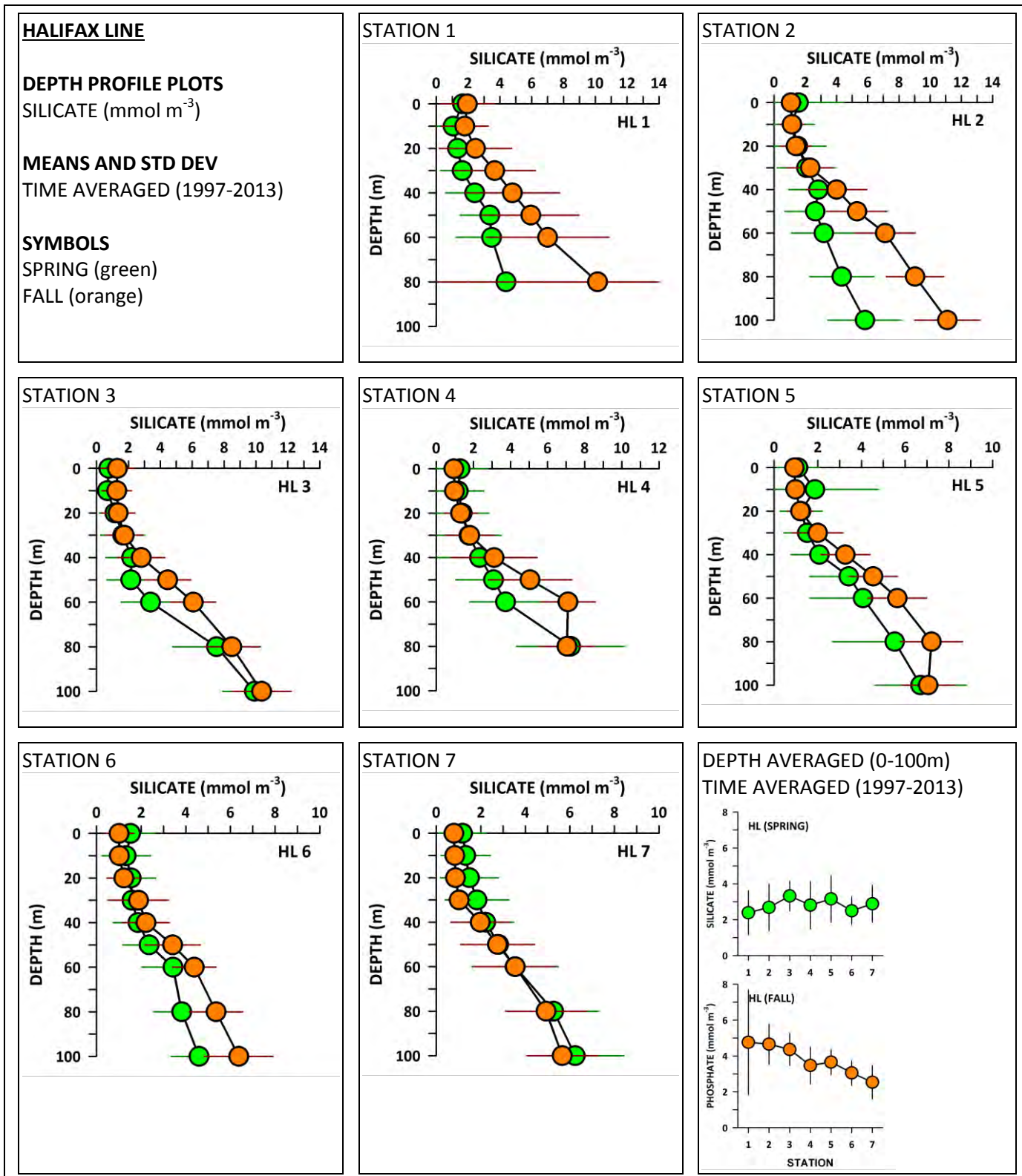


Figure 41

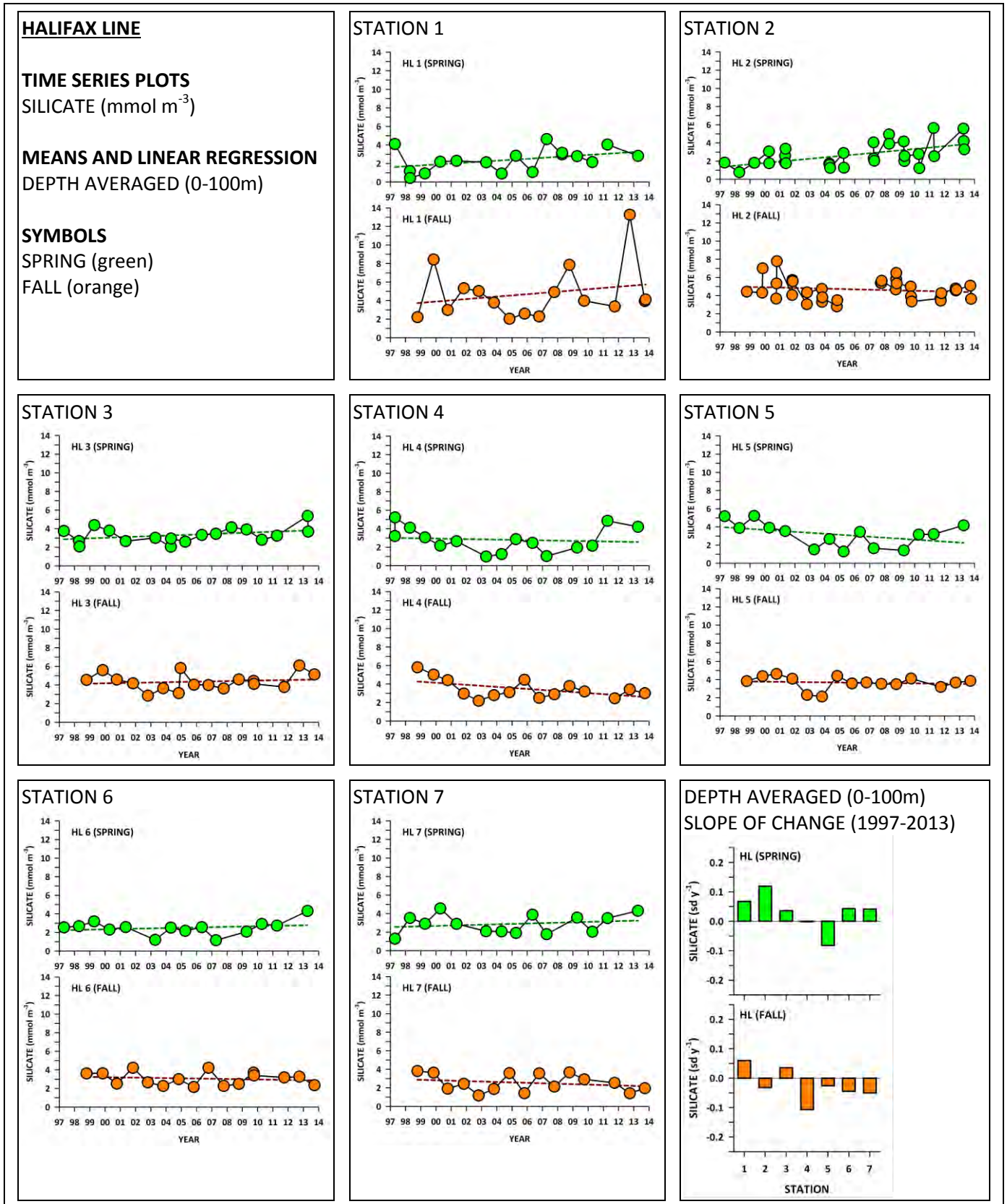


Figure 42

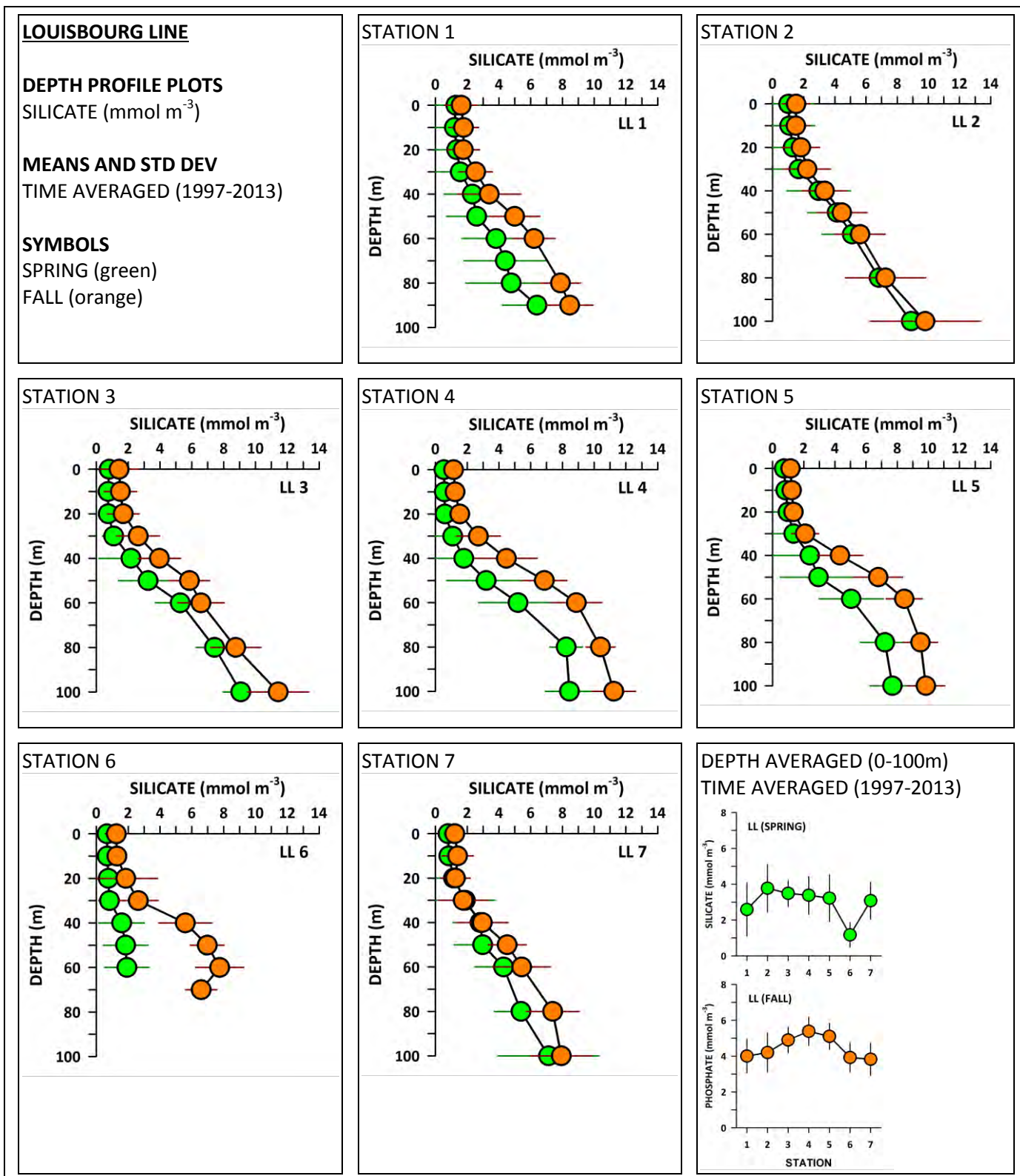


Figure 43

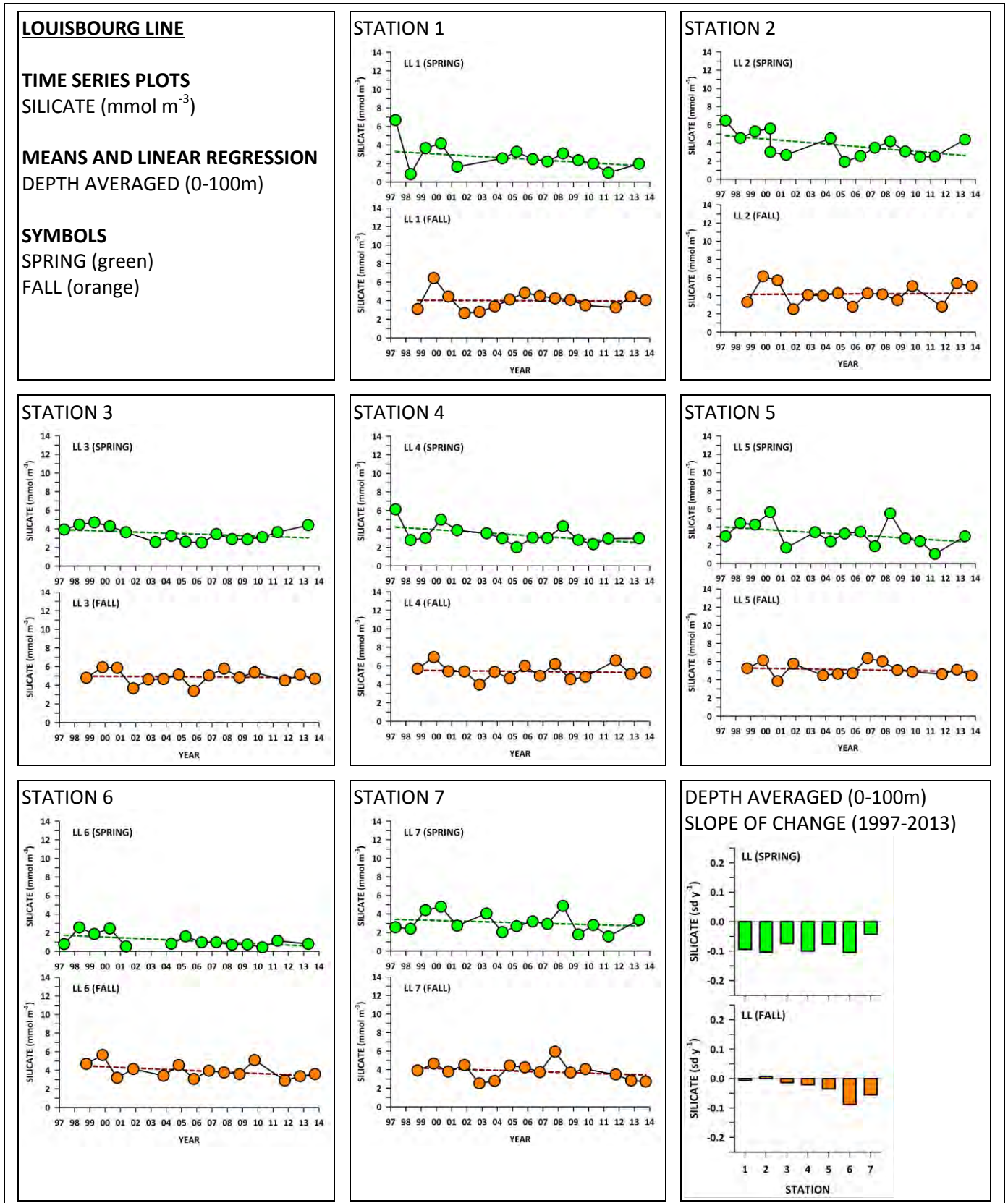


Figure 44

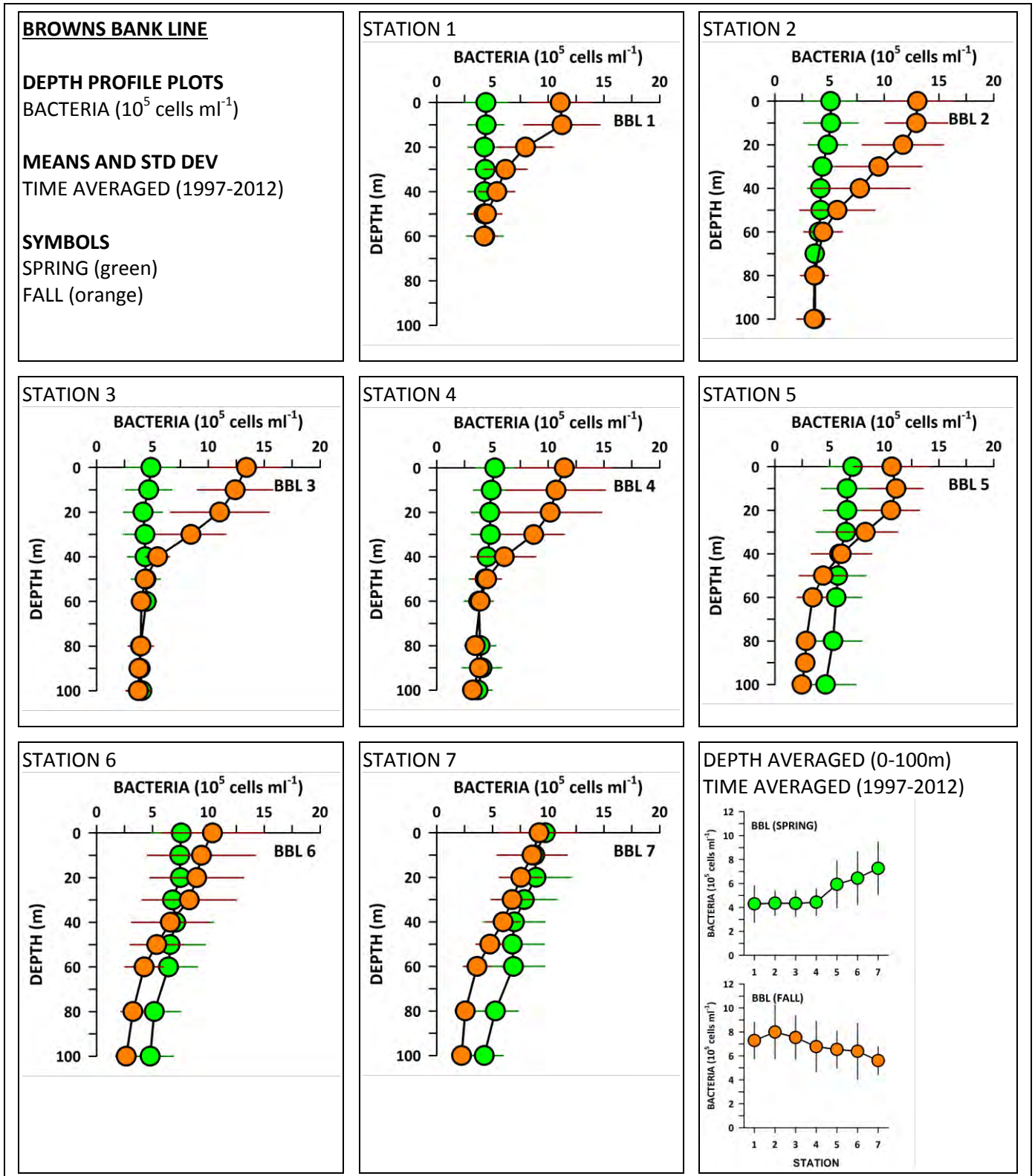


Figure 45

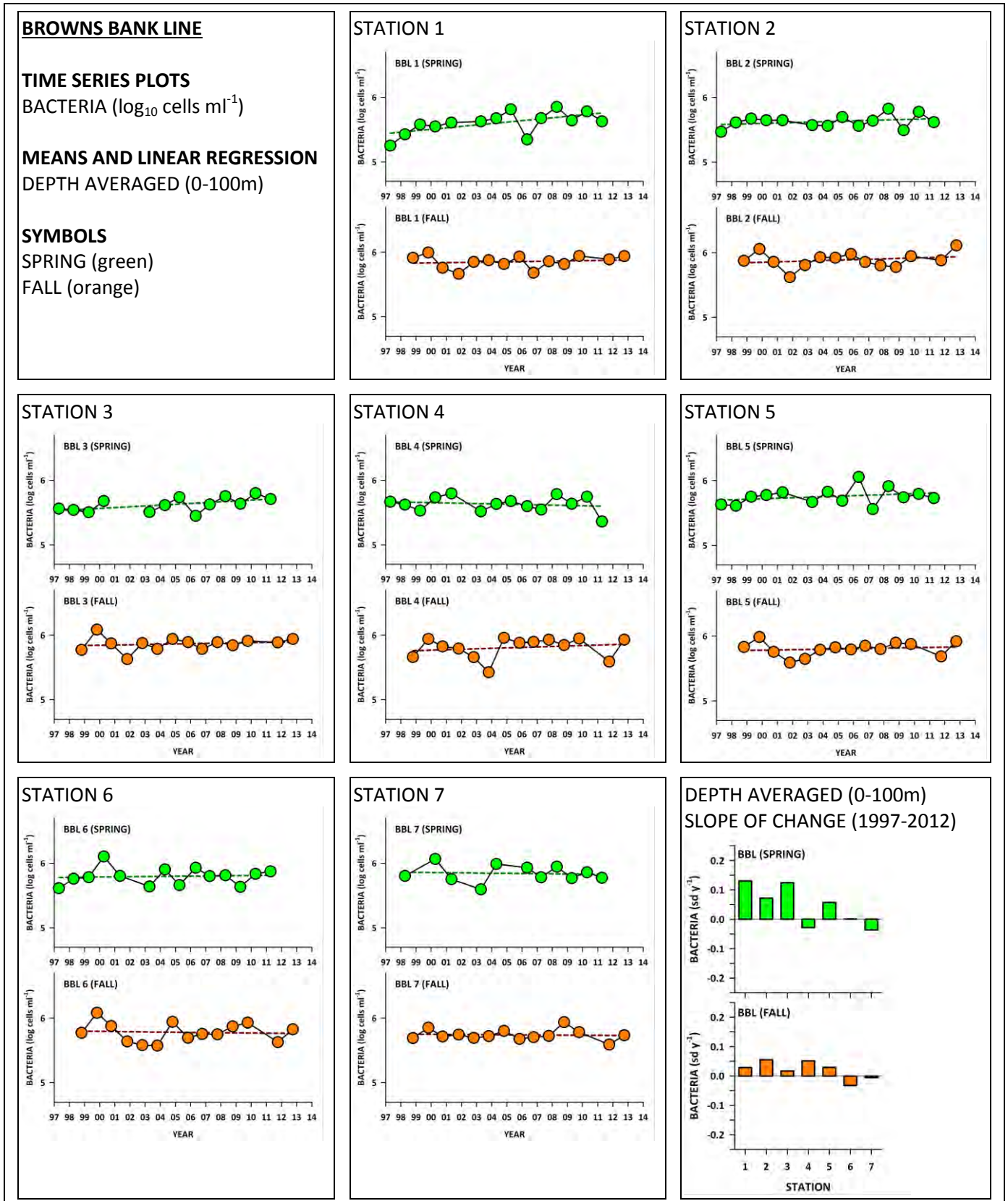


Figure 46

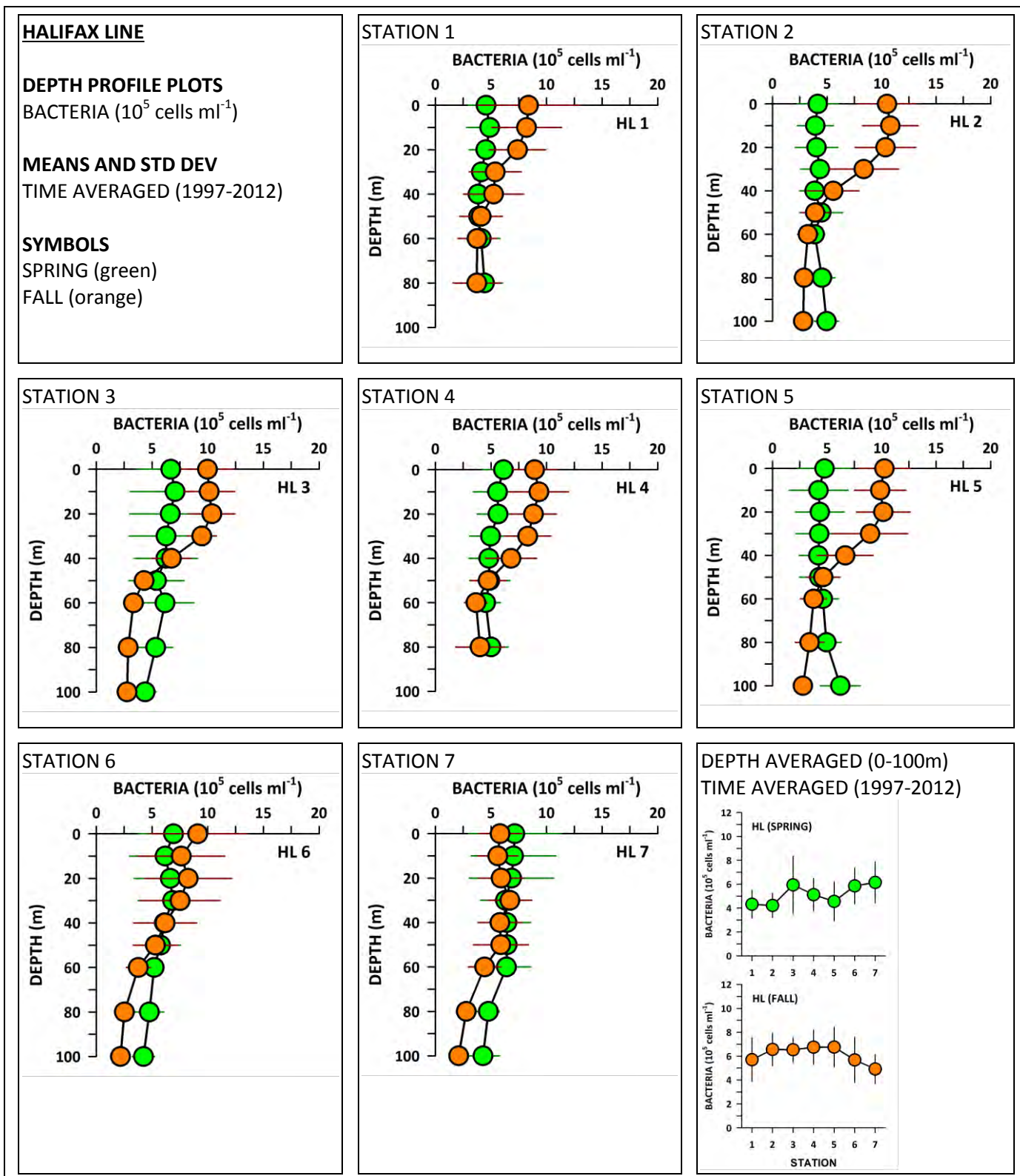


Figure 47

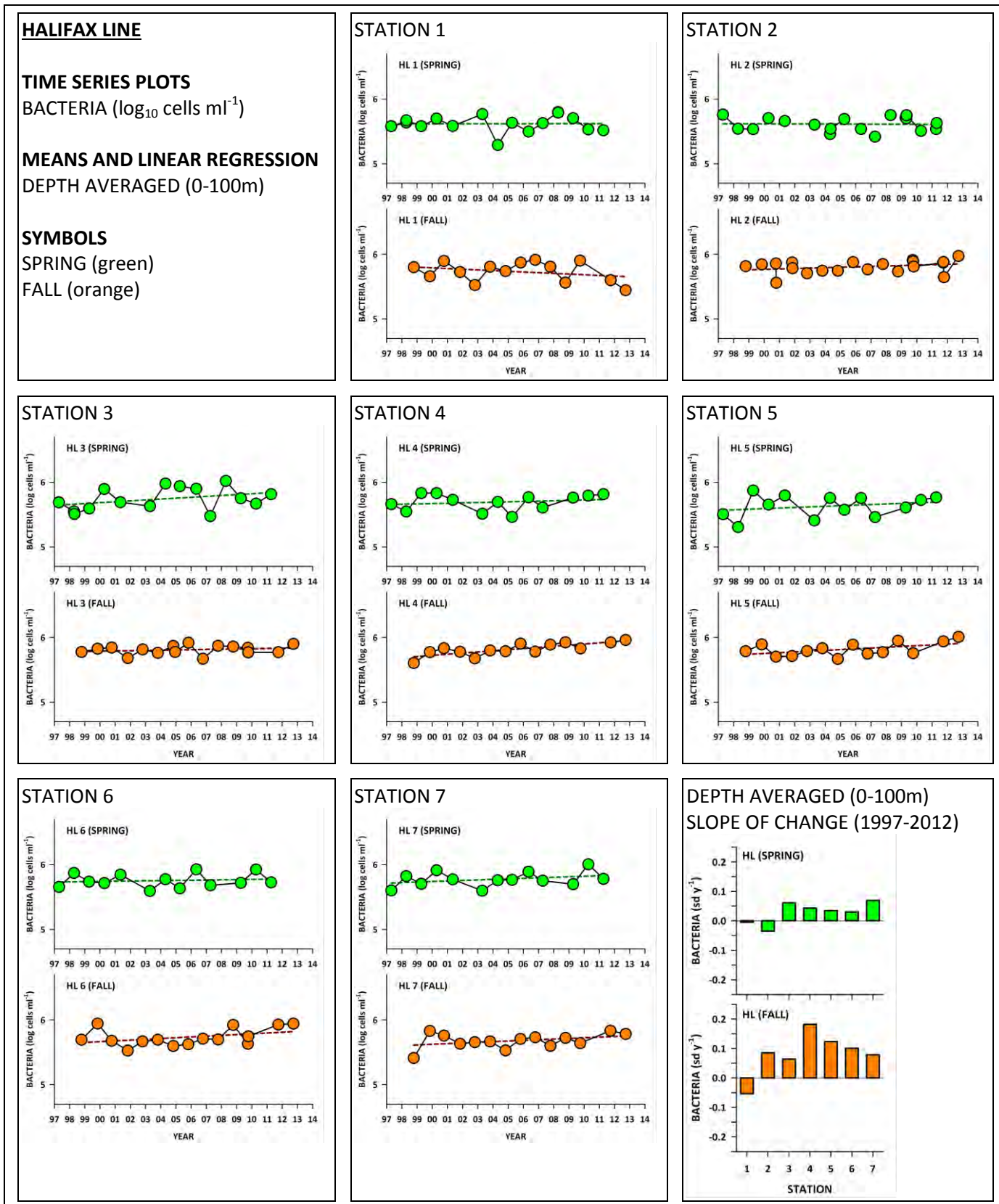


Figure 48

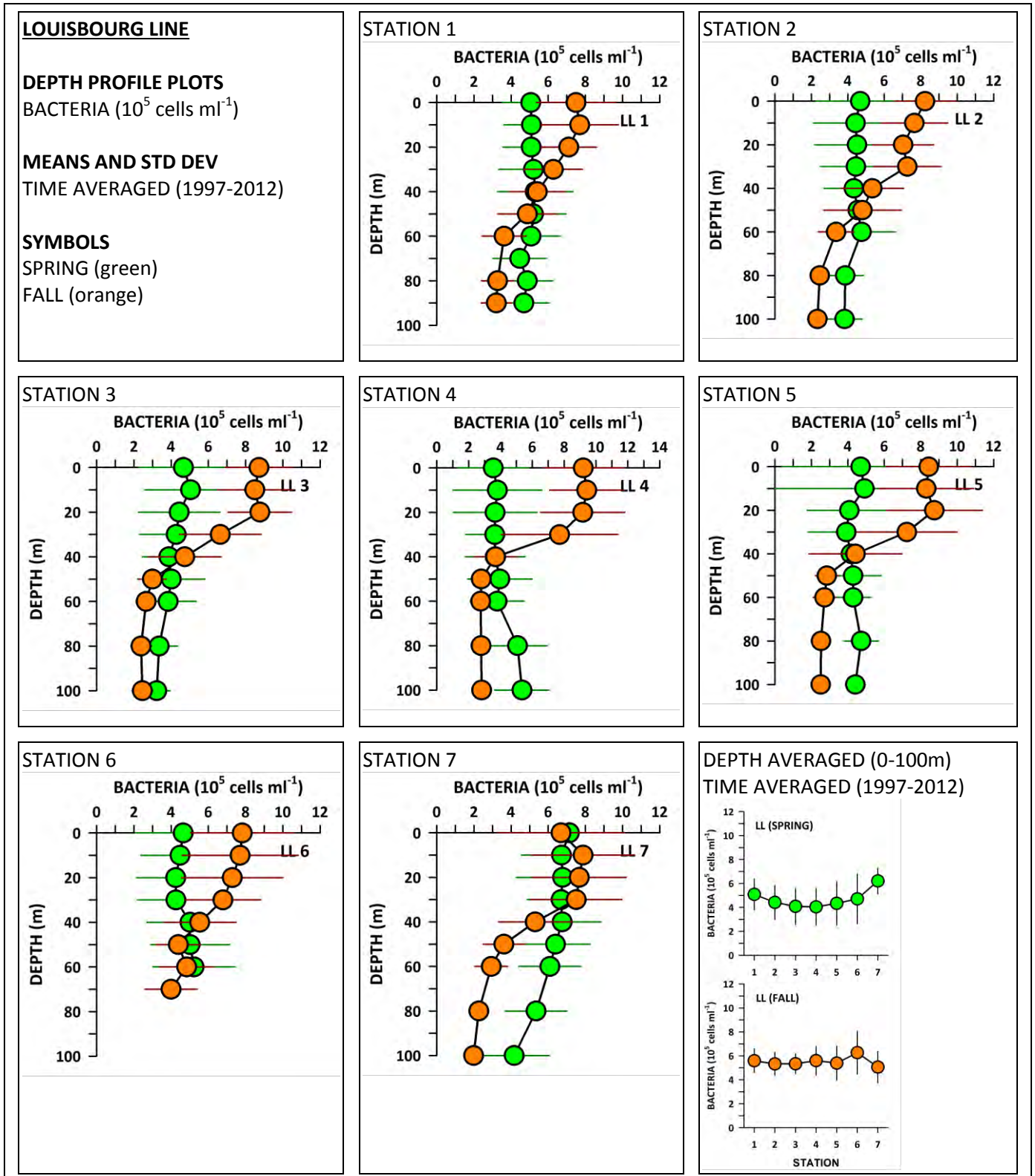


Figure 49

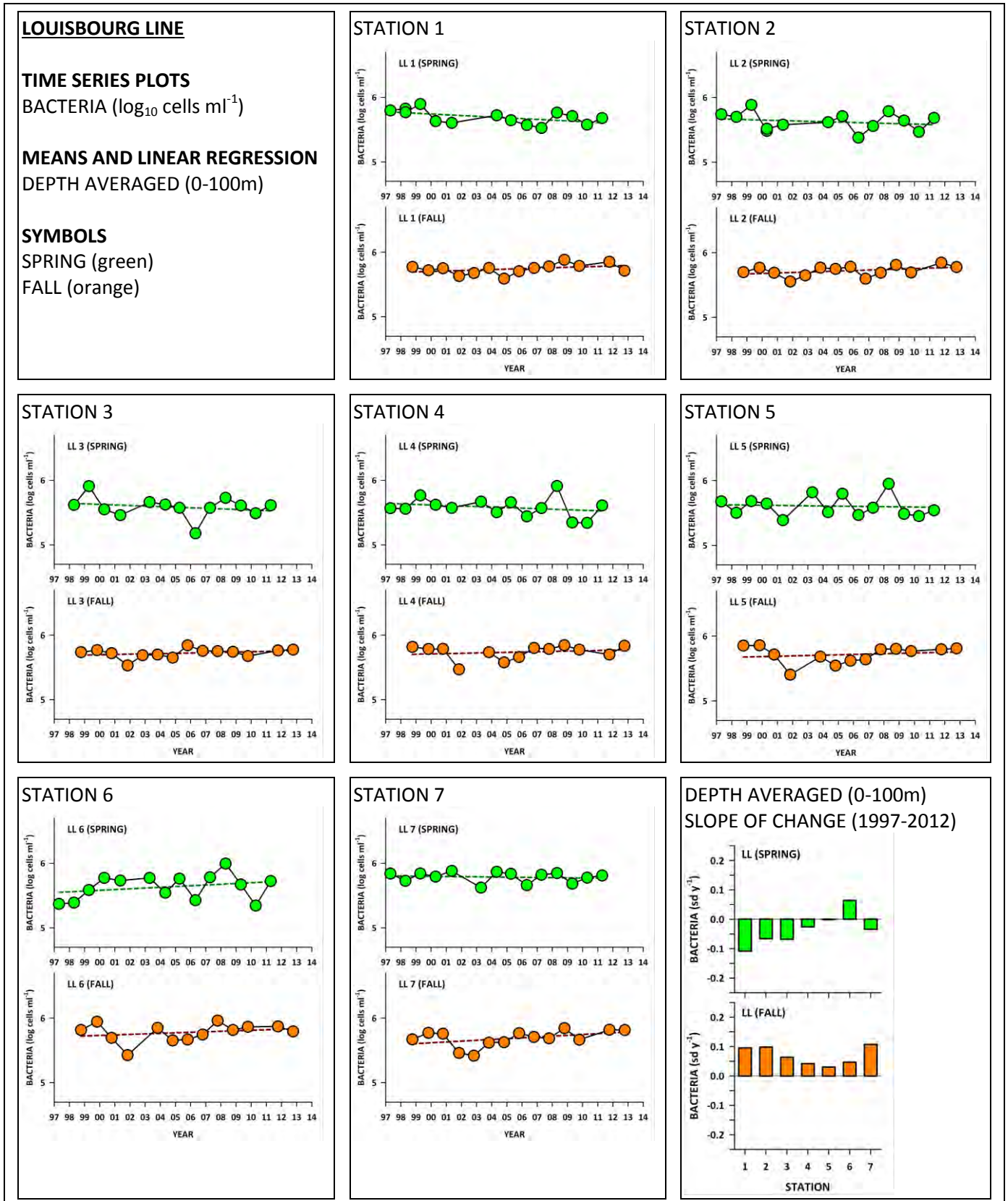


Figure 50

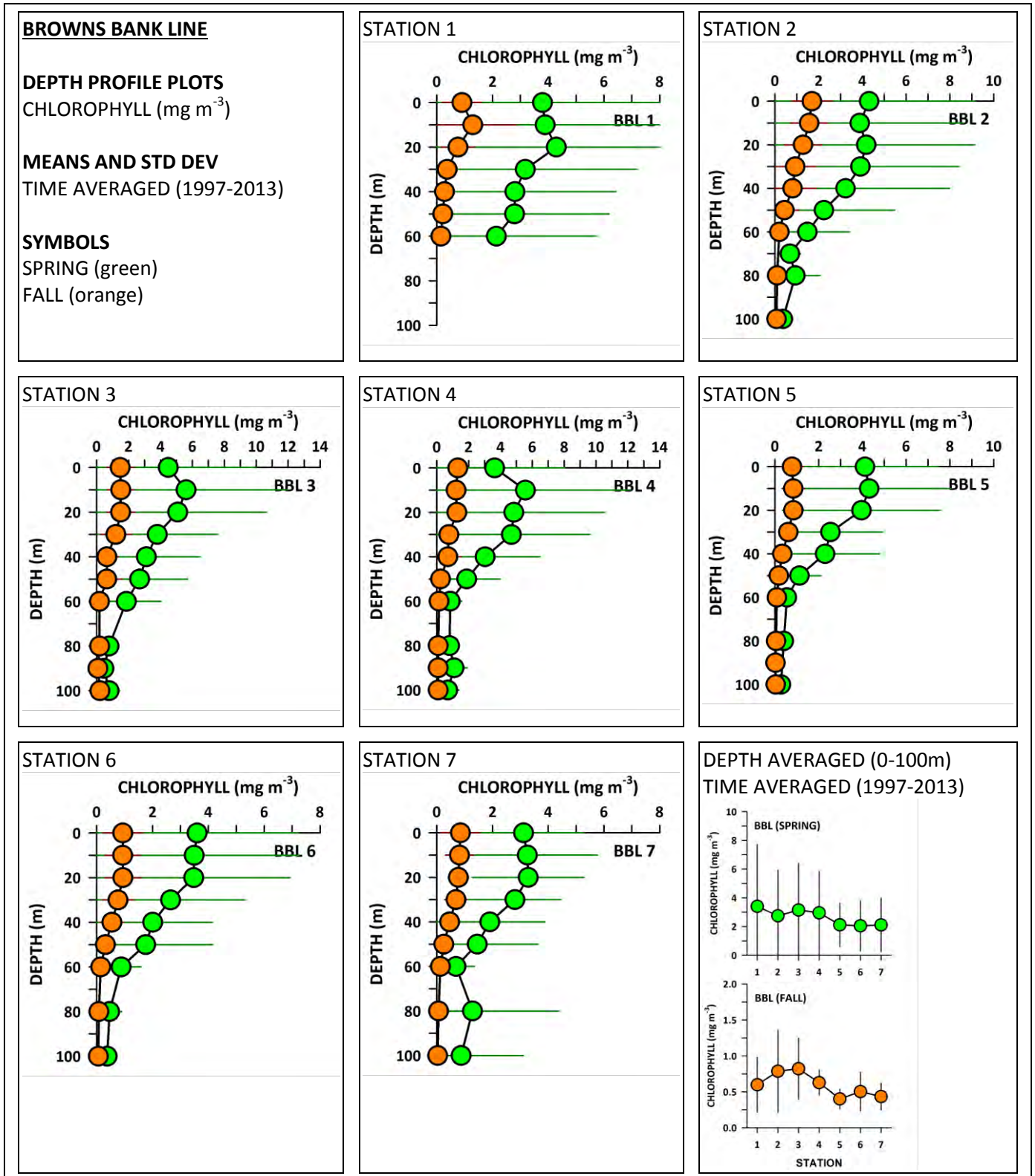


Figure 51

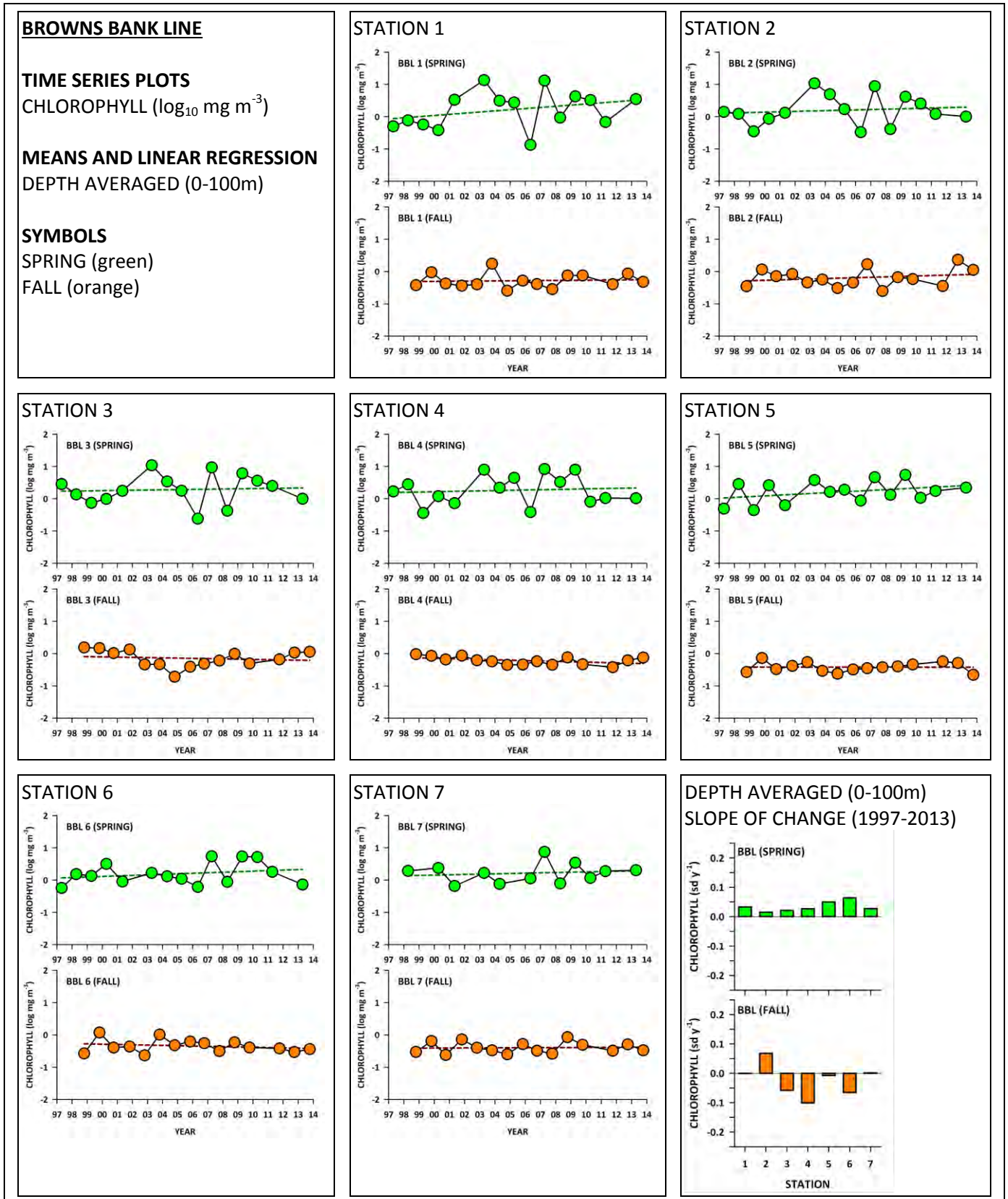


Figure 52

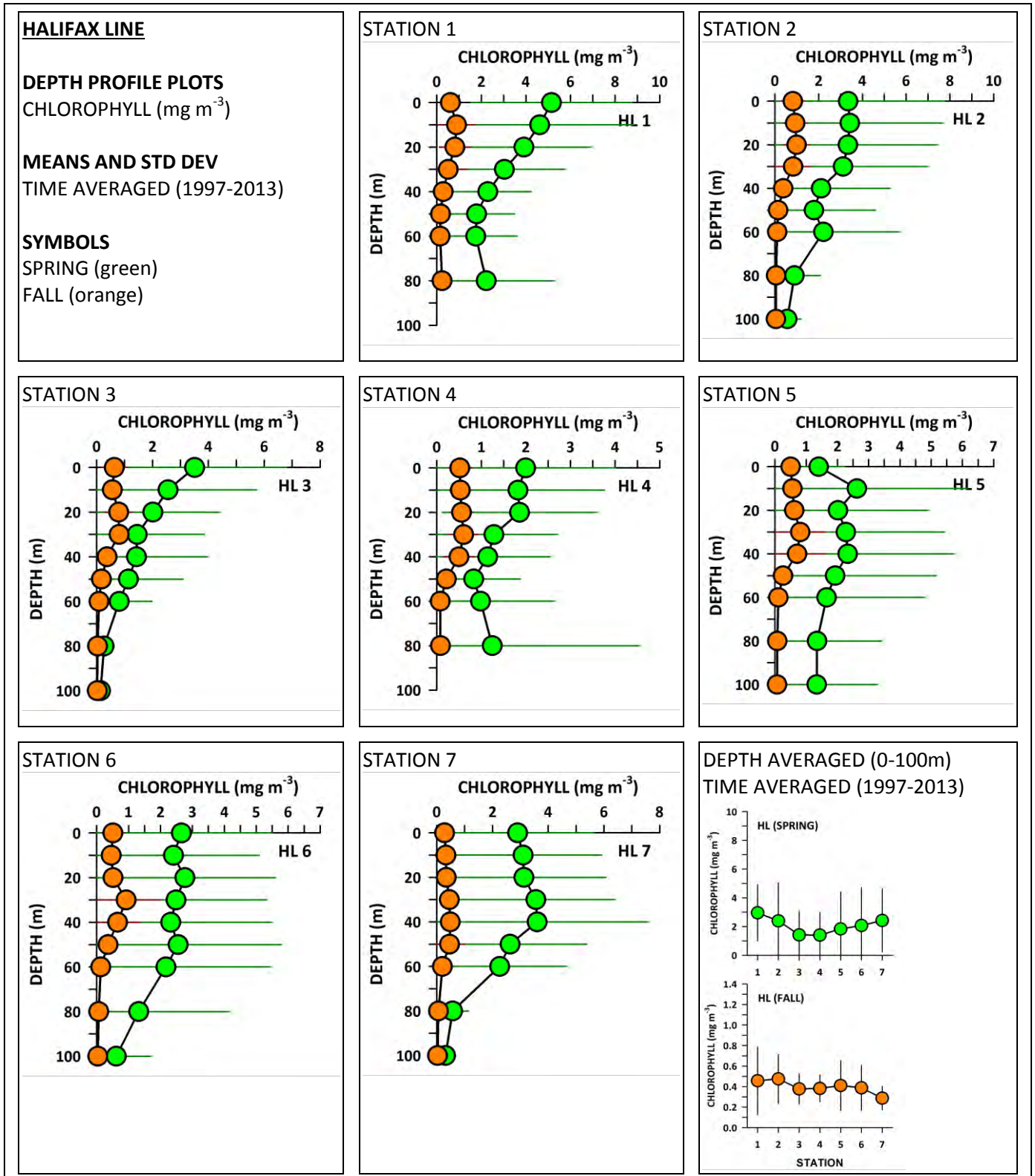


Figure 53

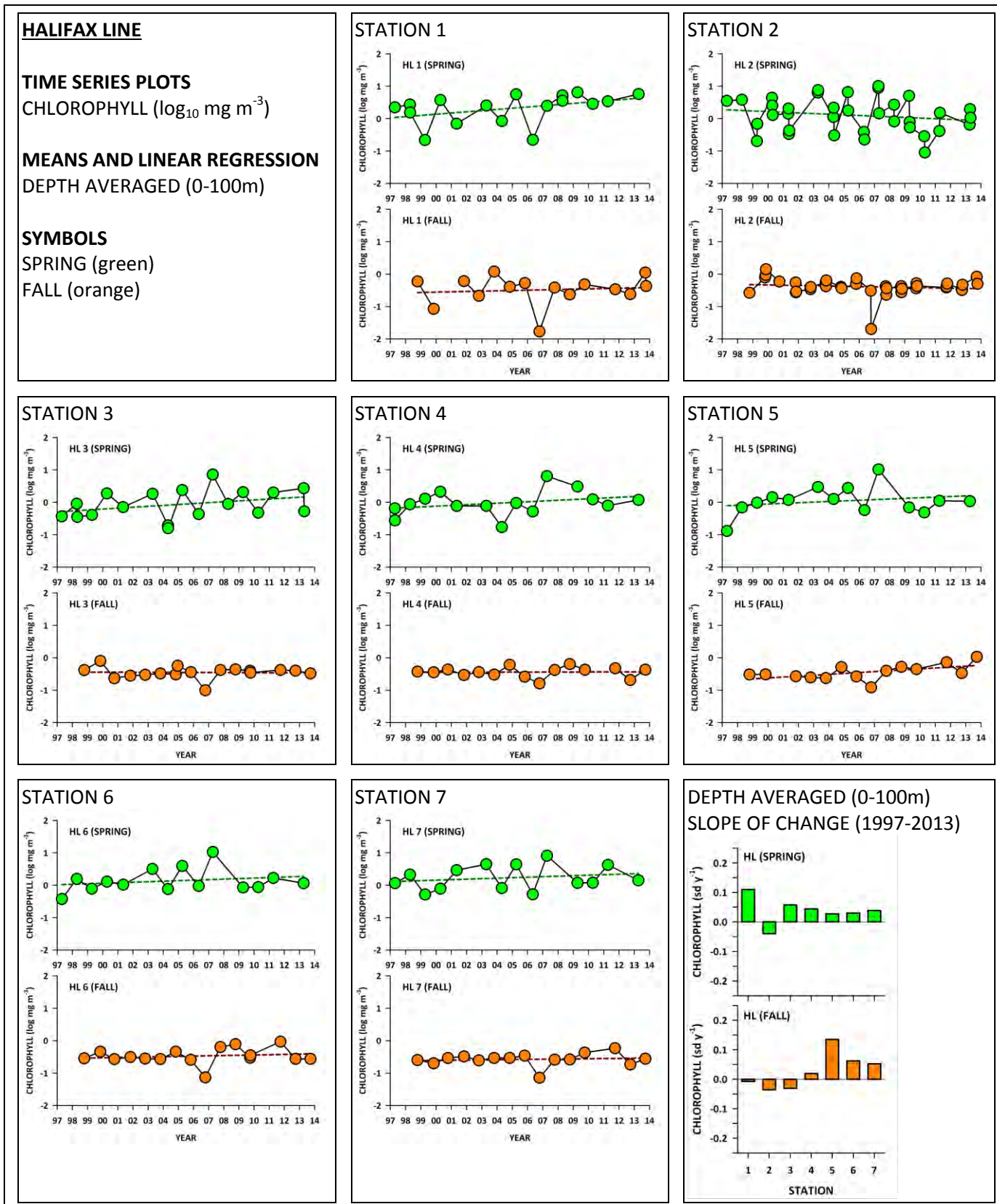


Figure 54

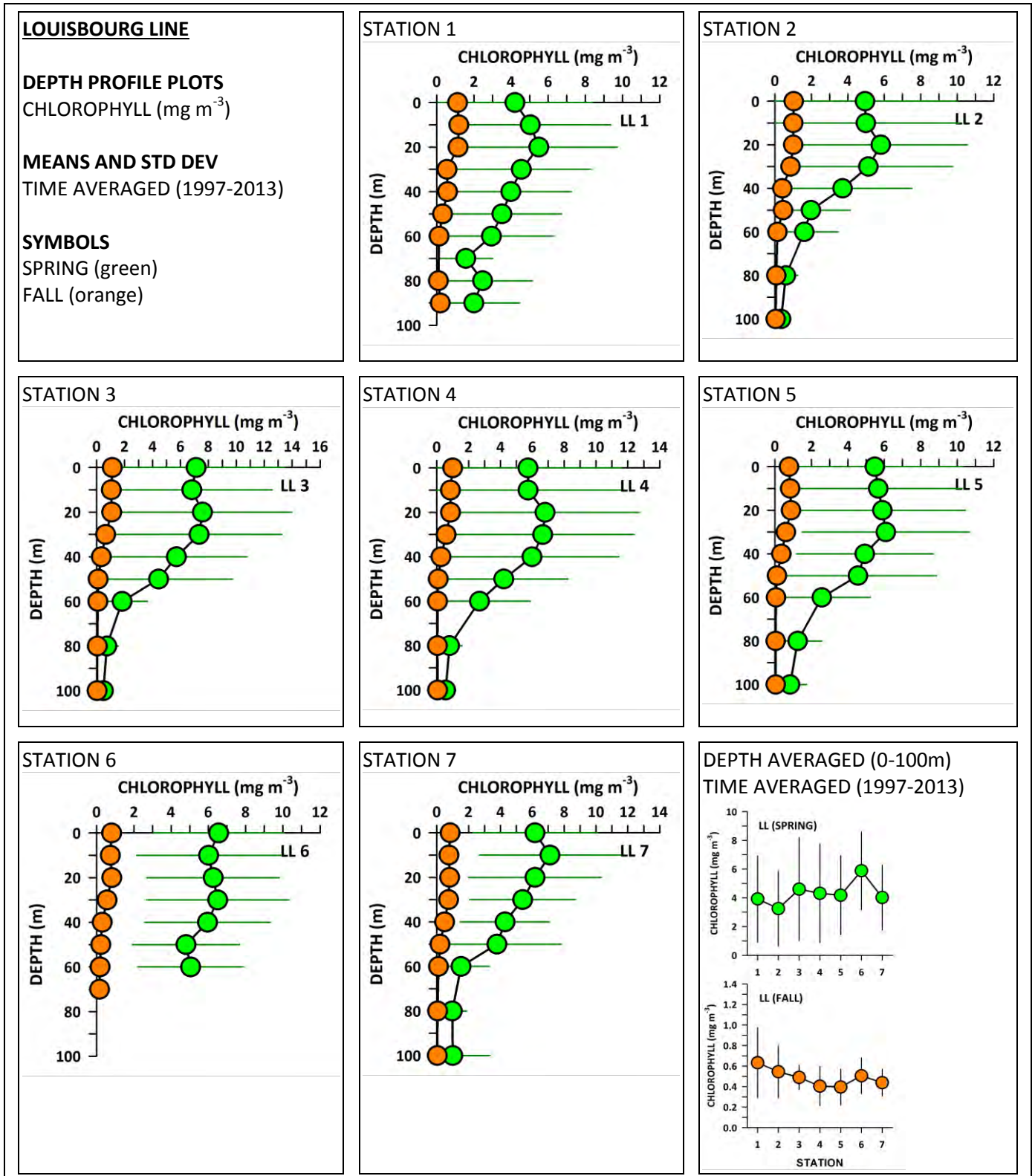


Figure 55

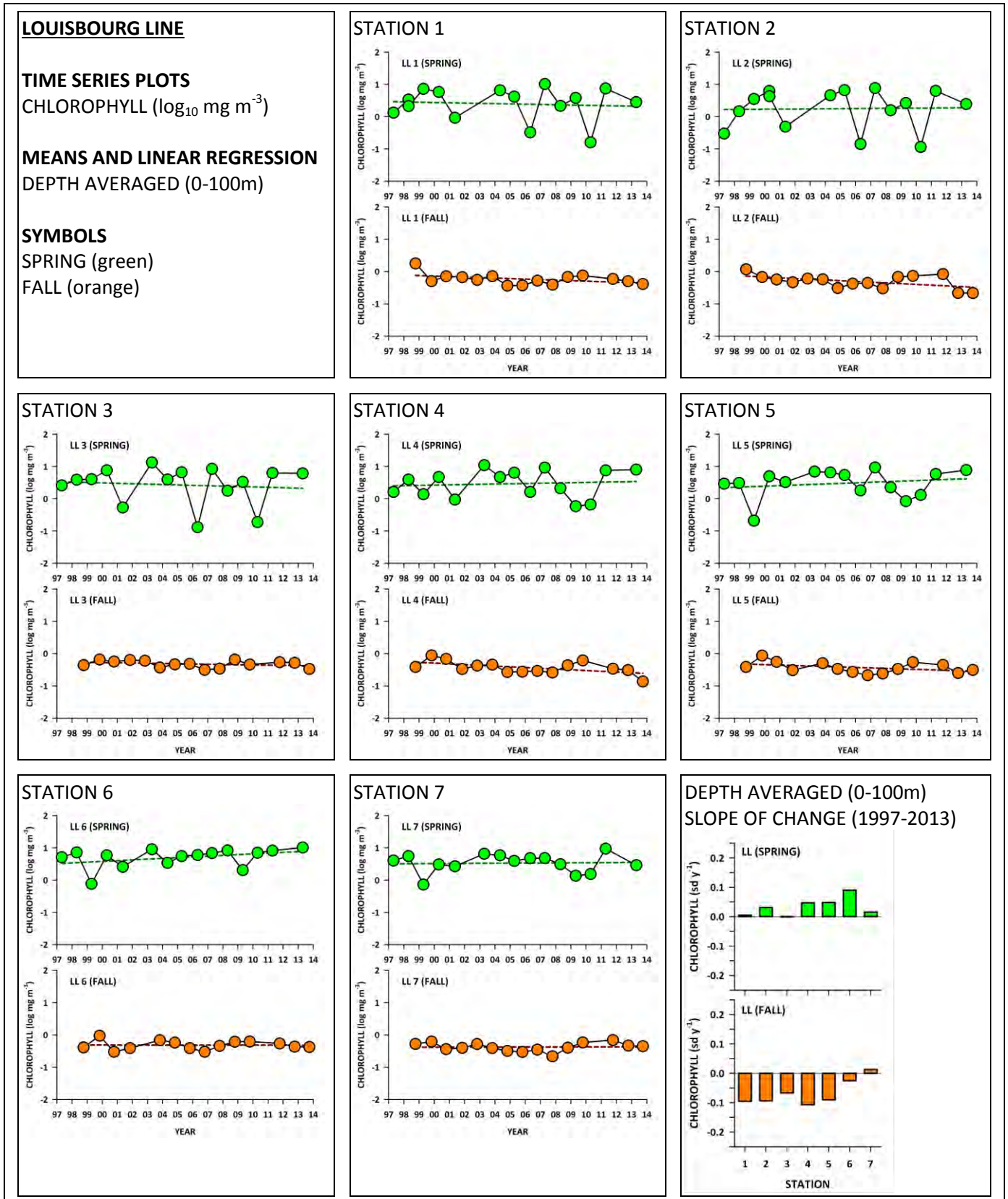


Figure 56

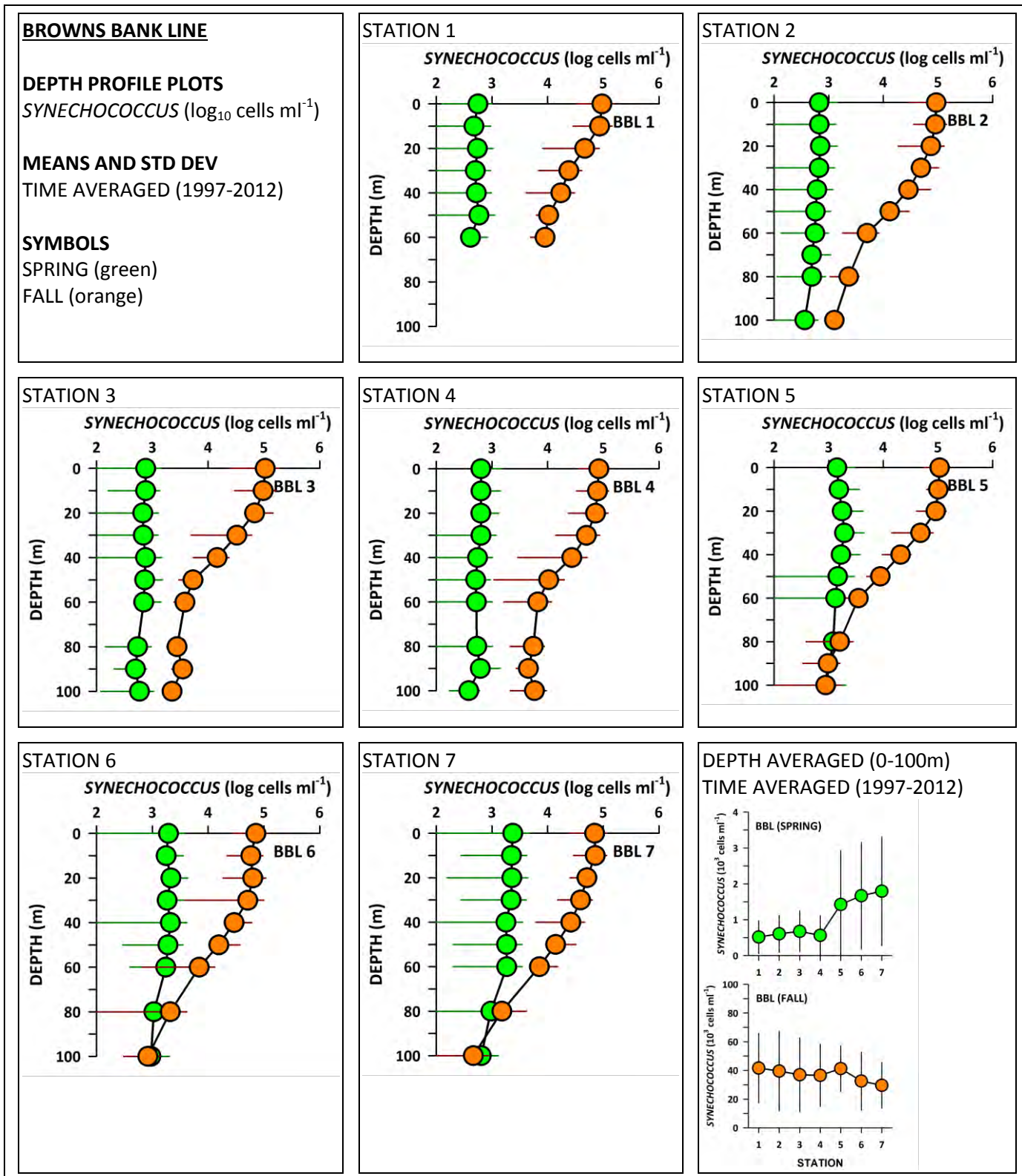


Figure 57

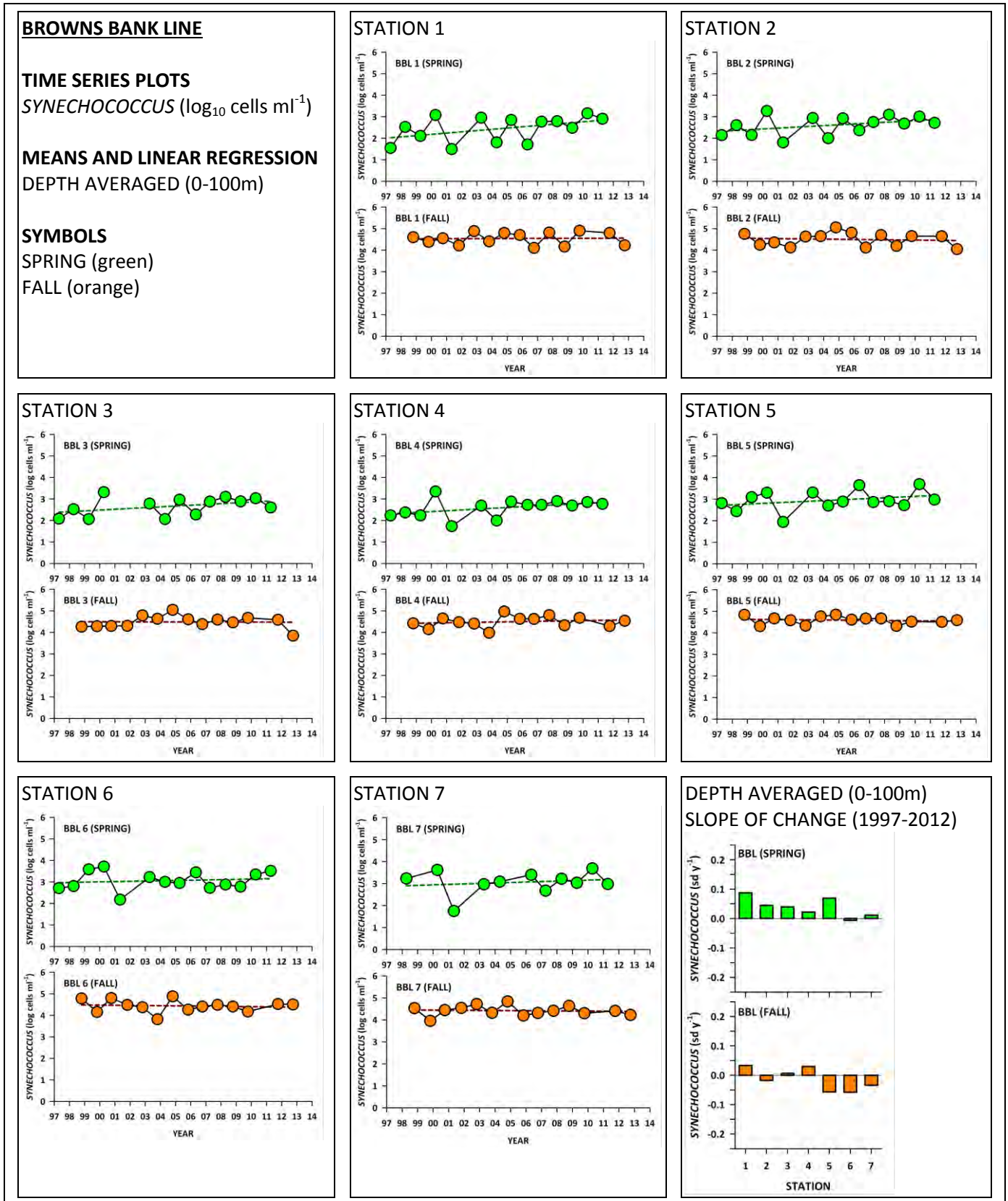


Figure 58

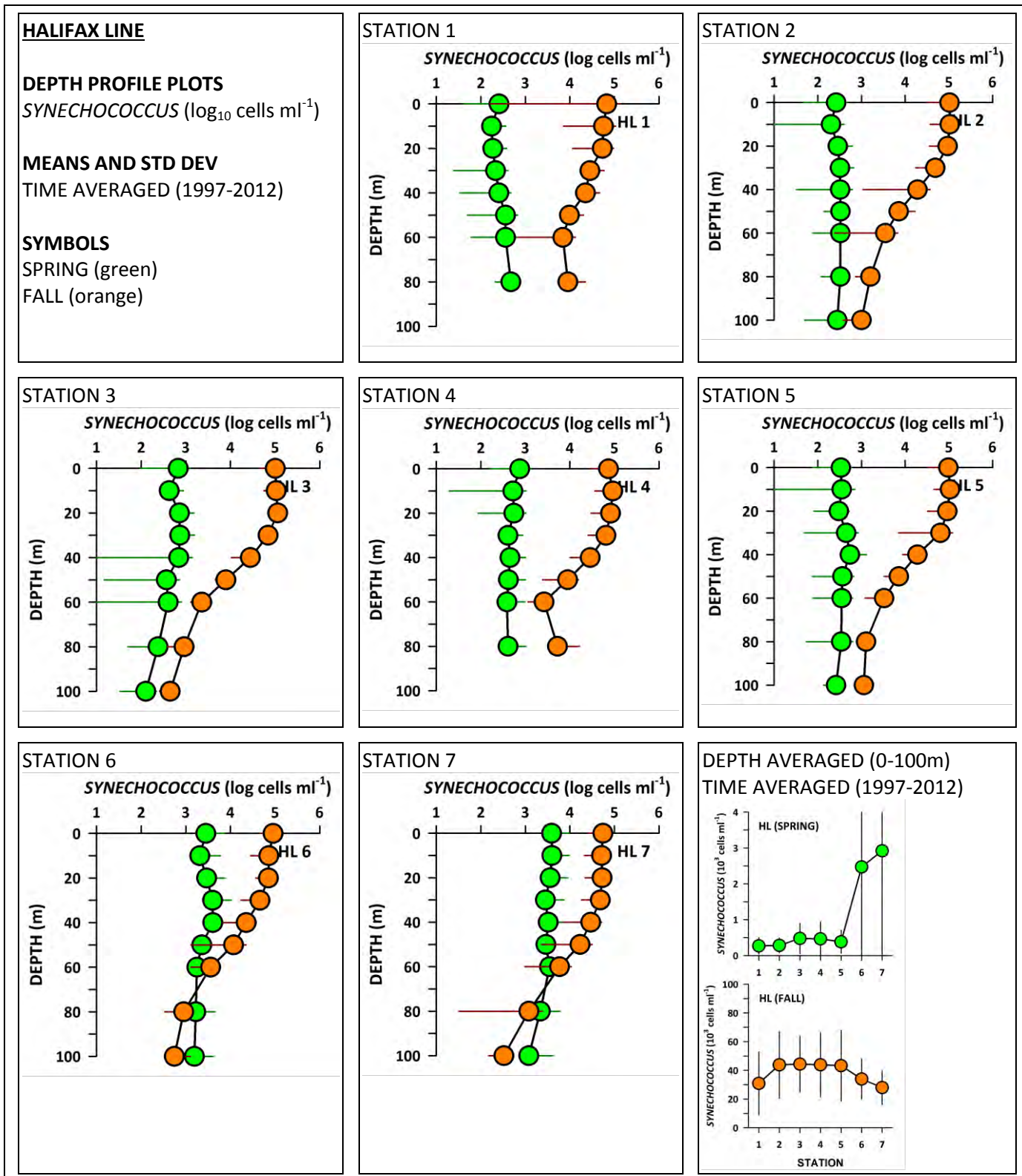


Figure 59

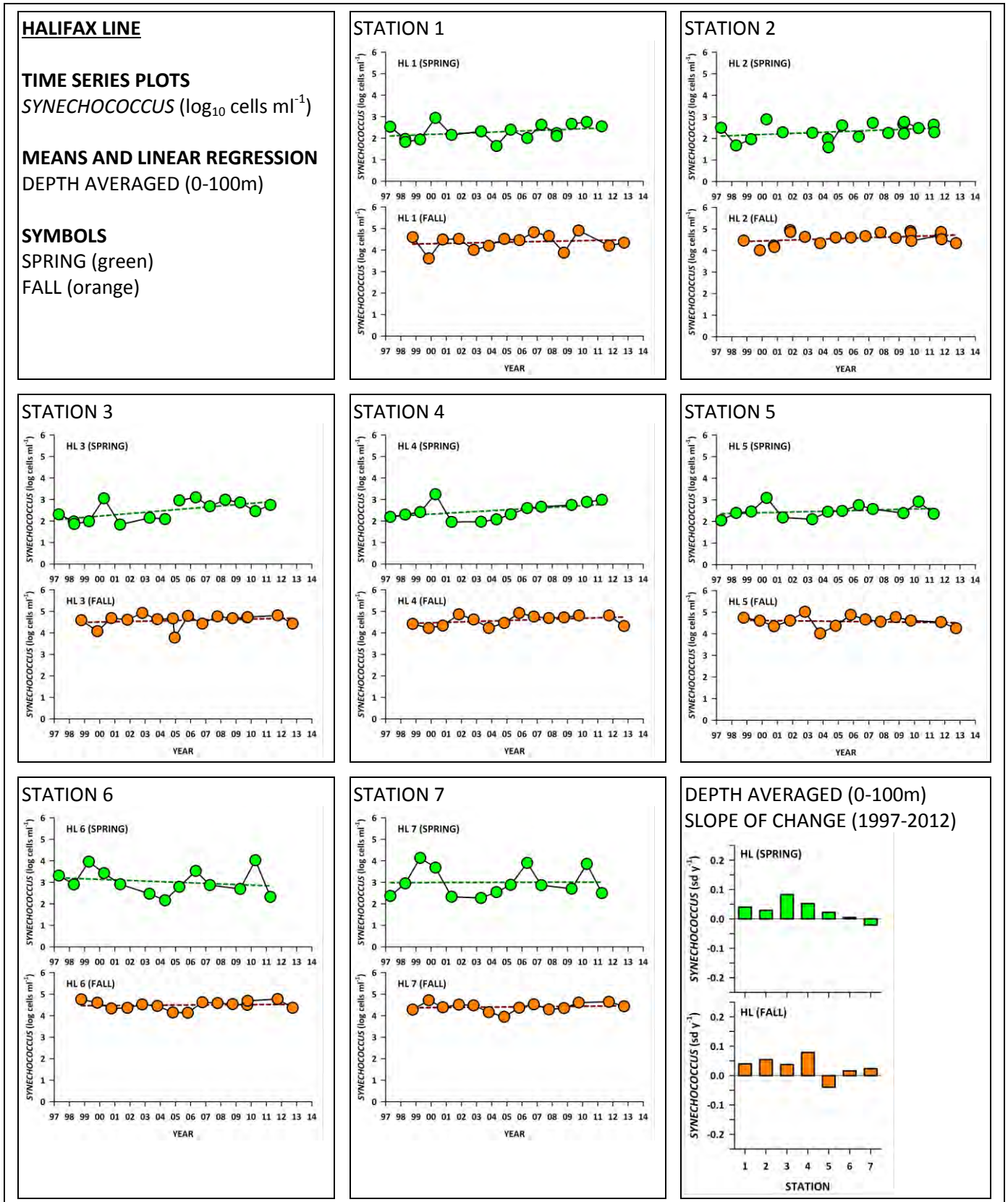


Figure 60

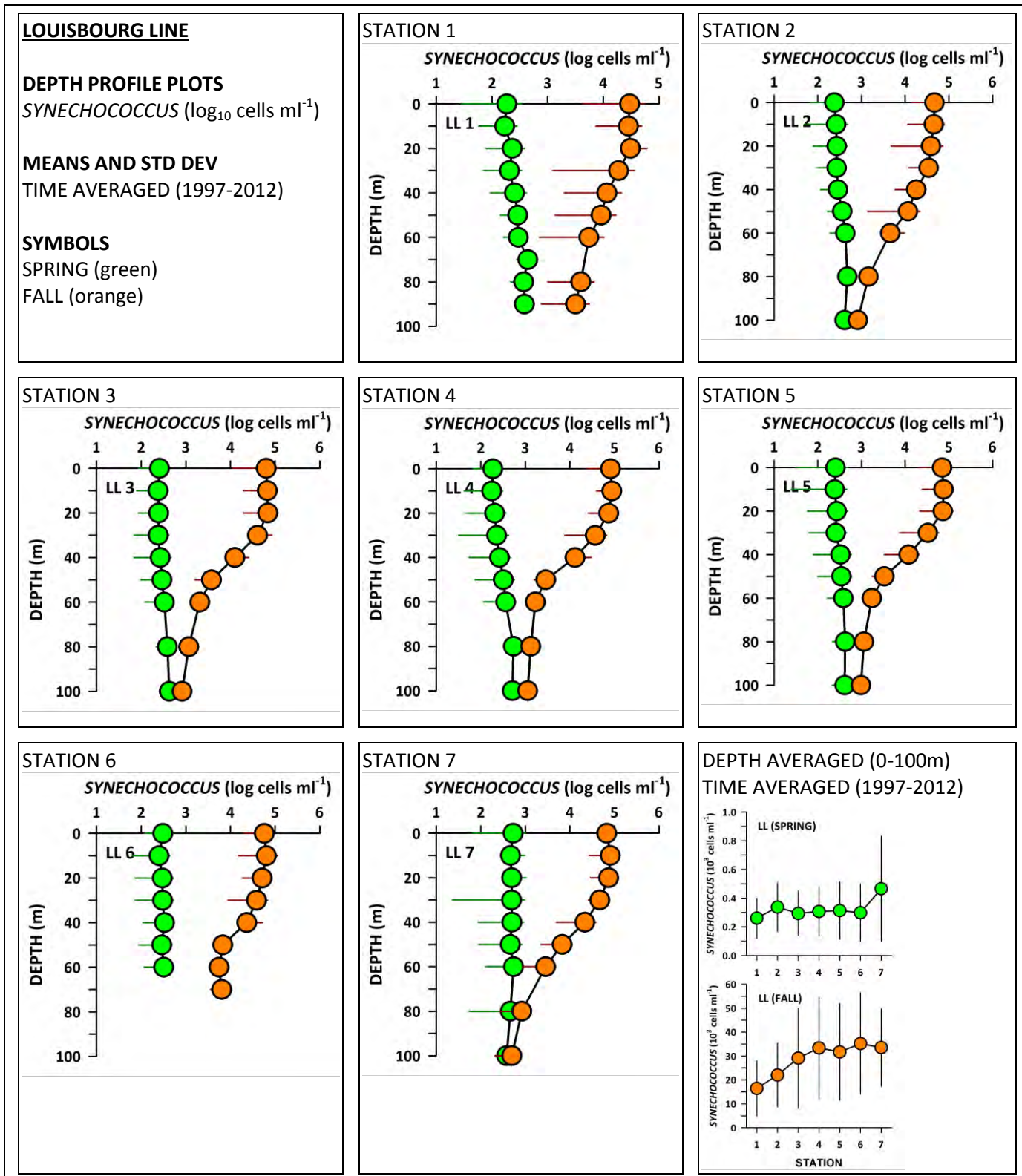


Figure 61

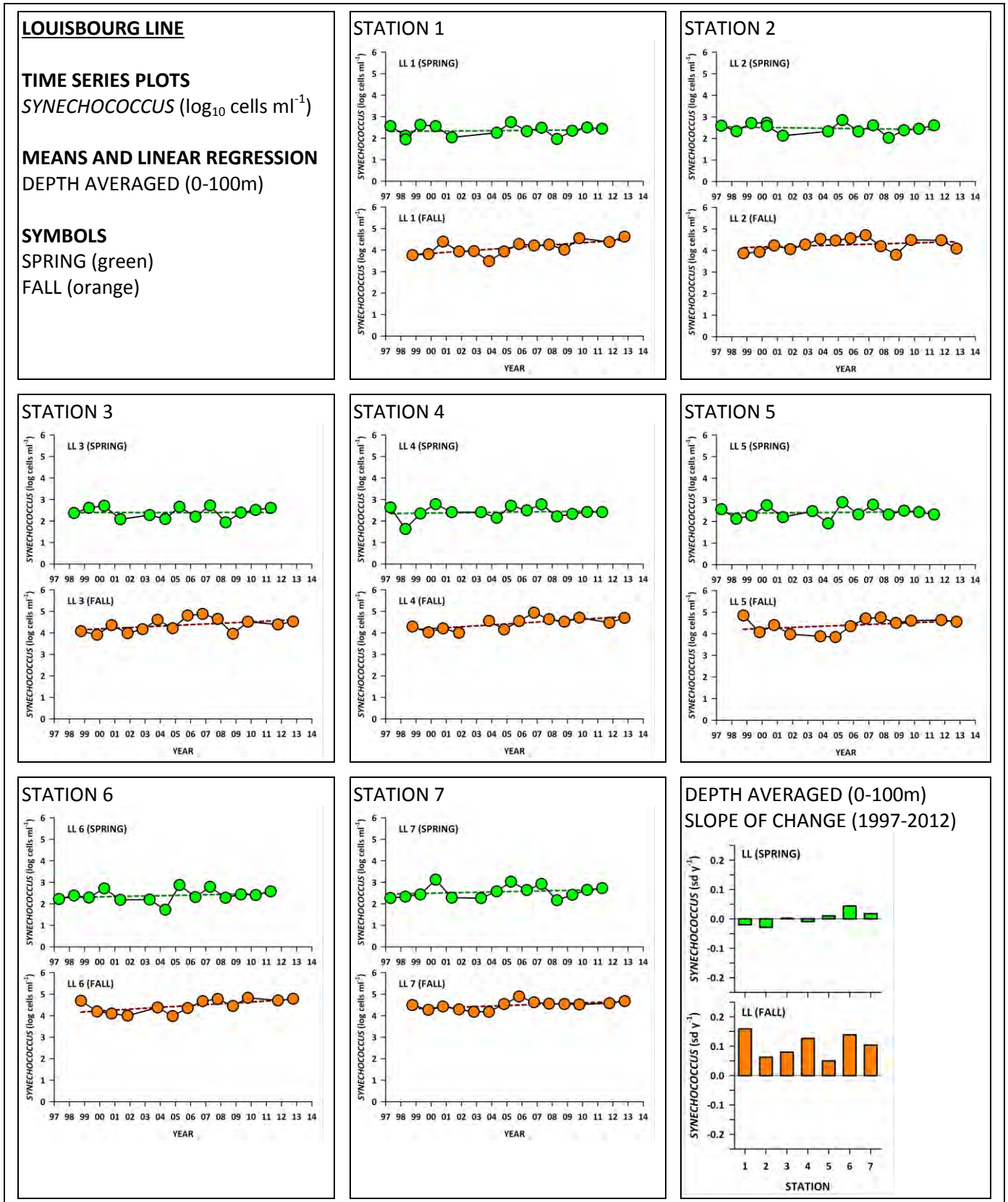


Figure 62

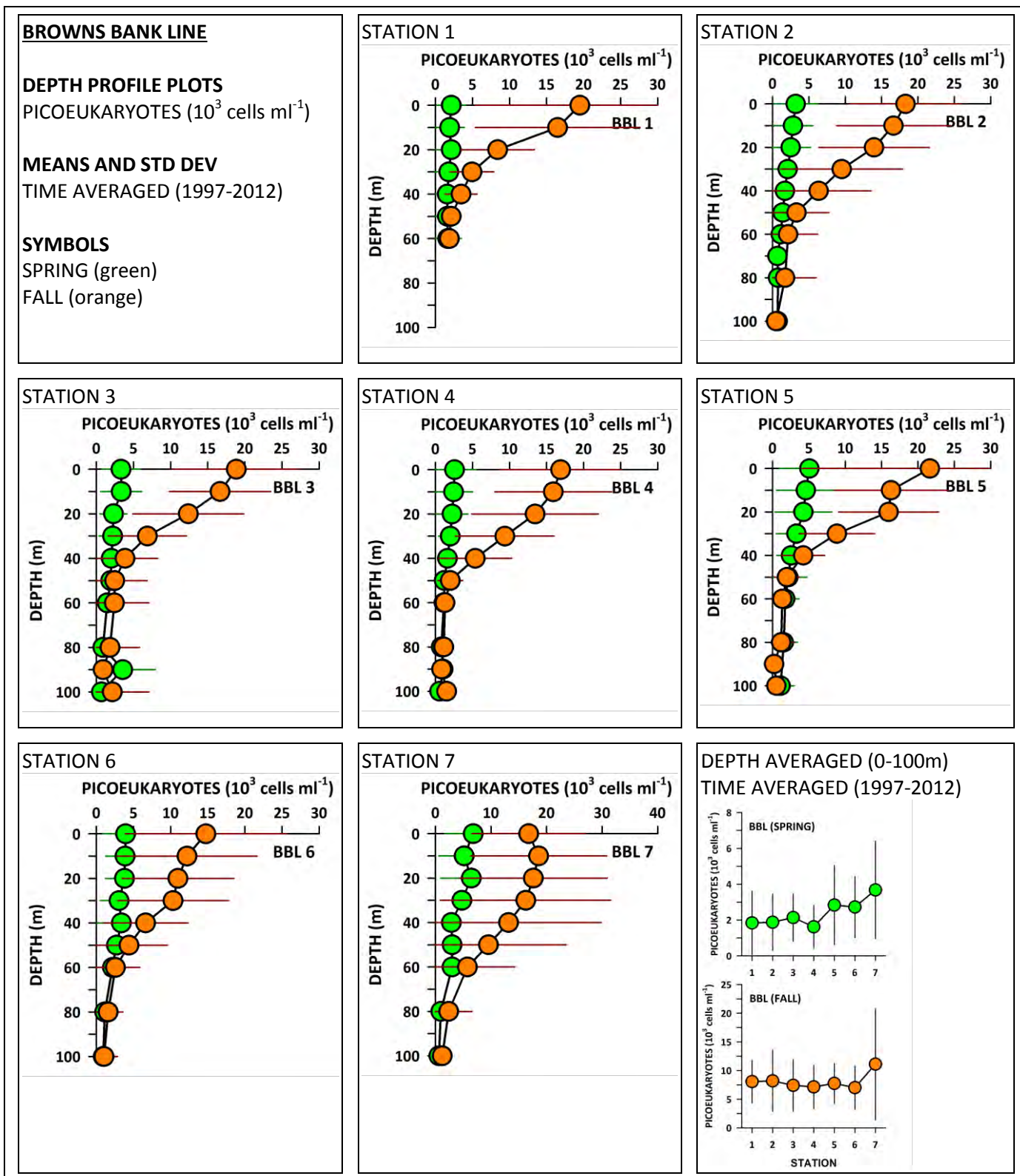


Figure 63

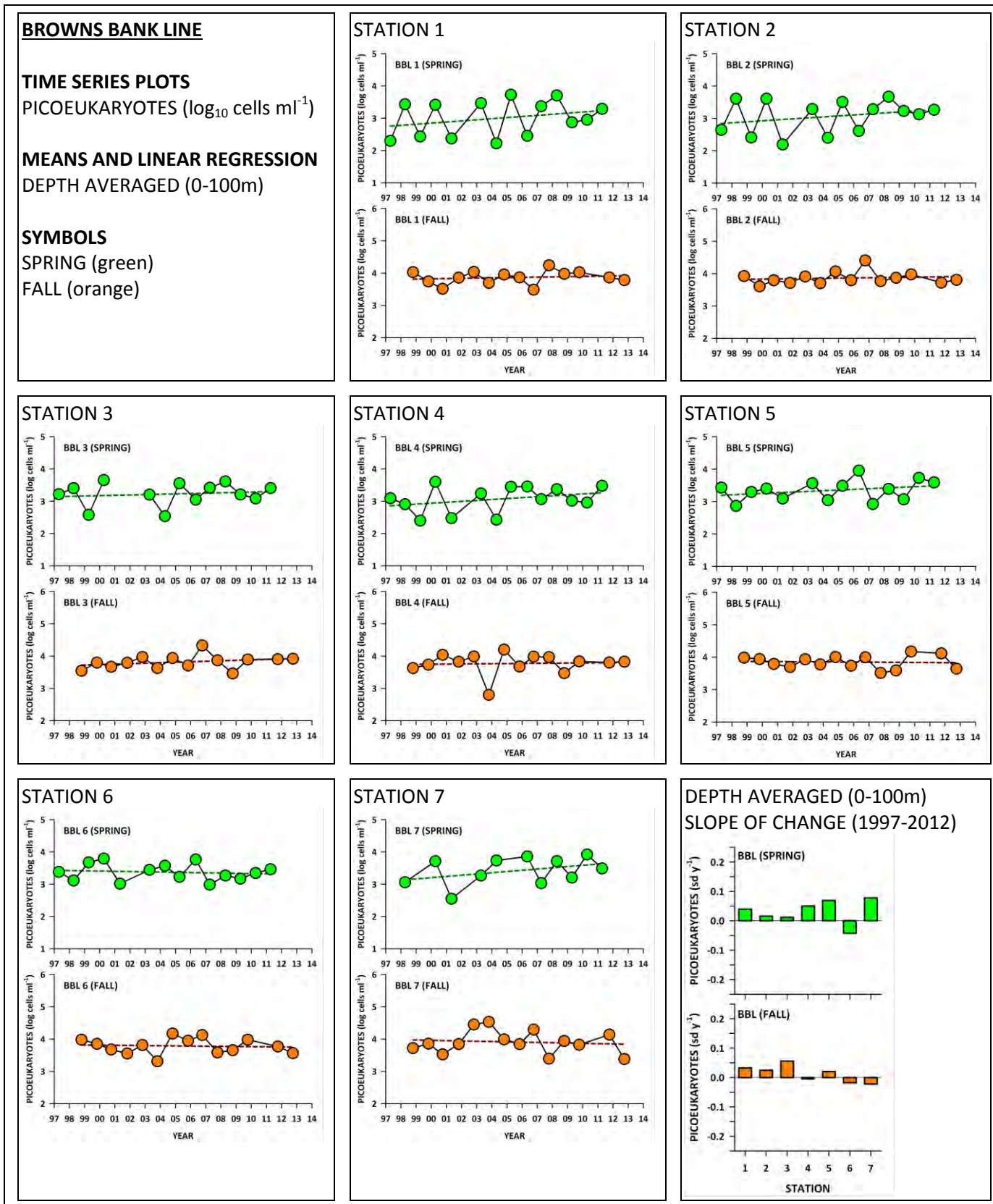


Figure 64

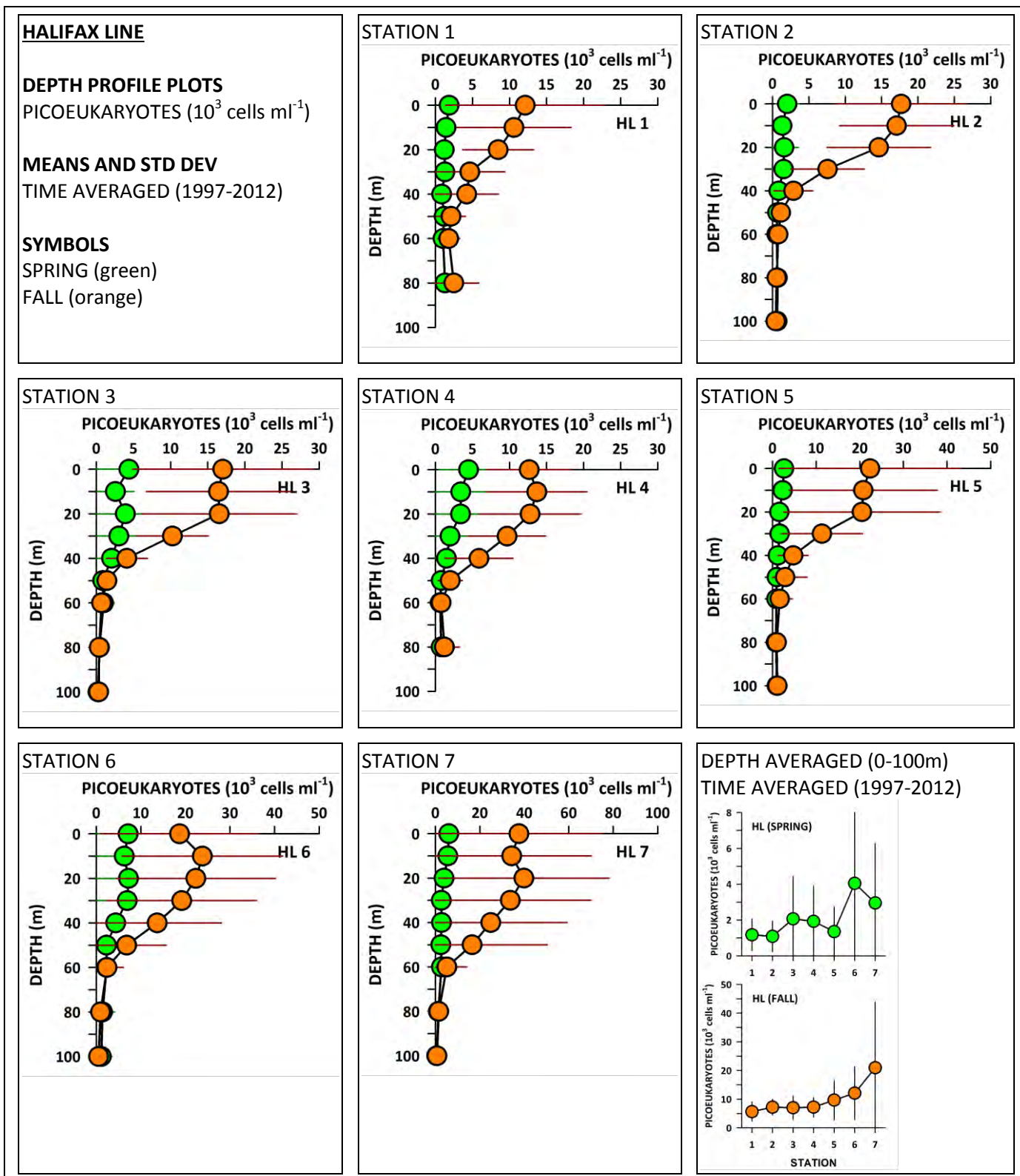


Figure 65

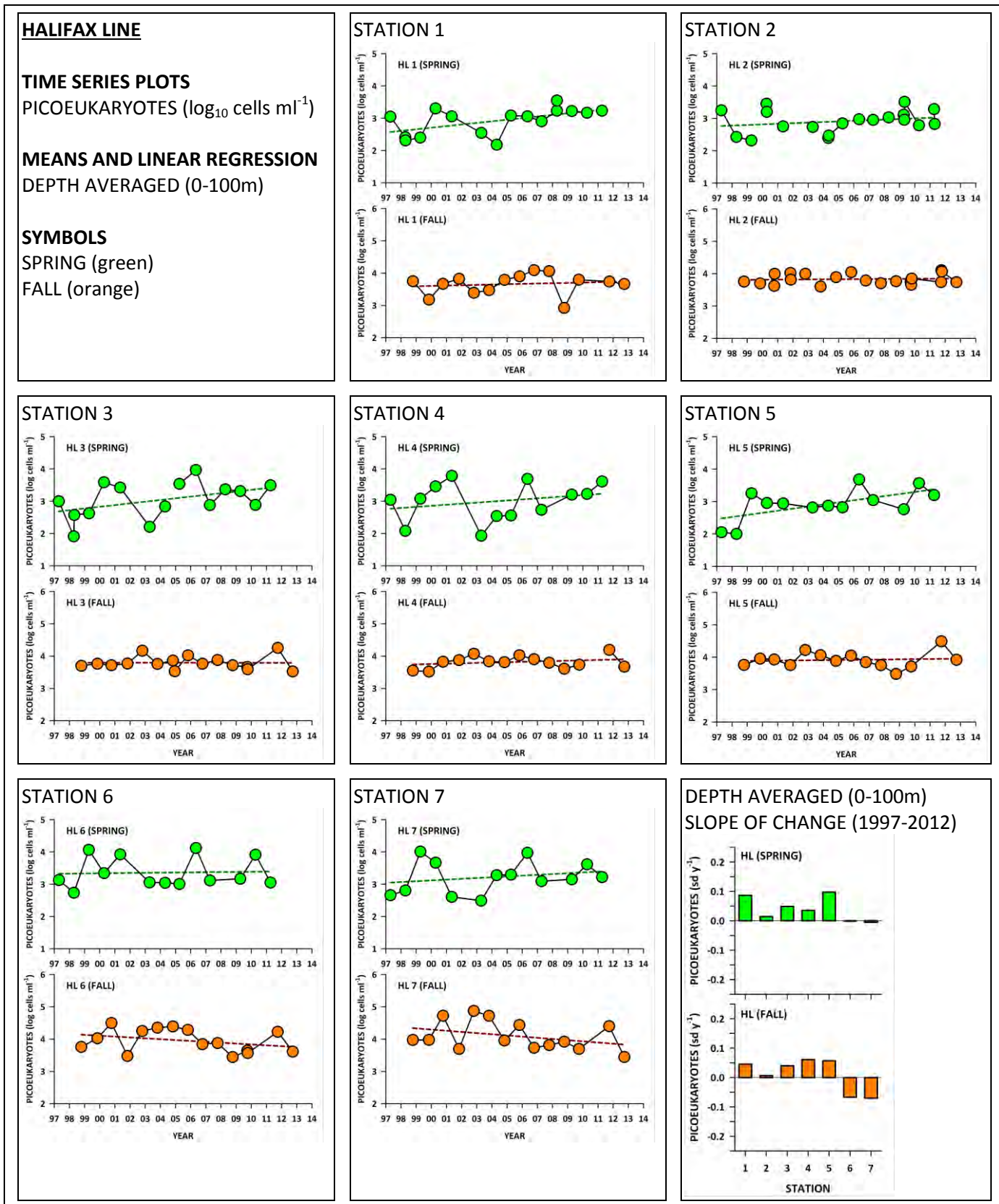


Figure 66

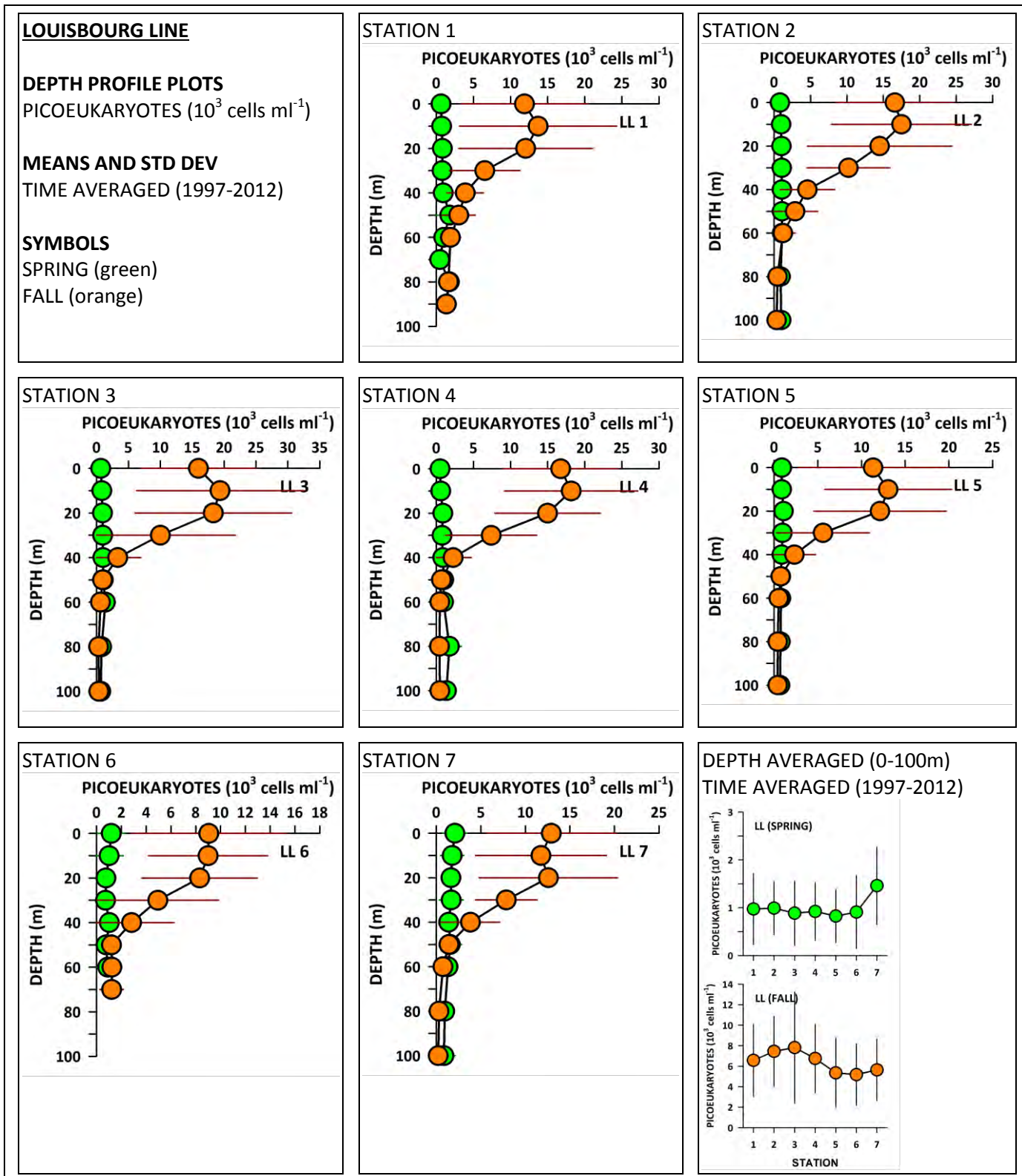


Figure 67

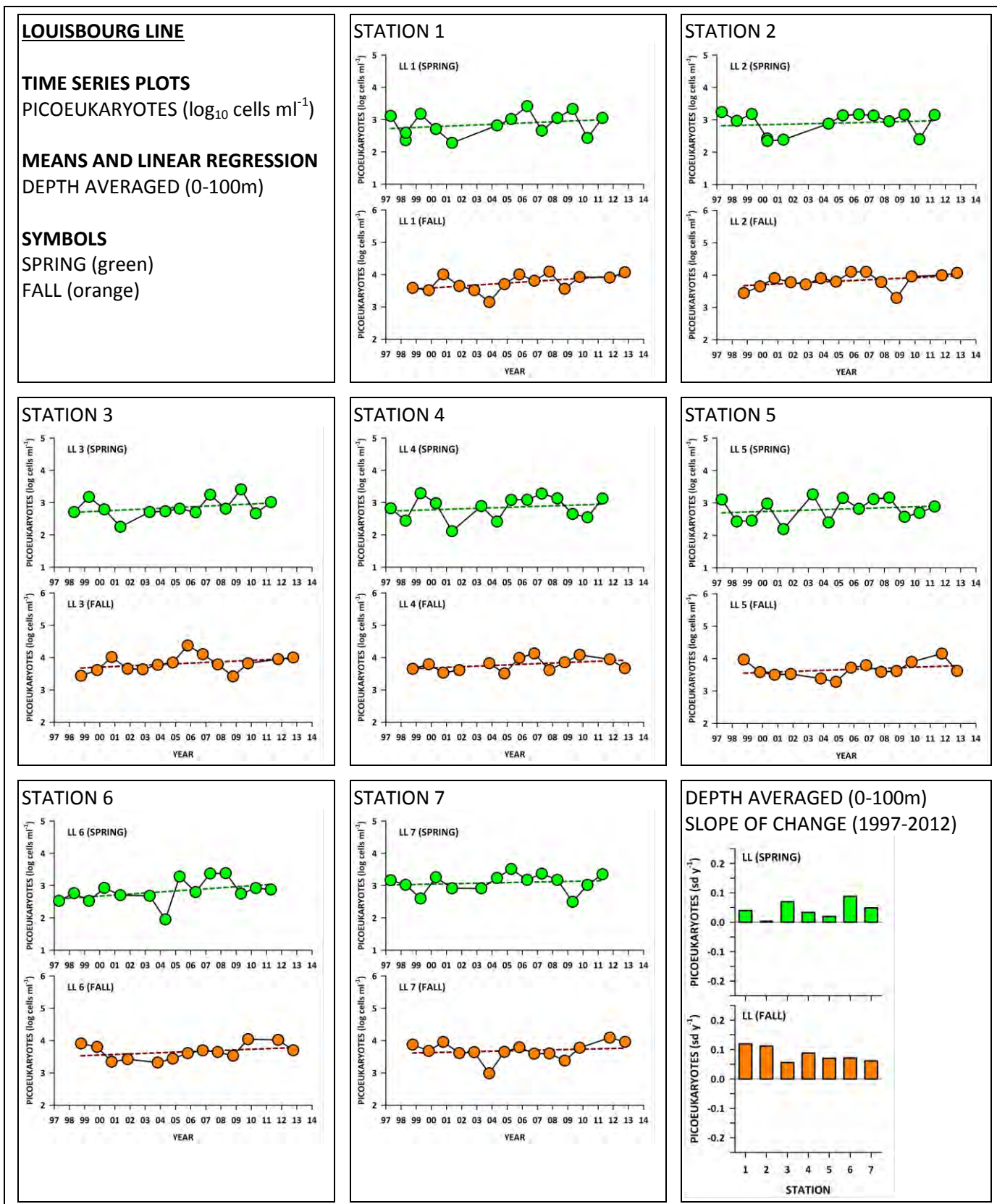


Figure 68

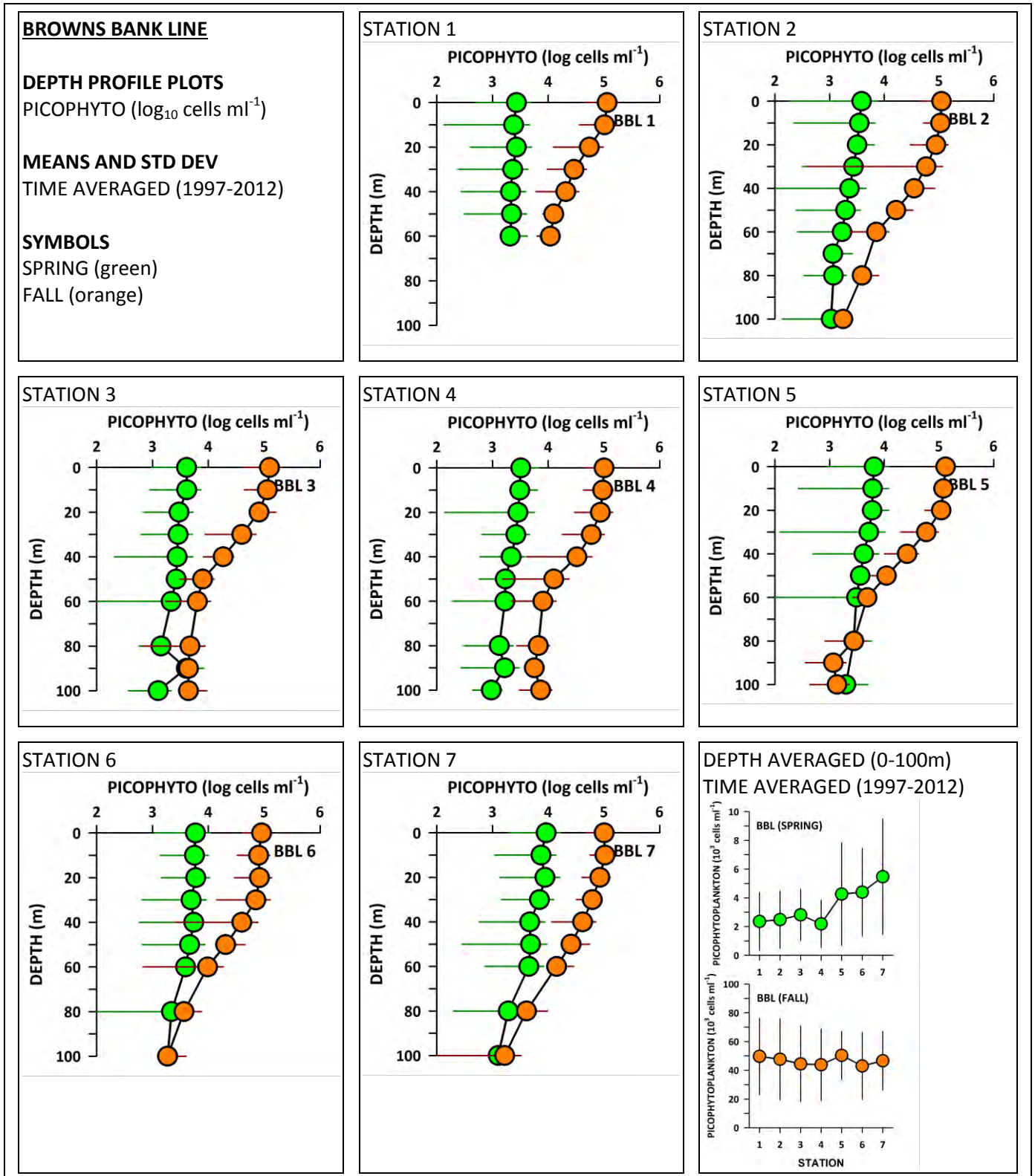


Figure 69

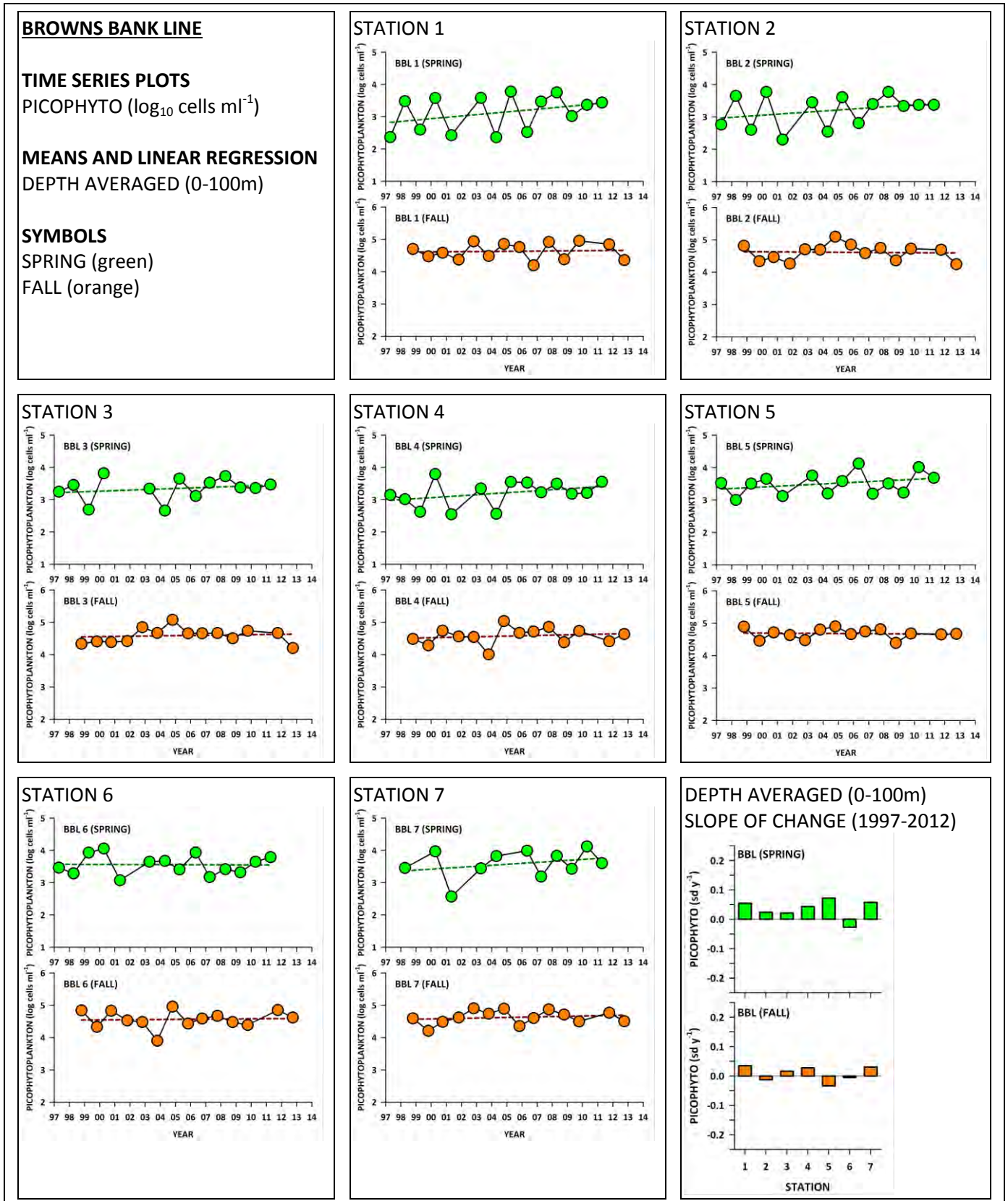


Figure 70

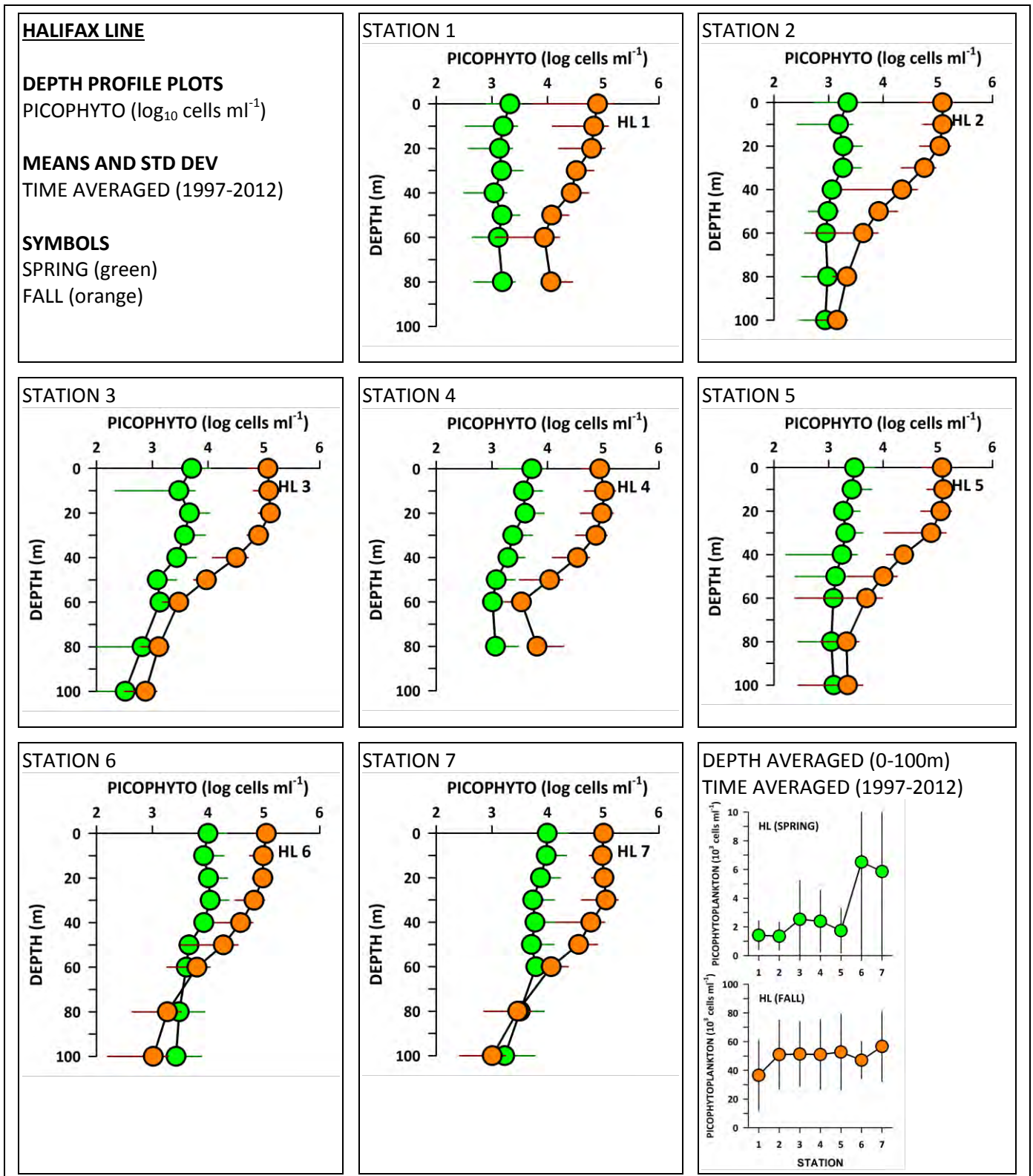


Figure 71

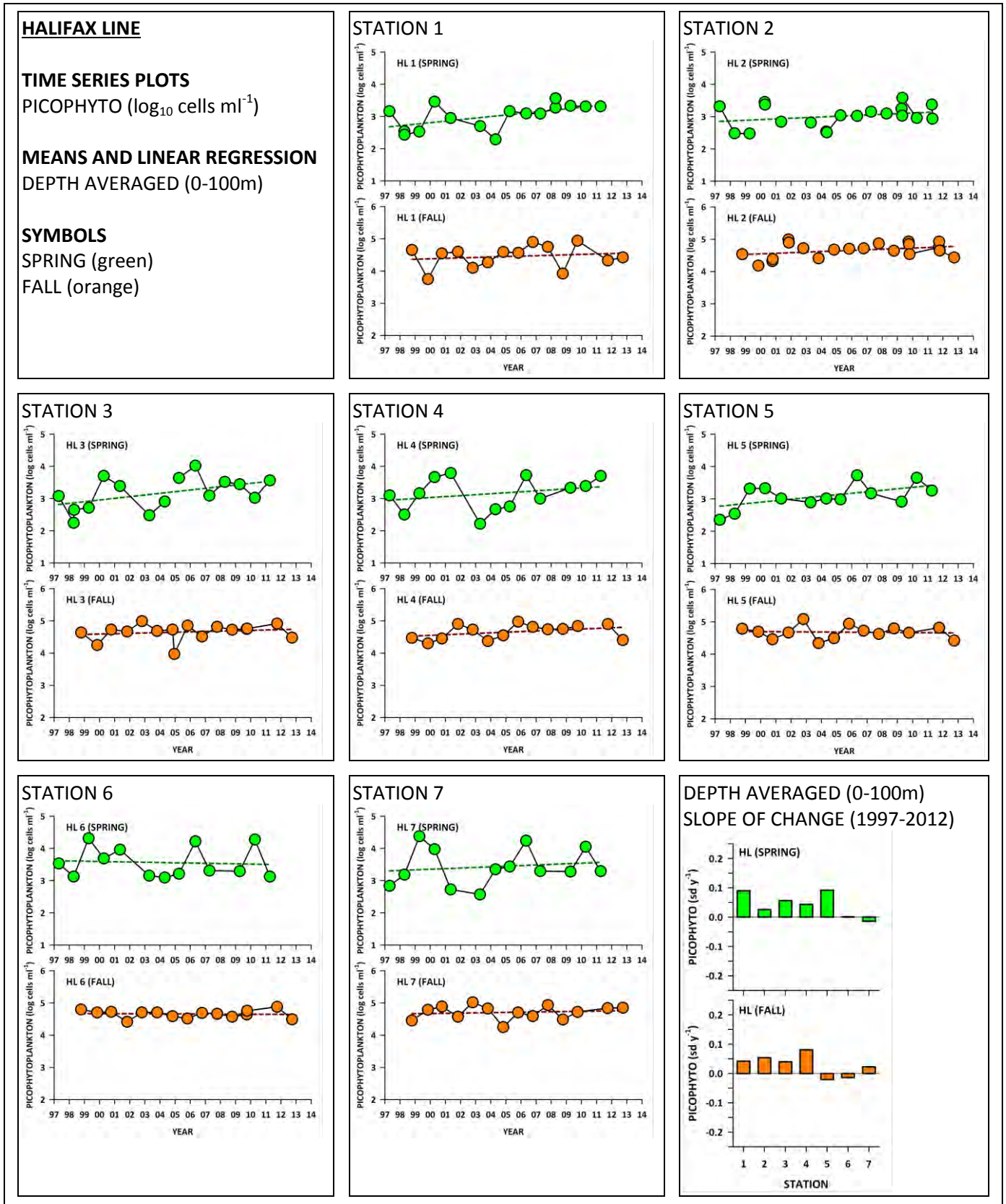


Figure 72

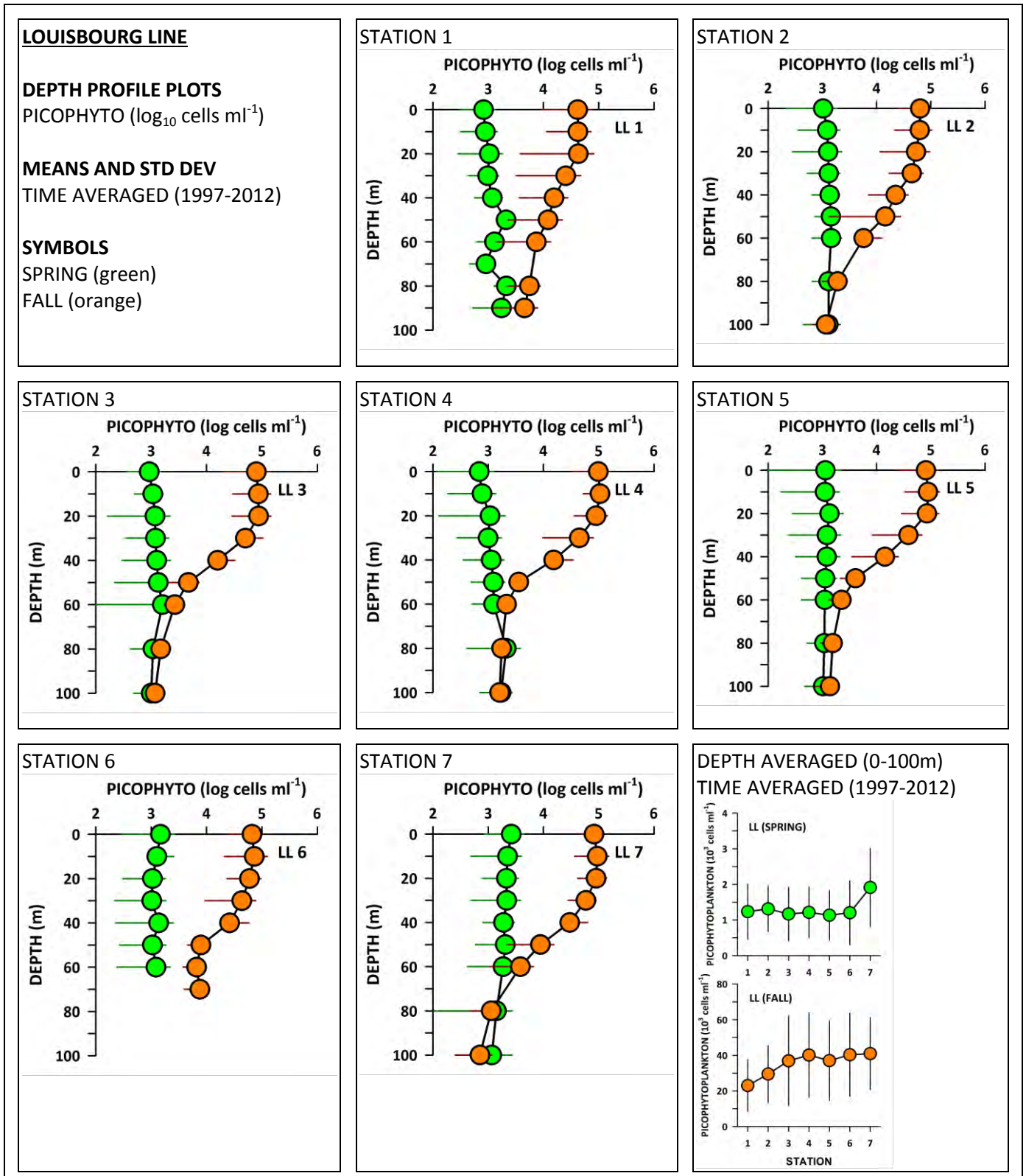


Figure 73

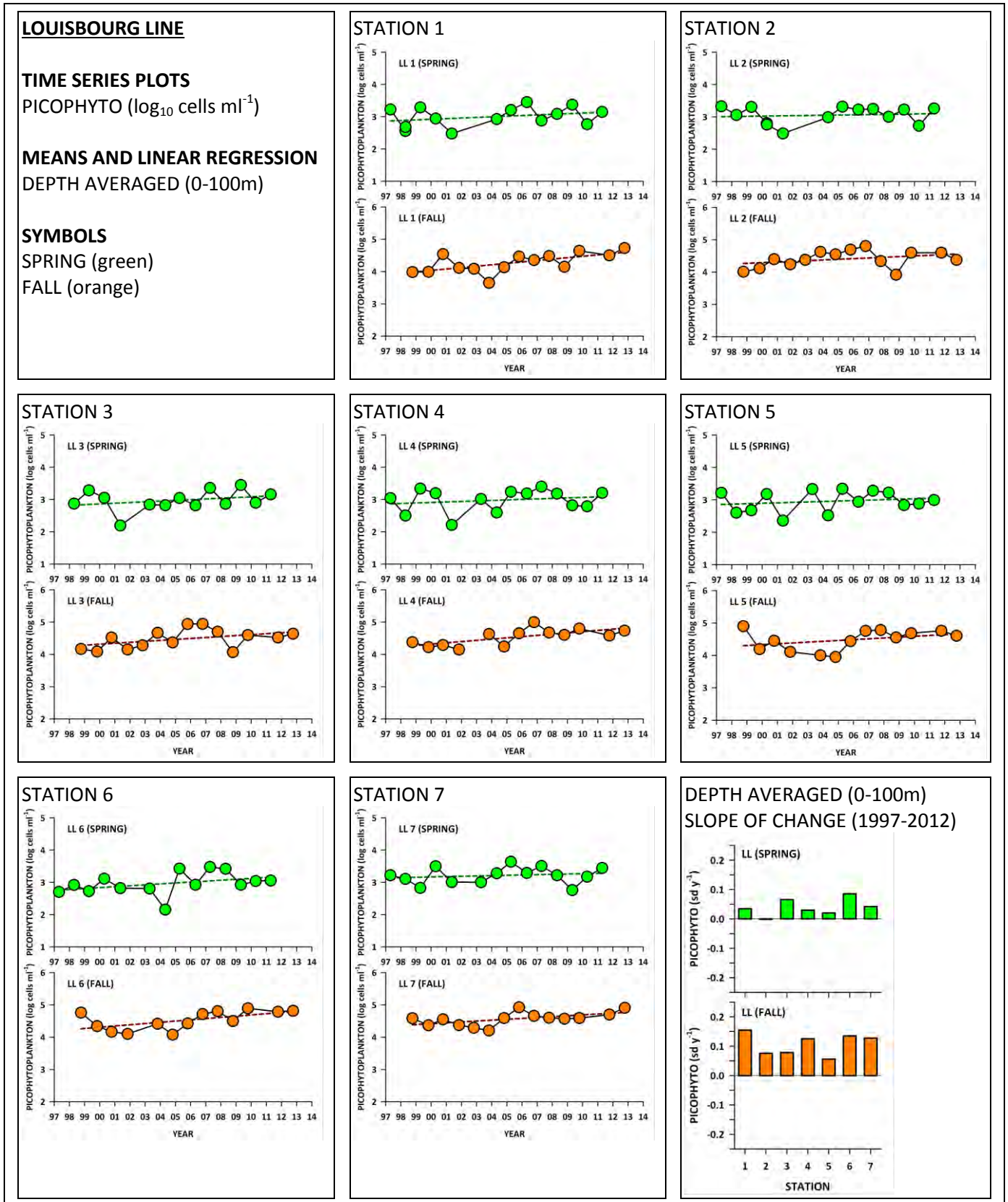


Figure 74

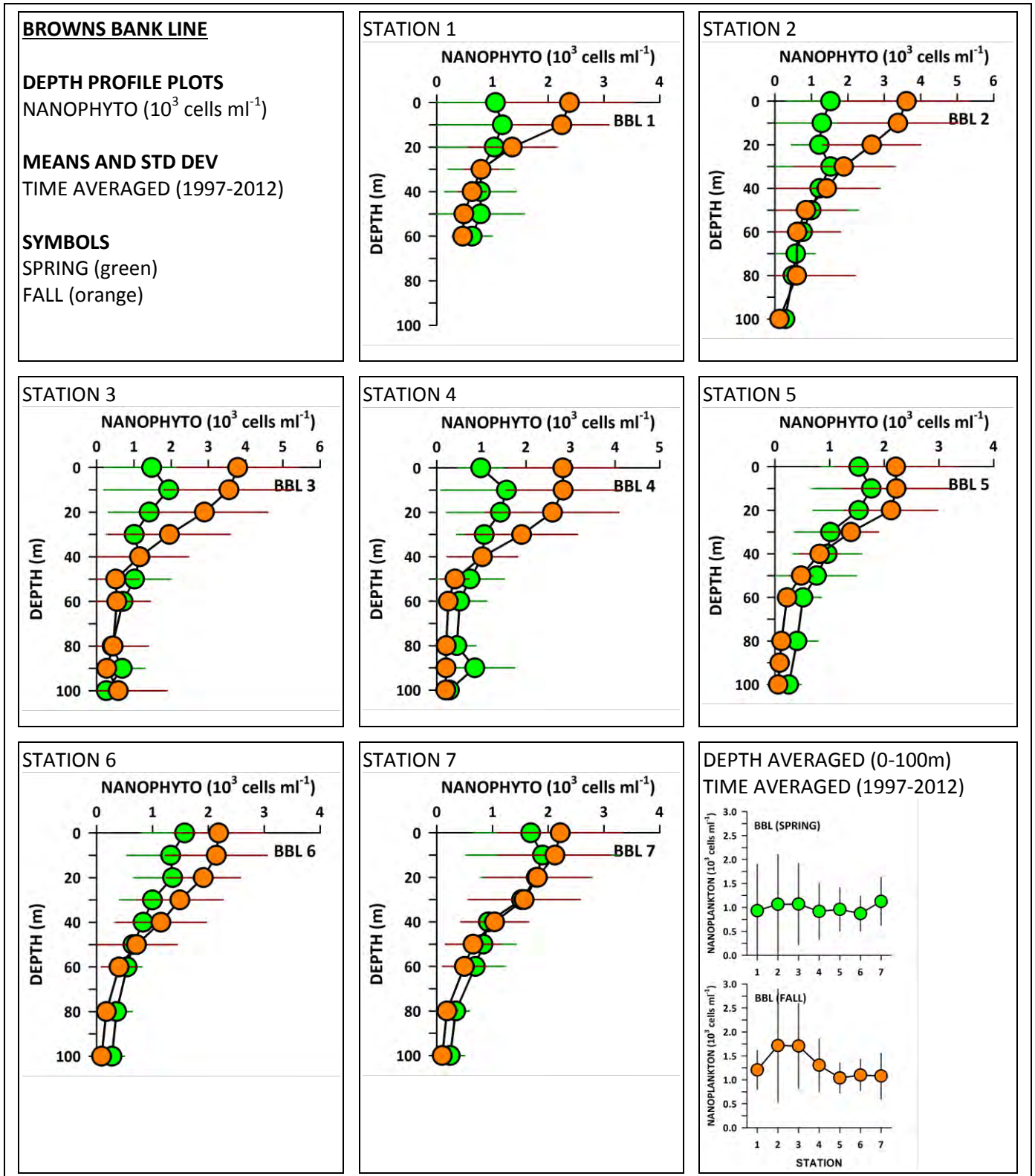


Figure 75

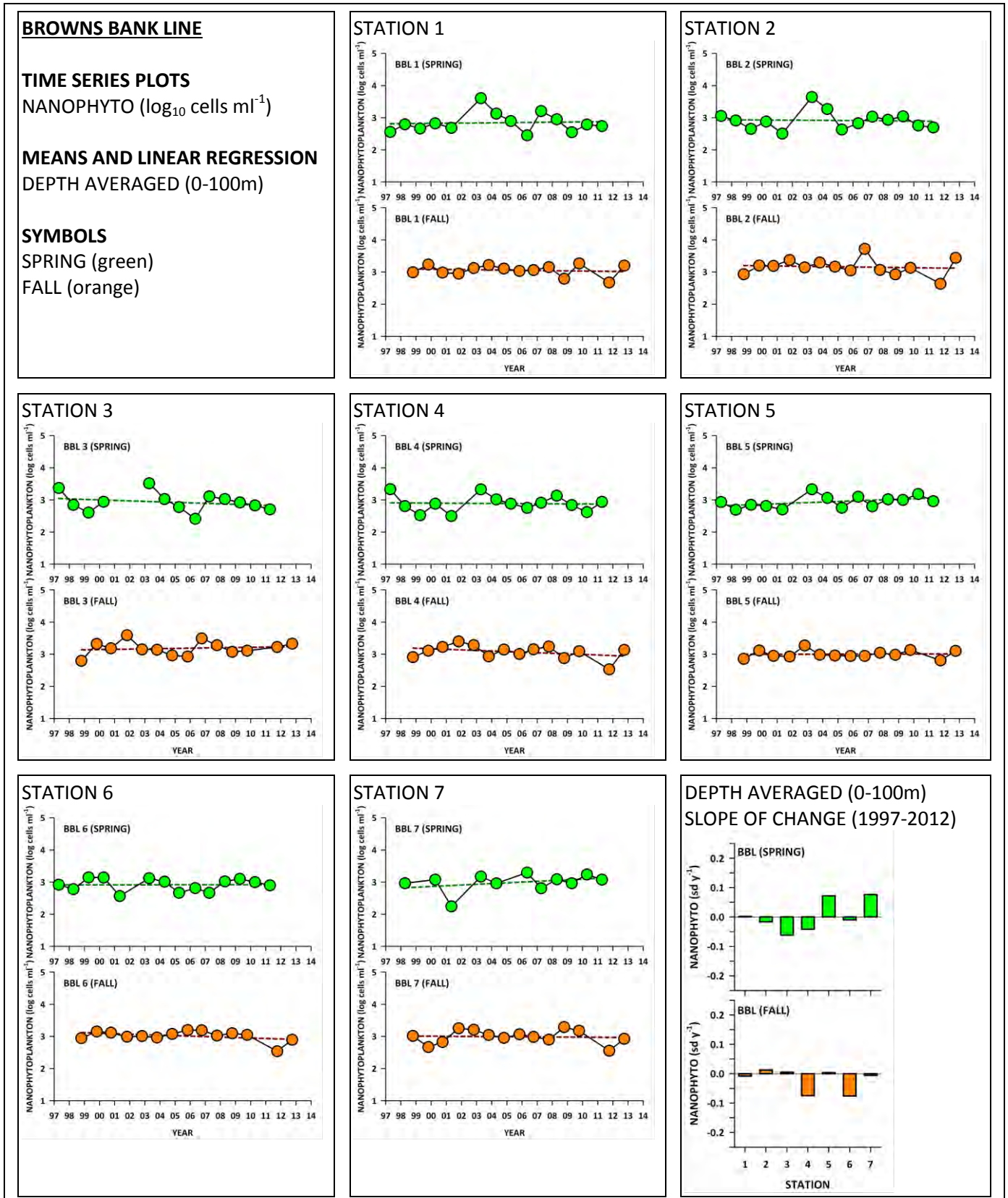


Figure 76

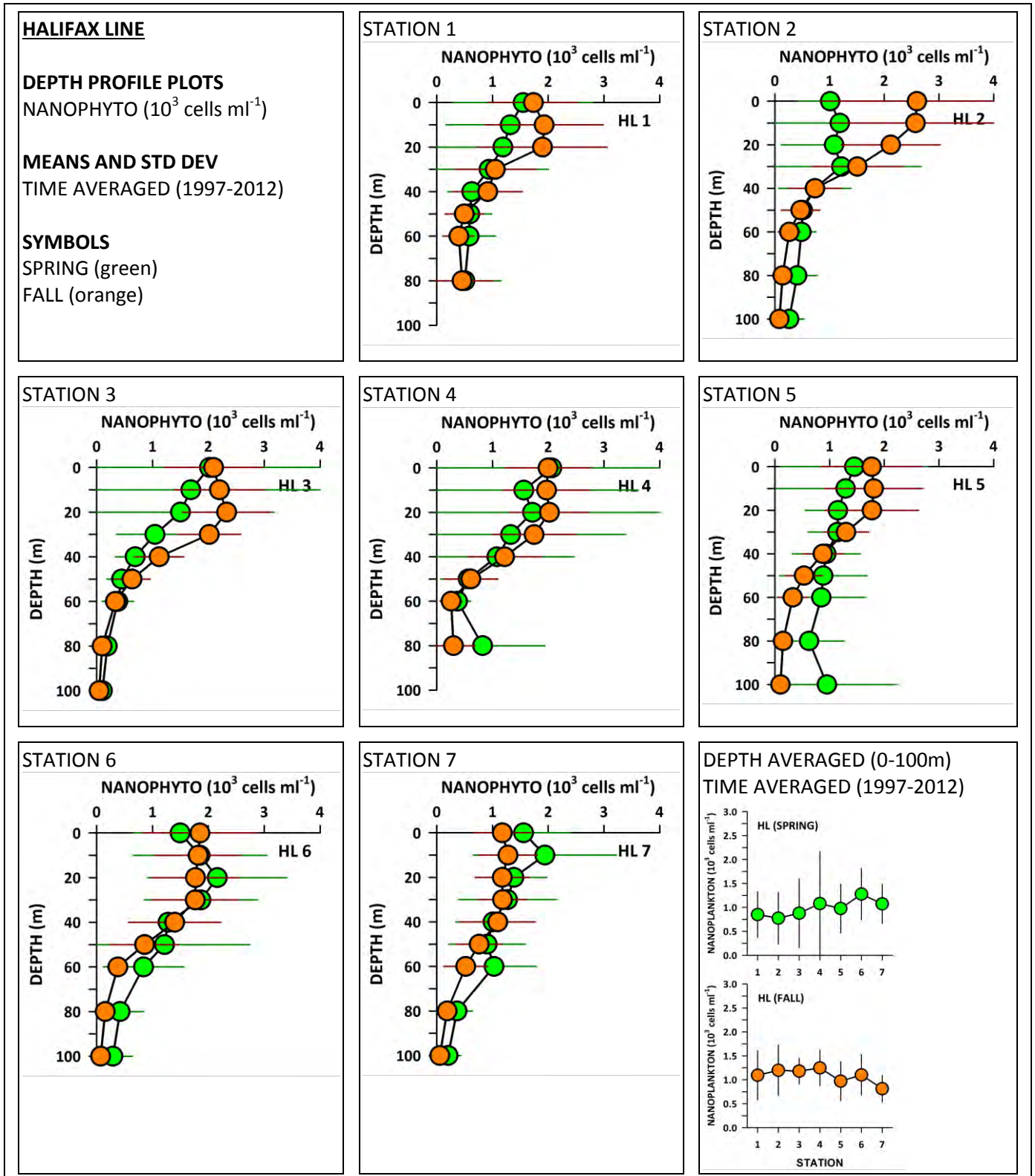


Figure 77

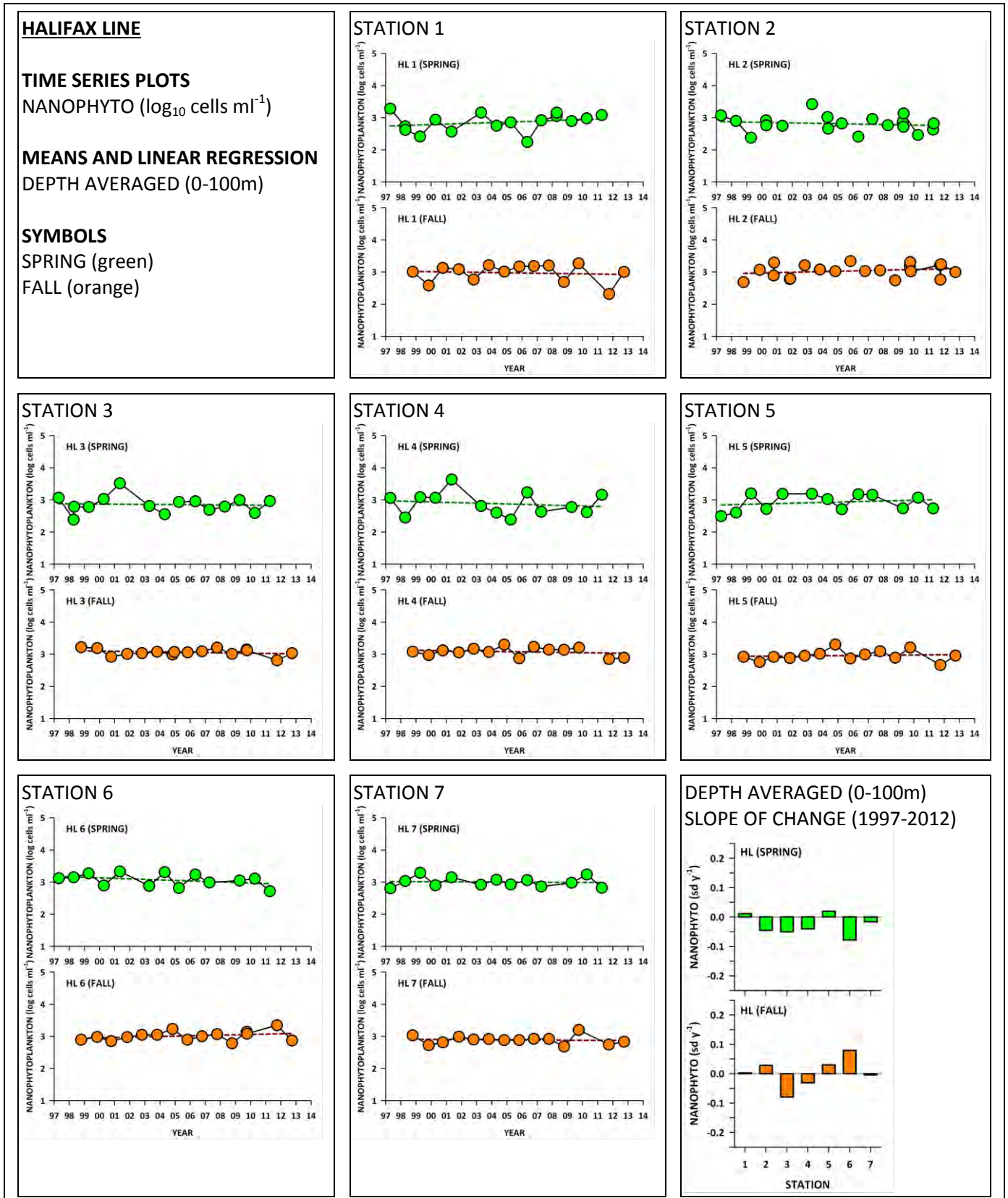


Figure 78

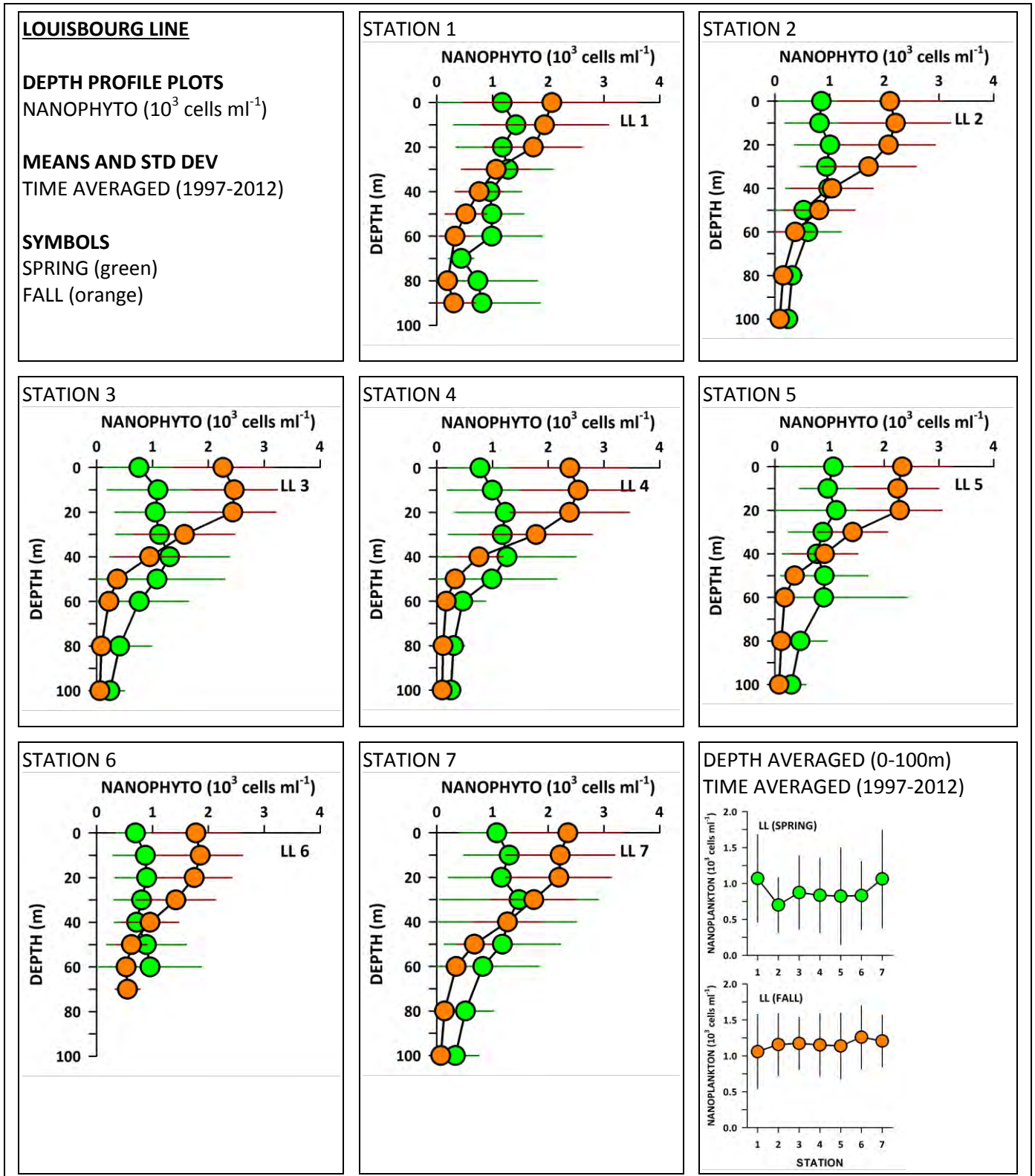


Figure 79

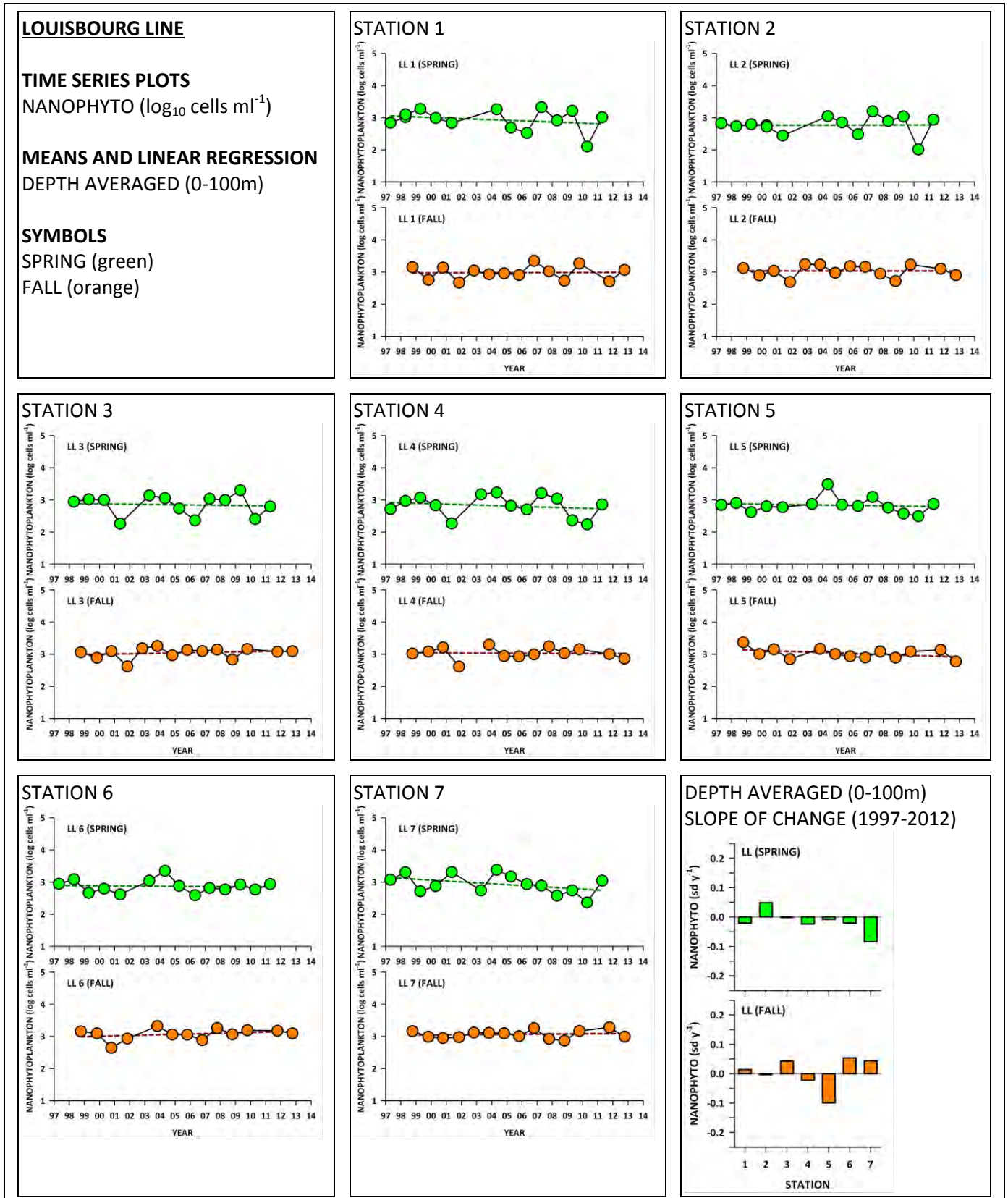


Figure 80

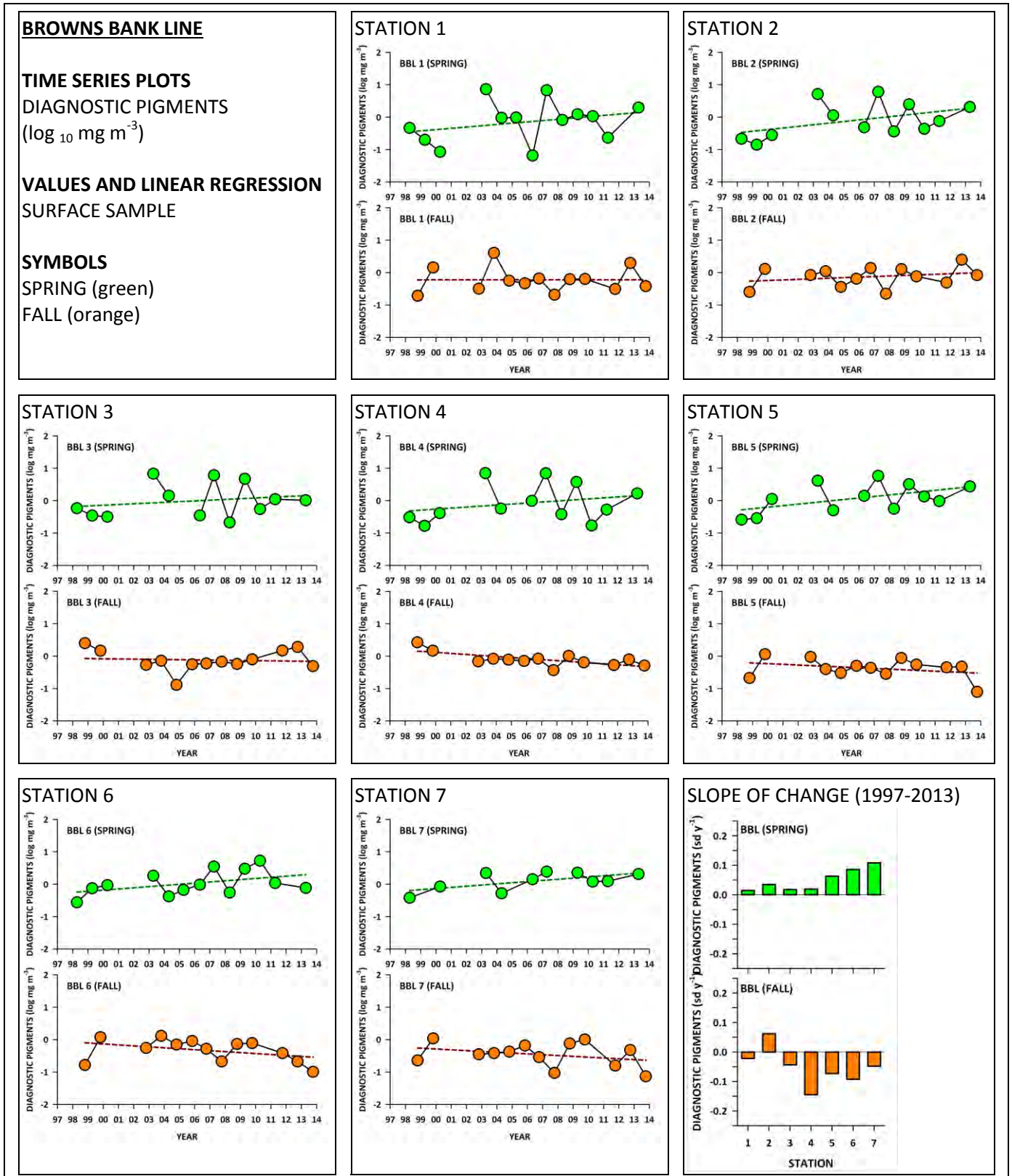


Figure 81

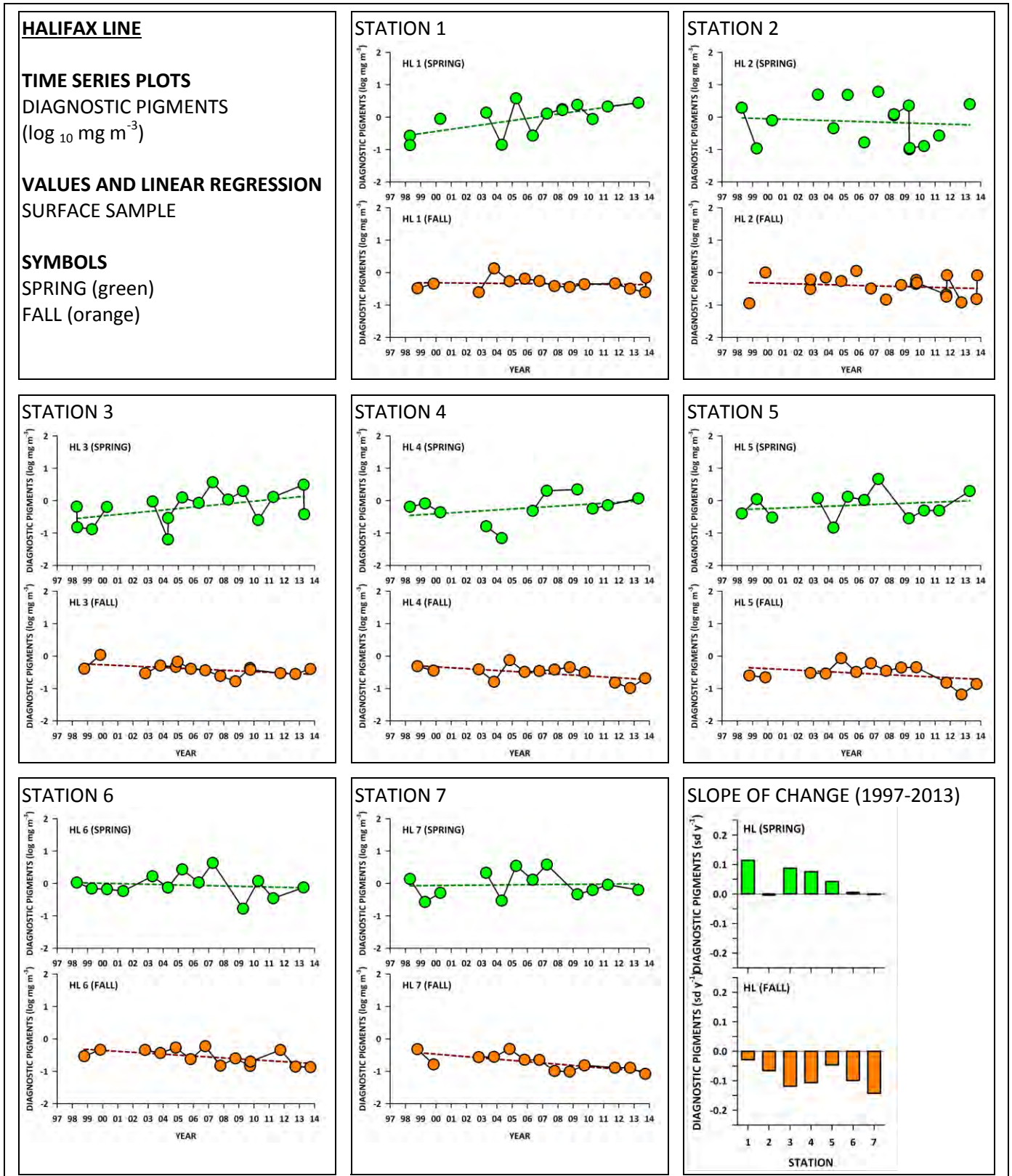


Figure 82

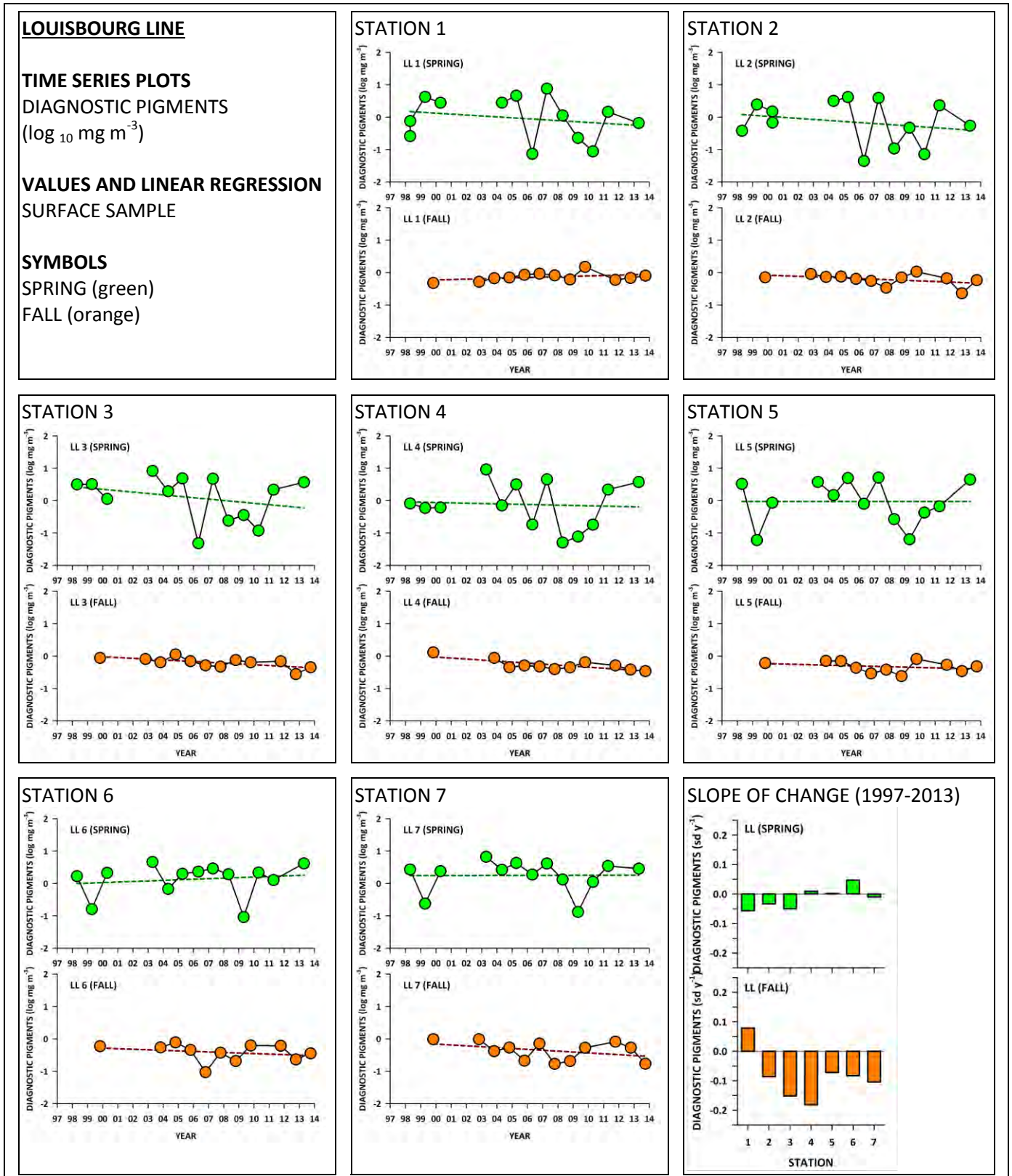


Figure 83

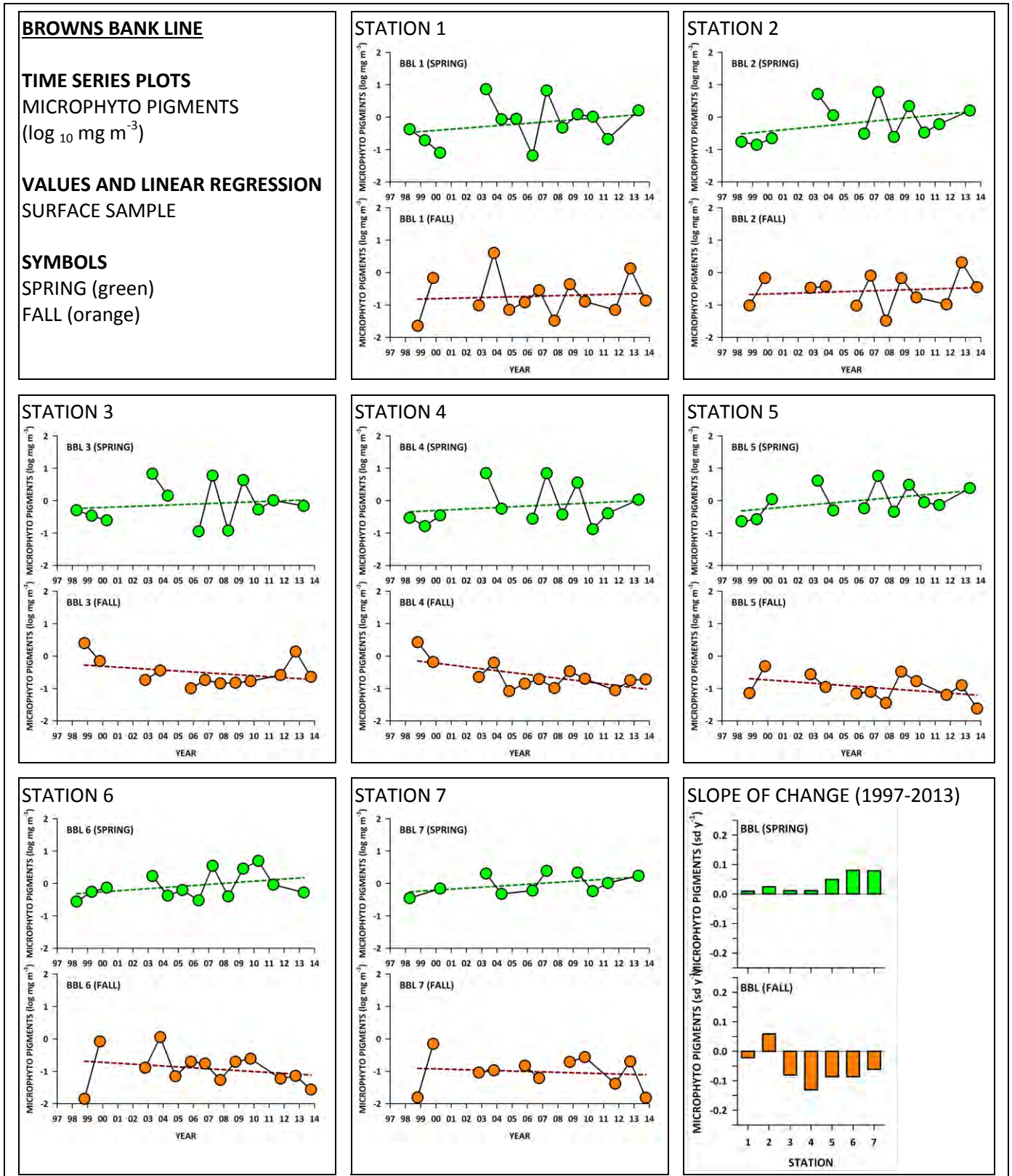


Figure 84

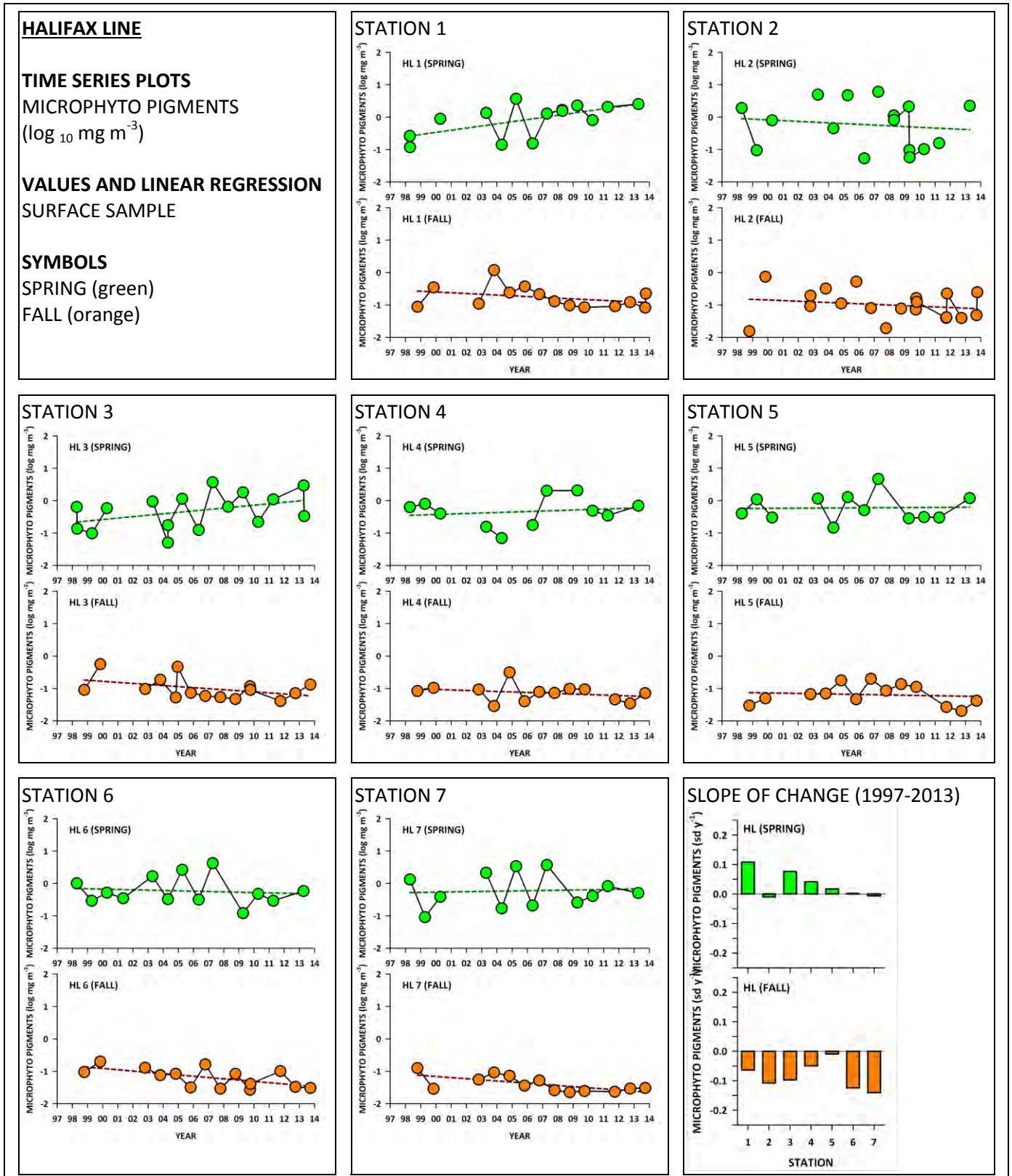


Figure 85

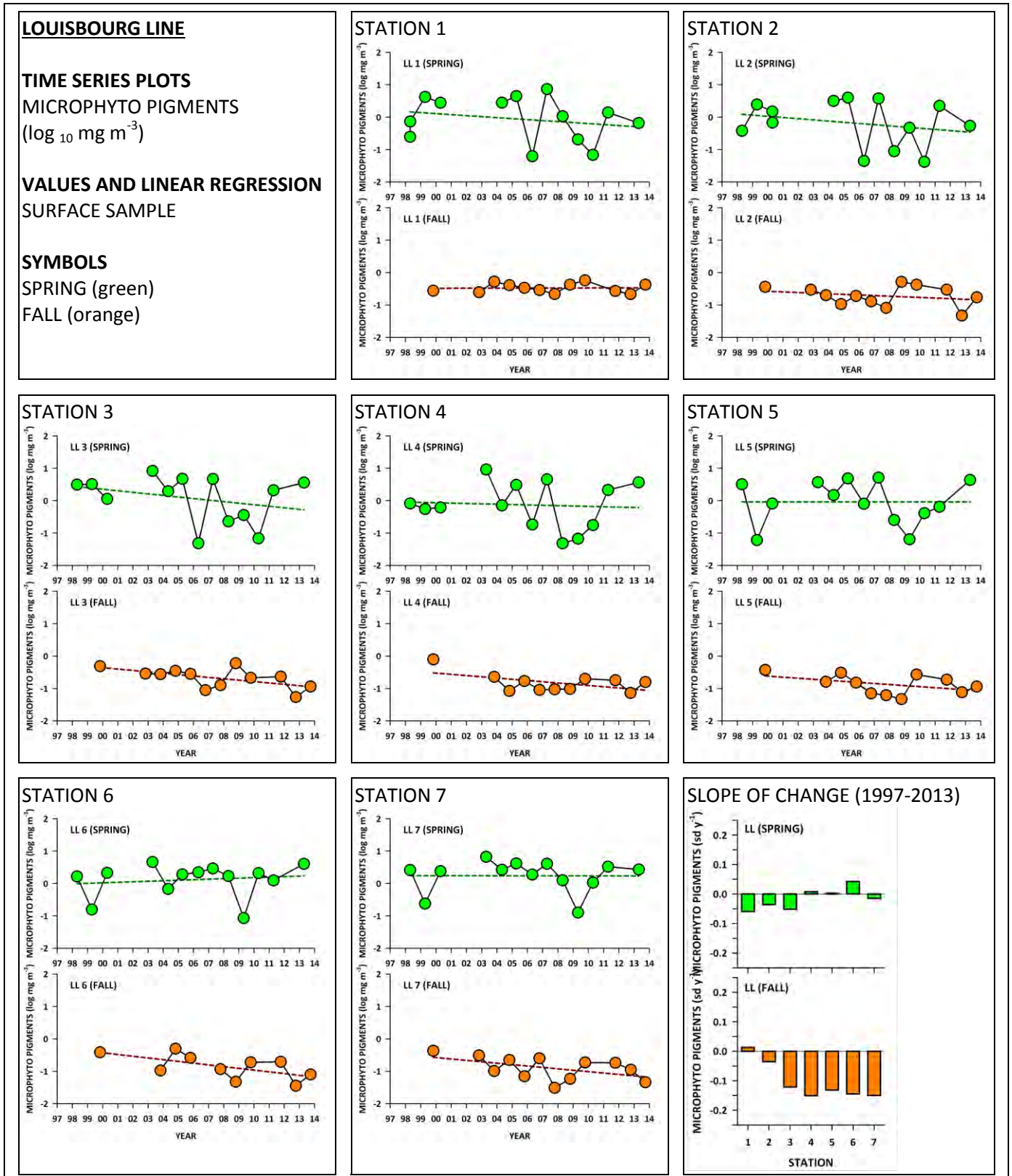


Figure 86

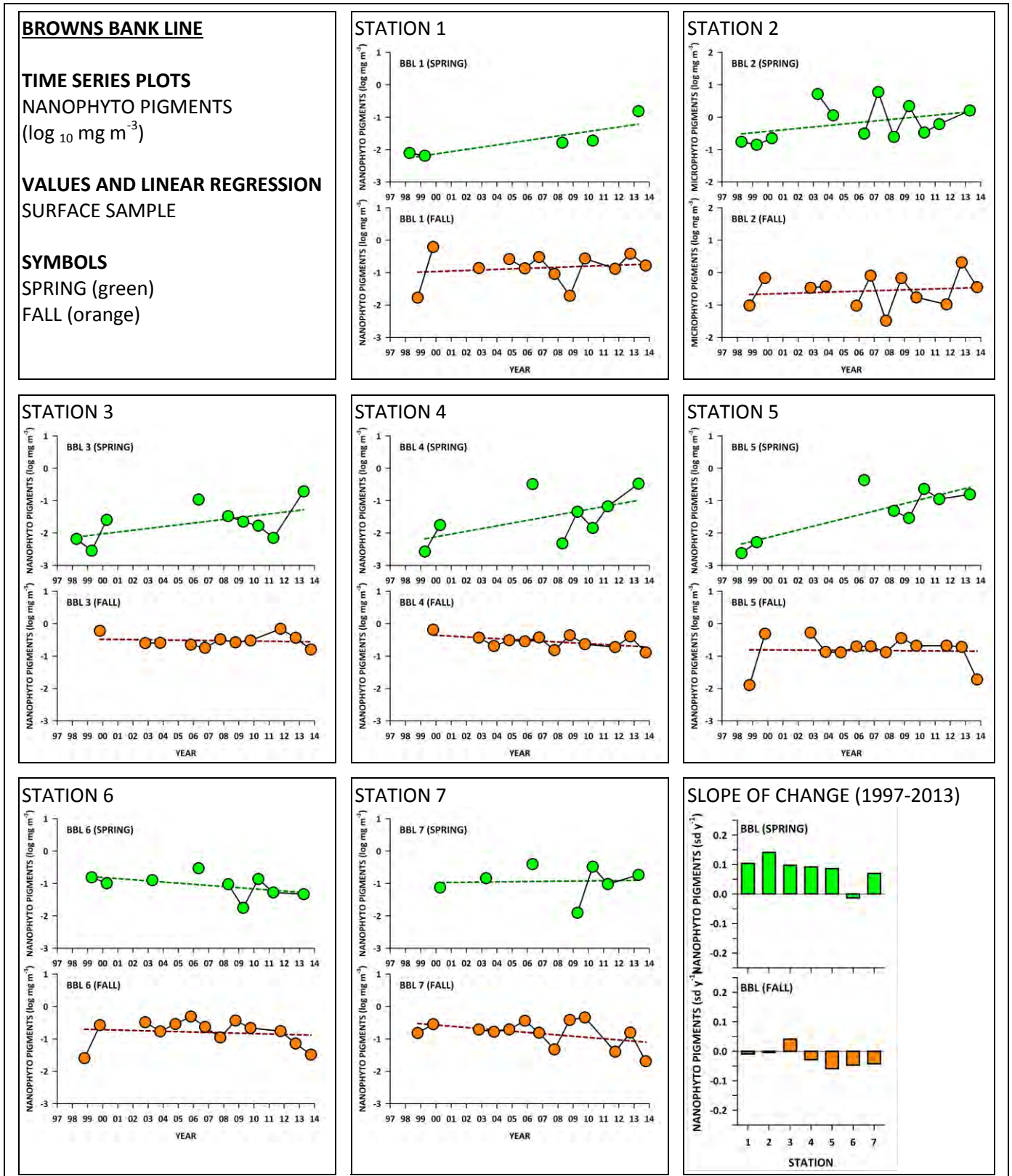


Figure 87

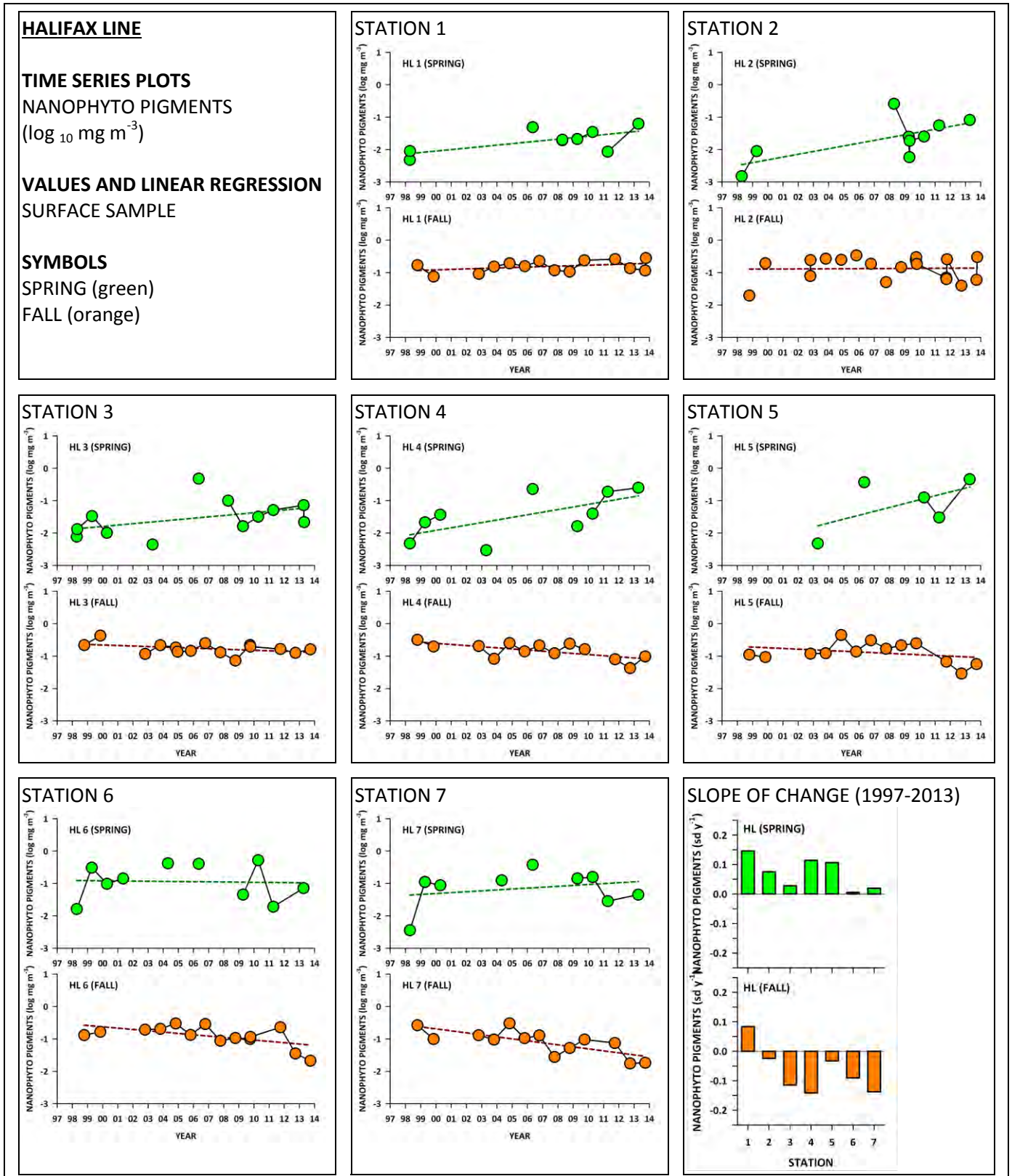


Figure 88

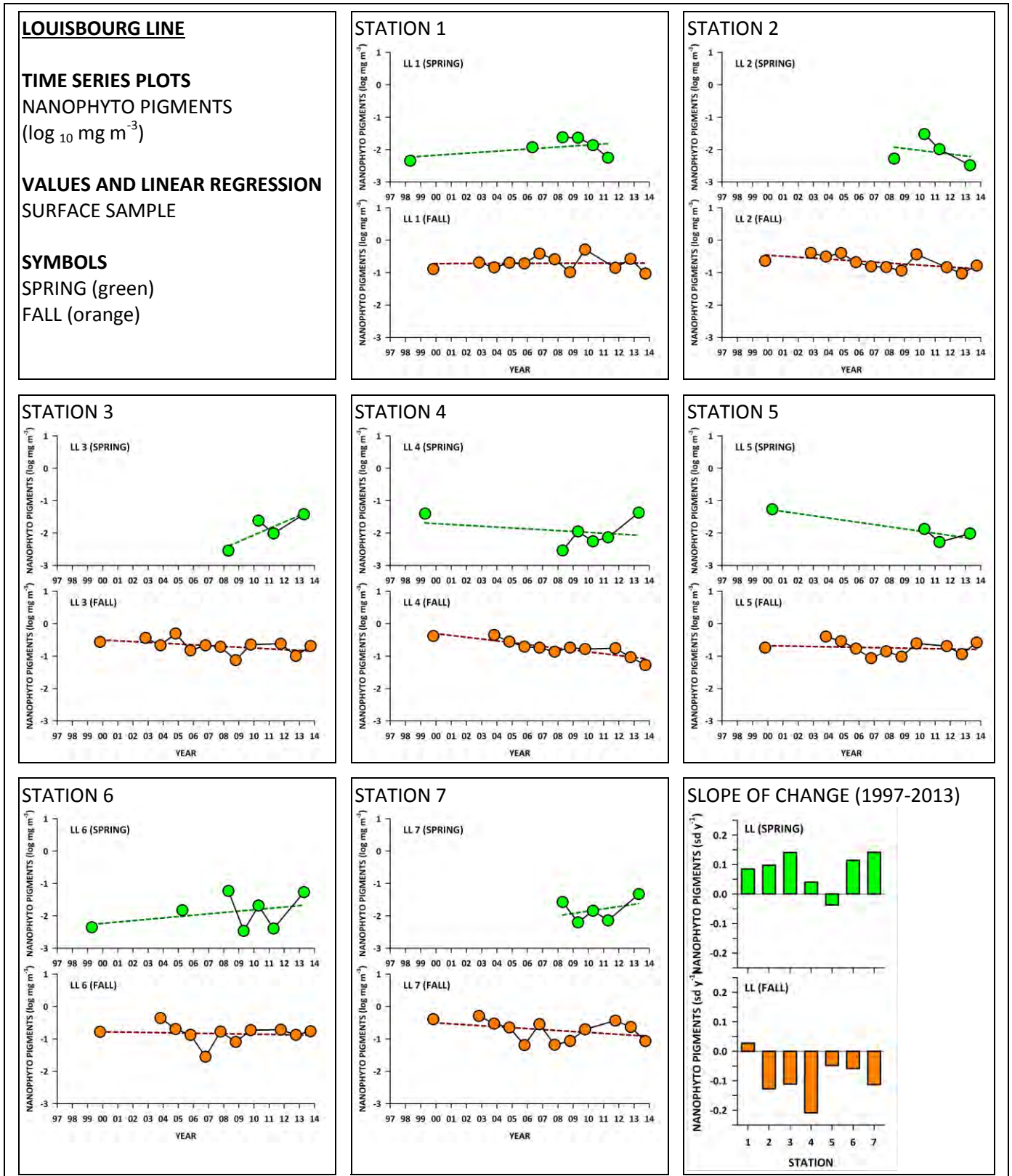


Figure 89

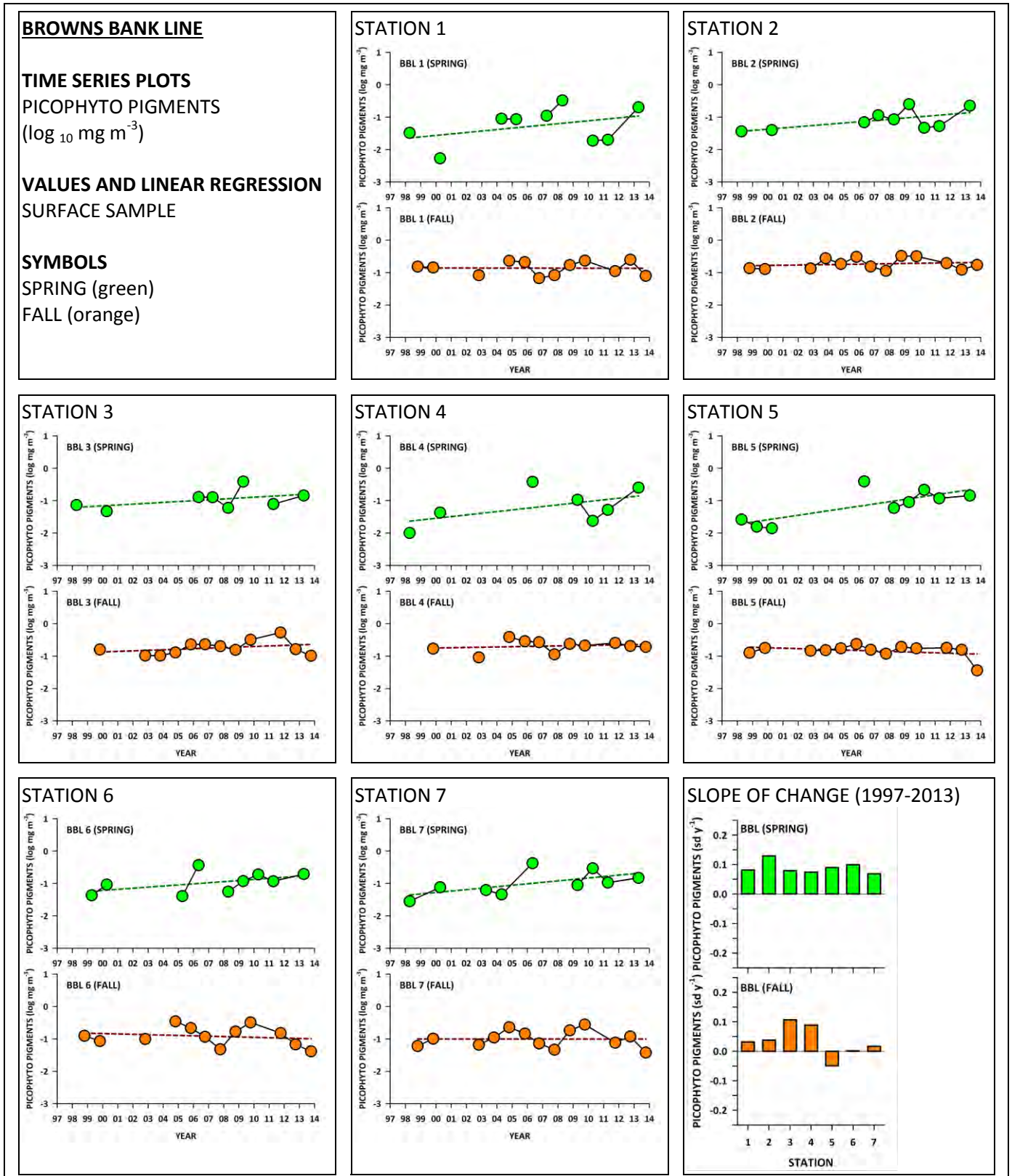


Figure 90

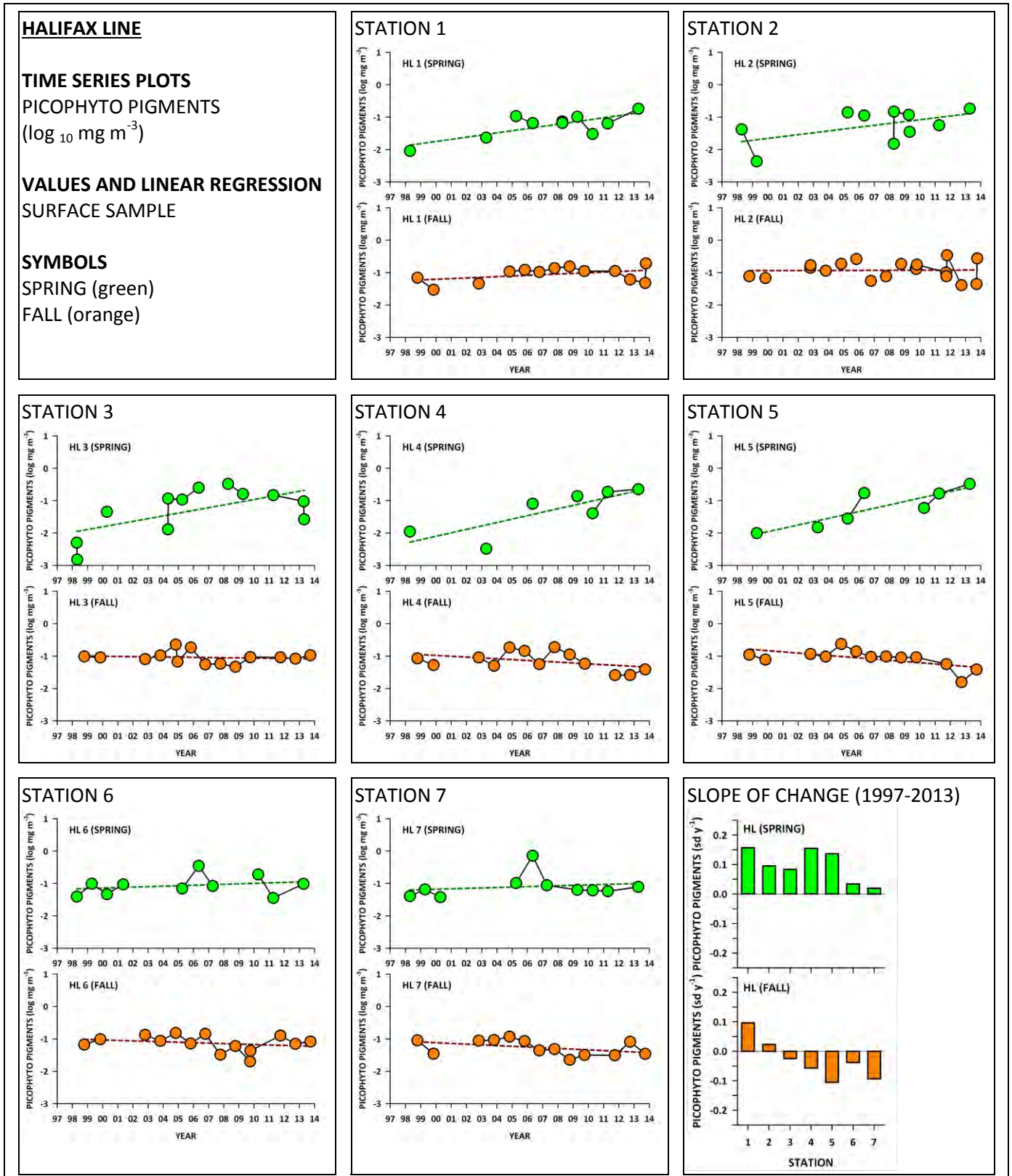


Figure 91

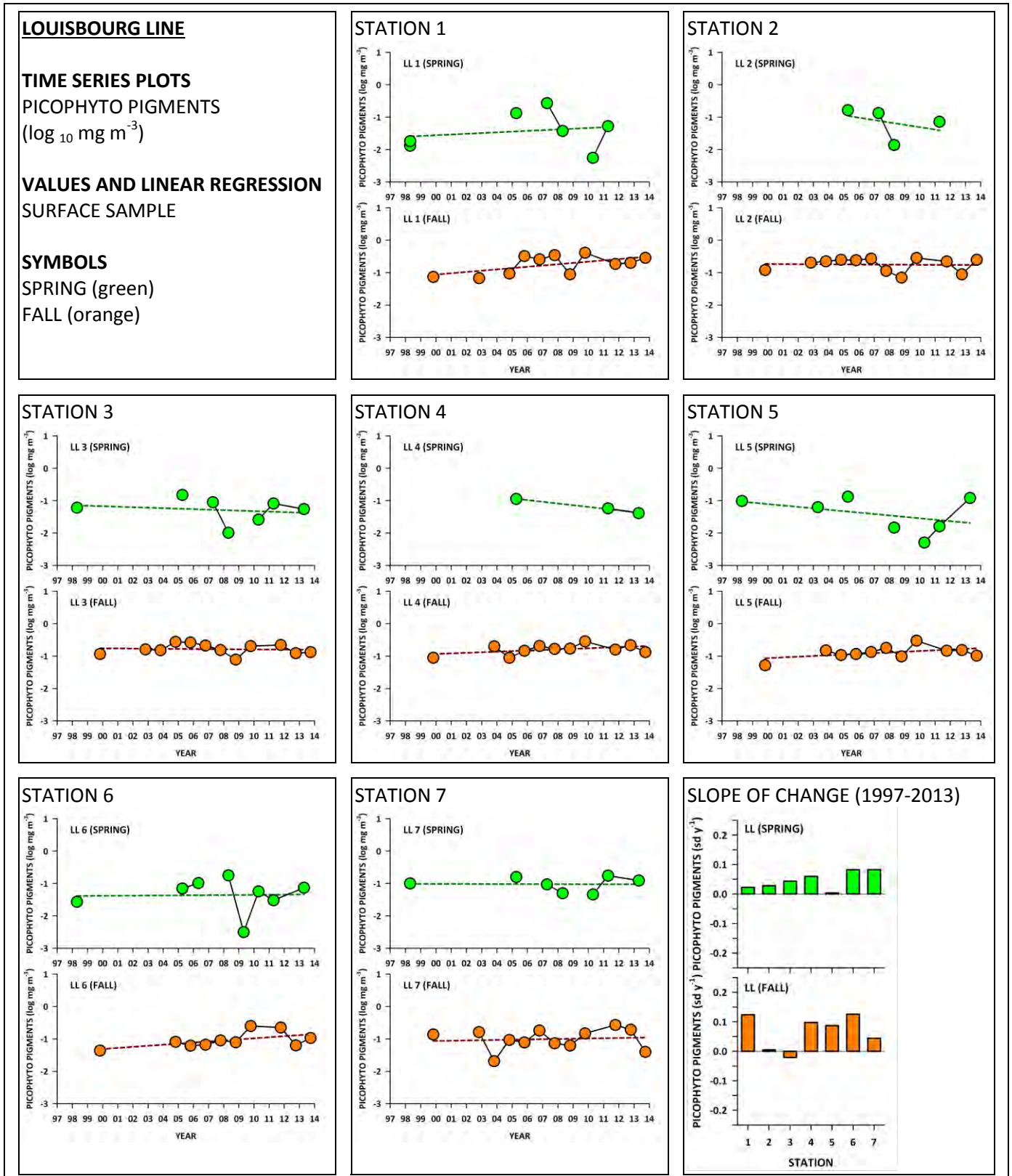


Figure 92

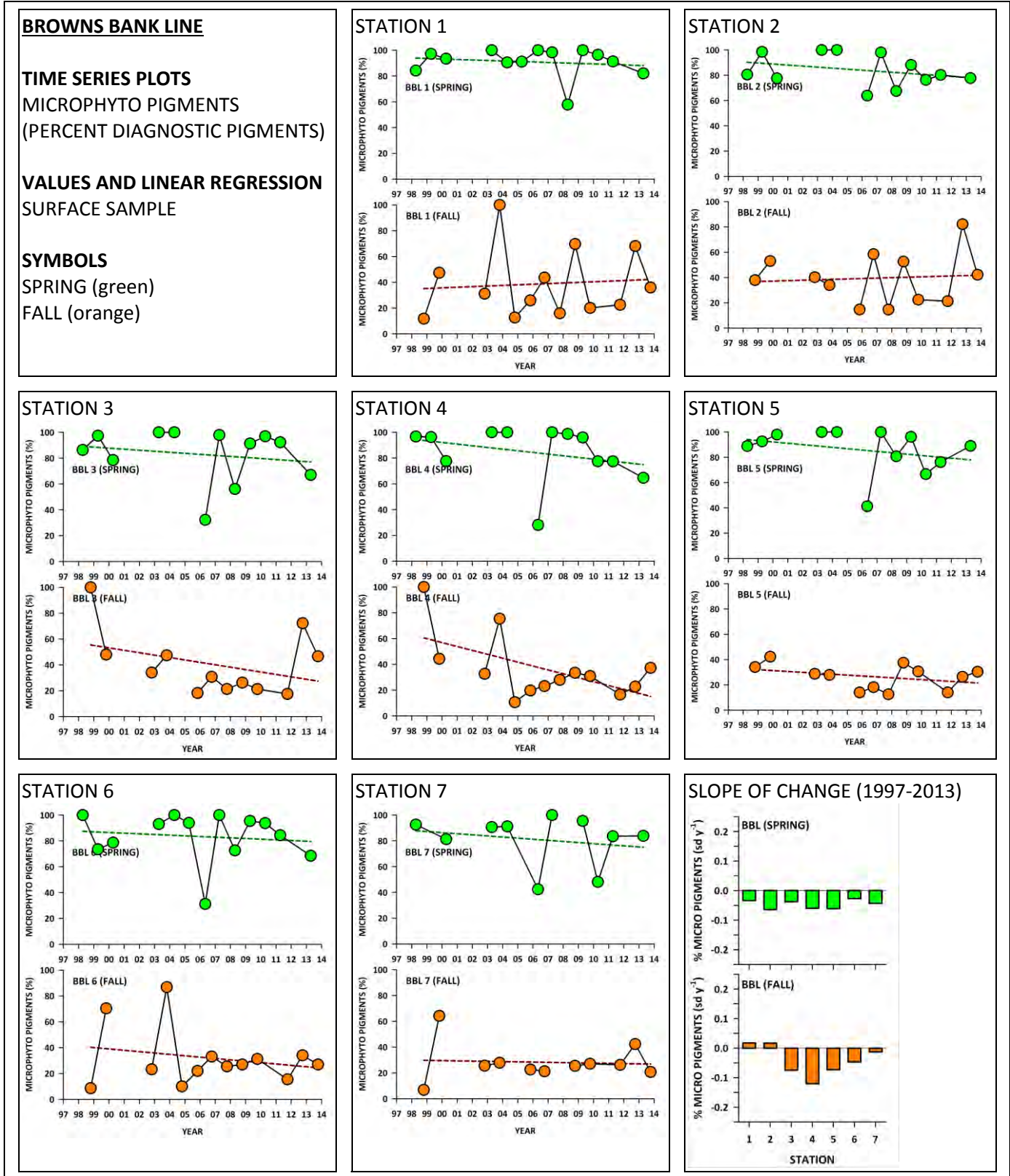


Figure 93

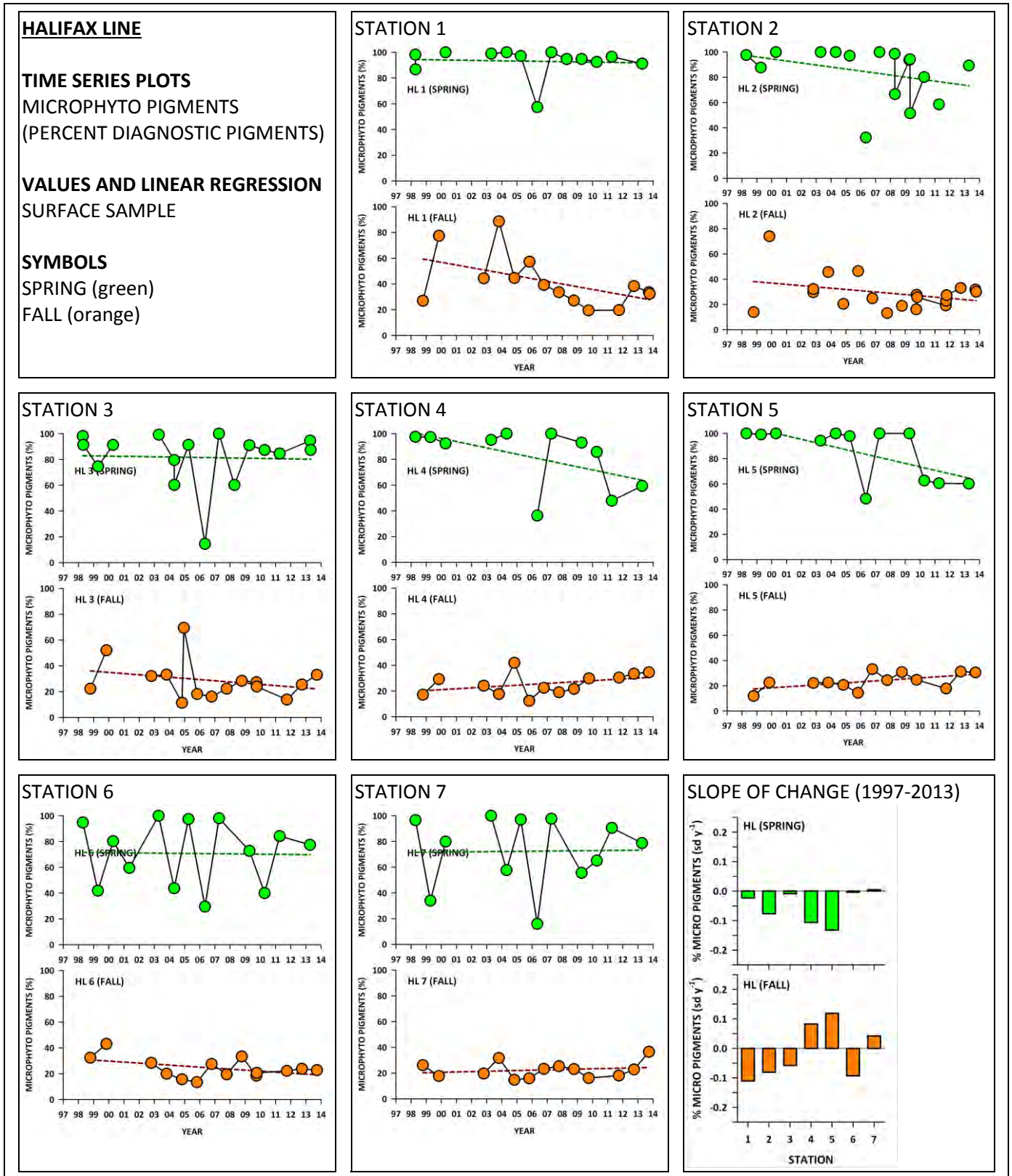


Figure 94

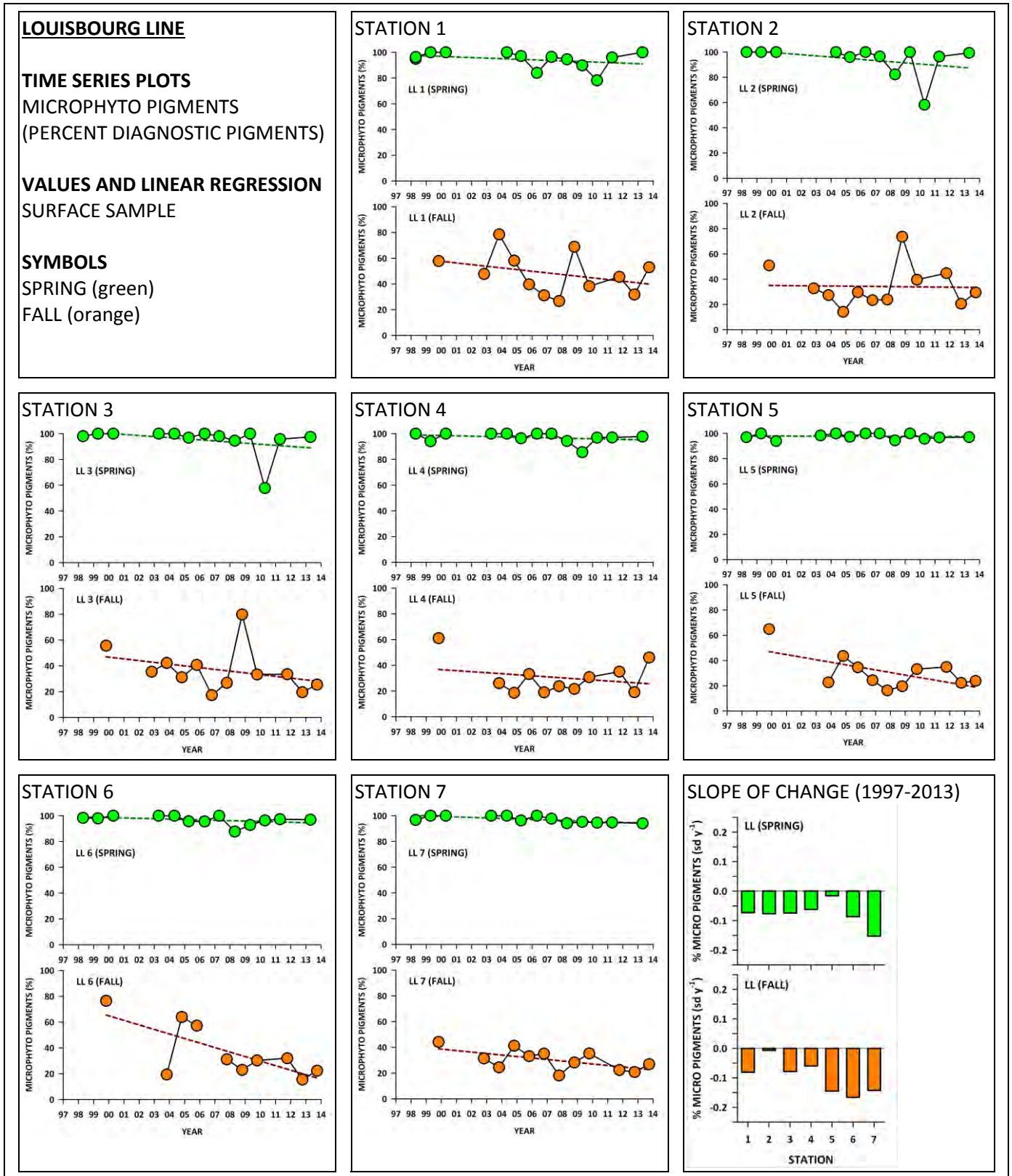


Figure 95

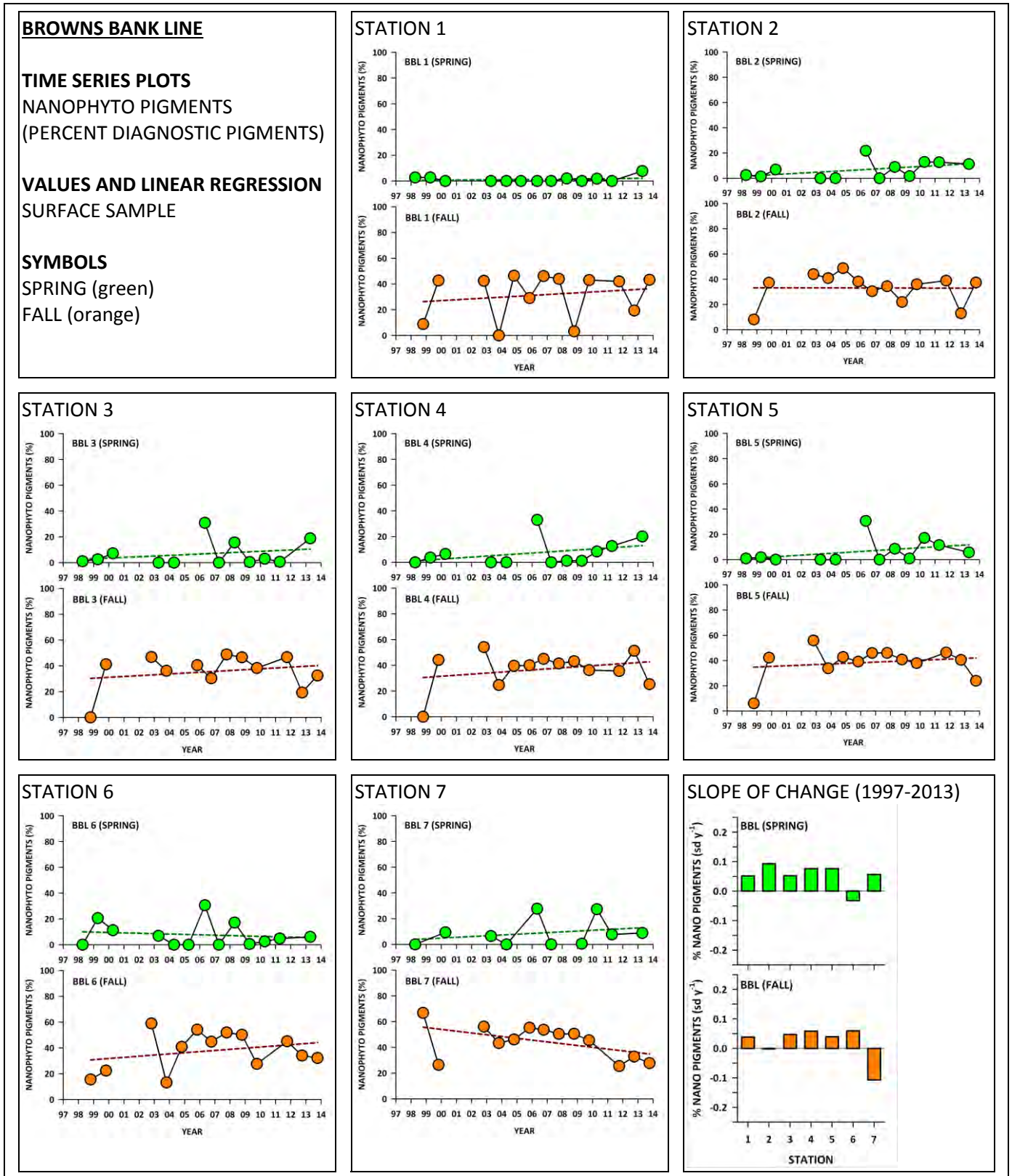


Figure 96

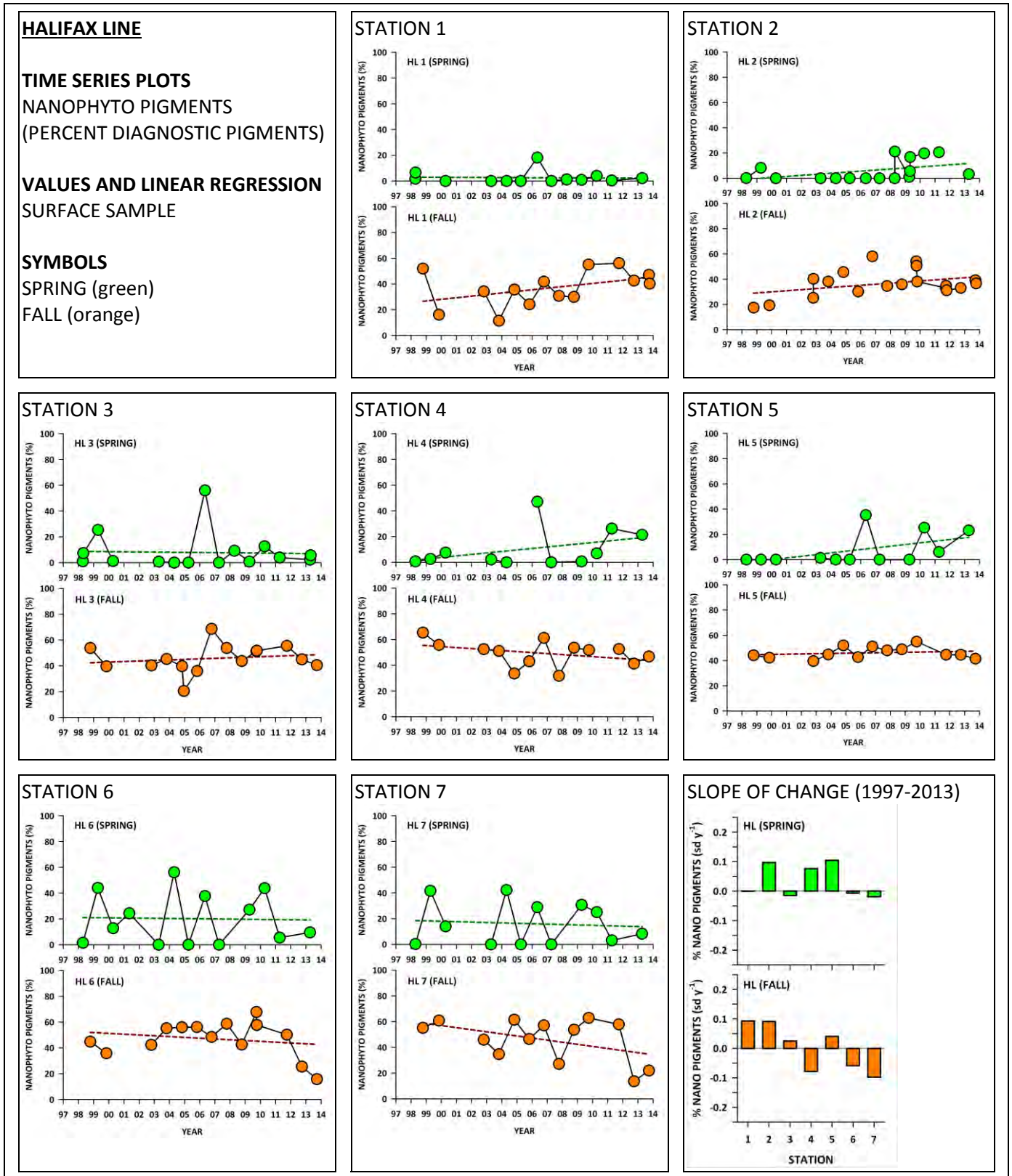


Figure 97

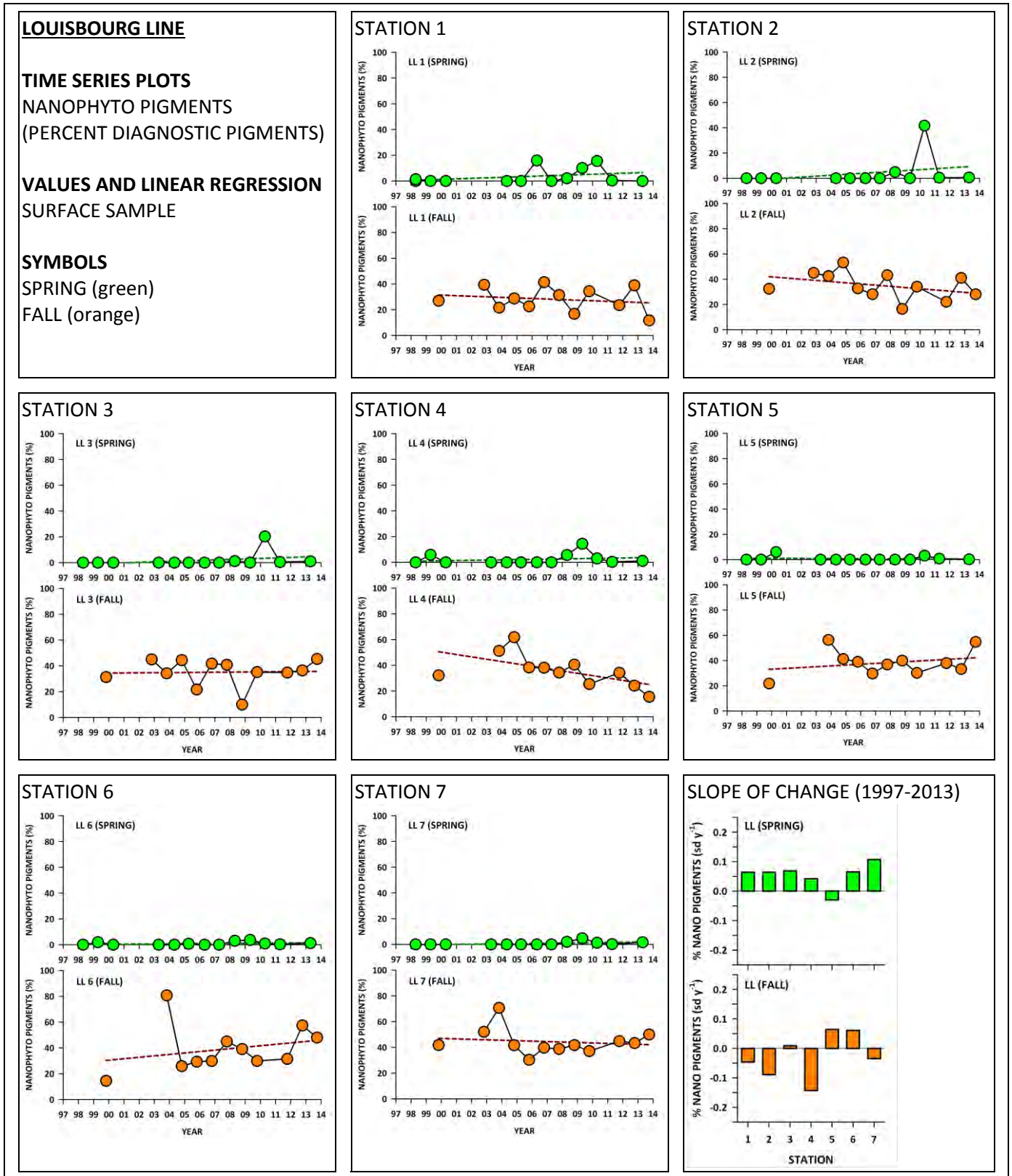


Figure 98

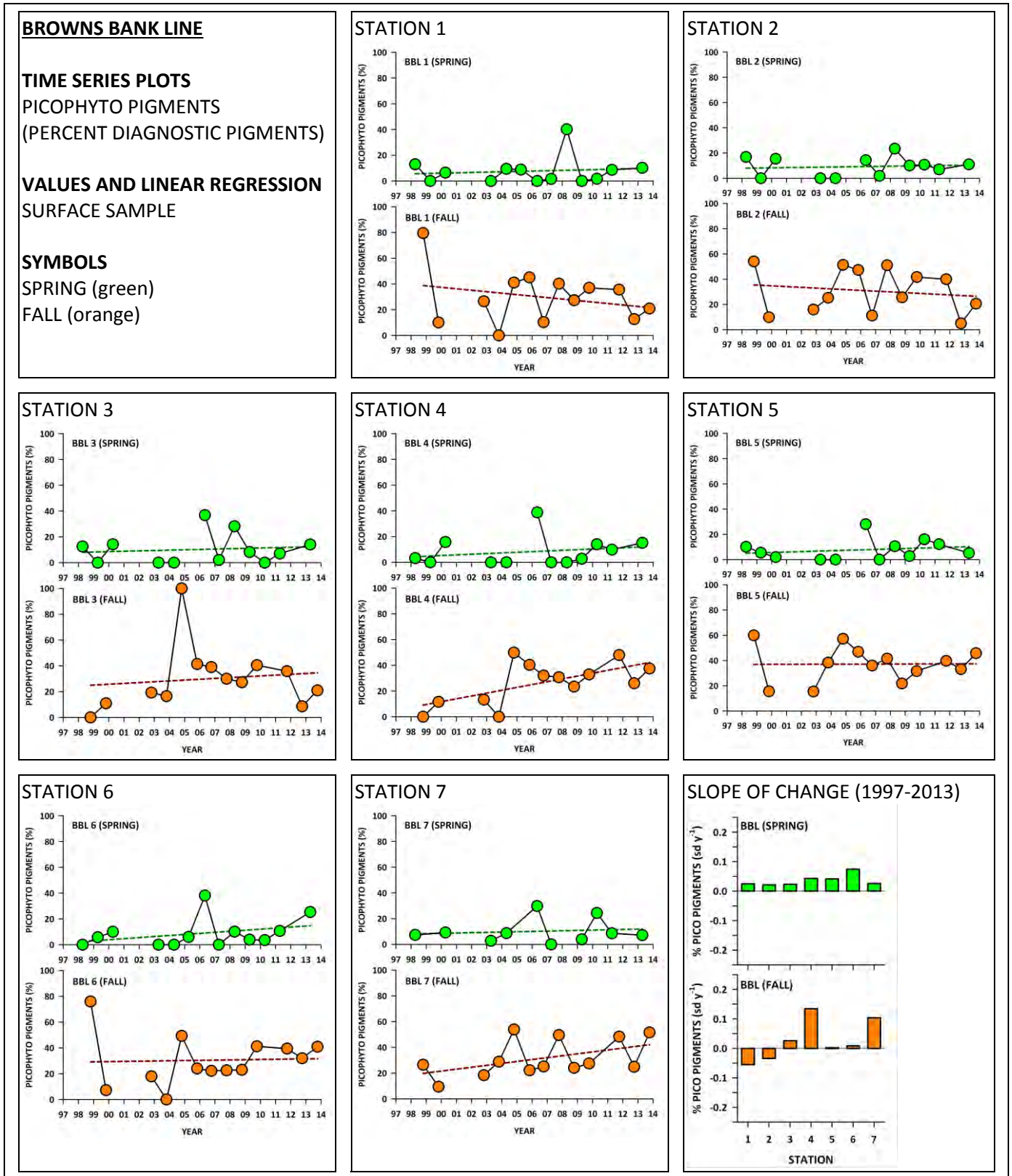


Figure 99

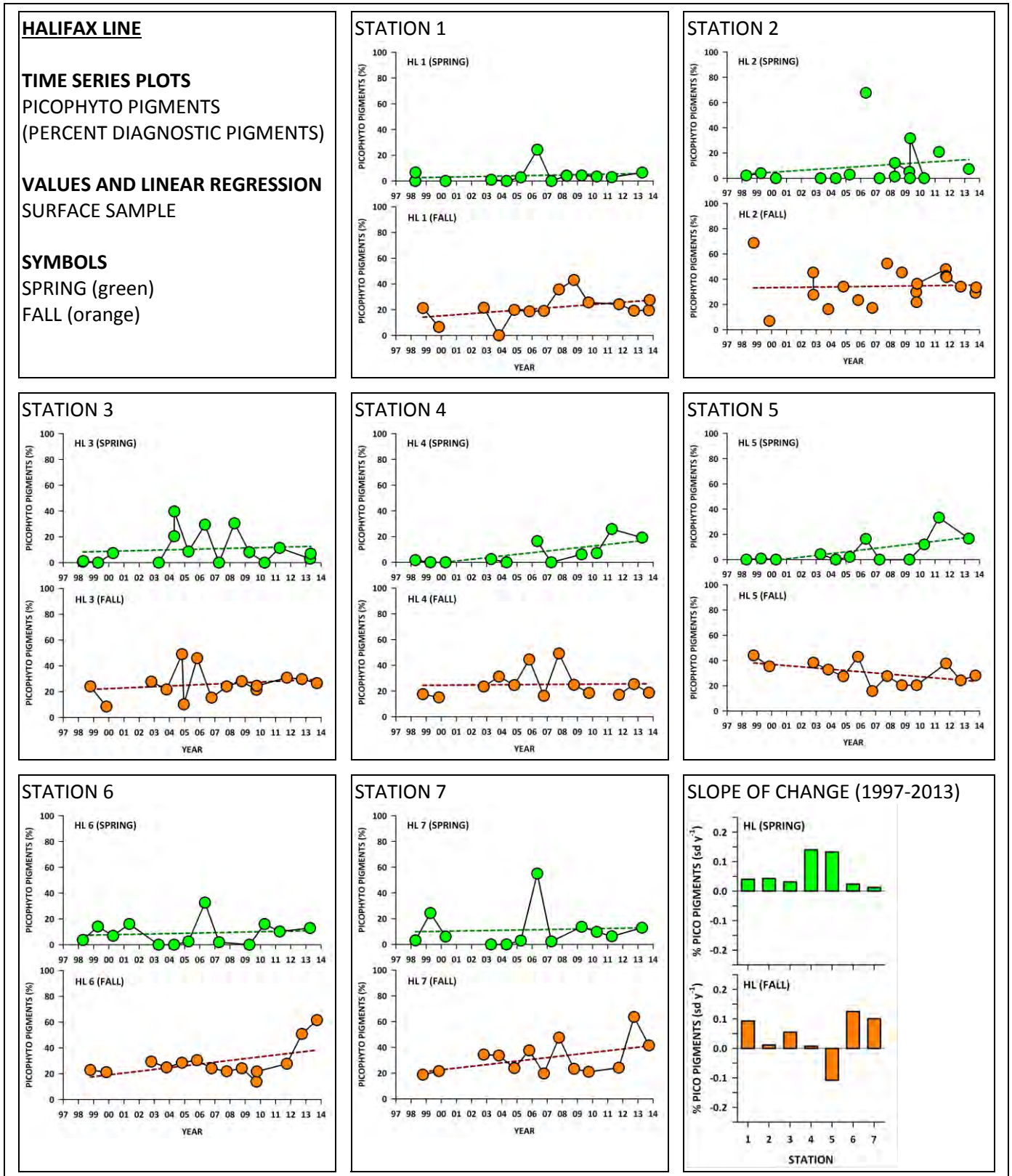


Figure 100

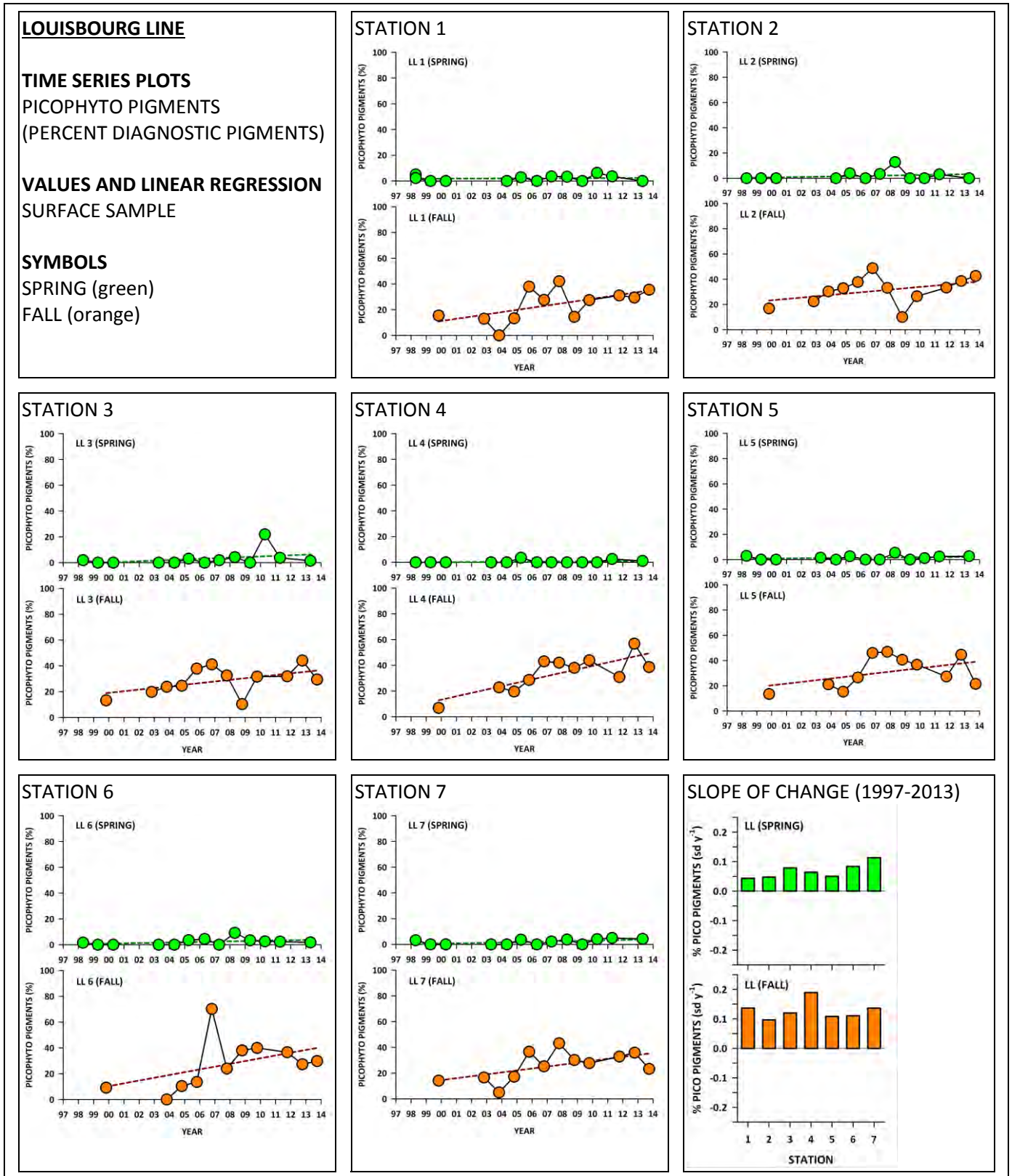


Figure 101

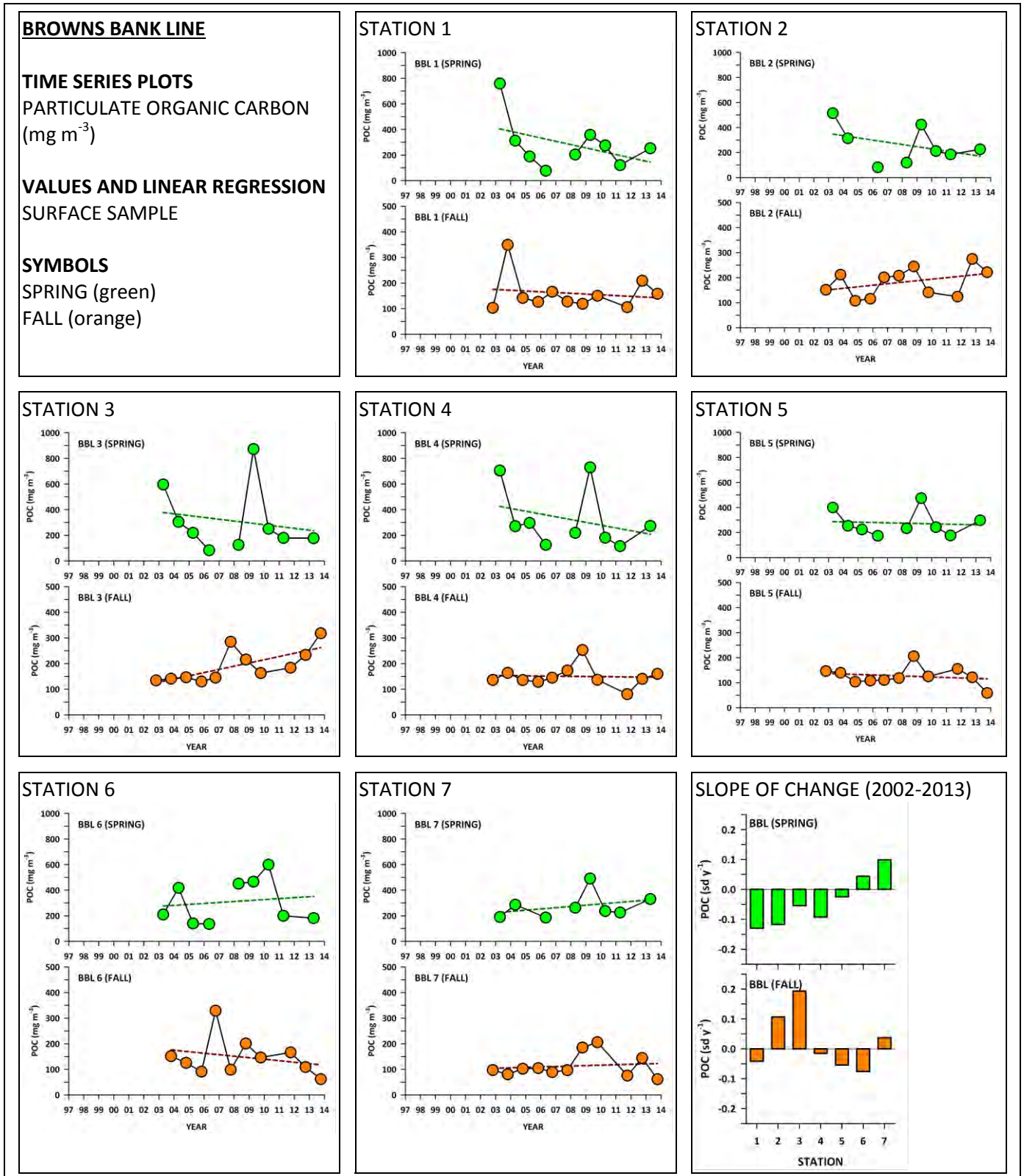


Figure 102

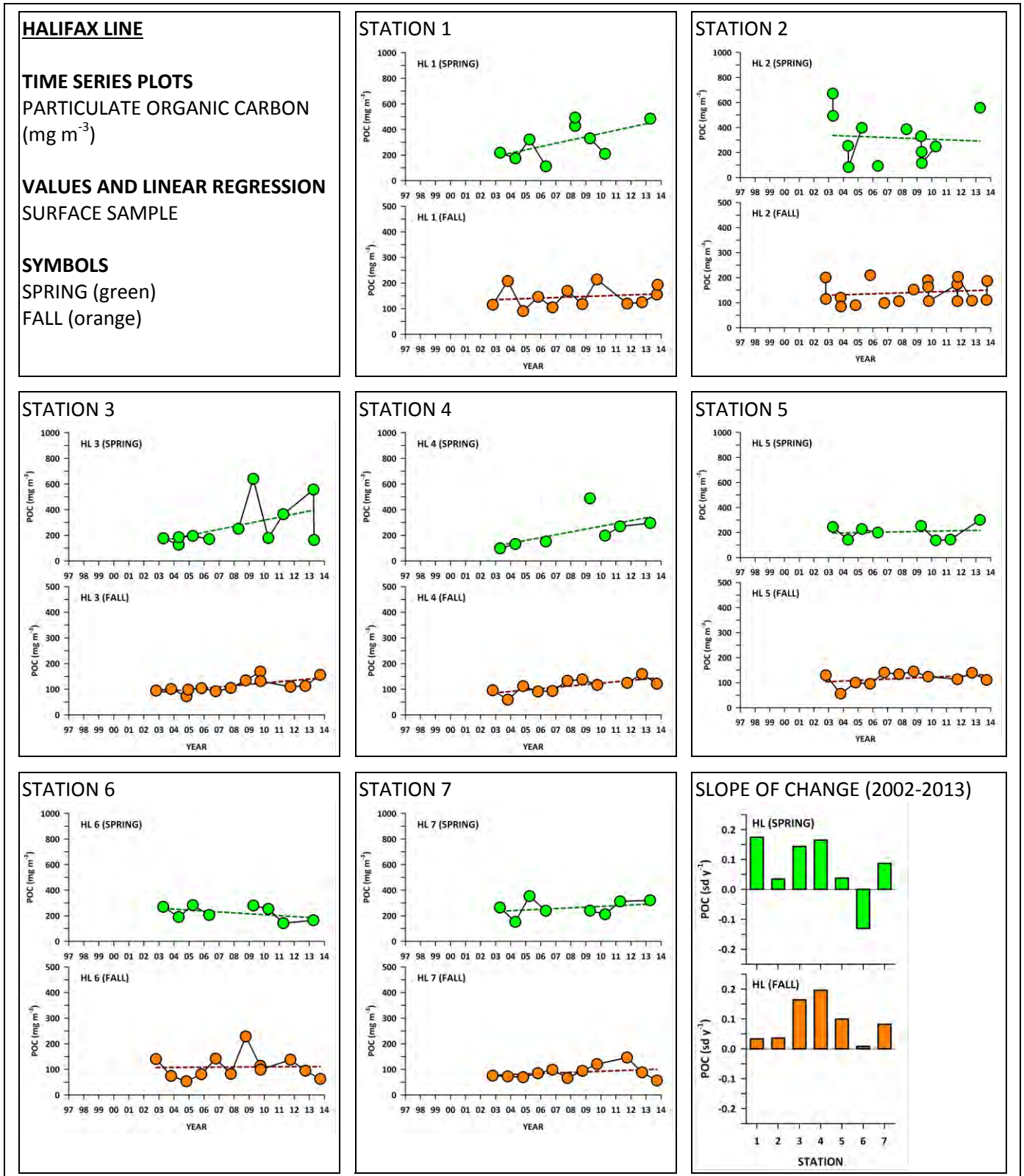


Figure 103

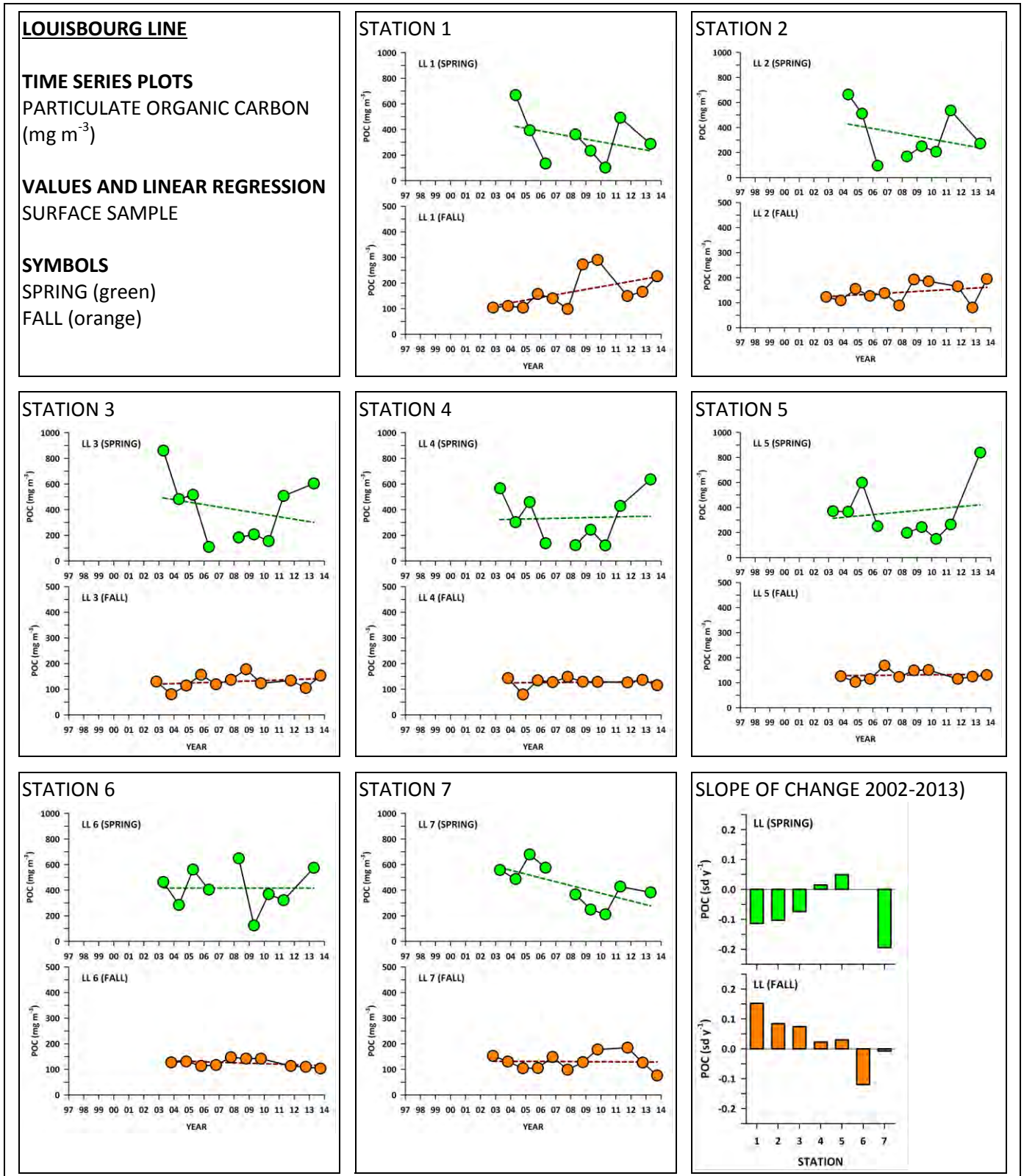


Figure 104

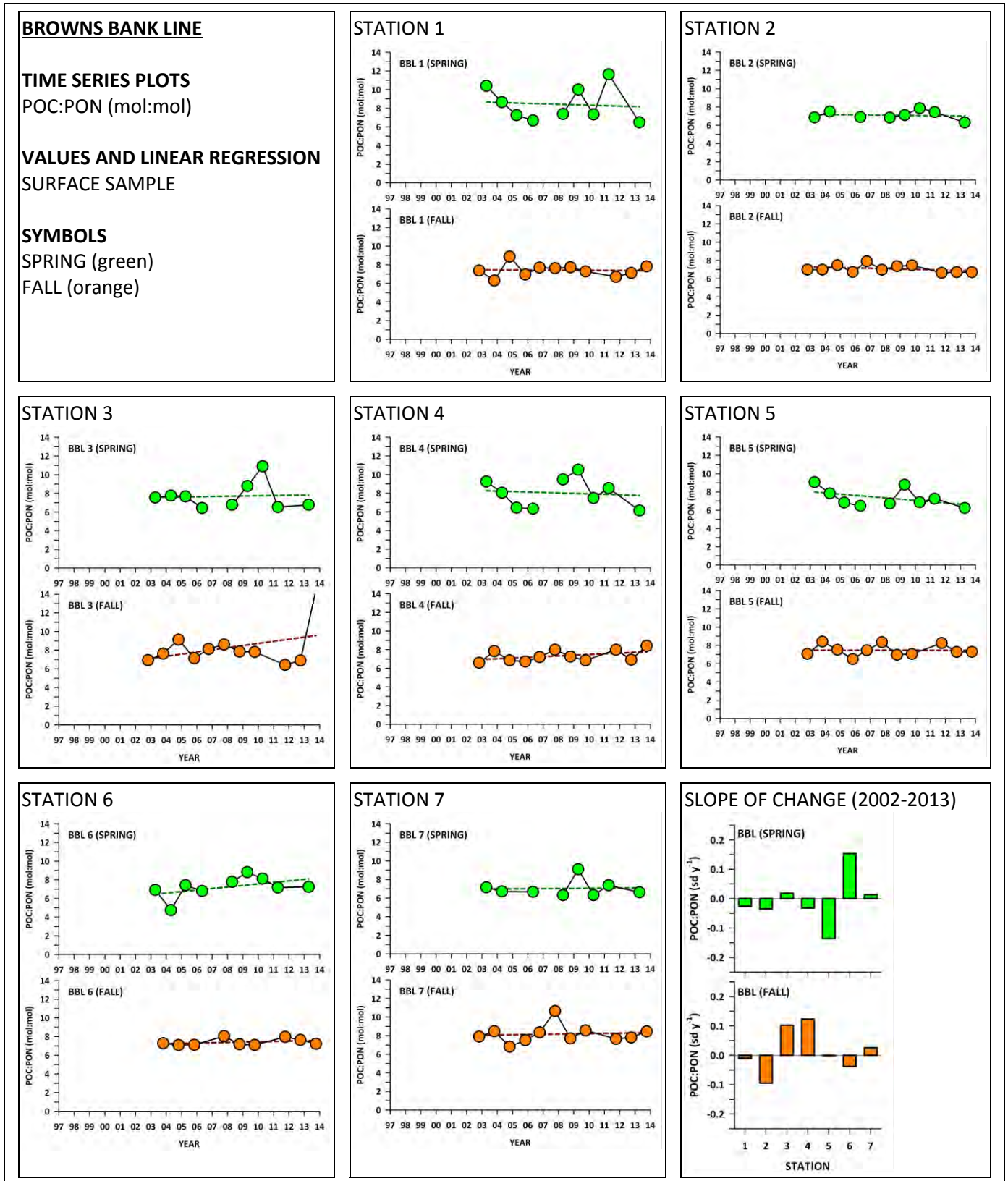


Figure 105

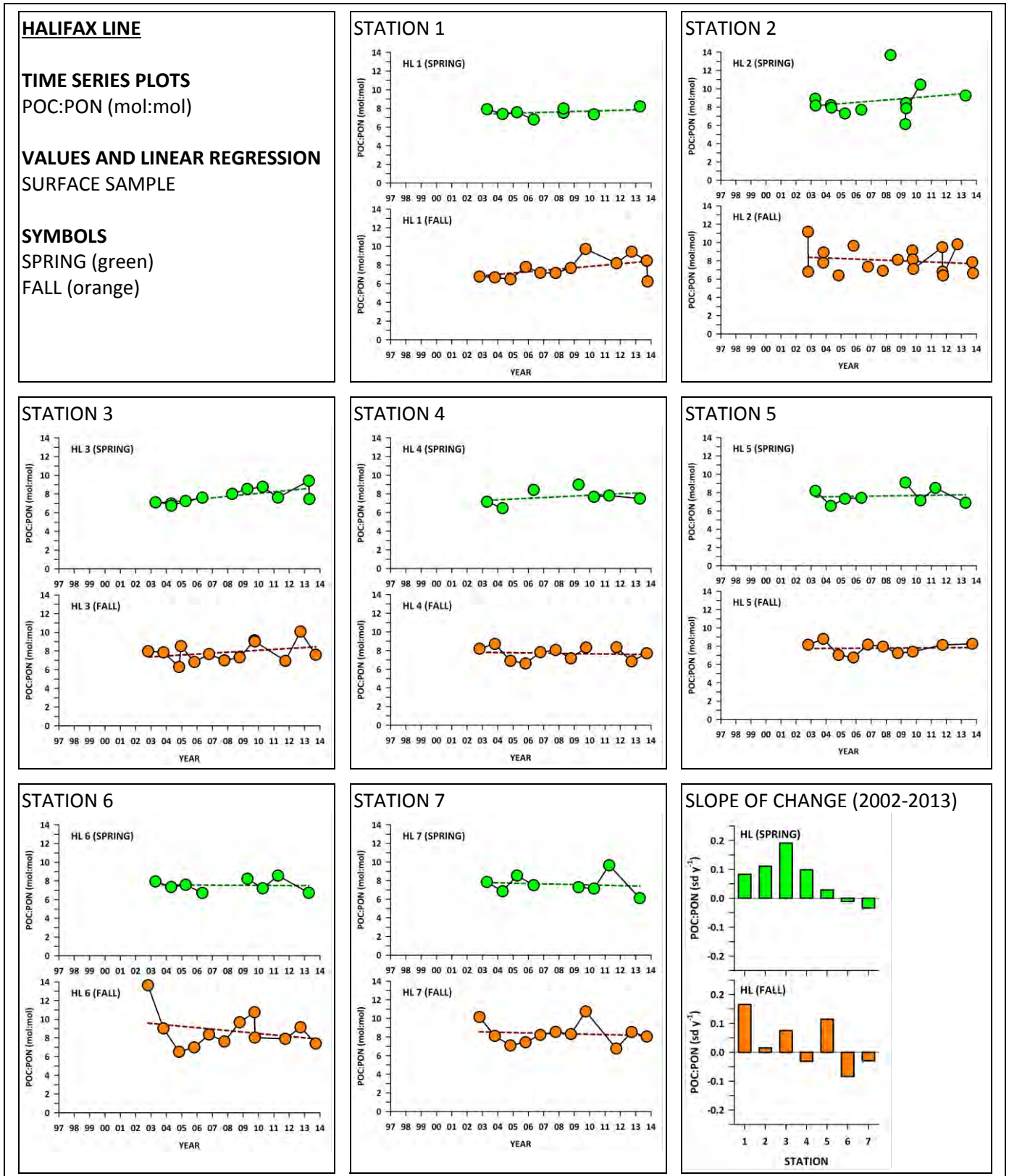


Figure 106

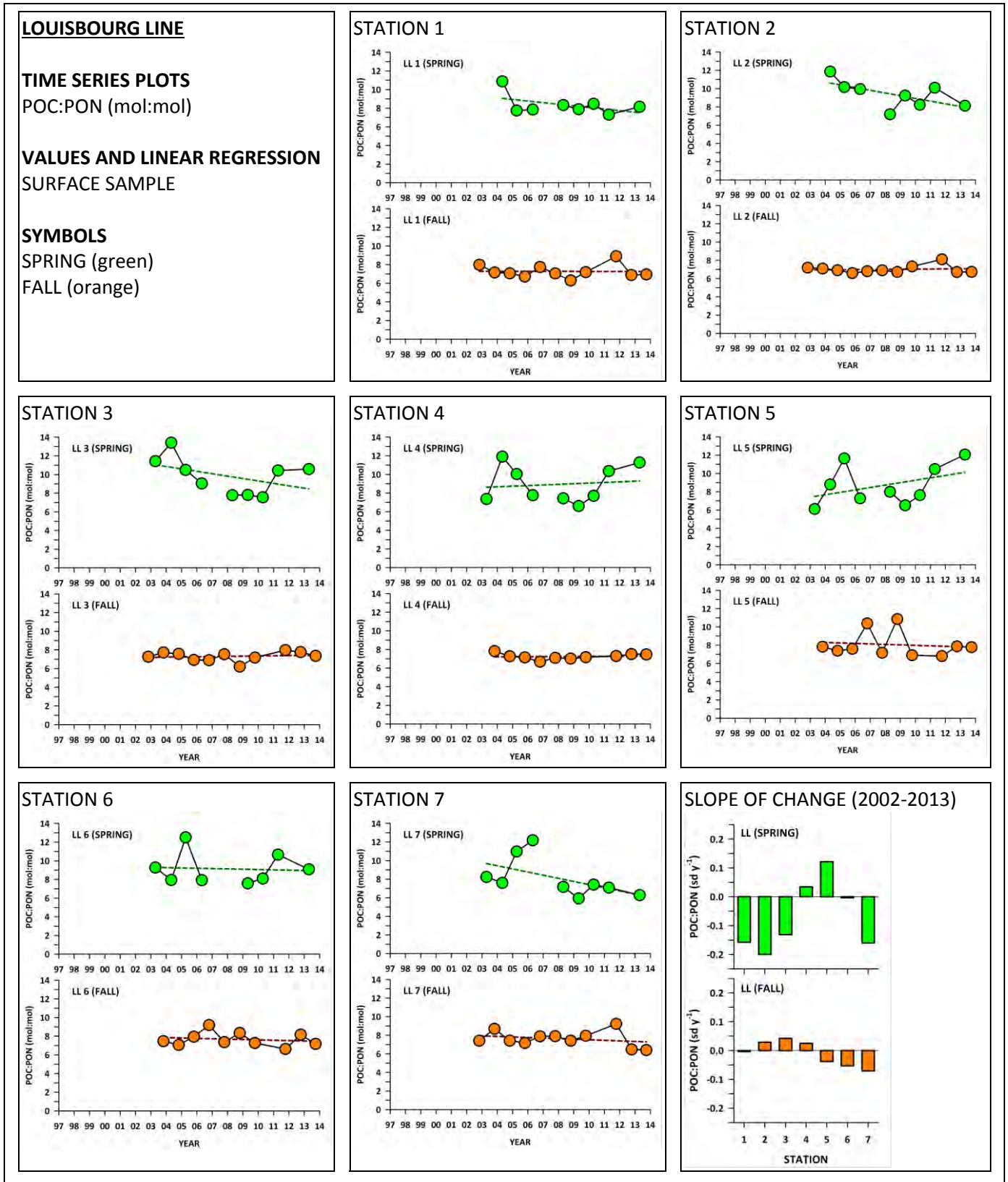


Figure 107

BROWNS BANK LINE

SLOPE OF CHANGE PLOTS

standard deviates per year

SYMBOLS

SPRING (green)

FALL (orange)

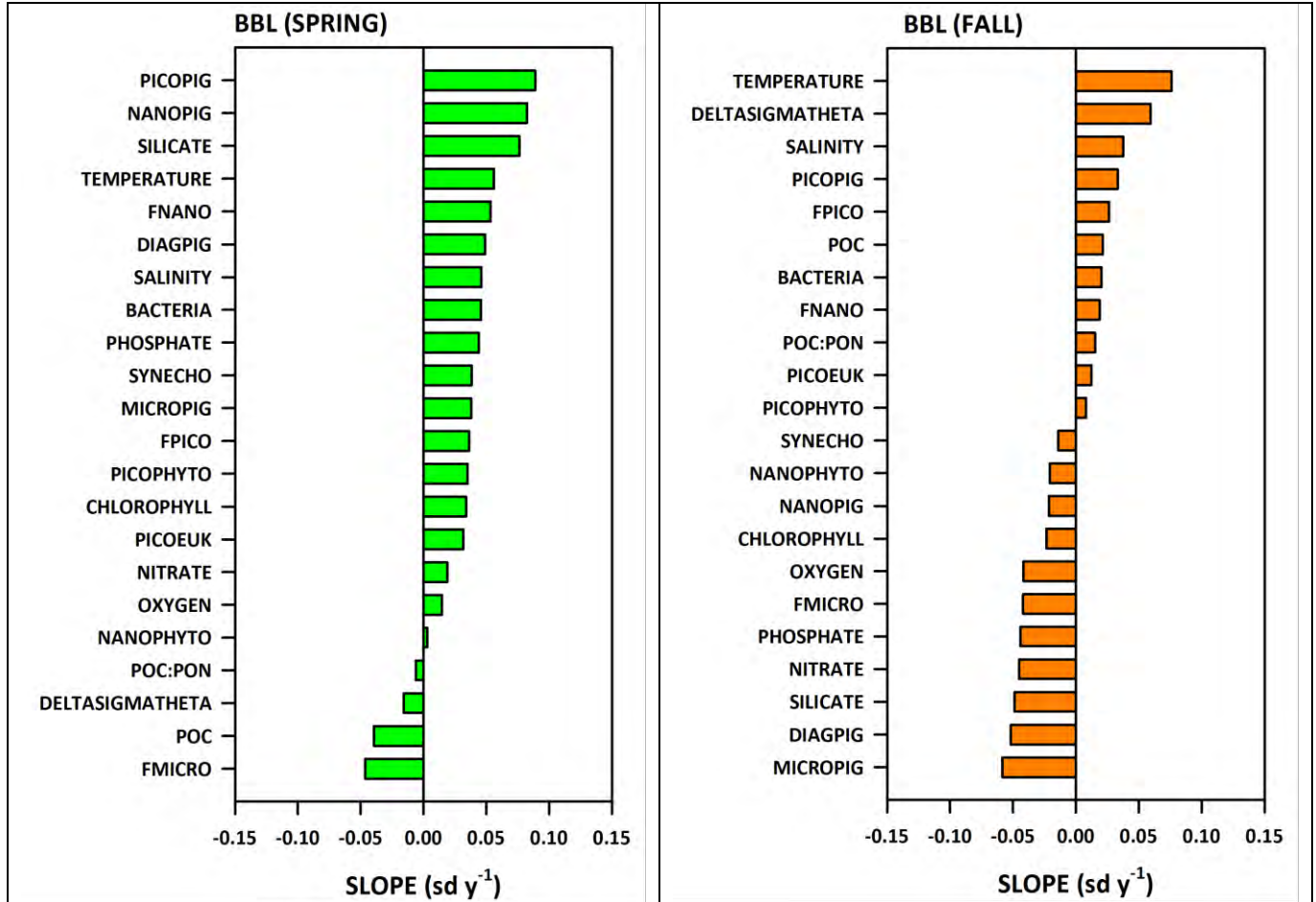


Figure 108

HALIFAX LINE

SLOPE OF CHANGE PLOTS

standard deviates per year

SYMBOLS

SPRING (green)

FALL (orange)

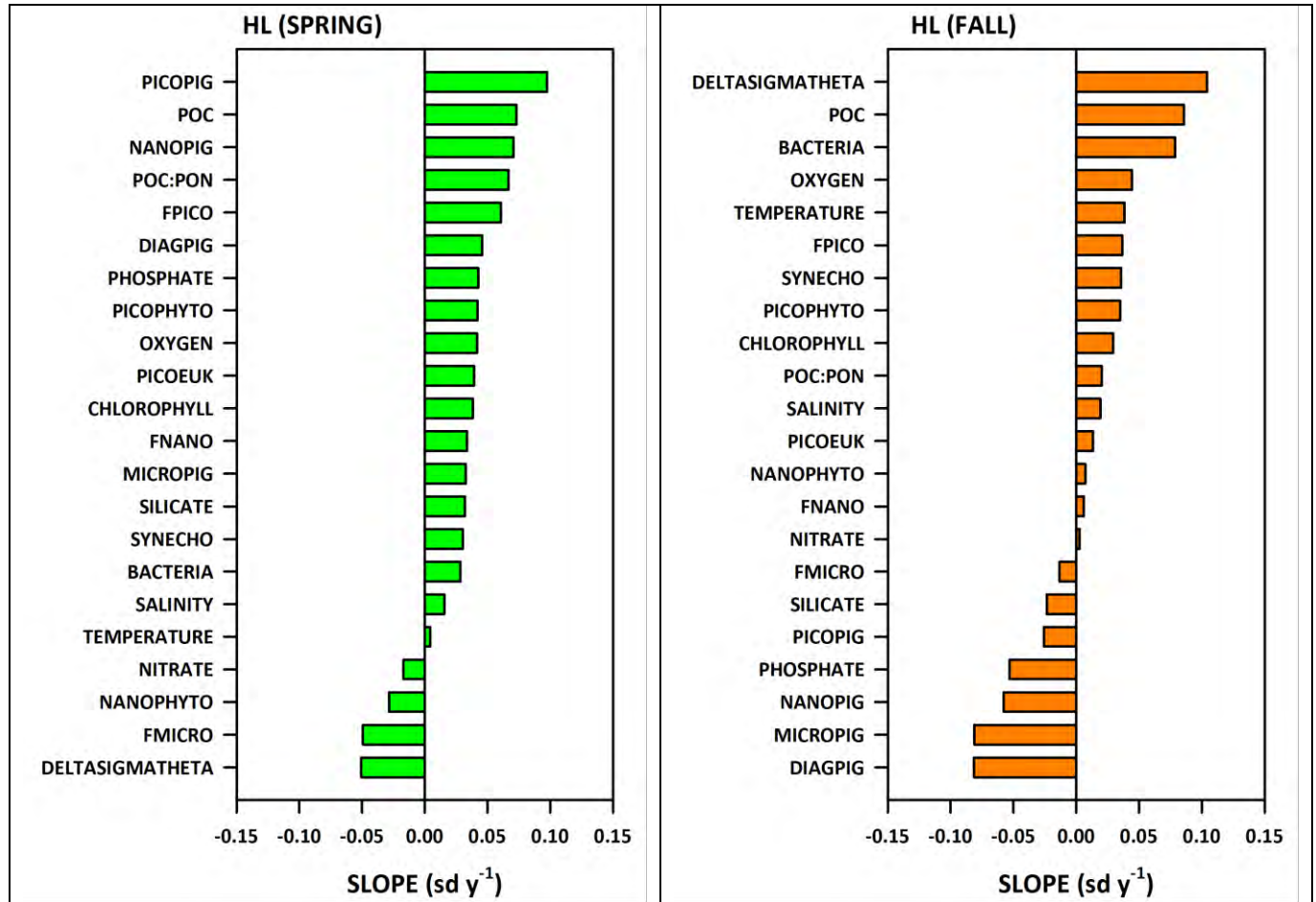


Figure 109

LOUISBOURG LINE

SLOPE OF CHANGE PLOTS

standard deviates per year

SYMBOLS

SPRING (green)

FALL (orange)

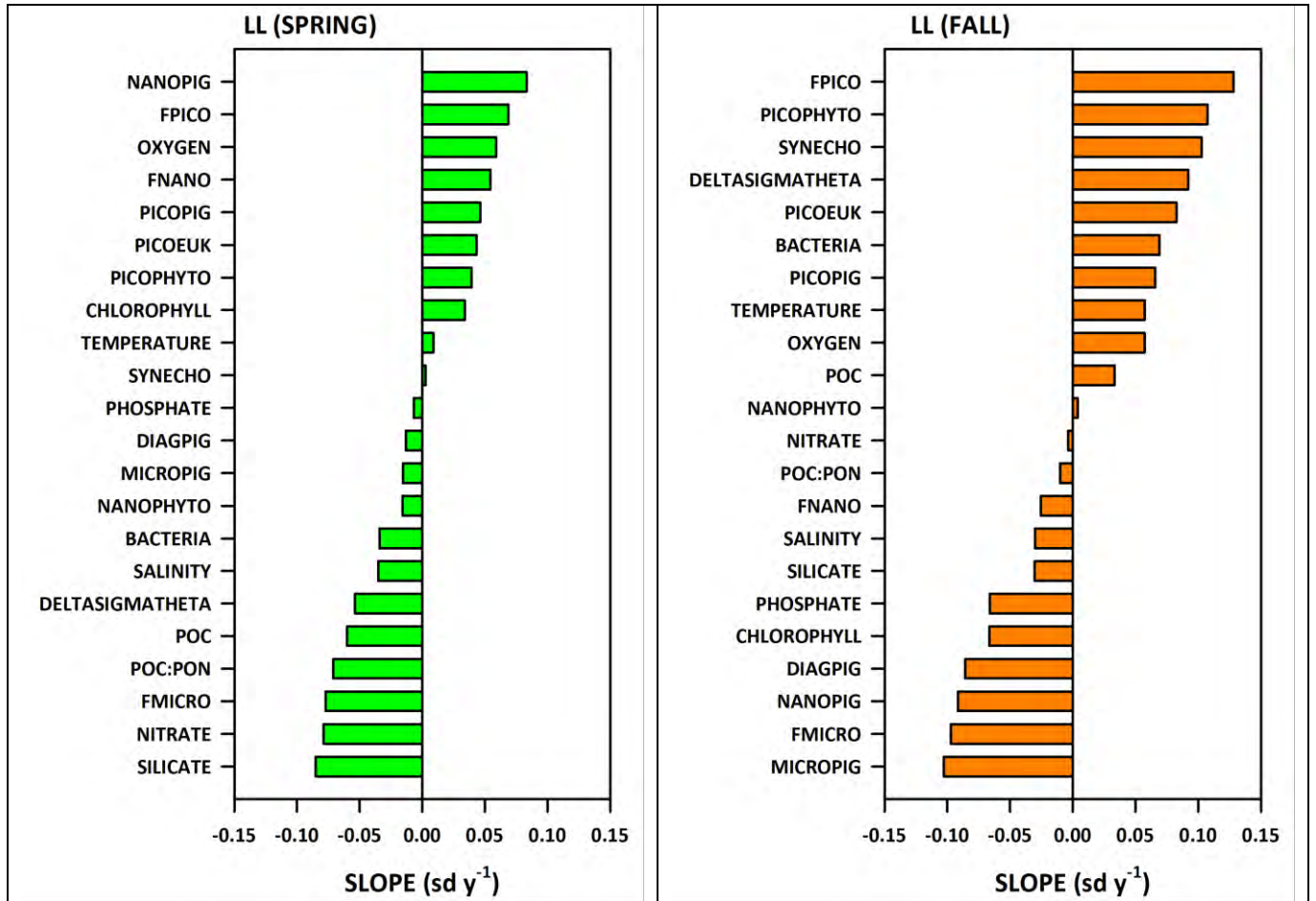


Figure 110

SCOTIAN SHELF (BBL, HL, LL)

SLOPE OF CHANGE PLOTS

standard deviates per year

SYMBOLS

SPRING (green)

FALL (orange)

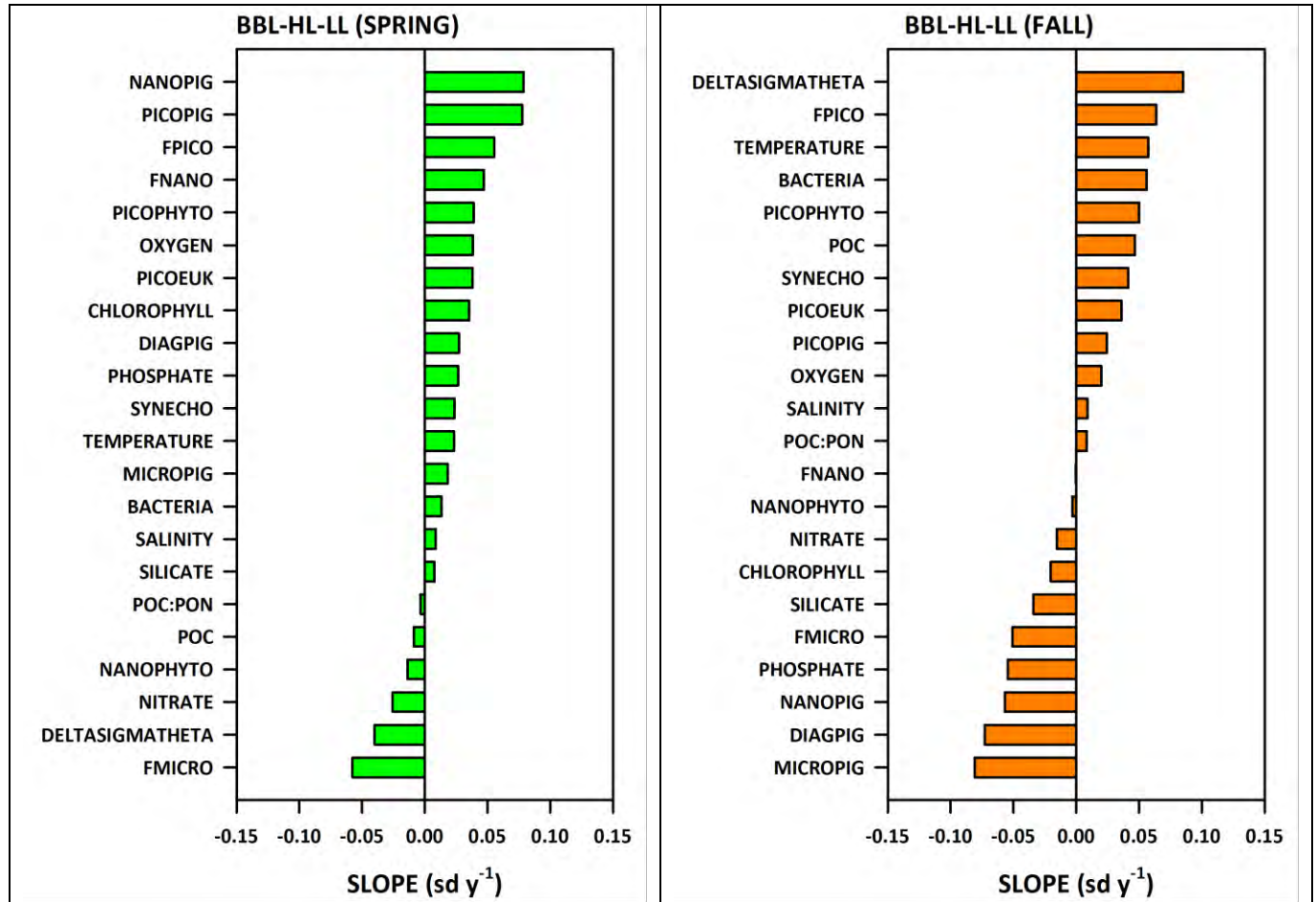


Figure 111

GRAND MEAN

SCOTIAN SHELF (BBL, HL, LL)

ANNUAL (SPRING,FALL)

SLOPE OF CHANGE PLOT

standard deviates per year

